The role of soil moisture on summer climate simulations over southern Africa

Marshall Lison Mdoka

Thesis Presented for the Degree of

DOCTOR OF PHILOSOPHY

in the Department of Environmental and Geographical Sciences
Faculty of Science

UNIVERSITY OF CAPE TOWN

February 2015

Abstract

This study aims to increase our perspective of the responses of Southern African climate to soil moisture forcings by drying or moistening the land surface using a regional climate model version 3, RegCM3. The sensitivity and response capabilities to soil moisture perturbations of the model are investigated. This includes identification of regions that may be influenced differently by antecedent soil moisture conditions as well as understand the implications of soil moisture conditions on frequency and intensity of rainfall. Exploratory analyses of soil moisture retention and comparison of climate model parameters with available observations or re-analysis data is done. The study then seeks out the large-scale atmospheric forcings under which the regional climate explicitly responds to perturbations in soil moisture using self-organising map technique. To investigate these underlying processes of atmosphere-soil moisture interactions a series of RegCM3 model experiments utilizing wet, dry and normal soil moisture conditions were designed. The experiments are based on changing the soil moisture field capacity in the RegCM3. The control simulations are run with RegCM3 nested in NCEP/NCAR reanalysis 2 data and using Emanuel convective scheme for the selected six summers (dry seasons – 1991/92, 1994/95 and 1997/98; wet seasons – 1995/96, 1996/97 and 1998/99). September to March simulations are performed with August as the spin-up month. The respective dry and wet soil moisture perturbation simulations are then initialised at field capacities of 25% (wilting) and 75% (saturation) within the land surface model, Bio-sphere Atmosphere Transfer Scheme. From the sensitivity studies, anomalously dry (wet) conditions have positive feedbacks with similar dry (wet) synoptic forcings of the regional climate. Anomalous dry forcing persists for longer and exacerbates the changes in the regional anticyclonic circulation especially during a drought or dry period. Soil moisture perturbations mostly affect the lower troposphere. Surface variables analysed especially surface temperature show strong responses to the soil moisture perturbations under all synoptic forcings but rainfall characteristics are strongly influenced by large-scale synoptic circulations. However, in some areas over southwestern parts of the region a weak feedback which can be either positive or negative depending on geographical and climatological setting has been detected.

List of Figures

1.1 Map of the southern African countries that constitute the domain used in this study. LS, SZ and DRC respectively stand for Lesotho, Swaziland and Democratic Republic of Congo……..**5**

2.1 Schematic illustration of the mean winds convergence and positions of the Inter-Tropical Convergence Zone (ITCZ) and Congo (formerly Zaire) Air Boundary (ZAB) over Africa and adjacent oceans in (a) January and (b) July (adapted from Lindesay, 1998)……**14**

2.2 Mean 500hPa geopotential heights using NCEP/NCAR reanalysis 2 data for the period (1979-2000). An anticyclone stretching from the Atlantic into the sub-continent is shown……**15**

3.1 Domain choice showing the (a) elevation of the topography and (b) land cover types over the southern Africa region. The inserted black quad shows the sub-domain that will be presented for most of the spatial maps on the chosen surface climate variables…….…….**42**

4.1 Mean soil moisture conditions for the (a) RegCM3 top-layer soil moisture; (b) mean soil moisture data measured as soil water index (SWI) obtained from Institute of Photogrammetry and Remote Sensing (IPF), Vienna University of Technology, IPF soil moisture and (c) bias of RegCM3 with respect to IPF. This soil moisture data's unit of measurement SWI (%) is for soil moisture content within the 1st metre of the soil layer in relative units that ranges from wilting level to field capacity as (%) and bias……..……**50**

4.2 Mean summer total precipitation (mm/day) of all the simulated seasons. On the left column (a) RegCM3 with precipitation over ocean masked out, (b) RegCM3 with precipitation over ocean; middle column is for (c) CRU reanalysis, (d) GPCP monthly data and left column is the biases from RegCM3 with the respect to (e) CRU and (f) GPCP…….**52**

4.3 Mean total precipitation (mm/day) of September to November (SON) for all the simulated seasons. On the left column (a) RegCM3 with precipitation over Oceans masked out, (b)

RegCM3 with precipitation over Ocean; middle column is for (c) CRU, (d) GPCP monthly data and right column is the biases for RegCM3 with the respect to (e) CRU and (f) GPCP……..**53**

4.4 Mean total precipitation (mm/day) for December to February (DJF) of all the simulated seasons. On the left column (a) RegCM3 with precipitation over ocean masked out, (b) RegCM3 with precipitation over ocean; middle column is for (c) CRU, (d) GPCP monthly data and right column is the biases for RegCM3 with the respect to (e) CRU and (f) GPCP……..**54**

4.5 Mean Air Temperature (°C) for a) control simulation, RegCM3 and b) CRU data and c) Bias for the summer season simulations. For temperature anomalies blue means negative and red is positive……...**58**

4.6 Mean Air Temperature (°C) for a) control simulation, RegCM3 and b) CRU data and c) Bias for the for SON period and d) RegCM3 e) CRU and f) Bias for DJF period for all the summers simulated. For temperature anomalies blue means negative and red is positive…….…..…**59**

4.7 The mean 10m wind fields (m/s) of the summer seasons for a) RegCM3 and b) NCEP/NCAR reanalysis 2 data……...…….……**60**

4.8 Temporal variations in the top-layer soil moisture (mm/day) for 1 September to 31 March of a) dry and b) wet season. The control simulation is represented in black, interactive wet soil moisture simulation is in blue and the dry soil moisture simulation is in red……...**63**

4.9 Mean Total Precipitation for the dry seasons on the left column with a) dry perturbation minus control; b) wet perturbation minus control; and for the wet seasons on the right column c) dry minus control; d) wet minus control. White lines enclose areas that are statistically significant at 95% confidence level……..**65**

4.10 Temporal variations in the mean total precipitation (mm/day) for the control, dry and wet soil moisture perturbations for the a) dry season and b) wet season. The control simulation is represented in black, interactive dry soil moisture simulation is in red and the wet soil moisture simulation is in blue……...**67**

4.11 Mean Surface Temperature (°C) for the dry seasons on the left column with a) dry perturbation minus control; b) wet perturbation minus control; and for the wet seasons on the right column c) dry minus control; d) wet minus control. For temperature fields, blue indicate decrease or negative responses whilst red is for an increase or positive response. White lines enclose areas that are statistically significant at 95% confidence level……...**69**

4.12 Temporal variations in the mean surface temperature (°C) for the control, dry and wet soil moisture perturbations for the a) dry season and b) wet season. The control simulation is represented in black, interactive dry soil moisture simulation is in red and the wet soil moisture simulation is in blue……...**70**

4.13 Total precipitation anomalies for interactive experiments for 1 September to 31 March 1991/1992 for a) dry run and b) wet run as well as for c) dry run and d) wet run for 1 September to 31 March 1995/1996. White lines enclose areas that are statistically significant at 95% confidence level……**72**

4.14 Anomalies of total precipitation (mm/day) for early summer, September to November, SON (left column) of 1991 and 1995 as well late summer, December to January, DJF (right column) of 1991/1992 and 1995/96. These are for all experiments of interactive dry perturbation (first and third rows) and interactive wet perturbation (second and bottom rows). White lines enclose areas that are statistically significant at 95% confidence level…….**73**

4.15 Temporal variations in the total precipitation for 1 September to 31 March of a) 1991/92 and b) 1995/96. The control simulation is represented in black, interactive dry soil moisture simulation is in red and the wet soil moisture simulation is in blue……...**78**

4.16 Surface Temperature (°C) anomalies for interactive experiments for 1 September to 31 March 1991/1992 of a) dry and b) wet perturbations and for 1 September to 31 March 1995/1996 of c) dry and d) wet perturbations. White lines enclose areas that are statistically significant at 95% confidence level…….**80**

4.17 Spatial distribution anomalies of Surface Temperature (°C) for early summer, September to November, SON (left column) of 1991 and 1995 as well as late summer, December to January,

DJF (right column) of 1991/1992 and 1995/96. These are for all experiments of interactive dry perturbation (first and third rows) and interactive wet perturbation (second and bottom rows). White lines enclose areas that are statistically significant at 95% confidence level…….**81**

4.18 Temporal variations in the surface temperature (°C) for 1 September to 31 March of a) 1991/92 and b) 1995/96. The control simulation is represented in black, interactive dry soil moisture simulation is in red and the wet soil moisture simulation is in blue…….**83**

4.19 Sensible heat flux (W/m^2) anomalies for interactive experiments of 1 September to 31 March 1991/1992 of a) dry and b) wet perturbations as well as for 1 September to 31 March 1995/1996 of c) dry and d) wet perturbations. White lines enclose areas that are statistically significant at 95% confidence level…….…..**85**

4.20 Spatial distribution anomalies of sensible heat flux (W/m^2) for early summer, September to November, SON (left column) of 1991 and 1995 as well late summer, December to January, DJF (right column) of 1991/1992 and 1995/96. These are for all experiments of interactive dry perturbation (first and third rows) and interactive wet perturbation (second and bottom rows). White lines enclose areas that are statistically significant at 95% confidence level…….....**87**

4.21 Temporal variations in the sensible heat flux (W/m^2) of 1 September to 31 March for a) 1991/92 and b) 1995/96 seasons. The control simulation is represented in black, interactive dry soil moisture simulation is in red and the wet soil moisture simulation is in blue……**88**

4.22 Latent heat flux (W/m^2) anomalies for interactive experiments for 1 September to 31 March 1991/1992 of a) dry and b) wet perturbations as well as for 1 September to 31 March 1995/1996 of c) dry and d) wet perturbations. White lines enclose areas that are statistically significant at 95% confidence level…….**89**

4.23 Spatial distribution anomalies of latent heat flux (W/m^2) for early summer, September to November, SON (left column) of 1991 and 1995 as well late summer, December to January, DJF (right column) of 1991/1992 and 1995/96. These are for all experiments of interactive dry

perturbation (first and third rows) and interactive wet perturbation (second and bottom rows). White lines enclose areas that are statistically significant at 95% confidence level…….**91**

4.24 Temporal variations in the latent heat flux (W/m^2) for 1 September to 31March of a) 1991/92 and b) 1995/96. The control simulation is represented in black, interactive dry soil moisture simulation is in red and the wet soil moisture simulation is in blue……...…….**92**

4.25 Incident solar radiation anomalies (W/m^2) for interactive experiments of 1 September to 31 March 1991/1992 of a) dry and b) wet perturbations as well as for 1 September to 31 March 1995/1996 of c) dry and d) wet perturbations. White lines enclose areas that are statistically significant at 95% confidence level……...**94**

4.26 Incident solar radiation anomalies (W/m^2) for early summer, September to November, SON (left column) of 1991 and 1995 as well late summer, December to January, DJF (right column) of 1991/92 and 1995/96. These are for all experiments of interactive dry perturbation (first and third rows) and interactive wet perturbation (second and bottom rows). White lines enclose areas that are statistically significant at 95% confidence level……...**96**

4.27 Temporal variations in the incident solar radiation (W/m^2) for 1 September to 31 March of a) 1991/92 and b) 1995/96 seasons. The control simulation is represented in black, interactive dry soil moisture simulation is in red and the wet soil moisture simulation is in blue……..…**97**

4.28 Planetary boundary layer height anomalies (m) for interactive experiments of 1 September to 31 March 1991/1992 of a) dry and b) wet perturbations as well as for 1 September to 31 March 1995/1996 of c) dry and d) wet perturbations. White lines enclose areas that are statistically significant at 95% confidence level……**99**

4.29 Anomalies of planetary boundary layer height (m) for early summer, September to November, SON (left column) of 1991 and 1995 as well late summer, December to January, DJF (right column) of 1991/92 and 1995/96. These are for all experiments of interactive dry perturbation (first and third rows) and interactive wet perturbation (second and bottom rows). White lines enclose areas that are statistically significant at 95% confidence level……**100**

4.30 Temporal variations in the planetary boundary layer height (m) for 1 September to 31 March of a) 1991/92 and b) 1995/96 season. The control simulation is represented in black, interactive dry soil moisture simulation is in red and the wet soil moisture simulation is in blue……...……**102**

5.1 Geopotential height anomalies at 700hPa for the soil moisture perturbations from the control for 1 September to 31 March 1991/92 RegCM3 a) dry run b) wet run, and for 1 September to 31 March 1995/96 with c) dry run and d) wet run……..**108**

5.2 Geopotential anomalies (gpm) at 700hPa for the soil moisture perturbation simulation from the control simulation of early summer of 1991/92 and 1995/96 (left column) and later summer of 1991/92 and 1995/96 (right column)……..**111**

5.3 Direction and magnitude of moisture flux (g kg^{-1} ms^{-1}) for (a) January 1992 and (b) January 1996 in the RegCM3 at 2 metres above surface……..…**113**

5.4 The direction and magnitude of 2m moisture fluxes anomalies (g kg^{-1} ms^{-1}) for January 1992, interactive a) dry run - control, b) wet run – control; January 1996, interactive c) dry run - control and d) wet - control……..**114**

5.5 Vertical profiles for cloud liquid water path (g m^{-3}) for the perturbed and control simulations in (a) 1991/92 and (b) 1995/96 seasons. Black represents the control run, red is the dry run and blue for the wet run……..**115**

5.6 Vertical analyses of air temperature anomalies of the soil moisture perturbations from the control simulations for 1991/92 (left column) and 1995/96 (right column) seasons at latitude 18ºS in the central part of southern Africa region…….……..**117**

5.7 Diurnal cycles of (a) Total precipitation, (b) Surface Temperature (c) Evapotranspiration for January 1992 and (d) Total precipitation, (e) Surface Temperature and (f) Evapotranspiration for January 1996……**120**

5.8 Diurnal cycles of (a) Sensible heat flux, (b) Incident solar radiation (c) Planetary boundary layer for January 1992 and (d) Sensible heat flux, (e) Incident solar radiation and (f) Planetary boundary layer for January 1996……....**121**

5.9 Rain days and Intensity for RegCM3 simulations; January 1992 a) Rain days, b) Intensity and January 1996 c) Rain days, b) Intensity. Rain day is considered to be 2mm/day……**123**

5.10 Total rain days anomalies between the interactive experiments from the control simulation for January 1992 a) dry - control, b) wet – control and 1996 c) dry - control and d) wet – control. Rain day is considered to have at least 2mm/day……**124**

5.11 Intensity anomalies between the interactive experiments minus the control simulation for January 1992 a) dry - control, b) wet – control and 1996 c) dry - control and d) wet – control……..**126**

6.1 A 3x4 SOM of daily average NCEP/NCAR 850hPa geopotential height from 1 September to 31 March 1991/92 and 1995/96……..…….**133**

6.2 A 3x4 SOM of daily average NCEP/NCAR 500 geopotential height from 1 September to 31 March 1991/92 and 1995/96……..……..**134**

6.3 A 3x4 SOM of daily average NCEP 700hPa precipitable water from 1 September to 31 March 1991/92 and 1995/96……...**135**

6.4 Median dates of occurrence of each of the SOM node for simulated seasons of 1 September to 31 March of 1991/92 and 1995/96…….……**136**

6.5 Frequency of occurrence for the simulated seasons, 1 September to 31 March 1991/92 (the grey shading bars) and 1995/96 (plain white bars) for each of the SOM nodes ……**138**

6.6 Planetary boundary layer (m) anomalies for the 4x3 nodes from the daily RegCM3 simulation of dry soil moisture perturbation – control of September 1991 to March 1992. Red shading indicates positive planetary boundary layer anomalies and blue shading indicates negative planetary boundary layer anomalies……..**139**

6.7 Planetary boundary layer anomalies (m) for the 4x3 nodes from the daily RegCM3 simulation of wet soil moisture perturbation – control of September 1991 to March 1992. Red shading indicates positive planetary boundary layer anomalies and blue shading indicates negative planetary boundary layer anomalies…….**140**

6.8 Planetary boundary layer anomalies (m) for the 4x3 nodes from the daily RegCM3 simulation of dry soil moisture perturbation – control of September 1995 to March 1996. Red shading indicates positive planetary boundary layer anomalies and blue shading indicates negative planetary boundary layer anomalies…….…….**141**

Figure 6.9 Planetary boundary layer anomalies (m) for the 4x3 nodes from the daily RegCM3 simulation of wet soil moisture perturbation – control of September 1995 to March 1996. Red shading indicates positive planetary boundary layer anomalies and blue shading indicates negative planetary boundary layer anomalies……..**142**

7.1 Zones selected for the sub-regional analysis of summer climate simulations to soil moisture perturbations. There is the *Domain, Central, South* and *West* areas…….…..….**146**

7.2 Top-layer soil moisture anomalies (mm/day) for the selected zones over *Central , South* and *West* for the soil moisture perturbation experiments from the control simulations of the respective early and late summer time periods of 1991/92 and 1995/96……..…...**147**

7.3 Total rainfall anomalies (mm/day) for the selected zones over *Central , South* and *West* for the soil moisture perturbation experiments from the control simulations of the respective early and late summer time periods of 1991/92 and 1995/96……..**148**

7.4 Surface (tg) and air (ta) temperature (°C) for the selected zones over *Central , South* and *West* for the soil moisture perturbation experiments from the control simulations of the respective early and late summer time periods of 1991/92 and 1995/96…….**150**

7.5 Latent heat (le) and sensible heat (h) fluxes as well as incident solar radiation (swi), (W/m^2) for the selected zones over *Central, South* and West for the soil moisture perturbation

experiments from the control simulations of the respective early and late summer time periods of 1991/92 and 1995/96……**151**

7.6 Planetary boundary Layer (m) for the selected zones over *Central, South* and *West* for the soil moisture perturbation experiments from the control simulations of the respective early and late summer time periods of 1991/92 and 1995/96……....**152**

7.7 Evaporative Fraction of the control (black), dry (red) and wet (blue) soil moisture perturbation simulations for summer season of 1991/1992…….……**153**

7.8 Evaporative Fraction of the control (black), dry (red) and wet (blue) soil moisture perturbation simulations for summer season of 1995/1996……**154**

7.9 Moist static energy of the control (black), dry (red) and wet (blue) soil moisture perturbation simulations for summer season of 1991/1992…….**156**

7.10 Moist static energy of the control (black), dry (red) and wet (blue) soil moisture perturbation simulations for summer season of 1995/1996……..……..**158**

List of Tables

Table 3.1 Land Cover or Vegetation classes as defined within GLCC dataset……..…..**37**

Table 6.1 Total days and frequency of occurrence of each SOM node for both simulated seasons…….**137**

Table 7.1 Zones selected for the sub-regional analysis to soil moisture perturbations……...…**147**

List of Acronyms

AGCM	Atmospheric Global Climate Model/ General Circulation Model
ANN	Artificial Neural Network
AVHHR	Advanced Very High Resolution Radiometer
BATS	Biosphere-Atmosphere Transfer Scheme
BATS1E	Biosphere-Atmosphere Transfer Scheme version 1E
BUH	Botswana Upper High
CAB	Congo Air Boundary
CAPE	Convective Available Potential Energy
CCM3	Community Climate Model version 3
CLIVAR	CLIimate VARariability and Predictability
CLM	NCAR Community Land Model
CLM3	NCAR Climate Model version 3 (NCAR CCM3)
CLWP	Cloud Liquid Water Path
CMAP	Climate Prediction Center Merged Analysis of Precipitation
CRU	Climate Research Unit
CSAG	Climate System Analysis Group
DJF	December January February

ECMWF	European Centre for Medium Range Weather Forecasting
EF	Evaporative Fraction
ENSO	El Niño Southern Oscillation
ERA-15	ECMWF 15-year Reanalysis data
ERA-40	ECMWF 40-year Reanalysis data
ERS	European Remote-Sensing Satellite
ET	Evapotranspiration
ETCCDMI	WMO/CLIVAR Expert Team on Climate Change Detection, Monitoring and Indices
FAO	Food Agriculture Organization
GCM	Global Climate Model/ General Circulation Model
GCOS	Global Climate Observing System
GES DISC	Goddard Earth Sciences Data and Information Services Center
GHGs	Greenhouse Gases
GLACE	Global Land-Atmosphere Coupling Experiment
GLCC	Global Land Cover Characterization
GPCP	Global Precipitation Climatology Project
GTS	Global Telecommunications Systems
H	Sensible Heat Flux

HadAM3	Hadley Centre climate model
IBIS	Integrated Biosphere Simulator
ITCZ	Inter-Tropical Convergence Zone
ICTP	International Centre of Theoretical Physics
IPF	Institute of Photogrammetry and Remote Sensing
LE	Latent Heat Flux
LS	Lesotho
LSM	Land Surface Model
MIT	Massachusetts Institute of Technology
MM4	Mesoscale Model version 4
MM5	Mesoscale Model version 5
MSE	Moist Static Energy per unit mass
MSLP	Mean Sea-Level Pressure
NCAR	National Center for Atmospheric Research
NCEP	National Center for Environmental Prediction
NE	Northeast
NHST	Null Hypothesis Significant Testing
NMC	USA National Meteorological Center
NOAA	National Ocean and Atmospheric Administration

OND	October November December
OISST	Optimized Interpolated SST
P-E	Precipitation to Evaporation
PBL	Planetary Boundary Layer
PRECIS	Providing Regional Climates for Impacts Studies
QBO	Quasi-Biennial Oscillation
RCM	Regional Climate Model
RegCM3	Regional Climate Model version 3
RSM	Regional Spectral Model
SAO	South Atlantic Ocean
SE	Southeast
SIO	South Indian Ocean
SOI	Southern Oscillation Index
SOM	Kohonen Self-Organised Mapping
SON	September October November
SST	Sea Surface Temperature
SSTA	Sea Surface Temperature Anomaly
SUBEX	SUB-grid EXplicit moisture scheme
SWI	Soil Water Index

SWIO	Southwest Indian Ocean
SWZ	Swaziland
TC	Tropical Cyclone
TTT	Tropical Temperate Trough
UK	United Kingdom
USA	United States of America
WMO	World Meteorological Organization
WRF	Weather Research and Forecasting
ZAB	Zaire Air Boundary

Acknowledgments

I would like to convey much gratitude to my supervisors Prof. Bruce Hewitson and Dr. Mark Tadross for their invaluable support and guidance throughout my PhD study.

My sincere thanks to Prof. Filippo Giorgi and Dr. Jeremy S. Pal who during my scientific visits to the International Centre of Theoretical Physics (ICTP) did magnificent jobs of contributing with brilliant ideas towards my modeling work with RegCM3 and the rest of the ICTP Science team for all the help and learning from them.

I would like to acknowledge and thank Phillip Mukwenha, Chris Jack, Igor Olivier and Jeremy Main for all the computer assistance they gave me at University of Cape Town (UCT).

I am grateful to the following for financial assistance throughout the period of this research: DAAD Third Scholarship, NRF and WRC.

I am most appreciative and indebted to my family, for instilling the thirst for knowledge and pushing me into taking up this opportunity.

Special mention should be made of Ruth Cerezo for taking time out to proof-read my thesis and make valuable comments.

Lastly but not least, I have also received invaluable support, suggestions and encouragement from friends and colleagues in CSAG and ICTP and my family especially my son Marshall Jr (6years now) who did not understand why Dad was ignoring him at times. Thank you all!

I dedicate this thesis to my Dad who could not live to see me graduate. MHSRIP!

Table of Contents

Abstract ..... **iii**

List of Figures ..... **v**

List of Tables ..... **xv**

List of Acroynms… ..... **xvii**

Acknowledgements ..... **xxiii**

Table of Contents ..... **xxv**

Chapter 1 Background **1**

1.1 Introduction 1

1.2 Need for the research…. 4

1.3 Aims and Objectives 7

1.4 Layout of thesis 8

Chapter 2 Literature Review **11**

2.1 Introduction 11

2.2 Climate Variability of Southern Africa 11

2.3 Soil Moisture Atmosphere Interactions 15

2.3.1 Feedback Mechanisms 15

2.3.2 Positive Feedback Mechanism 16

2.3.3 Negative Feedback Mechanism 20

2.4 Soil Moisture and Africa 22

2.5 Land Surface Models 25

2.6 Soil Moisture retention, initialization and seasonal predictability 26

2.7 Soil Moisture Sensitivity to Evapotranspiration 27

2.8 Soil Moisture and Hot Spots 28

2.9 Soil Moisture Dynamics and Uncertainties 29

2.10 Summary 31

Chapter 3 Data and Research Methods 33

3.1 Introduction 33

3.2 Data.....34

3.2.1 National Centers for Environmental Prediction/National Center for Atmospheric Research Reanalysis 2 Data.....34

3.2.2 Climate Prediction Center Merged Analysis of Precipitation 35

3.2.3 Climate Research Unit 0.5º Dataset 35

3.2.4 Global Precipitation Climate Project…….....36

3.2.5 Global Land Cover Characterization 36

3.2.5 Institute of Photogrammetry and Remote Sensing soil moisture data 37

3.3 Methodologies 38

3.3.1 Regional Climate Model 38

3.3.2 Experimental Set up.....40

3.3.3 Self-Organizing Mapping 42

3.3.4 Student's t Test 44

3.4 Other Soil Moisture Related Variables Calculated and Analysed 47

3.4.1 Cloud Liquid Water Path 47

3.4.2 Evaporative Fraction 47

3.5 Summary 48

Chapter 4 Summer Simulations 49

4.1 Introduction 49

4.2 Model Performance 50
4.2.1 Model Comparison to IPF Total Soil Moisture 50
4.2.2 Model Comparison to Total Precipitation 51
4.2.3 Model Comparison to Air Temperature 57
4.2.4 Model Comparison to 10m Wind Fields 60
4.2.5 Summary of Model's Performance…… 61
4.3 Spatial and Temporal Analysis of Model's Response to Soil Moisture Perturbations 62
4.3.1 Temporal Variation of Soil Moisture for dry versus wet seasons.....62
4.3.2 Spatio-temporal Analysis of Mean Precipitation for dry versus wet seasons.....64
4.3.3 Spatio-temporal Analysis of Mean Surface Temperature for dry versus wet seasons..68
4.3.4 Summary of spatio-temporal analysis of the dry versus wet seasons.....70
4.4 Sensitivity Analysis of the Driest and Wettest Season…….....71
4.4.1 Total Precipitation 71
4.4.2 Surface Temperature 77
4.4.3 Sensible Heat Flux 83
4.4.4 Latent Heat Flux 88
4.4.5 Incident Solar Radiation 90
4.4.6 Planetary Boundary Layer 95
4.5 Summary 102

Chapter 5 Synoptic Analysis and Mean January Responses 107
5.1 Introduction 107
5.2 Geopotential Heights 108
5.3 Moisture Fluxes 111
5.4 Vertical Analysis 115
5.4.1 Cloud Liquid Water Path 115

5.4.2 Atmospheric Analysis of Air Temperature 116
5.5 Mean January Climate Responses 118
5.5.1 Diurnal Cycles 118
5.5.2 Rain Days and Rainfall Intensity 122
5.6 Summary 127

Chapter 6 SOM Analysis of Synoptic Patterns in Summer Simulations 131
6.1 Introduction 131
6.2 Circulation Types 132
6.2.1 850 hPa Geopotential Heights 132
6.2.2 500 hPa Geopotential Heights 133
6.2.3 700 hPa Total Precipitable Water 135
6.3 Seasonal Evolution through the SOM Array 135
6.4 Frequency of Occurrence.....136
6.5 RegCM3 Simulations Mapping onto the Synoptic States 139
6.5.1 Planetary Boundary Layer Anomalies 139
6.5 Summary 141

Chapter 7 Sub-regional Analysis of Summer Simulations 147
7.1 Introduction 147
7.2 RegCM3 Top-layer Soil Moisture 147
7.3 Total Precipitation.....149
7.4 Surface and Air Temperatures 151
7.5 Heat Fluxes and Incident Solar Radiation 152
7.6 Planetary Boundary Layer 154
7.7 Evaporative Fraction 154

7.8 Moist Static Energy 158

7.9 Summary 161

Chapter 8 Conclusion 165

8.1 Overview and Summary 165

8.1.1 Introduction 165

8.1.2 Summer Climate Simulations 166

8.1.3 Synoptic Analysis and Mean January Climate Responses 170

8.1.4 SOM Analysis of Synoptic Patterns in Summer Climate.....172

8.1.5 Sub-regional Analysis of the Summer Climate Simulations 174

8.2 Caveats or Limitations 177

8.3 Recommendations for future work 184

8.4 Conclusion 186

References 187

Appendices 207

Appendix A: Model Validation……...207

Appendix B: SOM Analysis of Synoptic Patterns 211

Chapter 1

Background

1.1 Introduction

Soil moisture plays a fundamental role in the transfer of water and energy between the land surface and atmosphere particularly through the evapotranspiration process. This vital role within the hydrological cycle process is more important during the summer rainfall season over southern Africa as it has a major impact on the agricultural season (Tadross et al., 2010). Many meteorological, climatological, hydrological and/or agricultural applications require global or regional soil moisture data to be used for initialisation conditions of the soil moisture variables (Alfieri et al., 2008). These applications range from weather forecasts and seasonal climate predictions to models of global or regional climate, hydrology and crops or plant growth (Betts et al. 1996, Schär et al., 1999; Koster et al., 2004a, 2004b; Seneviratne et al., 2006a, 2006b, 2010; Alfieri et al., 2008; Tadross et al., 2010). Recently, the importance of soil moisture in the global climate system was highlighted by the Global Climate Observing System, GCOS[1] as an "Essential Climate Variable", ECV (World Meteorological Organization, WMO, 2010).

There are a limited number of studies on the role of soil moisture conditions on land-atmosphere interactions over southern Africa (Nicholson, 2001; Hulme et al., 2001; New et al., 2003; Cook et al., 2006; Mackellar, 2007; Mackellar et al., 2009). It is still unclear how antecedent soil moisture conditions may affect summer rainfall season over southern Africa. There is a gap in the understanding of the interactions of soil moisture with large-scale atmospheric circulations during the summer rainfall season. Different researchers have provided contrasting hypotheses on the existence of soil moisture feedback mechanisms over southern Africa. New et al. (2003) and Cook et al. (2006) have demonstrated the negative feedback phenomenon over the region. However, in some areas of the subcontinent a weak feedback which can be either positive or negative depending on geographical and climatological setting has been detected (Cook et al. 2006; Mackellar, 2007). Thus, explanation of the feedback processes between soil moisture and

[1] More information about the WMO publication and available data can be found at http://www.wmo.int/pages/prog/gcos/

subsequent summer season over southern Africa is further complicated. It remains unclear when and where soil moisture-atmosphere feedbacks are positive or negative over southern Africa.

Positive feedback mechanism occurs when soil moisture is reduced and leads to decreased precipitation. This mechanism has been confirmed over the United States (Eltahir and Pal, 1996; Eltahir, 1998; Pal and Eltahir, 2001, 2003) and over central Europe (Schär et al., 1999, Seneviratne et al., 2006a; Fisher et al., 2007; Jaeger, and Seneviratne, 2011). Decreased initial soil moisture leads to: (a) decreased latent heat fluxes (decreased evapotranspiration); (b) increased sensible heat fluxes (increased surface temperatures); (c) decreased total heat fluxes (d) increases in incident solar radiation along with decreased cloud cover (or no cloud type) and no or reduced precipitation. The converse would be true for increased soil moisture. However, these simplified one-dimensional explanations ignore the possibility of horizontal advection and changes in the atmospheric circulation. For instance, the above mentioned increased surface temperatures and sensible heat fluxes may lead to increased convection, drawing moisture from other regions and leading to an increase of both cloud cover (or rain producing clouds) and precipitation, resulting in a negative feedback (Seth and Giorgi, 1998). Such a different response to soil moisture indicates that drier soil moisture conditions might actually lead to increased precipitation via an increase in convective instability (Giorgi et al., 1996; Paegle et al., 1996; Seth and Giorgi, 1998).

The rainfall season characteristics such as onset and cessation of the rain season, rain days, rainfall intensity and probability of the occurrence of dry spells or droughts are a major concern to many stake holders (Matarira and Flocas, 1989, Matarira and Jury, 1992; Makarau and Jury 1997; Pal and Eltahir, 2001; Unganai and Mason, 2002; Usman et al., 2004; Tadross et al. 2005a, 2010). The dry spell information is required for tactical decision making while the drought information could be both tactical and strategic. In hydrology, consideration of rainfall amounts aid in assessing or predicting probable dryness to saturation level of soils, runoff, stream flow, water table and infiltration (Cheng et al., 2006). Whereas in agriculture, the decision making on planting, crop type and variety can be based on the soil moisture levels e.g. water logged soils will suit rice better than maize or probably planting of the drought resistant crops when below-average rainfall is predicted (Eltahir, 1998; Schär et al., 1999; Eltahir and Pal, 2001; Pal and Eltahir, 2002; R. Shulze, 2009 *pers. comm*.).

There are many regional forcing processes over the continent itself such as landuse change and the adjoining oceans which factor in on causing extreme dry or wet conditions (Lindesay, 1998; Nicholson, 2001). Seasonal predictability requires a solid understanding of the space-time characteristics of the major climatic processes of the region. There is also evidence that atmospheric variables such as seasonal 500hPa height patterns and 200hPa winds may be useful for enhancement in understanding of the upper atmosphere analysis (Torrance, 1981; Tyson, 1986). Land surface variables such as pre-season rainfall, soil moisture and vegetation may also affect coupled processes in a low frequency capacity similar to seasonal surface temperatures, yet so far studies of their effects over southern Africa are limited (Nicholson, 2001; Hulme et. al, 2001; New et al., 2003; Cook et al., 2006; Mackellar, 2007; Mackellar et al., 2009; Jack, 2012). These studies suggest that spring time soil moisture conditions have an effect on the next summer rainfall season. Yet so far, only a few studies have dealt with soil moisture-atmosphere interactions over southern Africa prompting the need for this investigation.

At daily time-scale, studies of climate extremes so far have been limited to South Africa, given the lack of sufficient data especially soil moisture for other Southern African countries (Tennant and Hewitson, 2002; Fauchereau et al., 2003; Tadross et al., 2005a ; New et al., 2006; WMO, 2011; Dorigo, 2011). Work to improve the understanding of the nature and characteristics of rainfall on an intra-seasonal time scale, particularly at the daily scale, is lacking in the region (Tennant and Hewitson, 2002). Tyson (1986) related rainfall over Southern Africa to variations in pressure and circulation patterns over the oceans surrounding Southern Africa. These studies revealed that distinct relationships exist between pressure anomalies and rainfall over the region (Mdoka, 2003). Besides the circulation patterns, moisture sinks and sources need to be understood or identified to enable further analysis of moisture transport (C. Jack, 2009 *pers comm*.). There is a need to look at large-scale dynamics such as circulation patterns and moisture trajectories to aid in the soil moisture-rainfall feedback mechanisms analysis. This suggests that the response might not only be a local phenomenon but an effect ensuing from a remote location.

Limited studies with contradictory findings done on soil moisture conditions over southern Africa (Hulme et. al, 2001;New et al., 2003; Cook et al., 2006; Mackellar, 2007), western Africa (Eltahir 1998; Nicholson, 2001; Findell & Eltahir, 2003; Moufouma-Okia & Rowell, 2009; Taylor et al., 2011) as well as the rest of the world (Delworth and Manabe, 1988a, 1988b;

Oglesby and Erickson 1989; Eltahir and Pal 1996; Findell and Eltahir 1997, Pal and Eltahir, 2002; Schär et al., 1999; Fisher et al., 2003; D'Odorico and Porporato 2004; Koster and Suarez 2004; Seneviratne et al., 2006a, 2006b, 2010; Fischer et al., 2007; Alfieri et al. 2008; Kohenegger, 2009, Mei and Wang, 2012) have motivated the pursuit of this research as the next section presents. An in-depth review of this previous research is presented in the next chapter.

1.2 Need for the research

Southern Africa's climate is highly variable as a result of its position, vastly variable topography and large land to ocean set up (Torrance, 1981).With the exception of Western Cape of South Africa, the region receives rainfall during austral summer (Buckle, 1996; Tyson and Preston-Whyte, 2000). Rainfall is the most important climatic parameter over the region as most countries are dependent on rain fed agriculture. Knowledge of the rainfall season, inter-seasonal dry spells or droughts, onset and length of growing season is very important especially among the communal farmers who have limited resources (Usman and Reason, 2004; Tadross et al. 2005a, 2010). The region is so vulnerable to climate variability and climate change related events with a spate of droughts, heat waves and floods which caused devastating landslides e.g. Mozambique and Durban 2007[2], fires, famine, diseases, human and economic losses (South African Weather Services, SAWS, 2011)[3]. Considering the vulnerability of southern Africa's community to climate, it is imperative to better understand factors that influence climate variability over southern Africa. Figure 1.1 shows the continental southern African countries that these issues relate to and the domain used in this study.

Despite the many studies that have looked at the impacts of climate variability and climate change, there are still few studies aimed at understanding the role of climate factors particularly how soil moisture conditions affect climate variability over the southern Africa region (Hulme et al., 2001; New et al., 2003; Cook et al., 2006; Mackellar, 2007). However, a great deal of work still needs to be carried out to further understand circumstances leading to positive or negative feedbacks occurrence between soil moisture and other climatic variables such as rainfall and temperature within southern Africa. There are several studies done over the northern hemisphere

[2] The Star newspaper online: www.iol.co.za, 2007.
[3] Weather related events and reports can be obtained at www.weathersa.co.za.

especially over United States of America (USA) and central Europe evaluating these feedbacks. Different researchers have revealed contrasting evidence supporting their theories. For example, Oglesby and Erickson (1989); Eltahir and Pal (1996); Findell and Eltahir (1997) established the existence of positive feedbacks whilst Giorgi et al. (1996); Seth and Giorgi (1998); Findell and Eltahir (2003b) and Cook et al. (2006) have shown the negative feedback mechanism. In western Africa, similar experiments have been done with more or less contrasting patterns being identified (Eltahir 1998; Entekhabi et al. 1991; Findell and Eltahir 2003b; Kunstmann and Jung, 2003). However, some of the experiments carried out over southern Africa do not reveal the clear-cut patterns found over the northern hemisphere areas. Most of the current findings have had contrasting conclusions about the role of antecedent soil moisture conditions on climate variability over southern Africa (New et al., 2003; Cook et al., 2006; Mackellar, 2007). More detailed review on the earlier research and findings will be discussed in chapter 2.

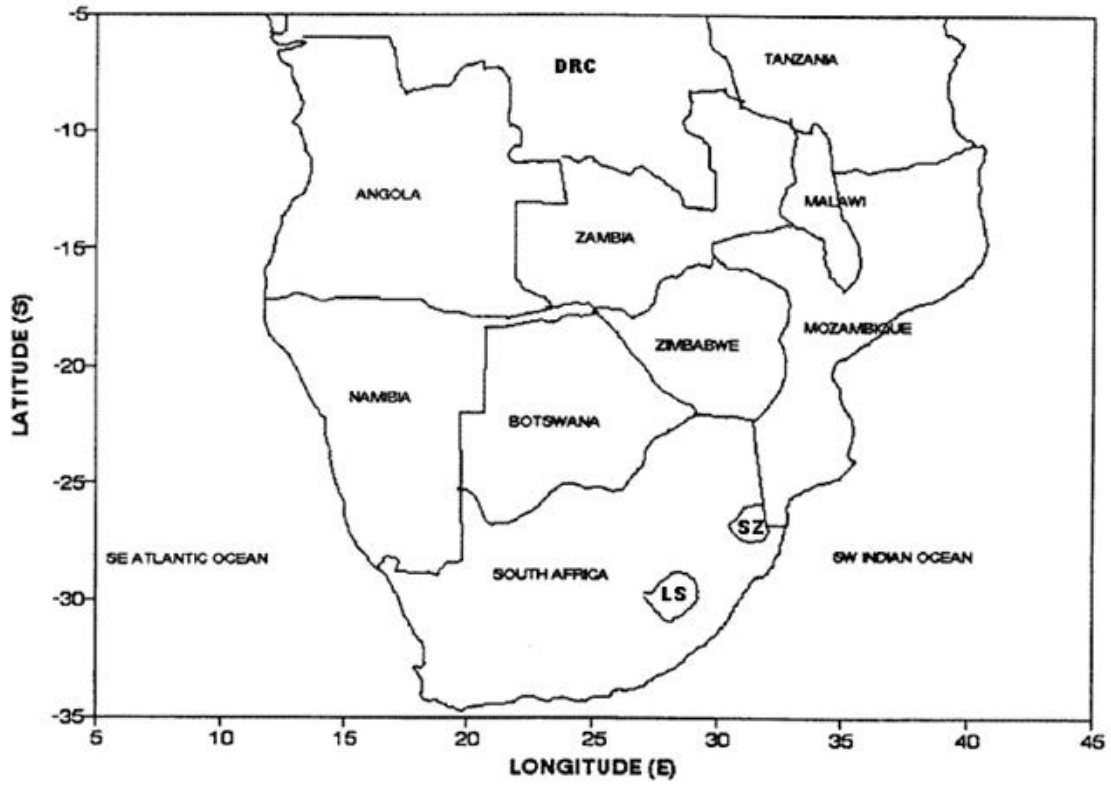

Figure 1.1 Map of the southern African countries that constitute the domain used in this study. LS, SZ and DRC respectively stand for Lesotho, Swaziland and Democratic Republic of Congo.

Due to limited soil moisture observation data over the region (WMO, 2010; Dorigo, 2011) most of the research taking place is based on simulated climate using global circulation models (GCMs) and regional climate models, RCMs (New et al., 2003; Cook et al., 2006 and Mackellar, 2007). The hydrological cycle of climate models depends on its configuration, which is important for accurately simulating the observed frequency or intensity and therefore changes associated to the soil moisture-atmosphere attributes. Little is known about the implications of soil moisture conditions on the characteristics of rainfall and resulting effects on rain-days, intensity as well as spatio-temporal distribution. Thus, a more rigorous study based on a better representation of the real climatology of southern Africa is proposed. It requires clear understanding of the model's physics and sensitivity experiments of the model. However, recent studies within the international programme Coordinated Regional Downscaling Experiment (CORDEX[4]) (Giorgi et al. 2009) have shown that neither of the various surface physics parameterizations results in a better or superior model performance (Diro et al., 2012).

In order to resolve the variability of a model's atmosphere to variable soil moisture conditions, experiments should be performed for various climate scenarios which range from extreme dry through normal to wet years as well as El Niño and La Niña years. Most experiments carried out have focussed only on extreme dry or wet events (Makarau and Jury, 1997; Pal and Eltahir, 1998, Unganai and Mason, 2002; New et al., 2003; Cook et al. 2006; Mackellar, 2007; Mackellar et al., 2009). This means that there are still some unresolved gaps in the soil moisture and climate variability studies.

Soil moisture retention or memory experiments are useful not only for assessing a model's response but also for forecasting purposes i.e. how an initial soil moisture perturbation persists and affects rainfall during a seasonal forecast (Koster and Suarez, 2001; Seneviratne et al., 2006b, 2010). Knowledge of antecedent soil moisture and how it couples to the overlying atmosphere could help improve the probabilistic forecasting of rainfall at seasonal to interannual scales. Other predictors such as vegetation, sea surface temperatures (SSTs), aerosols or knowledge of moisture trajectories may offer similar improvements in forecasting efforts (Koster et. al., 2004b; Tadross et al., 2010; Jack 2013).

[4] The official WCRP CORDEX page; http://wcrp.ipsl.jussieu.fr/SF_RCD_CORDEX.html

In light of the above, there is a need for further research on soil moisture-atmosphere interactions and an enhancement of the understanding of its overall role in climate variability over southern Africa. From herein, the following objectives were derived towards seeking to resolve some of the issues mentioned.

1.3 Aims and Objectives

Given the above discussion, this research aims to understand the interactions of soil moisture with the large-scale atmospheric circulation, during the summer rainfall season; identify regions where characteristics of early summer climate may be influenced by soil moisture; understand the implications of soil moisture conditions on frequency and intensity of rainfall. Thus, the research is focussed on soil moisture conditions and atmosphere interactions. The research could be relevant to both seasonal forecasting and long term climate or environmental change.

The study will focus on the soil moisture atmosphere interactions over southern Africa simulated using the International Centre for Theoretical Physics (ICTP), Regional Climate Model version 3,RegCM3 (Pal et al. 2007). It will seek to use these climate modelling simulations to assess the adjustment of the atmosphere and the surface state to enforced initial soil moisture anomalies. The study will also analyse the feedback mechanisms, soil moisture retention, on both inter-annual and seasonal timescales and comparison of climate model parameters with available observations or re-analysis data. An analysis of simulations focussing on aspects of boundary layer heights, compared to observations, can aid in evaluating the importance of this soil moisture-atmosphere mechanism relative to all the other forcings (local and global) that can also affect summer climate. Large-scale dynamics such as circulation patterns and moisture trajectories (Jack, 2013) allow a clearer understanding of where and when the feedbacks are vital. The research also seeks to look at the effects of anomalous soil moisture conditions on the important rainfall characteristics related to agriculture and hydrology, e.g. raindays and intensity.

Therefore, the specific research objectives for this study are:

1. To understand how antecedent soil moisture conditions influence the summer climate variability.
2. To determine if soil moisture plays a dominant role and which characteristics of rainfall get altered e.g. frequency and/or intensity.
3. To seek out the large-scale atmospheric forcings under which the regional climate significantly responds to perturbations in soil moisture.
4. To identify specific areas for which soil moisture has a substantial impact on surface climate variables.

1.4 Layout of thesis

Chapter 1 provides a general introduction to the soil moisture-atmosphere interactions and basic knowledge about southern Africa climate research focus. The need for this study is then discussed as well as its overall aims and objectives. A more detailed literature review of the work that has been done on soil moisture-atmosphere interactions across the globe is discussed in **chapter 2**. As a holistic approach, the chapter seeks to enlighten beyond aspects relating to this study on the fundamental role of soil moisture. **Chapter 3** describes the data and methodology employed in this study. Hypotheses, innovations and experimental designs are addressed. Results are then presented in **chapter 4** for the summer climate simulations and an evaluation of the sensitivity of the experiments to soil moisture is discussed. This chapter addresses the first and third objectives with discussions that relates to previous studies incorporated. Whilst still in line with the first objective, the second objective is also the focus of **Chapter 5** which presents a synoptic analysis of the summer climate simulations and diurnal variations as well as rain days and intensity using a close-up look at January month whilst addressing the second objective.

Chapter 6 deals with self-organising map characterization of synoptic patterns in the summer climate simulations. This chapter also addresses the third objective which seeks out large-scale atmospheric forcings under which the regional climate significantly responds to perturbations in soil moisture. **Chapter 7** then provides a sub-regional analysis of the summer climate simulations for the selected zones within southern Africa with emphasis on how soil moisture

perturbations affect those regions as the chosen surface climate variables' response depict (objective 4). This chapter substantiates some of the earlier findings from previous chapters as it incorporates most of the thesis objectives in the discussion. **Chapter 8** gives an overview, discussion of results and conclusion in which a synthesis of the findings is presented. The caveats including proposals for future research are also discussed.

Chapter 2

Literature Review

2.1 Introduction

Soil moisture is a key component of land surface-atmosphere interactions, which governs the energy and water exchanges within the boundary layer. Thus, the state of soil moisture is regulated by rainfall, temperature and potential evaporation amongst other parameters. Numerical models, such as Global Circulation Models (GCMs), (e.g. Shukla and Mintz, 1982; Paegle, 1996) and Regional Climate Models (RCMs), (e.g. New et al., 2003; Cook et al., 2006 and Mackellar, 2007) have been used over the years leading to conclusions discussed in the subsequent sections. Soil moisture atmosphere interactions research resulted in contradictory conclusions and various theories (Delworth & Manabe, 1993; Giorgi et al., 1996; Pal & Eltahir, 1996; Seth & Giorgi, 1997; Eltahir, 1998; New et al., 2003; Cook et al., 2006; Seneviratne et al., 2010; Jaeger & Seneviratne, 2011).

Feedback processes between soil moisture and the atmosphere are of a major importance for our climate system. Ecosystems are stabilised by a series of feedbacks driven by men, animals, soil, vegetation, aerosols and climate (Petersen et al. 2009). Land-atmosphere interaction is particularly important to adequately model these features in order to have a complete understanding of the climate variability in the region. The role of soil moisture-atmosphere interactions in the climate variability over southern Africa has become essential (Nicholson, 2001; Hulme et. al, 2001; New et al., 2003; Cook et al., 2006 and Mackellar, 2007). However, it will be necessary to briefly discuss findings of forcings affecting climate variability. Although the next section is not exhaustive of factors affecting the climate of the region besides soil moisture, an attempt will be made to give an insight of the major factors.

2.2 Climate Variability of Southern Africa

Southern Africa's climate is highly variable making it prone to many climate extremes. There is a persistence of interannual mid-season dry spells or droughts which highly impact on

agriculture during the summer rainfall season (Matarira and Jury, 1992; Makarau 1995; Tenant and Hewitson, 2002; Usman and Reason, 2004). The main rain-bearing systems affect a major part of southern Africa during summer (Torrance, 1981; Lindesay, 1998; Washington and Todd, 1998; Tyson and Preston-Whyte, 2000). Convection is the dominant rain-inducing process in the region, accounting for almost 90% of Zimbabwe's total rainfall (Unganai, 2002) and with similar traits in most parts of the region (Tyson and Preston-Whyte, 2000). Floods and droughts have repeatedly affected parts of the region since the last decade of the 20th century.

Some interannual and intraseasonal aspects of the rainfall season such as onset and end of the rainfall season, length of the growing season, wet or dry spell durations, droughts and floods, ENSO, SSTs and climatic trends have been given widespread consideration. Many studies have been done seeking to understand and explain the meteorological conditions, feedback mechanisms behind these aspects as well as the prediction processes (Torrance, 1981; Buckle, 1996; Lindesay, 1998; Tyson and Preston-Whyte, 2000; Nicholson, 2001; Hulme et al., 2001; Usman and Reason, 2004; New et al., 2006; Tadross et al., 2005a, 2010). Due to the variety in the physical explanation of the occurrence of these events one has to assess all the conditions from large scale circulation features of the atmosphere to synoptic and local forcings (Entekhabi et al., 1991).

Several studies explain the influence and contribution of phenomena such as El Nino Southern Oscillation (ENSO), Indian Ocean Dipoles, Sea Surface Temperatures (SSTs) in adjacent Indian and Atlantic oceans and Quasi-Biennial Oscillation to the occurrence of these events over southern Africa (Nicholson, 1986; Ropelewski and Halpert, 1987; Matarira, 1990a, 1990b; Rocha, 1992; Ogallo et al., 1993; Jury and Pathack, 1993; Mason et al., 1994; Makarau, 1995; Makarau and Jury, 1997; Rocha and Simmonds, 1997a, 1997b; Lindesay, 1998; Landman and Graham, 1999; Goddard and Graham, 1999; Reason and Mulenga, 1999; Richard et al., 2001; Tyson and Preston-Whyte, 2000; Goddard et al., 2001; Landman et al., 2001; Mason and Goddard, 2001; Richard et al., 2001; Unganai and Mason, 2001; Vigaud et al., 2009; Reason et al., 2003; Landman and Beraki, 2010). These do affect some of the main rain producing systems, that is; the position of the Inter-Tropical Convergence Zone, Angola Low, Tropical Jet Streams, and the paths of Tropical Cyclones or blocking high pressure belts.

Although not fully exploratory, a few studies on the findings of the effects of some of the systems particularly over contiguous southern Africa will be discussed hereafter. The latitudinal position of southern Africa results in the region being influenced by tropical, sub-tropical and midlatitude anticyclones and wind systems. As the near-equatorial trough migrates with the seasons, the Inter-Tropical Convergence Zone (ITCZ) lies south of the equator in austral summer and north of the equator in winter (Figure 2.1 a, b). The ITCZ in southern Africa is neither spatially continuous nor aligned east-west, particularly in summer (Figure 2.1a) when the major wind convergence over the eastern parts of the region is displaced southward as far as 20°S (Torrance, 1981; Buckle, 1996; Lindesay, 1998; Tyson and Preston-Whyte, 2000). Northeasterly airflow from the East African monsoon, deep tropical easterlies from the Indian Ocean and westerly airflow from the Atlantic Ocean converge over the eastern subcontinent along the ITCZ (Figure 2.1a). Over the western parts of the region, the main rain producing airstreams converge along the Congo (formerly Zaire) Air Boundary (ZAB) between Atlantic and Indian Ocean fluctuating in position from day to day and mark a region in which low pressure systems tend to form preferentially.

The ITCZ (and ZAB) is a region of pronounced convective activity and constitutes a region of major tropical latent heat release over southern Africa in summer (Torrance, 1981; Buckle, 1996; Lindesay, 1998; Tyson and Preston-Whyte, 2000). Just as diabatic heating in the tropics is influenced in part by moving towards the equator of midlatitude disturbances, tropical disturbances may exert important influences on midlatitude circulations (Tyson and Preston-Whyte, 2000). This is certainly the case over southern Africa, where the interaction between tropical and temperate disturbances (TTTs) has important consequences for the weather of the region (Washington and Todd, 1998; Tyson and Preston-Whyte, 2000; Usman and Reason, 2004).

Another important feature of southern Africa's rainfall season is the middle level (500hPa) anticyclone, which tends to establish a centre around Botswana (Torrance, 1981). This has a tendency of being a semi-permanent feature fluctuating only in strength and orientation. Subsidence from 500hPa level prevents the formation of cloud in the middle troposphere and fine weather prevails. Pressure falls more rapidly with height in the warm air and thus strengthens the upper anticyclone. Under this circulation pattern, rainfall over the southwestern

parts of the regions is drastically suppressed (Torrance, 1981; Tyson and Preston-Whyte, 2000). Deviations from the mean 500hPa level conditions are used to separate dry and wet years (Torrance, 1981; Mdoka, 2003). Tyson (1986) inspected the differences in annual geopotential heights at 850hPa and 500hPa levels at 16 stations over southern Africa and adjacent oceans and found that the 500hPa circulation field was more important than its near-surface counterpart as a control of annual rainfall. Figure 2.2 shows the mean 500hPa geopotential height using NCEP/NCAR reanalysis 2 data for the period 1979-2000. A three-month seasonal (DJF) deviation from the 500hPa geopotential height mean was used to determine circulation anomalies associated with wet and dry conditions within the last 2 decades of the twentieth century.

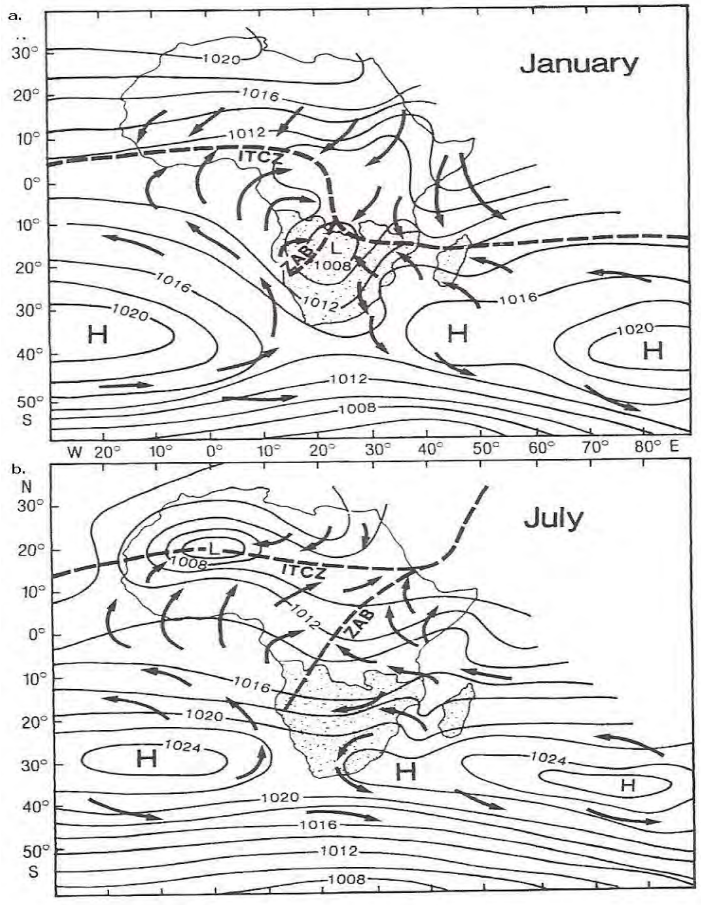

Figure 2.1 Schematic illustration of the mean winds convergence and positions of the Inter-Tropical Convergence Zone (ITCZ) and Congo (formerly Zaire) Air Boundary (ZAB) over Africa and adjacent oceans in (a) January and (b) July (adapted from Lindesay, 1998).

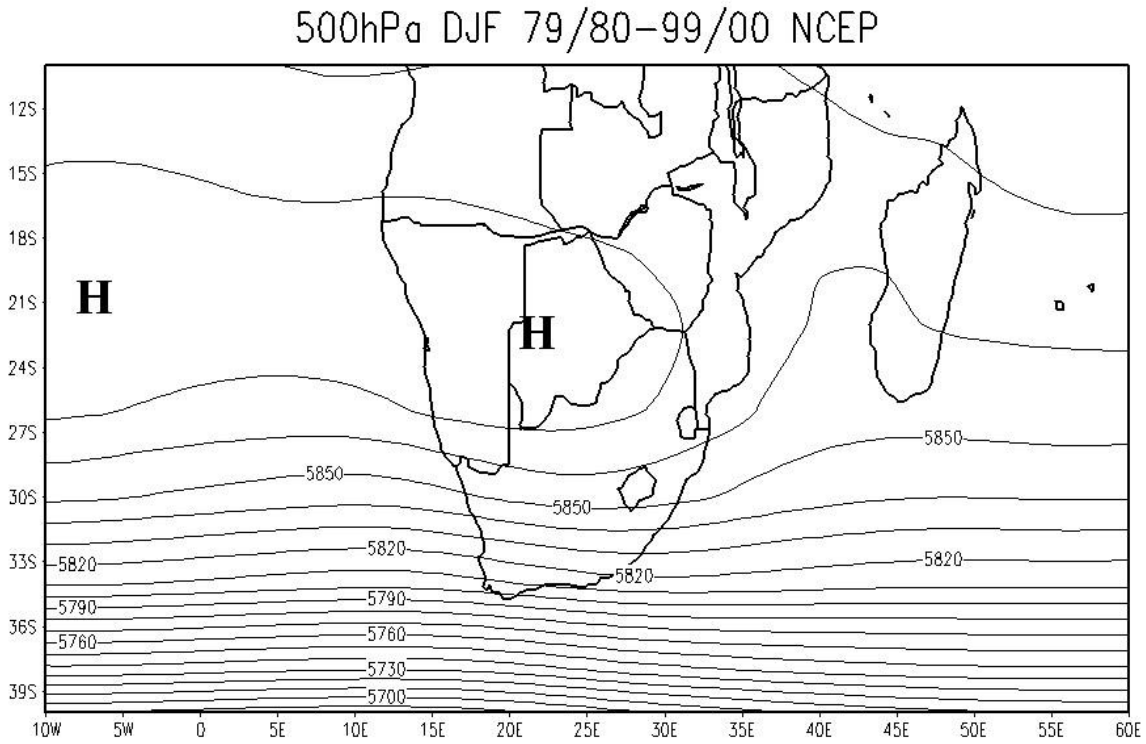

Figure 2.2 Mean 500hPa geopotential heights using NCEP/NCAR reanalysis 2 data for the period (1979-2000). An anticyclone stretching from the Atlantic into the sub-continent is shown.

2.3 Soil Moisture Atmosphere Interactions

2.3.1 Feedback Mechanisms

Feedback mechanisms have made interest in soil moisture-atmosphere interactions grow. Several key pathways and mechanisms through which antecedent soil moisture conditions affect subsequent rainfall have been investigated using GCMs and RCMs (Delworth and Manabe, 1993; Pal and Eltahir, 1996; Eltahir, 1998; Schär et al., 1999; Pal and Eltahir, 2001, Seneviratne et al., 2006a, 2006b, 2010; Rowell and Jones, 2006; Teuling et al., 2006; Kim and Hong, 2007; Vidale et al., 2007; Jaeger and Seneviratne, 2011). Although there are limited documented studies over Southern Africa (New et al., 2003; Cook et al., 2006; Mackellar, 2007), numerous studies over the rest of the world have shown that persistence in soil moisture is translated into persistence in near-surface humidity, temperature, and precipitation (Delworth and Manabe, 1993; Eltahir, 1998; Zheng and Eltahir, 1998; Schär et al., 1999; Findell and Eltahir 1999; Pal and Eltahir, 2001; Wu and Dickinson, 2004; Seneviratne et al., 2006a, 2006b, 2010; Rowell and

Jones, 2006; Teuling et al., 2006; Kim and Hong, 2007; Vidale et al. 2007; Jaeger and Seneviratne, 2011). Various studies show inconsistent feedback pathways or mechanisms (positive or negative) to soil moisture-atmosphere interactions over the same areas of analysis.

2.3.2 Positive Feedback Mechanism

Most of the earliest studies on soil moisture and atmosphere interactions were limited to the summer over North America using a wide range of GCMs (Kim and Hong, 2007). Atlas et al. (1993) demonstrated that anomalous dry soil moisture results in a greater reduction of precipitation and a significant rise in the surface temperature over the Great Plains. Using a GCM, Beljaars at al. (1996) investigated the 1993 United States of America (USA) summer floods for anomalous rainfall and demonstrated major improvements in simulated precipitation when wet initial soil moisture was prescribed. Models were also utilized to analyse regional soil moisture anomalies over Europe (Rowntree and Bolton, 1983) and the global sensitivity to soil moisture conditions (Yeh et al., 1984). Both experiments demonstrated that a positive soil moisture-rainfall feedback exists when above-normal soil moisture increases the chances of subsequent precipitation whilst the reverse could occur for dry soil moisture conditions. Most of the GCMs studies suggested a positive response between the soil moisture and the precipitation or temperature.

Earlier in 1982, Shukla and Mintz studied the response of a GCM to prescribed sea surface temperatures and soil moisture conditions across the globe. The study detected strong sensitivity of the precipitation and temperature responses with respect to evaporation. Thereafter, Mintz (1984) investigated the summer moisture budget over the USA to demonstrate the important role of local evaporation and also confirmed that a coupling exists between evaporation and precipitation, in the sense that precipitation increases over land when evaporation increases. The author suggested that if surface evaporation moistens the boundary layer it can stimulate convective instability and rising air masses, leading to condensation of moisture advected from the ocean and that evaporated from the land. This implies a positive feedback from the recirculation of precipitation through the soil moisture sink, which may lead to prolonged persistence of anomalous wet spells. Such persistence was also obtained by Oglesby (1991) from

model simulations in which lagged correlations were found at the 700hPa level over the Midwestern USA between spring and summer as well as from a correlation of spring precipitation anomalies and summer temperature anomalies (Betts et al. 1996). Numerous follow up studies using mostly RCMs were undertaken over North America and Europe (Pal and Eltahir, 1996; Eltahir, 1998; Schär et al., 1999; Pal and Eltahir, 2001, 2003; Seneviratne et al., 2006a; Hohenegger et al., 2009; Seneviratne et al., 2010; Jaeger and Seneviratne, 2011).

Eltahir (1998) describes the physical mechanisms and processes resulting in the positive feedback between initial soil moisture and future rainfall. The author proposes that anomalously high soil moisture conditions yield an increase in moist static energy (MSE) per unit mass of the planetary boundary layer (PBL) air and hence more rainfall in convective regimes. The mechanisms responsible for the feedback are directly linked to the surface energy budget. An increase in evaporation at the surface leads to reduced sensible heat flux, which reduces PBL temperature and MSE (Pal and Eltahir, 2001). However, this effect tends to be outweighed by the increase in MSE due to increased latent heat flux. Whereas, decreases in sensible heat flux reduce the depth of the PBL, thus MSE per unit mass within the PBL increases (Eltahir, 1998; Pal and Eltahir, 2001). Thus, Eltahir (1998) concluded that high soil moisture values induce a decrease in the albedo and the Bowen ratio, β thus favouring energy inflow from the soil surface and convective instability, hence a positive feedback between soil moisture and the triggering of convective rain.

The positive feedback mechanism findings were in agreement with Schär et al., (1999) in RCM experiments conducted for July 1990 and 1993 to study the sensitivity of the summertime European precipitation climate. However, in order to isolate the physical mechanisms underlying the soil moisture-precipitation feedback, Schär et al. (1999) recommends a detailed analysis that includes an investigation of the mean diurnal cycle throughout the integration period be performed. Lin et al. (2000) proposes that the diurnal cycle is one of the prominent cycles in the water and energy exchanges within the climate system and can be considered to be an ideal test-bed for GCMs and RCMs as well as their parameterisations. Feedbacks between cloud and radiative processes are key factors in determining the sensitivity of soil moisture-precipitation interactions. Careful consideration is required during the parameterization of these processes in

model simulations, especially the strength of their simulated feedback mechanism (Schär et al., 1999). Chen and Avissar (1994) evaluated the impact of soil moisture on the timing of cloud formation and the intensity and distribution of the resulting precipitation. The research demonstrates that land surface moisture discontinuities enhance shallow convective precipitation and seem to play an important role in a relatively dry atmosphere.

Jaeger and Seneviratne, (2011), concur with the positive feedback mechanism during their study of the European summer climate particularly for extreme years. The RCM experiments show that soil moisture-climate interactions have important effects on temperature extremes and slightly on precipitation extremes. Using the heat fluxes, extreme minimum (plant wilting point) and maximum (field capacity) soil moisture value experiments within the RCM shows that an increase in soil moisture leads to an increase in latent, LE (also in the evaporative fraction, EF) and a decrease in sensible (H) heat flux (and therefore also in the β). Similar to Eltahir, (1998), Schär et al., (1999) and Hohenegger et al., (2009) this anomalous positive soil moisture causes a shallower, moister and colder PBL as indicated by the decreased air temperature. This also leads to decrease in net short wave radiation whilst net long wave radiation increases as total cloud cover increase resulting in an increase in precipitation (Jaeger and Seneviratne, 2011). A decrease in soil moisture has the opposite effect. However, the experiments exhibit no clear relationship for the net radiation. This is contrary to the findings by Eltahir, (1998), Shukla (1999) and Schär et al., (1999) which shows symmetric relation with enhanced net radiation under anomalous wet soil moisture conditions and vice versa.

Earlier findings (Eltahir and Pal, 1996; Findell and Eltahir, 1997) supporting the existence of a positive feedback between soil moisture and subsequent precipitation have been backed by work from Koster and Suarez (2001), D'Odorico and Porporato (2004) and Alfieri et al. (2008). Such a positive dependence has been attributed to either autocorrelation of precipitation due to the persistence of large-scale forcings and the consequent occurrence of (stratiform) events longer than one day, or to the actual existence of an effective feedback between soil moisture and subsequent precipitation. However, Virtebo (1996) emphasises the importance of surface sensible heat flux upstream of the Upper Mississippi Basin for affecting convective activity through the destabilization of the vertical atmospheric thermodynamic profiles. The likelihood

for this feedback has been shown to be higher in the warm season due to the stronger coupling between land surface and the atmosphere as well as the favourable conditions for the formation of convective systems or regimes (Pal and Eltahir, 2003; Koster et al. 2003; Koster and Suarez 2004; Jaeger and Seneviratne, 2011).

Dry initial soil moisture conditions operate in the opposite of the above proposed mechanism, but with a stronger response associated with negative soil moisture anomalies (Eltahir and Pal, 1996; Pal and Eltahir, 2001; Kim and Hong, 2007; Seneviratne et al., 2010; Jaeger and Seneviratne, 2011). Therefore, it contributes towards enhancing the severity and persistence of droughts and floods. These findings were supported by a study over Western Africa in which Zheng and Eltahir (1998) pointed to the crucial role of radiative processes in the soil moisture-rainfall feedback. Whilst in Southern Africa some of the related studies focussing on boundary layer processes and causal mechanisms particularly rainfall characteristics near the surface were done by Matarira (1990a, 1990b); Matarira and Jury (1992) and Mackellar (2007).

The record breaking 2003 European summer heat wave was explored for the role of land surface-related processes and feedbacks using a regional climate model (Fischer et al., 2007). The investigation focussed on the contribution of soil moisture anomalies and their interactions with the atmosphere through latent and sensible heat fluxes. Sensitivity experiments were performed by perturbing spring soil moisture in order to determine its influence on the formation of the heat wave. Fischer et al. (2007) experiments of the hottest phase were realistically simulated despite the absence of an anomaly in total surface net radiation indicating the important role of partitioning of net radiation into latent and sensible heat fluxes, which to a large extent is controlled by soil moisture. Jaeger and Seneviratne, (2011) concur with these findings. Thus, lack of soil moisture strongly reduced latent cooling and thereby amplified the surface temperature anomalies. Experiments with perturbed spring soil moisture showed that without soil moisture anomalies the summer heat anomalies could have been reduced significantly in some regions. Drought conditions were revealed to influence the tropospheric circulation by producing a surface heat low and enhanced ridging in the mid-troposphere. This suggests a positive feedback mechanism between soil moisture and temperature. The surface temperature response to such circulation anomalies is amplified by a positive feedback due to suppressed

evapotranspiration owing to the lack of soil moisture (Eltahir and Pal, 1996; Eltahir, 1998; Pal and Eltahir, 2003; Seneviratne et al., 2006a, 2006b, 2010 and Jaeger & Seneviratne, 2011).

The impact of initial soil moisture on the East Asian monsoonal circulation was investigated by Kim and Hong (2007) using the National Center for Environmental Prediction (NCEP) Regional Spectral Model (RSM). Regional climate responses due to the soil moisture anomalies revealed a weak positive feedback to simulated precipitation. Kim and Hong,(2007) state that the changes in precipitation due to the initial soil moisture were geographically different in East Asia, whereas the sensitivity of precipitation was homogeneous in response to the initial soil moisture anomalies in North America (Atlas et al., 1993; Beljaars et al., 1996; Giorgi et al., 1996; Seth and Giorgi, 1998; Pal and Eltahir, 2001). The study also reveals that the soil moisture anomalies in the East Asian region have a conflicting impact on local feedback and dynamic forcing. This was cited as one of the reasons why the dynamical seasonal prediction skill was relatively low over this region and estimates of the limits of the impact of internal forcing by soil moisture can be provided through these sensitivity experiments (Kim and Hong, 2007).

2.3.3 Negative feedback mechanism

On the contrary, high soil moisture values can be associated with surface cooling and the possible stabilization of the planetary boundary layer resulting in subsidence and adiabatic heating (Seth and Giorgi, 1997; Cook et al., 2006; Grimm et al., 2007). This will prevent the triggering of convective rainfall. Similar surface feedbacks may develop due to the drying of the surface soil and the associated rise in its albedo (Idso et al., 1975). A similar phenomenon referred to as Charney bio-geophysical hypothesis and its variations have strongly influenced the treatment or explanation of drought in the literature (Charney et al., 1977; Entekhabi et al., 1991). Zhang and Dong's (2009) analysis of soil moisture influence on summertime air temperature over East Asia revealed that significant negative feedbacks appear over the transition zones between northern China and Mongolia.

Giorgi et al. (1996) also highlighted the discordant conclusions in the literature surrounding the significance of local processes in the enhancement or maintenance of droughts or flood conditions especially those primarily associated with surface evaporation and sensible heat flux.

According to Giorgi et al. (1996), surface sensible and latent heat flux have two opposite effects on summer convection:

1. Relatively wet soil conditions produce an increase in evaporation, which provides an additional moisture source for convective storm systems. This leads to an increase in precipitation and, for the drought and flood periods would provide a positive feedback mechanism capable of reinforcing the conditions. Or,
2. Relatively dry soils induce a decrease in evaporation and an increase in sensible heat flux which provides a source of buoyant energy that can enhance convection and deepen cyclonic systems. If sufficient atmospheric moisture is available, this process would increase precipitation, thereby providing a negative feedback that would alleviate the flood and drought conditions.

Using RCM RegCM2, Giorgi et al., (1996) showed that the USA 1988 drought and 1993 floods were due to anomalies in the large-scale circulations and that the local effects associated with surface evaporation played a minor role in maintaining and reinforcing the conditions. Sensitivity experiments of perturbing the soil moisture over USA resulted in a negative feedback mechanism over the Upper Mississippi basin. This negative feedback response was supported by Paegle et al., (1996) who used a limited area model nested within the National Meteorological Center (NMC) global model to study the effect of surface evaporation on precipitation over the Mississippi basin for July 1993.

Using RegCM3 and observed data, Grimm et al., (2007) explored the role of antecedent spring conditions and peak summer rainfall over eastern Brazil and through a surface-atmosphere feedback hypothesis proposed that reduced (enhanced) soil moisture in spring might produce the observed circulation as well as enhanced (reduced) precipitation anomalies in the peak summer monsoon season. Antecedent wet conditions in spring lead to opposite anomalies. The low response of monsoon rainfall anomalies in central-east Brazil during the austral summer was partially ascribed to the fact that the models do not well reproduce the topographical features and the land-atmosphere interaction that are important for the variability in that region (Grimm et al., 2007).

2.4 Soil moisture and Africa

Studies over Africa have often suggested contradictory feedback interactions as highlighted in other parts of the world. New et al. (2003) and Cook et al. (2006) have demonstrated the negative feedback phenomenon over southern Africa. Surface cooling associated with anomalously wet soil moisture conditions can result in large-scale subsidence and anomalous anticyclonic circulation which inhibits large-scale moisture convergence. However, in some areas over southern Africa a weak feedback which can be either positive or negative depending on geographical and climatological setting has been detected (Cook et al. 2006; Mackellar, 2007). The outcome also depends on the net energy contributions to the atmosphere thus making it even more difficult to explain the feedback processes between soil moisture and subsequent rainfall occurrence.

Mackellar (2007) investigated the response of southern Africa's summer climate to changes in land surface conditions using the non-hydrostatic Pennsylvania State University – National Center for Atmospheric Research's (NCAR) Mesoscale Model version 5 (MM5). The study evaluated the sensitivity of the RCM to initial soil moisture and consequent hydrological feedbacks by employing a perturbation in soil moisture of a magnitude and spatial variability that is within the bounds of uncertainty in soil moisture initialisation over southern Africa. Mackellar's (2007) findings over the region showed that latent heat fluxes in subsequent months are significantly affected in certain regions though there is little effect on sensible heat flux and near surface temperature as well as no noticeable impact on regional circulation or precipitation. Mackellar (2007) implied that the soil moisture–rainfall coupling in the model was weak. Therefore, the persistence of initial soil moisture anomaly and associated impacts on climate were based on location and time of initialization with a weak soil moisture anomaly memory of one to two months within the simulations. However, this approach evaluated all aspects in terms of pattern correlations i.e. how does the spatial pattern of the anomalies persist in time compared to the initial spatial pattern of soil moisture anomalies. Hence the surface variables show the highest correlations with atmospheric variables but only weakly correlated within the highly variable atmosphere. This does not clearly bring out the effect of the anomalies in space and time. Further analysis using a more robust approach can aid in understanding impacts on climate of the surface and atmospheric variables.

Williams et al. (2011) examined the influence of land cover on modelled rainfall and daily rainfall extremes over southern Africa using a GCM and an RCM. The study suggested that there is a strong land surface-atmosphere mechanism that exists in PRECIS model which is based on vegetation and directly modulates rainfall. In one of the experiments, the whole of southern Africa was turned into a desert leading to a decrease in the model's rainfall due to absence of vegetation thereby increasing the surface temperature and reducing the available moisture. This leads to decreased evaporation and vertical uplift is dampened. The study also showed the near-surface pressure and that associated anticyclonic flow was enhanced. Williams et al., (2011) strongly supported their findings by noting that the fact that both GCM and RCM results were similar therefore the results could not be due to biases within the RCM lateral boundary data and the precipitation changes from localised vegetation changes are not being driven by large-scale atmospheric forcings from the GCM but rather from small-scale influences. Although this current study does not use GCMs, this insight could aid in explaining some of the caveat or limitation when trying to determine if the internal variability (Giorgi and Bi, 2000; Kgatuke et al. 2008, Crẽtat et al. 2011) of the model is a major concern or not.

Over West Africa, Zheng and Eltahir (1998) developed a numerical model of the region's monsoons to investigate the hypothesis proposed by Eltahir (1998) which describes a soil moisture-rainfall feedback mechanism that was explained earlier (section 1.1). Some of the dominant pathways of the feedback were identified including the crucial importance of energy processes. The magnitude of rainfall anomalies depended on the magnitude of soil moisture anomalies and the details of the parameterizations. The results of the numerical experiments supported the proposed hypothesis (Eltahir, 1998) and highlight the importance of the radiative and dynamical feedbacks in regulating the rainfall anomalies that result from the soil moisture anomalies (Zheng and Eltahir, 1998). Taylor (2000) also investigated soil moisture-precipitation feedbacks in the Sahel and found a positive feedback between rainfall and soil moisture at scales of around 10-15km.

Earlier study by Walker and Rowntree (1977) found that the dryness of the surface in West Africa strongly influenced the simulated regional rainfall and that soil moisture anomalies

contributed to the persistence of drought. Kunstmann and Jung (2003) investigated the effects of agriculture growth in West Africa on precipitation applying MM5 for the identification of feedback mechanisms between land surface (soil moisture and vegetation) and atmosphere. Soil moisture-rainfall sensitivity was found to be variable over space, with both a positive and negative response. This is in direct contrast to the positive feedback mechanism found by Zheng and Eltahir (1998) and Taylor (2000) but similar to findings over southern Africa (Cook et al. 2006; Mackellar, 2007). Cunnington and Rowntree (1986) noted the importance of initial conditions of soil moisture and atmospheric conditions in numerical simulations of climate over West Africa.

Moufouma-Okia and Rowell (2009) used the Met Office Hadley Centre RCM, HadRM3P to investigate the impact of soil moisture and lateral boundary conditions (LBC) on simulations of the West Africa monsoon. The initial soil moisture conditions resulted only in minor random intraseasonal, interannual and spatial variations whilst the LBC dominated both magnitude and spatial coherency of the monsoon. However, Moufouma-Okia and Rowell (2009) noted that other RCMs or sources of soil moisture may lead to different responses. Taylor and Clark (2000) had been able to significantly improve the PBL evolution and therefore the simulation of convection triggering by using a more realistic land surface parameterization over the Sahel in the HadAM3 model.

Xue et al. (2012) have reviewed the recent developments in West African land/atmosphere interaction studies during the past decade as well as the future prospects. Evidence from satellite data analyses and modelling studies show that West Africa climate is sensitive to land surface processes and the exist a strong coupling between land surface process and regional climate at intraseasonal or seasonal scales. Important developments in better understanding of the West African monsoon or land interaction at intraseasonal/interannual/interdecadal scales have been made, particularly under the African Monsoon Multidisciplinary Analysis (AMMA) Project (Taylor et al., 2011).

2.5 Land Surface Models

RCMs use different land surface model (LSM) schemes for their representation or parameterization of the vegetation, soils and hydrological processes associated with these schemes. Studies have assessed the improvements that different LSMs coupled with the RCM can have on soil moisture-atmosphere interactions in other parts of the world. Recent study by Steiner et al., (2009) show that coupling of the NCAR Community Land Model (CLM3; Sellers et al. 1997) to the RegCM3 atmosphere substantially improves the simulation of mean climate over West Africa. Some of the findings include soil texture boundary condition with the hydrologic treatment of the soil column leading to greater infiltration, less water storage in the soil, evapotranspiration components of water cycle which return less total water to the atmosphere than Biosphere-Atmosphere Transfer Scheme (BATS), Steiner et al., 2009.

Winter et al., (2009) coupled RegCM3 with Integrated Biosphere Simulator (IBIS; Foley et al., 1996) which introduces several advantages such as vegetation dynamics, the explicit modeling of soil/plant biogeochemistry, additional soil layers, an improved method for initialization of soil moisture and temperature. This shows that there are more dynamic models which can now be coupled with RCMs to improve on the land surface-atmosphere interactions. This improvement reinforces the concept that changes in land surface conditions can cause substantial changes in the atmospheric circulation (Steiner et al., 2009).

Diro et al., (2012) recently carried out sensitivity experiments to investigate RegCM4's sensitivity to LSMs (CLM and BATS) over Central America and found out that BATs has a more realistic simulation of the occurrence of the mid-summer drought over that region. Their study also showed that the use of CLM instead of BATS leads to a warmer and drier land surface and a better representation of the seasonal mean spatial pattern of precipitation. However, there is a need for validation of these couplings with LSMs over southern Africa to assess these findings as there are also some advantages or limitations of using BATS which are observed in these studies (Steiner et al., 2009; Winter et al., 2009, Diro et al., 2012). Thus coupling a particular LSM with RCMs for southern Africa studies does not necessarily lead to superior model simulations.

2.6 Soil moisture retention, initialization and seasonal predictability

The significance of soil moisture in seasonal predictability of atmospheric circulation has also being investigated. Soil moisture plays a fundamental role in the initial conditions of weather forecasting models, a dependence that is well recognized at several forecasting centres (Schär et al., 1999, Seneviratne et al., 2010). The presence of a strong soil moisture-precipitation feedback in conjunction with the persistence of soil moisture anomalies opens additional concepts for seasonal forecasting (Schär et al., 1999). Schär et al., (1999) propose that further work is required regarding the predictability of precipitation anomalies in response to soil moisture anomalies. Fennessy and Shukla (1999) using a GCM suggests that seasonal atmospheric prediction could be improved by using a realistic initial state of soil wetness. Whilst, Mahanama and Koster (2005) support the concept that a reduction in climate biases in the GCM leads to more appropriate transformation of soil moisture initialization into the seasonal prediction skill. In a hydrological study, Haga et al.(2005) conclude that consideration of antecedent soil moisture conditions as well as rainfall amount and intensity is essential for understanding the regional characteristics of lag times and subsurface water movement.

Delworth and Manabe (1988a) pioneered the study of soil moisture memory in atmospheric general circulation models (AGCMs), using a first-order Markov process model to relate memory to potential evaporation and soil-water holding capacity. Namias (1988, 1991) suggests that reduced soil during late winter and/or spring over central USA could help induce and amplify a warm, dry summer over the same region partially due to reduction of the local evaporation and by modifying the large-scale atmospheric circulation. Wu and Dickinson (2004) analysed the time scales of layered soil moisture memory in the CLM coupled with the NCAR Climate Model version 3 (NCAR CCM3) 50-year climate simulations which showed substantial variation with geography, season and depth. The major findings were consistent with previous studies (Delworth and Manabe ,1988b; Liu and Vissar, 1999); i.e. time scales are (1) shorter in the tropics increasing with latitude, (2) relatively longer in the arid regions and (3) increasing with soil depth (Wu and Dickinson, 2004)

Soil moisture memory as a key aspect of land-atmosphere interaction and its implications for seasonal forecasting has also been an international topic of discussion through The Global Land-

Atmosphere Coupling Experiment (GLACE) data (Seneviratne et al., 2006b). Due to its inherent memory, soil moisture is one of the major slow drivers of the climate system and possibly the chief source of forecast skill for summer precipitation over land in the midlatitudes (Koster et al., 2000). A detailed understanding of the processes controlling soil moisture memory is therefore necessary for assessing the predictability associated with soil moisture on subseasonal to seasonal time scale and for characterizing important mechanisms impacting land-atmosphere interaction on these time scales (Seneviratne et al., 2006b, 2010). An analysis of the processes controlling soil moisture memory in the AGCMs demonstrated that it is mostly controlled by evaporation's sensitivity to soil moisture, which increases with decreasing soil moisture content, and runoff's sensitivity to soil moisture, which increases with increasing soil moisture content. Soil moisture memory was observed to be highest in regions of medium soil moisture content, where both effects are small (Seneviratne et al., 2006b, 2010)

Using probability density function, the land-atmosphere coupling strength during summer over the USA subregions on the USA is confirmed by use of observations, reanalysis data and numerical models (Wei and Wang, 2012). The study identified hot spots for strong land-atmosphere coupling within the sub-regions, soil moisture-precipitation coupling is weaker than the soil moisture-temperature coupling and that the coupling is stronger in observational and reanalysis data than the coupling strength in numerical models.

2.7 Soil Moisture Sensitivity to Evapotranspiration

It has been shown that sensitivity of evapotranspiration (ET) to soil moisture storage also plays an important role in the land-atmosphere system. Teuling et al. (2006) notes that little is known about its magnitude, its dependence on soil, vegetation and/or climate characteristics due to the lack of connected observations of ET and soil moisture at similar time scales. The sensitivity of ET to soil moisture is a central parameter within the coupled land-atmosphere system. Several studies with GCMs and RCMs suggest that it might influence low frequency atmospheric variability in precipitation and temperature (Koster et al., 2004, Teuling et al., 2006; 2006; Seneviratne et al., 2006a, 2010 and Jaeger & Seneviratne, 2011).

Teuling et al. (2006) related the soil moisture sensitivity to the timescale of ET decay during wet-dry transitions in the absence of rainfall and showed that it can thus be derived from time series of ET alone. Calibration or validation of LSMs can lead to improved model-dependent parameters or configurations for example rooting depth and leaf area index (Steiner et al., 2009; Winter et al., 2009). This might lead to more realistic simulations of land surface-atmosphere or land surface hydrology under a range of varying climatic conditions (Teuling et al. 2006). Schär et al. (1999) confirmed that summertime European climate in a belt between the wet Atlantic and the dry Mediterranean climate is heavily dependent on the correct representation of soil moisture content. The study showed that changes in monthly mean precipitation amounted to about half the change in mean evapotranspiration.

2.8 Soil Moisture and Hot Spots

Hotspots are specific locations on the Earth's surface for which soil moisture anomalies have a substantial impact on precipitation (Koster et al., 2004a). The identification of such hot spots has important implications for the design of seasonal prediction systems. If soil moisture impacts on precipitation are found to be localised, these hot spots are important for the measuring and monitoring of soil moisture as well as for understanding the climate system. According to Koster et al. (2004a), the positions of these hot spots are not unexpected, particularly if the soil moisture influence is presumed to be local rather than remote. In wet climates for which soil water is plentiful, evaporation is controlled not by soil moisture but by net radiative energy.

The fraction of evaporation variance explained by soil moisture variations is lowest when soil moisture is high. Thus, when evaporation in wet climates is not highly sensitive to soil moisture variations, precipitation should not be sensitive to them either (Koster et al., 2004a). Within dry climates evaporation rates are sensitive to soil moisture but are also generally small; small evaporation rates should have a limited ability to affect precipitation. Whereas, for transition zones between wet and dry climates, where the atmosphere is open to precipitation generation, particularly where boundary-layer moisture can trigger moist convection and where evaporation is high enough but still sensitive to soil moisture, we can expect soil moisture to influence precipitation. This was recently confirmed by Jaeger and Seneviratne, (2011). It is within these transition zones where the major hot spots lie. This suggests that for southern Africa, semi-arid

or deserts of Namibia and Botswana and the rest of the southern parts should expect different responses to soil moisture than the rest of the subcontinent. Hotspots should be expected to lie within the zones separating these dry climates from the wet climate areas of the region.

2.9 Soil Moisture Dynamics and Uncertainties

Most of the studies on soil moisture atmosphere interactions discussed above do not focus on the southern African region. In essence, some of the noted observations might not apply to the region, especially in the mid-latitude regions. Several uncertainties or assumptions in these studies were highlighted; Zheng and Eltahir (1998) assumed in their model a constant depth for the boundary layer. Therefore, several of the important feedback mechanisms, i.e. the cloud-radiation feedback, suggested in Eltahir (1998) are not represented in this model. Schär et al. (1999) included an interactive cloud scheme, but the proposed impact of soil moisture on net radiation remained unchanged. This was confirmed by Jaeger, and Seneviratne, (2011).

Similarly the soil moisture-rainfall feedback is also dependent on the convective parameterization scheme used for model simulations. Pal and Eltahir, (1998) utilised the Kuo scheme whilst Giorgi et al., (1996) used the Grell scheme to study the droughts and floods over USA. For the Kuo scheme, significant rainfall anomalies were found following initial soil moisture anomalies whereas the Grell scheme showed little sensitivity to the soil moisture perturbation. However, a comparison of the Grell scheme with the Emanuel scheme (Emanuel, 1994), which is also physically based, suggests that the Grell scheme results should not be altered qualitatively (Findell and Eltahir, 1999). Recent CORDEX-Africa regional climate simulations point to the fact that most or all RCMs simulate the seasonal mean and annual cycle quite accurately, although individual models can show significant biases in some parts of the regions and seasons (Nikulin et al. 2012)

Land surface model schemes influence the soil moisture-atmosphere interactions. Different LSMs have different responses due to the dynamics, soils and hydrological processes. Coupled in RegCM3, LSMs such as BATS; CLM3 and IBIS have their advantages and limitations (Steiner et al., 2009; Winter et al., 2009, Diro et al. 2012). Thus, unresolved uncertainties exist on the best LSM coupling in RCMs for southern Africa.

There should be careful consideration of domain choice and location of boundaries when applying limited-area models. Seth and Giorgi, (1998) focused on the effect of model domain on seasonal, summertime precipitation simulation and its sensitivity to initial soil moisture. The motivation for Seth and Giorgi (1998) had originated from the contradictory results obtained by Beljaars et al. (1996), Paegle et al. (1996) and Giorgi et al. (1996) who looked at the sensitivity of simulated precipitation to surface soil wetness for the summer of 1993 over the central USA. The simulated soil moisture feedbacks from the three studies varied from strong positive, to strong negative, to generally weak. Although the models employed by Beljaars et al. (1996), Paegle et al. (1996) and Giorgi et al. (1996) utilized different physics parameterizations, there were also differences in the model domain. Seth and Giorgi (1998) proposed that the incompatible results may be an indication that interactions between boundary conditions and internal model forcings played an important role not only in the actual simulation of the events, but also in the model sensitivity to soil moisture forcing.

On climate change, Seneviratne et al. (2006a) suggest the enhanced role of soil moisture feedbacks in influencing summer climate variability and the potential for shifts in climatic zones with strong coupling being a consequence of global warming. Several other studies have also suggested that the projected changes in future summer climate rely on soil moisture-atmosphere interactions (Rowell and Jones 2006; Vidale et al., 2007).

In their statistical analysis of land-atmosphere feedbacks in GCMs and the possible pitfalls evaluation, Orlowsky and Seneviratne (2010) point to the fact that "most importantly, apparent soil moisture-precipitation feedbacks can often as well as or even better be attributed to the influence of sea surface temperatures (SSTs) on precipitation……Results for soil moisture-temperature feedbacks complement the precipitation analysis.". Land-atmosphere feedbacks have been identified as one of the key sources of uncertainty in climate models and are thus of central importance for climate change projections (Seneviratne et al., 2006a; Orlowsky & Seneviratne, 2010).

2.10 Summary

Although the assessment of the previous studies might not be exhaustive, the gaps in the field especially the limited exploration over the role of soil moisture on climate variability over southern Africa prompted this research. Inspired and motivated by this soil moisture-atmosphere interactions research, key questions were asked and led to the objectives discussed in chapter 1. Aspects emanating from above research discussions, prompted this study seeking to understand the interactions of soil moisture with the atmosphere, during the summer rainfall season of southern Africa. Adopting the concept of hot spots, the study will seek to identify regions where characteristics of early seasonal rainfall may be influenced by soil moisture. The soil moisture sensitivity to various surface and radiative parameters will be used to understand the implications of soil moisture conditions on the frequency and intensity of rainfall. The soil moisture memory aspects can aid the study on antecedent soil moisture conditions and climate variability over southern Africa. In structuring the study various aspects of the earlier research (i.e. from the basic dynamics, uncertainties to actual rainfall response to soil moisture perturbation) covered here will be useful in explaining and discussing of the results.

Chapter 3

Data and Research Methods

3.1 Introduction

Climate affects a wide range of human activities and sectors across the world including agricultural and hydrological practices, economic planning and development; international relations and health. Observations of climate data including soil moisture are, however, limited on both spatial and temporal scales, particularly over Africa (Tennant and Hewitson, 2002; Fauchereau *et al*, 2003; Tadross et al., 2005b, 2010; New et al. 2006)). In the wake of sparse data in some parts of the developing world, reanalysed datasets have been produced by assimilation of observed values from a number of sources including land stations, satellite and ship rawinsondes (Kalnay et al.,1996; Xie and Arkin, 1996; Kistler et al., 2001).

Research methodologies and tools have also improved over the years, from the earlier years typified by low resolution climate models (GCMs) to the high resolution models (RCMs) that are now being used. Dynamic methodologies have improved by utilizing model ensembles of several GCMs to improve on product output or downscaling to get a representation at a better resolution (Hewitson and Crane, 1996; IPCC AR4, 2007\). This has helped improve understanding of climate variability, resulting in a better appreciation of climate change as well as improving climate prediction methods and skill. State-of-the-art statistical methodologies (linear and non-linear approaches) are also now used in climate studies. A new project initiative, CORDEX (Giorgi et al., 2009; Nikulin et al., 2012) described earlier is aiming to fill the gap on knowledge transfer between projects and regions as well as dissemination of climate information that is useful to the end-user community too. Hewitson et al. (2013) argue that any downscaled information must address the criteria of being plausible, defensible and actionable. The study illustrated the potential consequences of methodological choices of interpreting downscaling results as well as explores the benefits and limitations of using statistical downscaling. From this general view and vital perception, data utilised in this research and chosen methods as well the adopted RCM will be discussed.

3.2 Data

3.2.1 National Centers for Environmental Prediction - National Center for Atmospheric Research Reanalysis 2 Data

The U.S. National Centers for Environmental Prediction (NCEP) - National Center for Atmospheric Research (NCAR) Reanalysis 2 Data (Kalnay et al., 1996; Kistler et al., 2001, Kanamitsu et al., 2002) has a spatial resolution of $2.5^{o} \times 2.5^{o}$, is available at a time resolution of 6 hours with surface variables and free atmosphere variables distributed at 17 pressure levels (8 for humidity). This global data set describes the state of the global atmosphere and comprises a GCM with assimilation of observed values from a number of sources including land station, satellite and ship rawinsonde. It is a retroactive record of more than 50 years of global analyses of atmospheric fields in support of the needs of the research and climate monitoring communities. Kalnay et al. (1996) outline the quality and methods used to generate the reanalysis data[5] . NCEP/NCAR Reanalysis 2 is an improved version of NCEP Reanalysis I mode that fixed errors and updated parameterizations of the physical processes.

The data quality prior to 1979 for the southern African region is suspect since the climatology before 1979 (pre-satellite) is dominated by the model climatology in data-sparse areas (Kistler et al., 2001). The reanalysis data can be used for daily to seasonal and interannual time scales, depending on the variable. The accessibility and spatial coverage of NCEP/NCAR reanalysis 2 data make it an essential choice to conduct climate studies across southern Africa because of sparse observational data. Problems and limitations of the NCEP/NCAR reanalysis 2 data are available on its webpage[6]. Bromwich and Fogt (2004) and Marshall (2003) conclude that NCEP/NCAR reanalysis 2 data unlike many of the available analyses has the positive benefit of a fixed state-of-the-art assimilation scheme. Highlighted differences between NCEP/NCAR reanalysis 2 data and other analyses data are available[7].

[5] also available on http://atom.umd.edu/~ekalnay/

[6] http://www.cpc.ncep.noaa.gov/gov/products/wesley/reanalysis.html#problem

[7] http://www.esrl.noaa.gov/psd/data

3.2.2 Climate Prediction Center Merged Analysis of Precipitation

The 2.5° x 2.5° Climate Prediction Center, United States of America (U.S.) Merged Analysis of Precipitation (CMAP) dataset merges satellite and rain gauge data from a number of satellite and rain gauge sources. These data start in January of 1979 and continue through to the present. Xie and Arkin (1996) provide details on the component datasets and the method used to merge these data. Although the data is suitable for climate studies, there are limitations for some climate applications. These include discontinuities in the component data sets, differences in the calibration methods, and the methodology used to weight the individual rain estimates (Xie and Arkin, 1996).

3.2.3 Climate Research Unit 0.5° Dataset

The Climate Research Unit (CRU), University of East Anglia, UK dataset is a monthly mean data set with a spatial grid resolution of 0.5˚ x 0.5˚, using only meteorological station observations (New et al., 2000, Mitchell and Jones, 2005). The data includes six climate elements and extends over the global land surface for the period 1901-2002. An automated method that refines previous methods (New et al, 2000) was used to check for inhomogeneities in the station records. Through the use of incomplete, partially overlapping and/or information from different sources about a station, a reference series was developed. The reference series enables 1961-90 normals to be calculated for a larger proportion of stations (Mitchell and Jones, 2005). This dataset is known as CRU TS 2.1[8].

CRU rainfall estimates are generally lower than those of 2.5° x 2.5° Climate Prediction Center, United States of America (U.S.) Merged Analysis of Precipitation (CMAP) dataset (Xie and Arkin, 1996). This is more prevalent over the Democratic Republic of Congo and Angola where only a very small number of observation stations with a few records are available. New et al., (2000) state that where the station density is low, CMAP relies heavily on the satellite estimates whereas CRU data tends to climatology. It is unclear which analysis is a better representation of reality (Tadross et al., 2005b). These discrepancies or uncertainty in the observations complicate

[8] Publicly available at http://www.cru.uea.ac.

the validation of climate models and training of area-average rainfall forecasting methodologies over Southern Africa. However, CRU datasets utilise a higher number of observing stations than CMAP.

3.2.4 Global Precipitation Climatology Project

The Global Precipitation Climatology Project monthly precipitation analysis (Huffman et al., 2009) is a globally complete, monthly estimate of surface precipitation. Data from rain gauge stations, satellites, and sounding observations have been merged to estimate monthly rainfall on a 2.5-degree global grid from 1979 to the present. The careful combination of satellite-based rainfall estimates provides the most complete analysis of rainfall available to date over the global oceans, and adds necessary spatial detail to the rainfall analyses over land. In addition to the combination of these data sets, estimates of the uncertainties in the rainfall analysis are provided as a part of the GPCP products. The August 2012 GPCP v2.2 used upgraded emission and scattering algorithms and the Global Precipitation Climatology Centre (GPCC) precipitation gauge analysis.

Constantly improving GPCP key strength lies in that the monthly dataset is now considered the standard for global precipitation which in now often used in model evaluation e.g CORDEX projects and comes with estimates of uncertainty. However, it is only available at 2.5x2.5 grid resolution and over the oceans where satellite data are used; estimates may be biased low at low precipitation rates. The GPCP[9] products are also available as pentad and daily analyses.

3.2.5 Global Land Cover Characterization

Global Land Cover Characterization (GLCC) data is provided by the USA Geological Survey's Earth Resources Observation System Data Center (Loveland et al., 1999). This data is a climatology based on vegetation type (Table 3.1). This is a vegetation data set that is derived from 1 km advanced very high resolution radiometer (AVHHR) data. The data should provide

[9] Retrieved from https://climatedataguide.ucar.edu/climate-data/gpcp-monthly-global-precipitation-climatology-project.

for a more accurate representation of land surface processes in RegCM3 than those of the original 13 RegCM/MM4 vegetation data types (Haagenson et al., 1989). The soil texture class is prescribed according to the vegetation characterization. The GLCC vegetation dataset is prescribed as part of the initial surface conditions in RegCM3 and was thus deemed necessary to be described here.

Table 3.1 Land Cover or Vegetation classes as defined within GLCC dataset.

1	Crop/mixed farming	11	Semi-desert
2	Short grass	12	Ice cap/glacier
3	Evergreen needleleaf tree	13	Bog or marsh
4	Deciduous needleleaf tree	14	Inland water
5	Deciduous broadleaf tree	15	Ocean
6	Evergreen broadleaf tree	16	Evergreen shrub
7	Tall grass	17	Deciduous shrub
8	Desert	18	Mixed Woodland
9	Tundra		
10	Irrigated crop		

3.2.6 Institute of Photogrammetry and Remote Sensing soil moisture data

Soil moisture data measured as soil water index (SWI) obtained from Institute of Photogrammetry and Remote Sensing (IPF), Vienna University of Technology[10] is a global set with a 50km spatial resolution and 10days temporal resolution. This soil moisture data unit of measurement in SWI (%) which is the soil moisture content in the 1st metre of the soil in relative units ranging between wilting level and field capacity. To retrieve a relative measure of soil moisture, instantaneous European Remote-Sensing Satellite (ERS) scatterometer measurements are corrected for the influence of vegetation phenology and relating the vegetation corrected measurement to a dry and wet backscatter reference. The moisture content in the profile is then

[10] Soil moisture data available for download at www.ipf.tuwien.ac.at or www.ukzn.ac.za/sahg/share.

estimated from the surface measurements using a red noise filtering approach (Wagner et al., 1999; Ceballos et al., 2005).

Some of the problems include:

- The method used to retrieve soil moisture in principle is a change detection method. Thus, temporal variations can therefore be retrieved accurately, whereas the absolute level of soil moisture can be biased in certain regions especially in extreme climates (deserts, arctic regions);
- The azimuthal viewing geometry of the sensor is not taken into account during the retrieval. Azimuthal artefacts occur mainly in mountainous and sand desert regions;
- Retrieval of soil moisture is not possible under snow and frozen soil conditions and;
- Open water surfaces are known to cause errors in retrieval and will not be compared with simulations done.

3.3 Methodologies

3.3.1 Regional Climate Model

RCMs simulate the climate by solving the fundamental physical equations of the atmosphere-land-ocean system. However, it is necessary to parameterize certain sub-grid scale processes. Therefore RCMs such as MM5, RegCM3 and RegCM4 contain several options for representing different atmospheric processes such as the planetary boundary layer (PBL), cumulus convection, radiation and cloud microphysical processes. The models are based on the physical laws of fluid dynamics; thermodynamics and the governing equations of conservation of energy, mass and momentum.

The dynamical core of RegCM, originally developed by Dickinson et al. (1989) and Giorgi (1990), is based on the hydrostatic version of the Pennsylvania State University – National Center for Atmospheric Research's Mesoscale Model version 4 (MM4). RegCM3 employs a terrain-following σ-vertical coordinate model, where $\sigma = (p-p_{top})/ (p_s-p)$, p is pressure, p_{top} is the pressure specified at the top of the model and p_s is the prognostic surface pressure. The

atmospheric radiative-transfer computations are performed using the radiation scheme from the Community Climate Model version 3 [CCM3; Kiehl et al., 1996] and the PBL computations are calculated using the non-local formulation developed by (Holtslag et al., 1990). The vertical eddy flux within the PBL is given by an eddy diffusion term plus a "countergradient" term, which describes nonlocal transport due to deep convective plumes in the PBL. The eddy diffusivity term follows a parabolic profile between the surface and the PBL top.

Resolvable (large-scale) cloud and precipitation processes are computed using a sub-grid explicit moisture scheme (SUBEX) (Pal et al., 2000). The unresolved convective precipitation processes in RegCM3 are represented by three schemes; the modified Anthes-Kuo (Anthes, 1977; Giorgi 1991) , the Grell scheme (Grell, 1993) with the Fritsch and Chappell (1980) closure assumption and the newest cumulus convection option being the Massachusetts Institute of Technology (MIT) Emanuel Scheme (Emanuel, 1991; Emanuel and Zivkovic-Rothman, 1999). The MIT scheme assumes that the mixing ratio in clouds is highly episodic and inhomogeneous (as opposed to a continuous entraining plume) and considers convective fluxes based on an idealised model of sub-cloud-scale updrafts and downdrafts. Convection is triggered when the level of neutral buoyancy is greater than the cloud base level. Between these two levels, air is lifted and a fraction of the condensed moisture forms precipitation while the remaining fraction forms the cloud. Some advantages of the MIT-Emanuel scheme over other RegCM convection option includes a formulation of the auto-conversion of cloud water into precipitation inside cumulus clouds and the precipitation is added to a single, hydrostatic, unsaturated downdraft that transports heat and water (Giorgi et al., 2012; Pal et al., 2007; Emanuel, 1991; Emanuel and Zivkovic-Rothman, 1999). The third option to represent cumulus convection in RegCM3, the modified Anthes-Kuo (Anthes, 1977; Giorgi 1991) was the most erroneous in resolving the climate over southern Africa.

The surface physics calculations are performed using BATS1E (Biosphere-Atmosphere Transfer Scheme, BATS version 1E), described in detail by Dickinson et al., (1993). BATS scheme is designed to describe the role of vegetation and interactive soil moisture in modifying the surface-atmosphere exchanges of momentum, energy and moisture. It has a vegetation layer, a snow layer, a surface soil layer (10cm thick), a root zone layer (1-2m thick) and a third deep soil layer

(3m thick). These are the three soil layers modulated in the experiments for this study. Prognostic equations are solved for the soil layer temperatures using a generalization of the force-restore method of Deardoff (1978). The soil hydrology calculations include predictive equations for the water content of the soil layers. These equations account for precipitation, canopy foliage, evapotranspiration, surface runoff, snowmelt, infiltration below the root zone and diffusive exchange of water between soil layers. The scheme also has functions accounting for soil water movement, surface runoff, sensible heat, water vapour and momentum fluxes. BATS has 20 vegetation types; soil textures ranging from coarse (sand), to intermediate (loam), to fine (clay) and different soil colours (light to dark) for the soil albedo calculation (Dickinson et al., 1986). Additional modifications have been made to BATS in order to account for subgrid variability of topography and land cover using a mosaic-type approach (Giorgi et al., 2003). This parameterization showed a marked improvement in the representation of the surface hydrological cycle in mountainous regions. A more detailed description of RegCM3 and refereed articles can be found in Pal et al. (2007)[11]. A new version, RegCM4 (Giorgi et al., 2012) has since been launched at the end of 2010 after most of this study's experiments had been completed using RegCM3.

3.3.2 Experimental Set up

RegCM3 requires initial conditions and time dependent lateral boundary conditions for wind components, temperature, mixing ratio, surface pressure and water vapour. An accurate representation of these boundary conditions is often essential for RCM applications. The initial conditions and lateral boundary conditions for each simulation are taken from NCEP/NCAR reanalysis 2 data (Kalnay et al., 1996). SSTs are prescribed using data provided by the National Ocean and Atmospheric Administration (NOAA) – decadal Optimized Interpolated SSTs (OISST).The vegetation is specified using the Global Land Cover Characterization (GLCC) data (Loveland et al., 1999). The model domain is centred near northeastern South Africa at 17.5S and 35.0E while the grid is defined on a normal Mercator projection. In the horizontal, the grid is 109 points in the east-west direction and 102 in the north-south with a resolution of 50km. Figure 3.1 depict the domain of choice with the (a) surface elevation and (b) landcover types over

[11] Also available at user.ictp.it/RegCNET/

southern Africa. This resolution captures the main topographic features of the domain, such as the mountains of Lesotho and the main central watershed over Zimbabwe (Figure 3.1a). This substantiates the improvements brought by the inclusion of the mosaic type of approach (Giorgi et al., 2003) within BATS. The vegetation or land cover types in Figure 3.1b represent various landuses over the region – ranging from crop/mixed farming to mixed woodland. Table 3.1 show the vegetation classes as defined within GLCC dataset.

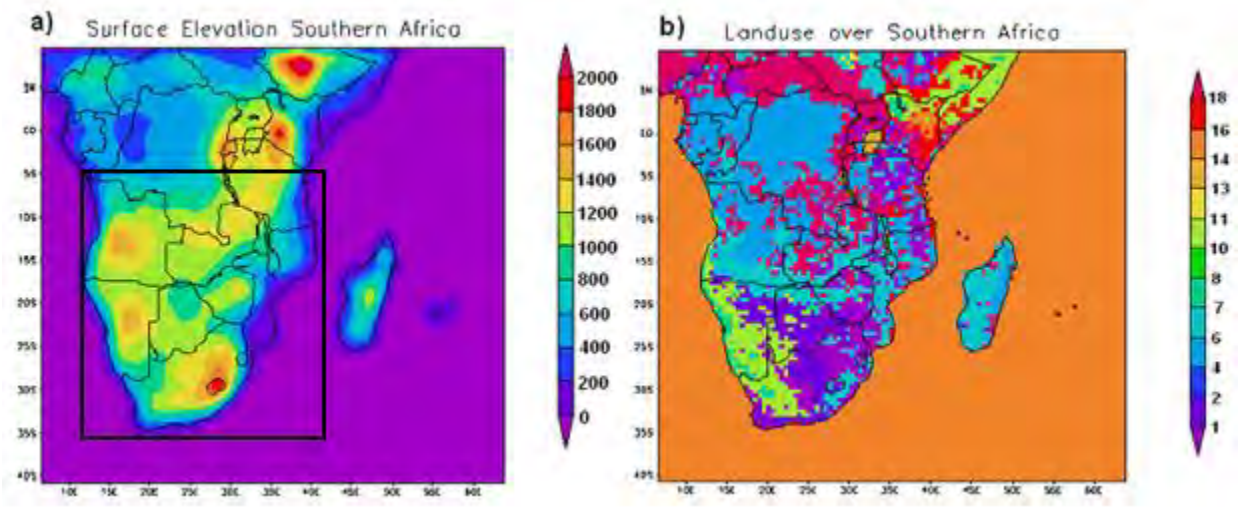

Figure 3.1 Domain choice showing the (a) elevation of the topography and (b) land cover types over the southern Africa region. The inserted black quad shows the sub-domain that will be presented for most of the spatial maps on the chosen surface climate variables.

In this study, the response of the atmosphere to soil moisture changes is considered through the use of a RCM, RegCM3 (Pal et al.,2007), evaluating in particular, the feedbacks between the atmosphere and land surface as well as the effect on precipitation extreme events, including frequency and intensity of the precipitation. The preliminary control simulations focused on January month) being driven by NCEP/NCAR re-analysis 2 data for the initial boundary conditions. Perturbation soil moisture experiments were based on changing the soil moisture field capacities within the BATS scheme. The moisture is initialised at percentages of 25% and 75% of the field capacity which represent the wilting point and saturation state within the scheme. The FORTRAN code within the BATS scheme is altered so that the model simulates with soil moisture being interactive for the selected capacities. The interactive factor implies that the soil moisture does respond to the atmosphere but initialization will only start at chosen soil

moisture perturbation values (Pal and Eltahir, 2002). Preliminary one-month simulations are performed with a 1 month spin up period using the Emanuel convective Scheme (Emanuel, 1993; Tadross et al., 2010). Thereafter, longer simulations are performed on a seasonal time scale from September to March for 6 seasons of three dry seasons 1991/92, 1994/95 and 1997/98 as well as wet 1995/96, 1996/97 and 1998/99 to 19978/99 with a 1 month spin up (August) for all the seasonal summer simulations. 1 month spin-up was deemed substantial to revolve the moisture around within the model for a 7months simulation. This was selected after some extensive testing, analysis, and consultation from some of the RegCM3 model developers; Jeremy Pal, Bi Xinquang and Filippo Giorgi (pers. communication 2005). Experimental set up remained similar to that of shorter simulations done earlier for a control, drier and wetter soil moisture perturbations. Initial experiments were done with a 15 day spin-up and did show some variability.

The analysis focuses on aspects such as the feedback, soil moisture memory, the seasonal cycle and comparison of model parameters with available reanalysis data observations. Aspects of water vapour in the planetary boundary layer and vertical cross-section plots on both latitudinal and longitudinal scales will be analysed. Antecedent conditions analysis on the summer situation will be carried out by splitting the season into early summer (September to November, SON) period and late summer (December to February, DJF) period in an effort to seek out more intraseasonal information. The analysis of the atmospheric levels will be required in seeking to fully explain the surface-atmosphere interaction process and identify internal model variability showing distinct responses to the effects of soil moisture anomalies within the boundary layer. The 850hPa or 700hPa for near surface features are analysed looking at these variables, horizontal u wind, the vertical v wind, moisture flux and the geopotential height (hgt) for all the different experimental set ups described above. The detailed understanding of dynamics of the soil moisture-atmosphere is important because of its critical implications on local to synoptic and large-scale circulations.

3.3.3 Self-Organizing Mapping

A non-linear statistical method, Kohonen Self-organizing mapping, SOM (Kohonen, 1995) of the simulations will be used to disaggregate the synoptic states and seek to explain how the

regions of southern Africa are being impacted. Diagnosis of the daily simulations based on synoptic states further allows the non-linearity of land surface-climate feedbacks to be more clearly assessed.

The SOM technique is a method for evaluating the distribution of modes of variability within a high-dimensional data set. It is able to capture variability in e.g. rainfall patterns and express these patterns (or nodes) across a non-linear two-dimensional continuum (Hewitson and Crane, 1994, 2002; Main, 1997). Additionally it separates patterns where there is more data to warrant such a separation. Once patterns of a dataset have been characterised the original data may be mapped to these characteristic patterns and a frequency of occurrence of each pattern generated. As a powerful utility in capturing the modes of variability in atmospheric patterns and expressing these synoptic types across a two-dimensional continuum, SOM has recently been adopted in synoptic climatology. The SOM has been broadly described as an Artificial Neural Network (ANN) and has an inherent ability for classification, which makes it potentially applicable for use in synoptic climatology (Hewitson and Crane, 1994, 2002; Main, 1997).

Main (1997) used SOMs to investigate seasonal cycles in GCMs; Hudson (1998) utilized SOMs to evaluate frequency changes of synoptic events in a GCM perturbation experiment; Tennant and Hewitson (2002) used SOMs to seek particular seasonal modes in the atmospheric circulation. Walawege (2002) used it in examining spatially extensive heavy rainfall events over South Africa. Crane and Hewitson (2003) used SOMs to combine precipitation records of individual stations into a regional data set by extracting the common regional variability from the locally forced variability at each station. Mdoka (2005) used the SOM technique on CMAP reanalysis data to characterize precipitation and frequency of occurrence over southern Africa. Alexander et al. (2009) utilised SOM to diagnose the synoptic influences driving changes in climate extremes over southern Australia during the last century whilst Mackellar et al., (2010) did synoptic-based evaluation of climatic response to vegetation change over southern Africa.

SOM technique is a method for mapping high dimensional input vectors to a two dimensional array of nodes. It can be interpreted as a “nonlinear projection” of the probability density function of the high-dimensional input data onto the two-dimensional display (Hewitson and

Crane, 2002). SOM maintains some measure of the distance between data points in the high dimensional space. The technique is different from traditional cluster algorithms in the way in which groups are defined. Output of SOM analysis is analogous to some form of data clustering; however, unlike clustering algorithms the basic SOM methodology is not primarily concerned with grouping data or identifying clusters (Hewitson and Crane, 2002). SOMs attempt to find nodes or points in the measurement space that are representative of the nearby cloud of observations and when taken together describe the multi-dimensional distribution function of the data set. For this work, the most important attributes of the SOM technique are the ability to classify input data based on non-linear relationships between the input elements and to visualise the continuum of the data space.

SOMs are developed through an iterative training procedure in which elements of the SOM are mapped to representative regions of the input data space (Kohonen, 1995; Main, 1997; Hewitson and Crane, 2002; Crane and Hewitson 2003). Training is implemented with one of the two possible neighbourhood kernels which are vital to the SOM algorithm, bubble or Gaussian which relates time and learning rate together to determine how a particular node's weights are updated. Learning rate determines how easily a node's weights may be changed. The user determines the size and shape of this update kernel. Quality of learning is based on initial values and applying different sequences of training vectors and different learning parameters. Thus an appreciable number of random initializations of the initial values ought to be tried and the map with the minimum quantisation error selected. The SOM technique also provides means of knowing how similar or dissimilar nodes are to each other through the Sammon mapping.

More detailed theoretical discussion on SOMs is well described in the literature especially the techniques by Kohonen, (1995). A practical SOMs software package[12] and its extensive references are freely available. Kohonen package is also available in R[13]

3.3.4 Student's t Test

[12] http://www.cis.hut.fi/research/som-research/

[13] http://www.cbtio.uct.ac.za

Zwiers and von Storch, 1995 states that statistical comparisons of means are frequently conducted in climatology to intercompare observed and/or simulated climates among themselves or against fixed reference values. These comparisons are conducted by employing a paradigm in which:

- a statistical model is imposed upon the samples of climate data,
- a *null hypothesis* H_o that is to be tested is specified,
- an *alternate hypothesis* H_a that guides the interpretation of the test is specified, and
- a test statistic is computed to determine how unusual the observed difference of means is in context of the model and null hypothesis, *null distribution* (Zwiers and von Storch, 1995; von Storch and Zwiers, 1999; Wilks 2006,).

The student's *t* test is a parametric test used to compare the means of two samples so as to establish whether they are significantly different from each other and thus represent two separate populations. Parametric tests are those conducted in situations where we know or assume that a particular theoretical distribution is an appropriate representation for the data and/or the test statistic (von Storch and Zwiers, 1999; Wilks 2006). In the present study, the test is used to determine if there are statistically significant differences between control and soil moisture perturbation model simulations. The variance of the two samples is assumed to be the same. An F test is used to decide whether two samples came from populations with equal variances (von Storch and Zwiers, 1999). The *F* test is not only used for *t* tests, but for any occasion when comparing the variation in two data sets is required. The *F* distribution (ratio of their variances differences should be close to 1), is then compared to the critical values of the *F* distribution (F_{CRIT}) from a Statistical table[14]. If $F < F_{CRIT}$, we can assume the sample variances are equal. Student *t* test is performed at each grid point of the daily data concerned and the confidence levels are calculated. Null hypothesis for each grid point is that there is no significant difference between the corresponding grid point means of the control and anomalous soil moisture simulations for the chosen variable. There are some

[14] Critical values of the F distribution are tabulated and are available from statistical websites or in Appendices of textbooks e.g. Appendix G (von Storch and Zwiers, 1999).

After the hypothesis testing criteria mentioned earlier, the last step is to compare observed test statistic to the null distribution (Wilks, 2006). If the test statistic falls in a sufficiently improbable region of the null distribution, H_o is rejected as too unlikely to have been the observed evidence. If the test falls within specified values described by the null distribution, the test statistic is seen as consistent with H_o, which is then not rejected. Note that not rejecting H_o does not mean that null hypothesis is necessarily true, only that there is insufficient evidence to reject this hypothesis. When it is not rejected, we can only say that it is not inconsistent with the observed data (Wilks, 2006). A 95% confidence level has been selected for this study.

When the samples are not serially correlated the appropriate classical tests for comparing means are utilised where the key assumption is the mutually independence of the individual observations. However, the data in this study are time means, and the persistence (or time dependence) is likely not to satisfy the mutual independence assumption but be serially autocorrelated. The lack of independence due to ignoring the time dependence leads to underestimation of the variance of sampling distributions of the classical test statistics, which in turn results in an inflated value of the test statistic (Wilks, 2006). One solution to this problem is to estimate the effective sample size or an equivalent number of independent samples, n′, anticipate that n′< n of independent values for which the sampling distribution of the average has the same variance as the sampling distribution of the average over the n autocorrelated values in the data (Zwiers and von Storch, 1995; von Storch and Zwiers, 1999; Wilks, 2006). Then n′ can be in *t* test equations and the classical tests can be carried through as before.

The effective sample size can be estimated using the approximation:

$$n' \cong n\,(1-\rho 1)/(1+\rho 1) \qquad 3.1$$

Where, ρ_1 is the lag-1 autocorrelation coefficient. When there is no time correlation, $\rho_1=0$ and n′=n. The ratio $(1+\rho_1)/(1-\rho_1)$ acts as a variance inflation factor, which adjusts the variance of the sampling distribution of the time average to reflect the influence of serial autocorrelation (Wilks 2006). In this study, the *t* test was applied to the control and soil moisture perturbation data for the chosen surface variables. There were varying statistically significant results for a number of grid points for the different variables analysed. Changes invoked by the anomalous

forcing does not lead to marked differences between the soil moisture perturbation experiments and the control grid point values with respect to the effective sample size, n′, to cause rejection of null hypothesis. According to Hudson (1998), von Storch and Zwiers, (1999) and Mackellar et al. (2009), statistically insignificant result does not imply a climatologically insignificant finding. Focus is on the consistency of the changes in spatial distribution from the anomalous forcing between the month and seasons of analysis. However, the student's *t* test examines the point-wise response but does not take into account the spatial response to the perturbation (Hudson 1998; Mackellar et al., 2009). Statistically significance acts as a relative guide to aid in identifying the possible key regions of importance.

3.4 Other Soil Moisture Related Variables Calculated and Analysed

3.4.1 *Cloud Liquid Water Path*

Cloud liquid water path (CLWP) is the column amount of liquid water in the cloud. CLWP is used to derive cloud optical thickness which is a very important component in the radiation scheme. CLWP plays an important role in the transport of energy (latent heat) in the earth-atmosphere system (Goddard Earth Sciences Data and Information Services Center GES DISC, 2008). Its major applications include (1) Global energy budget, (2) Climate Change, (3) Greenhouse effect and (4) Global warming. Thus effects of soil moisture perturbations within the PBL become important.

3.4.2 *Evaporative Fraction*

According to Farah et al. (2004) evaporative fraction is required on daily as well as longer time-scales for applications in hydrology, agriculture, forestry and environmental studies in general. Evaporative fraction, EF is the ratio between the latent heat and the available energy at the land surface. EF is the ratio of latent heat flux to the sum of latent and sensible heat fluxes. It has been used to characterize the energy partition over land surfaces and has potential for inferring daily energy balance information based on midday remote sensing measurements (Nichols and Cuenca, 1993). The variability of EF is due to environmental factors i.e. air temperature,

incoming solar radiation, wind speed, soil water content or leaf area index (Lhomme and Elguero, 1999; Farah et al., 2004; Gentine et. al., 2007).

Shukla (1999) and Fischer et al. (2007) show the important role of partitioning of net radiation into latent and sensible heat fluxes, which to a large extent is controlled by soil moisture. The classical energy partitioning indicator is the Bowen Ratio, β (Farah et al., 2004), which is a ratio of the sensible heat flux (H) and latent heat flux (LE). According to its definition evaporative fraction is thus presented as:

$$EF = \frac{LE}{\mathrm{Rn} - G} = \frac{LE}{LE + H} = \frac{1}{1 + \beta} \qquad 3.2$$

Where, R_n is the net radiation and G the soil heat flux. EF is directly related to β (equation 3.2).

3.5 Summary

A concise description into the datasets and research methods that were employed in this research has been presented. The strengths and weaknesses of the data and techniques have been outlined and should be borne in mind when considering some of the results obtained. Issues of discontinuity or missing data, spatial and temporal resolution are vital. The research methods included the description of the regional climate model, RegCM3 and its physics incorporating the schemes that are coupled with it particularly the LSM, BATS Scheme which is important in the current study of the soil moisture-atmosphere interactions. One of the key methods, SOM technique has also being discussed and some of the statistical methods that are used in spatial representation of the selected atmospheric variables have been described highlighting their advantages and disadvantages. It should be noted that additional material about some of the sections' data and/or methodology will be introduced within the discussion of results in the chapters remaining.

Chapter 4

Summer Climate Simulations

4.1 Introduction

The aim of the soil moisture experiments was to use the RegCM3 model to determine how soil moisture and surface heat fluxes affect the boundary layer climate of Southern Africa. The state of soil moisture, as described by the level of saturation in the soil levels, is regulated by rainfall and potential evaporation. Both of these atmospheric forcings exert substantial control on the evolution of the soil moisture state. To investigate these underlying processes, a series of simulations utilizing wet, dry and normal soil moisture conditions were designed. The experiments are based on changing the soil moisture field capacity in the RegCM3. The control simulation is run with prescribed conditions for the default setting of RegCM3. The soil moisture is then initialised at percentages of 25% (wilting) and 75% (saturation) of the field capacity within the land surface model, BATS scheme.

RegCM3 FORTRAN code within the BATS scheme was altered so that the model simulates with soil moisture being interactive for all selected capacities. These model's interactive simulations imply that the surface impacts the atmosphere and thus the soil moisture does respond to the atmosphere but starting the initialization at specific soil moisture perturbations of either wilting or saturation points (Pal and Eltahir, 2002).

As previously discussed, the mean summer climate will be studied using the six simulations of the chosen dry seasons (1991/92, 1994/95 and 1997/98) and the wet seasons (1995/96, 1996/97 and 1998/99). These summer simulations are performed with a 1 month spin up period using Emanuel convective scheme. To better understand the role of antecedent soil moisture conditions an analysis of soil moisture for early summer (September to November, SON) is carried out. This analysis would aid us to appreciate how the soil moisture is incorporated into the later part

of the summer season (December to February, DJF). Thus, interactive summer climate simulations are useful for assessing the model's persistence to the soil moisture perturbations.

4.2 Model performance

4.2.1 Model Comparison to IPF Total Soil Moisture

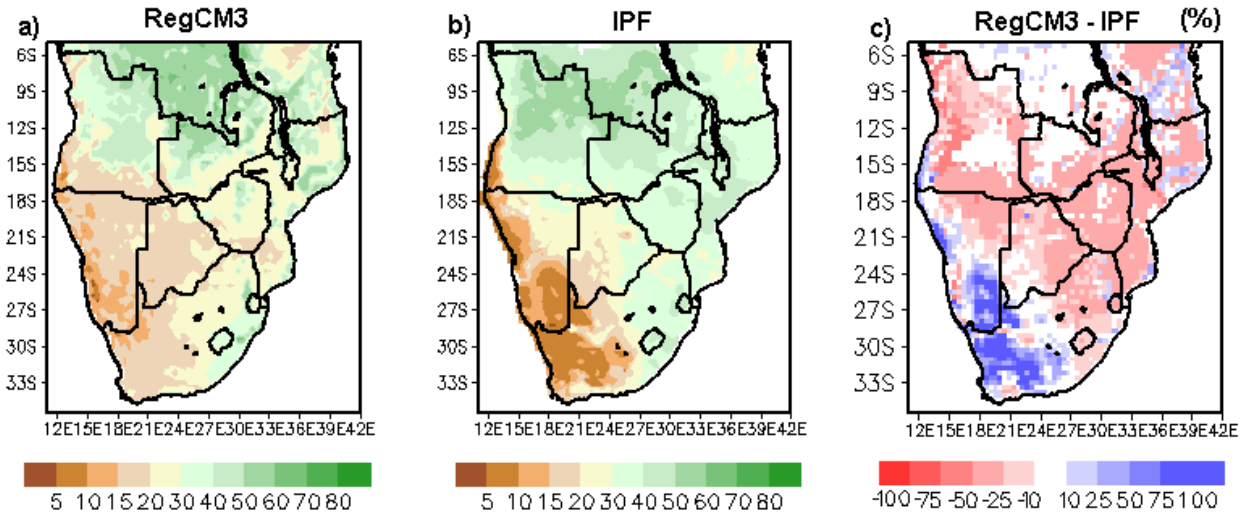

Figure 4.1 Mean soil moisture conditions for the (a) RegCM3 top-layer soil moisture, (b) mean soil moisture data measured as soil water index (SWI) obtained from Institute of Photogrammetry and Remote Sensing (IPF), Vienna University of Technology, IPF soil moisture and (c) bias of RegCM3 with respect to IPF. This soil moisture data's unit of measurement SWI (%) is for soil moisture content within the 1st metre of the soil layer in relative units that ranges from wilting level to field capacity as (%) and bias.

Figure 4.1 shows the mean soil moisture conditions for the (a) RegCM3 top-layer soil moisture, and (b) mean soil moisture data measured as soil water index (SWI) obtained from Institute of Photogrammetry and Remote Sensing (IPF), Vienna University of Technology which is IPF soil moisture and (c) is the bias of RegCM3 with respect to IPF. This soil moisture data's unit of measurement SWI in percentage (%) is for soil moisture content within the 1st metre of the soil layer in relative units that ranges from wilting level to field capacity as (%). RegCM3 captures appropriately the observed spatial distribution of soil moisture traversing from the very dry southwestern areas to moist northern tropical areas (fig. 4.1). The west-east moisture gradient is not clearly depicted due to the lower soil moisture especially over southern Angola, northeastern Namibia, Botswana, Zimbabwe and southeastern parts of the region (fig. 4.1a, c). However, the

model simulates less soil moisture over most areas but overestimates the soil moisture over southern Mozambique, southern Zimbabwe and southeastern Botswana. RegCM3 does well to capture the peaks to the east of Lesotho and to the west of Swaziland as well as parts of the moist tropical region over Republic of Democratic Congo (DRC). Wettest bias is simulated by the model over the southwestern areas and driest bias being over a small part of western Angola. It should be noted that this IPF soil moisture data is good reference database to how well RegCM3 simulated its top-layer soil moisture.

Although there are biases observed for the simulated soil moisture, the margin of error or point of major concern cannot be clearly assessed since there is not much knowledge on the evaluation of the IPF data. This is a limitation which is now being addressed by collecting of in-situ soil moisture data over South Africa. For the IPF data, the method used to retrieve soil moisture in principle is a change detection method (Wagner et al., 1999; Ceballos et al., 2005). Thus, temporal variations can therefore be retrieved accurately, whereas the absolute level of soil moisture can be biased in certain regions especially in extreme climates (deserts, arctic regions). This could aid in explaining the wet biases over parts of the Namib Desert. The azimuthal viewing geometry of the sensor is not taken into account during the retrieval. Azimuthal artefacts occur mainly in mountainous and sand desert regions thus can be reason behind the wet biases found over the southwestern areas (fig. 4.1). Thus without so much knowledge about the evaluation of the soil moisture data, we consider the spatial distribution aspect only.

4.2.2 Model Comparison to Total Precipitation

The mean total precipitation (mm/day) for the control simulation, RegCM3 is evaluated with respect to the CRU and GPCP datasets for all the summer seasons (fig. 4.2). Two forms of RegCM3 simulation maps are presented with precipitation over the ocean being masked out (fig. 4.2a) so as to compare it with land-based only measurements of CRU data (fig. 4.2c) whilst RegCM3 with precipitation over the ocean (figure 4.2b) for comparison with the GPCP analysis data (fig. 4.2d). Although we are mainly concerned with land surface- atmosphere interaction, the adjacent Oceans and other remote forcings such as ENSO are not being totally excluded. Thus the model's performance even over the Oceans needs to be understood.

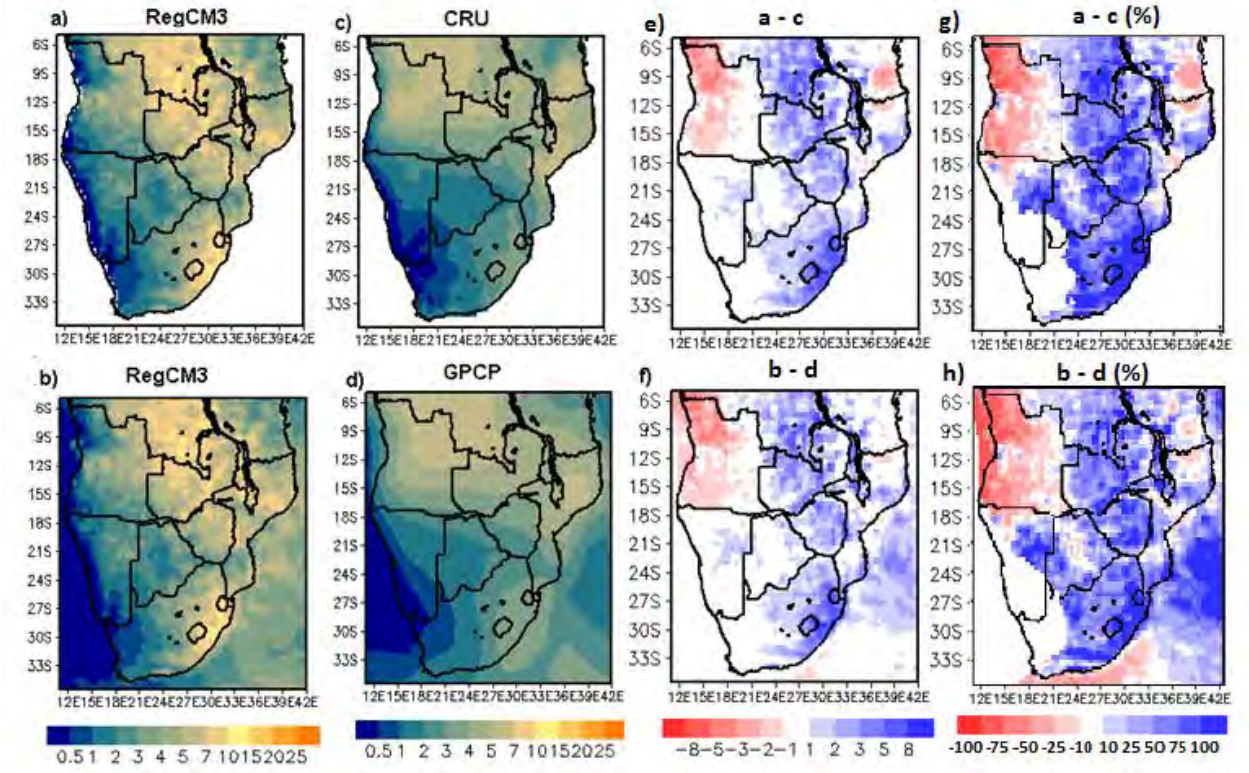

Figure 4.2 Mean summer total precipitation (mm/day) of all the simulated years (1991-1999) On the left column (a) RegCM3 with precipitation over ocean masked out, (b) RegCM3 with precipitation over ocean; middle column is for (c) CRU reanalysis, (d) GPCP monthly data, third column is the biases from RegCM3 with the respect to (e) CRU and (f) GPCP and last column (g,h) is in percentage of the biases from CRU and GPCP respectively

In general, the model (fig. 4.2a, b) does reasonably well to capture the full spatial distribution of the rainfall in comparison to the observations (fig. 4.2 b, c) whilst being able to almost reproduce the rainfall magnitude over a greater part of the southwestern areas. However, RegCM3 fails to simulate close to the rainfall magnitudes as compared to the observations (fig. 4.2a, b) particularly over Angola and southeastern areas. RegCM3 does well in simulating areas of rainfall maxima such as east of Lesotho, Swaziland, central Mozambique and border regions of DRC and Zambia (fig. 4.2a, b) although at a higher precipitation magnitude than for CRU data (fig. 4.2b). Underestimation of precipitation is observed from the dry biases over Angola and southern Tanzania in CRU data (fig. 4.2e) but only over Angola in the GPCP analysis. The model reproduces appropriately the observed west-to-east precipitation gradient over the southern parts of the region. It should be noted that the model's soil moisture spatial pattern (fig

4.1a) is similar especially to that of the GPCP and CRU spatial distribution (fig. 4.2c, d). This is supported by drier areas (low soil moisture) being represented by the dark brown colours whilst the wetter areas (high soil moisture) are being depicted with greener colours as part of a "dark brown to green" vegetation gradient representation. The model does well in reproducing the magnitude of precipitation over a greater portion of the region as well as over the adjacent oceans (fig. 4.2f). Although not quantified, the model seems to spatially agree better with GPCP than CRU data. The same conclusion can be reached through the soil moisture spatial distribution too (fig. 4.1a).

Figure 4.2e and 4.2f show that excessive precipitation biases of 8mm/day are observed only over higher ground areas within the Drakensburg escarpment and in south DRC. Although not covering a wide region, these areas also fall within the region where RegCM3 overestimates precipitation by 100% (figure 4.2 g, h). However, the rest of the areas (southeastern half of South Africa, Zimbabwe, west Botswana and eastern Namibia) within the 100% overestimation region (figure 4.2 g, h) fall within the little (1-2mm/day) or no biases range (figure 4.2e, f). There is 100% underestimation subregion (figure 4.2 g, h) but at a rate of about 5mm/day (figure 4.2e, f) over the northwestern Angola. This area is also associated with sparse rain gauge stations and thus increasing the rainfall uncertainty or margin of error to have an ascertained model's biases magnitudes (Zhang et al. 2013).

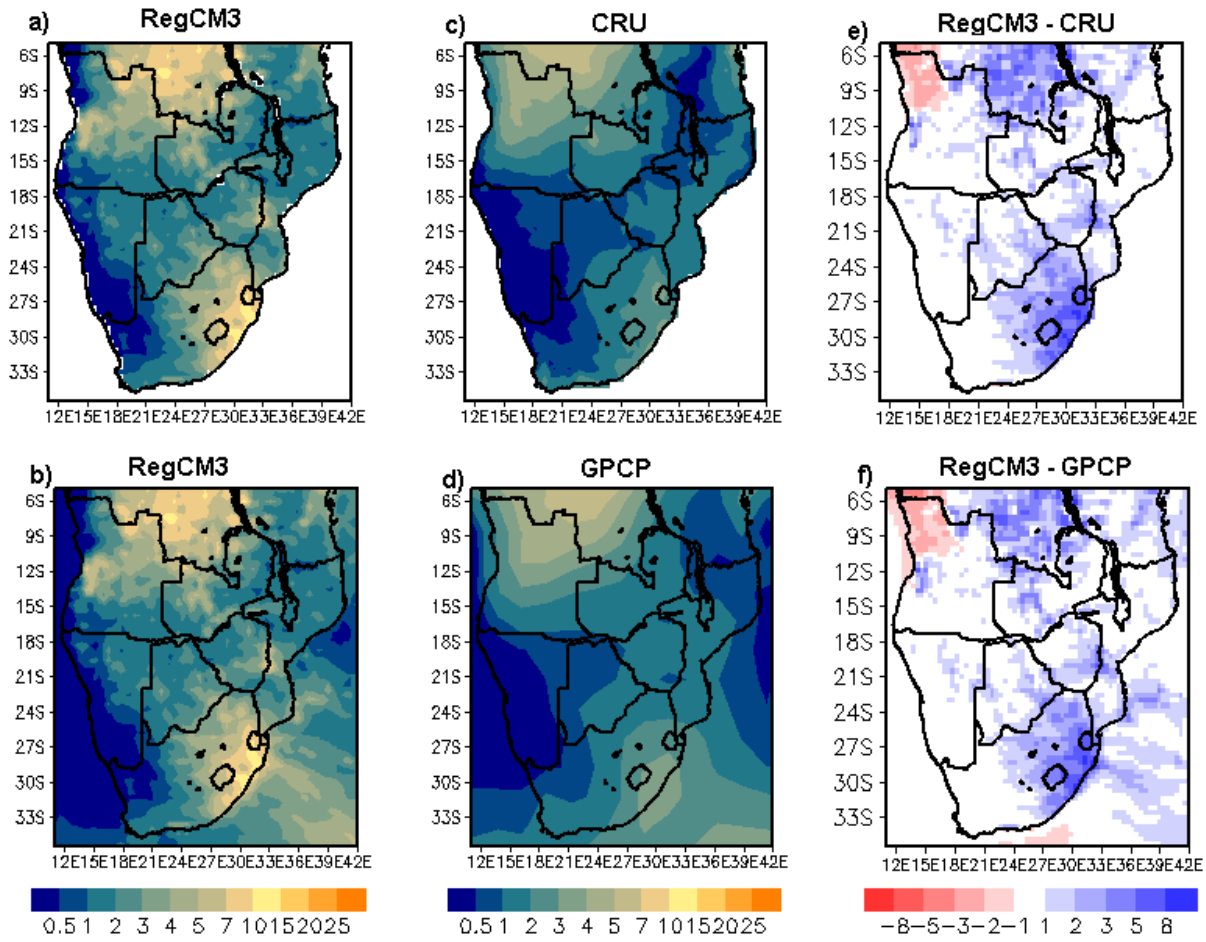

Figure 4.3 Mean total precipitation (mm/day) of September to November (SON) for all the simulated seasons. On the left column (a) RegCM3 with precipitation over Oceans masked out, (b) RegCM3 with precipitation over Ocean; middle column is for (c) CRU, (d) GPCP monthly data and right column is the biases for RegCM3 with the respect to (e) CRU and (f) GPCP.

Figure 4.3 and figure 4.4 show the mean total precipitation (mm/day) distribution patterns between the early summer (SON) and late summer (DJF) for all the simulated years. In the early summer, RegCM3 captures the spatial extent of the precipitation distribution over the region (fig. 4.3). However, the model overestimates precipitation especially over DRC and southeastern South Africa which is distributed in a northwest-southeast inclination whilst it underestimates over Angola. The maximum over DRC (figure 4.3a) is larger (by about 8mm/day) than in the CRU (fig. 4.3b). The model still captures the E-W rainfall distribution over South Africa and does fairly well in reproducing the spatial distribution and magnitude over the adjacent oceans (fig. 4.3b, d, f). Based on comparison of the seasonal maps (figure. 4.2c, f; figure 4.3c, f and

figure 4.4e, f), the model does best in reproducing the spatial extent and magnitude during the early summer period, SON. Thus, RegCM3 nested in NCEP/NCAR reanalysis 2 data and using the Emanuel convection scheme does well in capturing the spatial distribution over the region; reproduces the magnitude over the southwestern areas and adjacent Oceans but overestimates precipitation especially over most of the tropics but has some systematic cold bias over Angola. Although not shown here, it should be noted that there is 100% overestimation of percentage bias over south DRC. Given the scarcity of rainfall data over this region, such uncertainty and systematic errors observed would be helpful when translating this information to other applications.

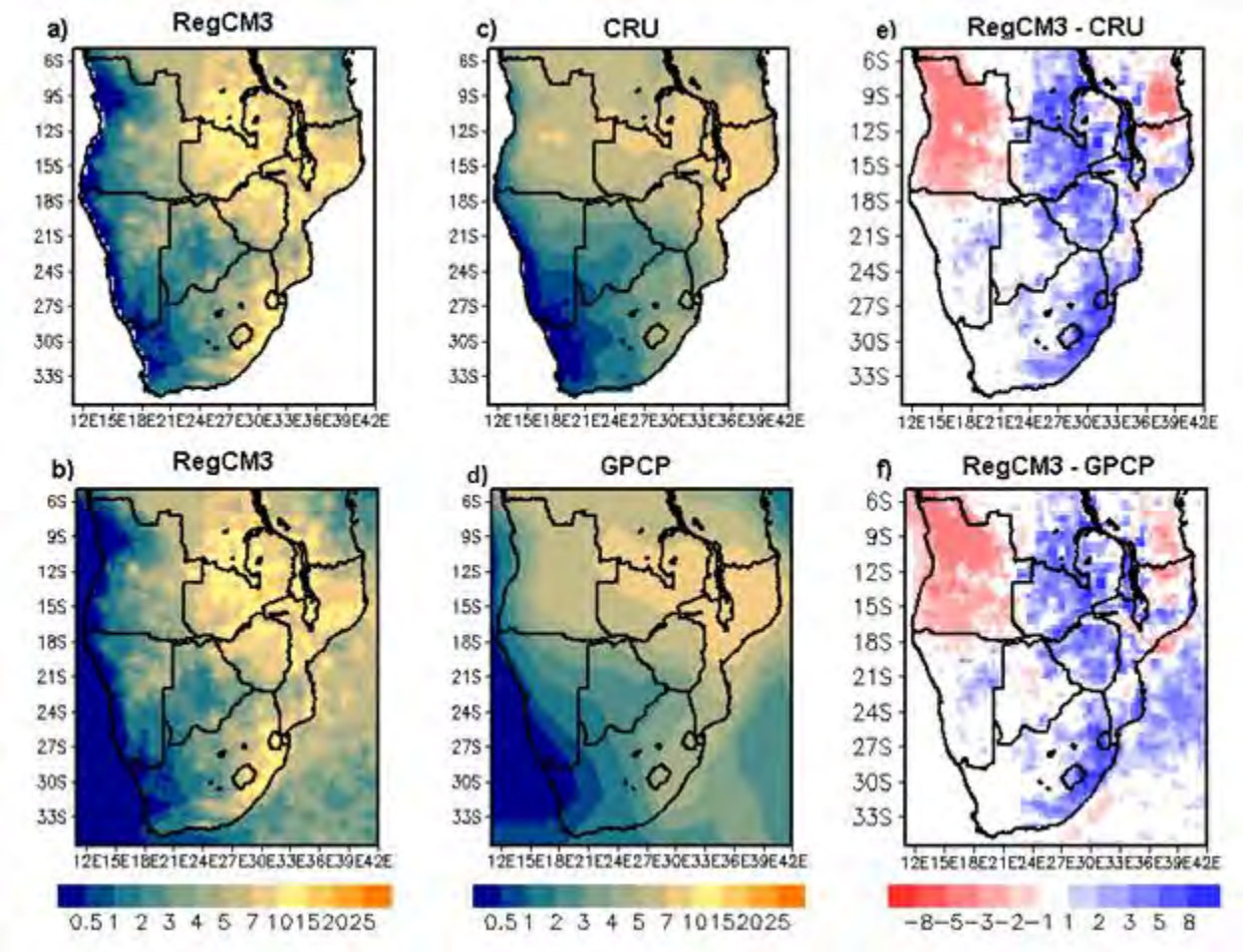

Figure 4.4 Mean total precipitation (mm/day) for December to February (DJF) of all the simulated years. On the left column (a) RegCM3 with precipitation over ocean masked out, (b) RegCM3 with precipitation over ocean; middle column is for (c) CRU, (d) GPCP monthly data and right column is the biases for RegCM3 with the respect to (e) CRU and (f) GPCP.

As for DJF period, the spatial distribution of precipitation is still being produced but the area of overestimation in rainfall widens to cover much of the eastern half of the region (figure 4.4c). Even though the wet biases are high, in comparison with the analyses, the model captures the exact positions for the localised maxima over the northeastern Zambia, northern Mozambique and still shows the persistent wet biases over Lesotho and Swaziland. The model underestimates precipitation over Angola and southern Tanzania (fig. 4.4e and fig. 4.4f). The seasonal variation between the early and late summer is evident from the increase in intensity and more wide-spread rainfall or increase in numerical or grid point storms during DJF period (figure 4.4c).

Thus, in both sub-seasonal periods analysed and over the entire region, RegCM3 does reproduce well the magnitude of rainfall over the southwestern areas and fittingly captures the spatial extent of precipitation over most of the region when compared with the analyses data. RegCM3 persistently overestimates the precipitation over most of the southeastern parts of the region and DRC but underestimates over Angola. During the SON period, the model captures the observed NW-SE band with the maximum precipitation (from DRC to southeastern South Africa). The band inclination could be possibly associated with the tropical temperate troughs that occur during this time (Washington and Todd, 1998). In the DJF period, the model's precipitation distribution is more inconsistent and widespread. There is an increase in the wet biases over the sub-tropics but still maintain west-east spatial gradient as compared to GPCP. Over the adjacent Oceans, the model does fairly well for both the spatial extent and magnitude with some slight biases of ±2mm/day (fig 4.2f; fig. 4.3f and fig. 4.4f). The overestimation of precipitation in the tropics could imply that Emanuel scheme tend to enhance convergence along the ITCZ.

In general, RegCM3 does well in capturing the spatial distribution of precipitation over most of the region. The model does fairly well in reproducing the rainfall magnitudes over the southwestern areas which are generally dry during the austral summer. Some persistent wet biases are observed over the northern and southeastern areas whilst some dry biases occurred over Angola and southern Tanzania. However, it should be noted that CRU tends to underestimate precipitation over tropical areas such as Angola and DRC due to sparse data and a few meteorological observation stations with a few records are available. New et al., (2000) state that where the station density is low, CRU data tends to climatology. The area of wet biases in

the mountainous region of the Lesotho is probably due to the model overestimating the effects of the local orographic forcing. Sylla et al. (2013) confirm this as a common problem in regional models over East Africa as well. Although there are uncertainties in CRU data, it still provides the most useful information about precipitation and variability. CRU and GPCP datasets agree well with each other and have temporal correlation of above 0.7 or higher except over Angola and DRC which is attributed to the sparse number of rain gauge stations in this region (Zhang et al., 2013).

One of the biggest challenges in climate modelling over southern Africa tends to be the simulating of rainfall. Previous studies over southern Africa have shown some substantial wet and dry biases over particular areas of the region (Tadross et al., 2005; Engelbrecht et al., 2009, Mackellar et al., 2009, Tummon et al., 2010; Sylla et al., 2010, 2012; Jack, 2013). Most of the CORDEX Africa project work has also noted these significant biases (Nikulin et al., 2012; Endris 2013; Gbobaniyi, 2013 and Kalognomou, 2013). Despite such a major limitation, some meaningful contribution to regional climate dynamics work has been produced from these studies. Such biases may probably be due to the model set up such as convection parameterization (Crẽtat et al., 2012); boundary conditions, simulated circulation anomalies, and moisture transport (Sylla et al., 2010, 2012; Nikulin et al., 2012; Zhang et al., 2013; Jack, 2013). Kalognomou, (2013) concur and highlighted the following potential sources of bias in each of the CORDEX models: the internal solvers of the models themselves, the physics packages like the PBL, and cumulus schemes as well as their subschemes like trigger, closure, and entrainment functions. Additionally, the representation of the land surface processes and circulations will also have an influence on the model rainfall bias. Thus understanding of the nature of the biases can aid in improving climate model simulations and avoid the translation of errors to model's applications (Sylla et al., 2012).

Optimisation of the RCMs requires very robust testing of the whole model package. In seeking to improve the model's simulation of the real climatology, the challenges come from the model's package itself, choice of domain, convection scheme and moderation of some parameter values (Seth & Giorgi, 1998; Crẽtat et al. 2012; Giorgi et al. 2012; Sylla et al., 2012). Sylla et al., (2012) honestly stated that "*Choice of domain, convection scheme and some parameter values*

also contributed to this improvement, although it is difficult to clearly identify the contributions of these different elements……" In the sensitivity tests over four CORDEX domains using the new RegCM4 model, Giorgi et al. (2012) also show that the model has consistent level of performance in different climatic regimes across the domains although some systematic model biases persist. RegCM4 model shows a significant sensitivity to different parameterizations and parameter settings which can thus be used to optimize model performance over different domains. However, Giorgi et al. (2012) quickly stress that the settings appear to perform generally well over most of these domains, there is still no single parameter setting that performs best in all domains tested; thus conducting a customisation exercise for our very sensitive southern Africa region before carrying out specific model applications will be required.

In future work, there is a need to consider the new reanalyses datasets such as the European Center for Medium Range Weather Forecast (ECMWF) ERA Interim reanalyses (Dee et al., 2011; Uppala et al., 2008) which is now commonly used as a boundary forcing field especially in most CORDEX projects (Nikulin et al, 2012; Gbobaniyi et al., 2013, Endris et al., 2013; Kalognomou et al., 2013). Recent reanalysis datasets have improved through the use four dimensional data assimilation, use of forecast models, ensemble data assimilation increase in the horizontal and vertical resolution as well as extension of the temporal coverage (Zhang et al., 2013).

4.2.3 Model Comparison to Air Temperature

In RegCM3, the air temperature is simulated at 2m level above the surface. Figure 4.5 presents mean air temperature (°C) of the control simulations and from the CRU dataset. In comparison to the CRU dataset, RegCM3 captures well the spatial distribution over most of the region. Noteworthy is how the simulated temperature matches the observation over some high altitude areas, such as Lesotho. Also the model does well in reproducing the magnitude of temperature in the Kalahari and Namib Deserts, Zambezi valley central and southern Mozambique and northwestern South Africa. Cold biases are observed over the northeastern parts of the region and southeastern areas with coldest bias of about 3°C. However, the model overestimates along the west coast of Namibia. The percentage biases for mean air temperature show that there is no

excessive underestimation or overestimation (less than 25%) for the whole region (fig. 4.5c, d). Thus, the temperature biases which are mostly falling within ±2°C are fairly acceptable.

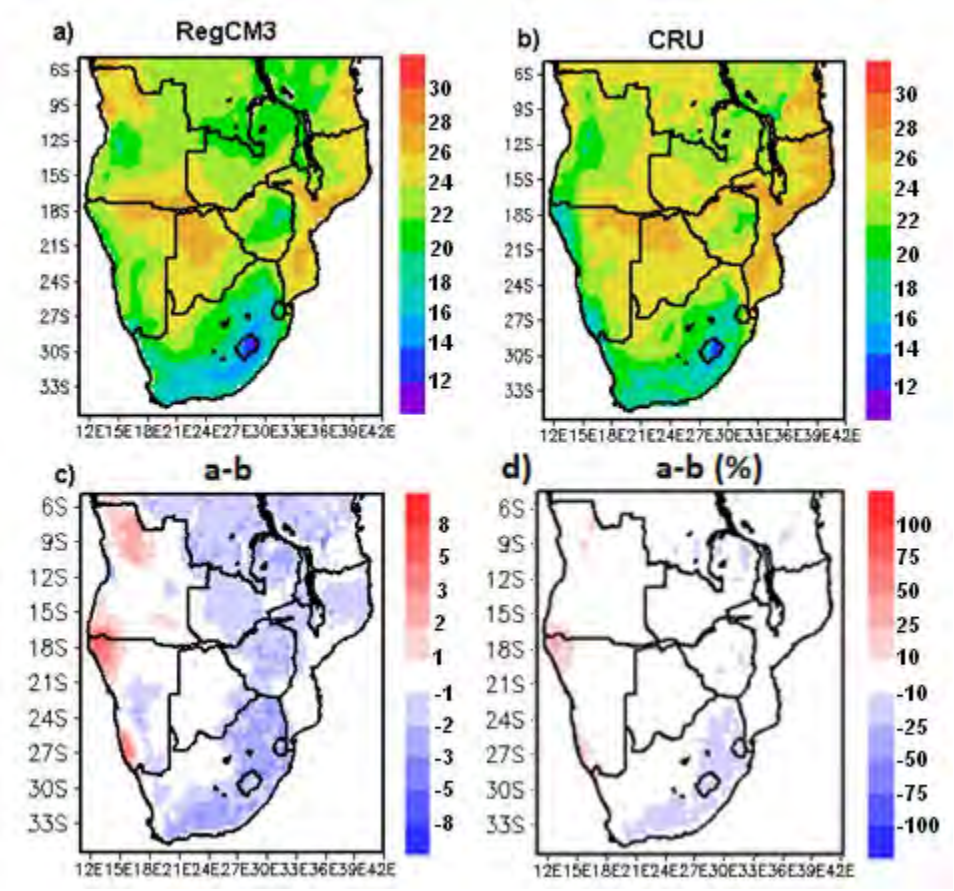

Figure 4.5 Mean Air Temperature (°C) for a) control simulation, RegCM3 and b) CRU data and c) Bias and d) Bias in percentage for the simulations. For temperature anomalies blue means negative and red is positive.

Figure 4.6 shows the both sub-seasonal, SON (fig. 4.6 a, b, c) and DJF (fig. 4.6 d, e, f) spatial representation of the mean air temperature for all the seasons simulated. The model captures well the magnitude and spatial distribution of the air temperature over the bulk of southern Africa as compared to CRU dataset (figure 4.6c). There is a persistent warm bias that occurs over the coast of Namibia (fig. 4.6 c, f). The sub-seasonal variations between the early and late summer analysed (figures 4.6 and 4.7) are well captured especially over the southern parts of the subcontinent where cooler air temperatures are simulated for SON period (fig. 4.6) which is associated with the wet biases observed over the same area for precipitation (fig 4.3a). However, the wet biases observed for SON precipitation do not translate to vital cold biases especially over

DRC with less than 2°C difference between RegCM3 and CRU data. For DJF, the model does well to capture the temperatures particularly the maxima over the Kalahari Desert, Botswana (fig. 46 d). The percentage biases for mean air temperature show that there is no excessive underestimation or overestimation (less than 25%) for the whole region (figures not shown here for brevity as it is almost similar to figure 4.5d)

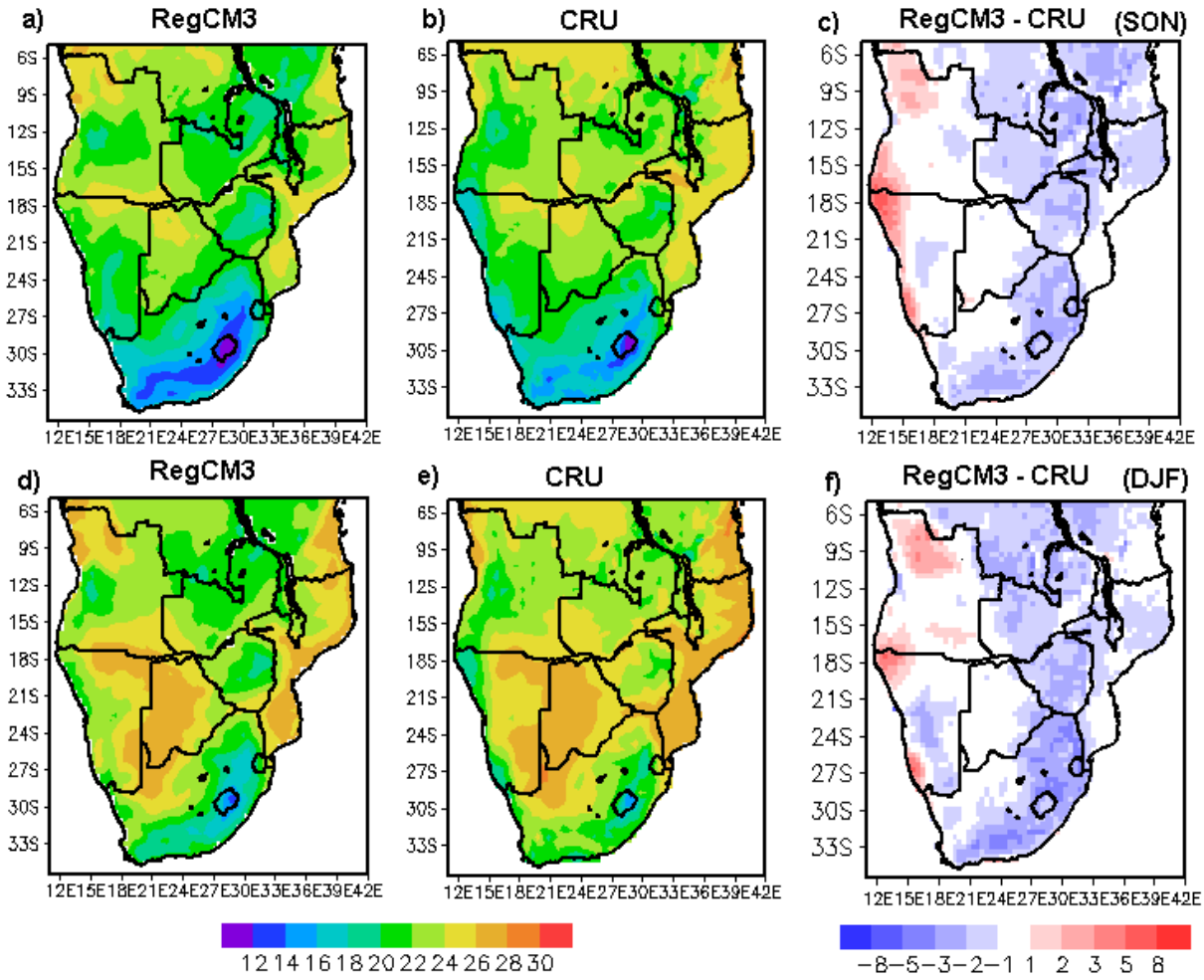

Figure 4.6 Mean Air Temperature (°C) for a) control simulation, RegCM3 and b) CRU data and c) Bias for the for SON period and d) RegCM3 e) CRU and f) Bias for DJF period for all the simulations. For temperature anomalies blue means negative and red is positive.

In general, RegCM3 captures both the spatial distribution and the magnitude of the mean air temperature with most of the existing biases within ±2°C range. The mean air temperature fields show a cold bias at seasonal and sub-seasonal scales. This cold bias in the simulated temperature fields is generally consistent with the corresponding wet rainfall bias. However, although

precipitation is certainly a vital factor in determining of surface temperatures, these cold biases can be attributed to a combination of various climate parameters, including radiation fluxes, clouds, surface albedo and temperature advection (Giorgi et al., 1998; Tadross et al., 2006; Sylla et al., 2012). In addition, dust particles and aerosols affect the insolation that reaches the surface and thus the air temperature (Petersen et al. 2010; Sylla et al. 2010; Tummon et al. 2010). As cited in Sylla et al. (2012) such uncertainties and considering that in most RCMs biases for seasonal surface temperature are within the range of ±2°C, RegCM3 biases are congruent with other state-of-art regional models.

4.2.4 Model Comparison to 10m Wind Fields

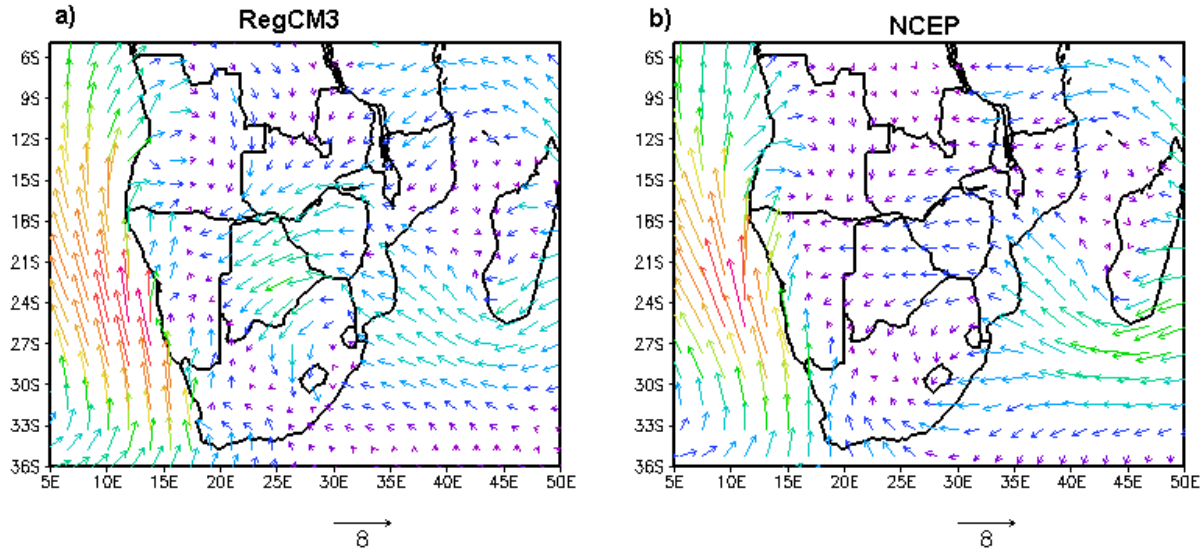

Figure 4.7 The mean 10m wind fields (m/s) of all the years for a) RegCM3 and b) NCEP/NCAR reanalysis 2 data.

The mean wind pattern at 10m above the surface level for the summer seasons simulate stronger winds for RegCM3 (figure 4.7a) than the NCEP/NCAR reanalysis 2 data (figure 4.7b). However, RegCM3 simulates well the main rain bearing circulation airmasses for the region as discussed earlier (see section 2.2 and figure 2.1). Figure 4.7a depicts the monsoonal easterly winds from West Indian Ocean, the southeasterly Trades from the Mozambican Channel and the recurving northwesterly over Angola and DRC (ZAB) which constitutes well the ITCZ position during the summer season (Lindesay, 1998; Tyson and Preston-Whyte, 2000). The areas of convergence are clearer in the RegCM3 over the western areas, through the northeastern parts of the regions and

into the central Mozambican Channel (figure 4.7a). For the NCEP/NCAR reanalysis 2 data, the convergence occurs in the same zones but the winds are lighter and variable over most of the interior region (figure 4.7b). The air circulation is distinctively stronger anticyclonic over Zimbabwe, Botswana and northwestern South Africa (figure 4.7a) than the weaker easterly flow for NCEP/NCAR reanalysis 2 data (figure 4.7b). This stronger northeasterly airflow inland could imply more moisture is advected from the Mozambican Channel. This possibly aids in explaining or relate to the wet and cold biases observed over the southern parts of the region (figures 4.2 and 4.5). Besides the isolated portions of varying wind strengths and weaknesses observed inland, RegCM3 does well in capturing the wind patterns and zones of convergence or divergence.

4.2.5 Summary of Model's Performance

Although the model validation is not so robust, the model's behaviour has been studied using the soil moisture, precipitation, air temperature and 10m wind fields for the 6 seasons of simulations. Besides the precipitation, the other variables do fairly well in capturing the climate dynamics. There is overestimation of precipitation in some areas where there is an underestimation of soil moisture. This is mainly observed over the eastern half of the region (figures 4.1 and 4.2) especially over the higher terrain of the Drakensburg Mountains and Lesotho. This may be attributed to RegCM3 overestimating evapotranspiration. More variables on geopotential, moisture flux and diurnal characteristics will be analysed in the next chapter on synoptic analysis and a close-up review of the January month. Some studies are available that provide an intensive validation of RegCM3 using the same boundary forcings (Sylla et al., 2010,12) and show that the model is able to be used for climate applications even in the presence of some biases. Knowledge of previous studies done over Africa and the region, show that even though the RCMs had some existing significant biases, the RCMs have been able to capture the climate dynamics and those studies have contributed to the regional climate studies over southern Africa and to the regional climate community (Tadross et al. 2006; Mackellar, 2007, Mackellar et al., 2009; Engelbrecht et al., 2009; Tummon et al. 2010; Sylla et al. 2010, 2012; Nikulin et al., 2012, Kalognomou et al. 2013; Jack 2013).

Southern Africa being very sensitive to a change of physical schemes (Crẽtat et al., 2012), lateral boundary forcings (Sylla et al., 2012) and aerosol radiative forcings (Tummon et al., 2010) could also influence the radiative feedbacks. There is also the existence of internal variability in regional model simulations which can influence the daily solution of climate parameters and can be a physical response (Giorgi and Bi, 2000; Kgatuke, 2008 and Crẽtat et al., 2011). In addition to that there are some global and regional climate forcings that also affect the region as discussed in Chapter 1 and 2. ENSO and SSTs cannot be excluded from its influence in the seasons selected in this study as it affects the region's climate (Tyson & Preston-Whyte, 2000; Richard et al., 2000, 2001; Landman & Beraki, 2010). Orlowsky and Seneviratne (2010) statistically analysed the relationship between precipitation, soil moisture and SSTs and found some very strong covariability.

Backed with all this knowledge about RCMs and challenges, some sensitivity experiments were then done. The main goal seeks to provide a clear understanding of the role of seasonal soil moisture on climate variability over southern Africa. The discussion of these results will start by looking at some mean conditions of the six simulations. This is to give credibility to the rest of the findings. To avoid on missing out some information that can be dampened by mean, detailed discussion and comparative analysis will then focus of the two main seasons of interest in this study: 1991/92 as the driest and 1995/96 as the wettest year. These two seasons have been used in many various regional climate studies set-up and will also be the focus for this study so that comparative analysis of the findings can be easily done with other land surface work on vegetation, aerosols and moisture projections (Tadross et al. 2006; Mackellar, 2007, Mackellar et al., 2009; Tummon et al. 2010; Tadross et al., 2010; Jack 2013).

4.3 Spatial and Temporal Analysis of Model's Response to Soil Moisture Perturbations

4.3.1 Temporal Variation of Soil Moisture for dry versus wet seasons

Figure 4.8 shows the temporal variations in the top-layer soil moisture for the summer climate simulations of the chosen dry seasons (1991/92, 1994/95 and 1997/98) and the wet seasons (1995/96, 1996/97 and 1998/99). The control simulation (black line) and interactive wet

simulation (blue) tend to be similar in magnitude and variability for most of the season. The interactive dry run (red) shows the least top soil moisture over the period but tends to vary similarly with the control simulation towards the end. The model can keep different soil moisture levels due to the respective initializations content until around mid-December (figure 4.8).

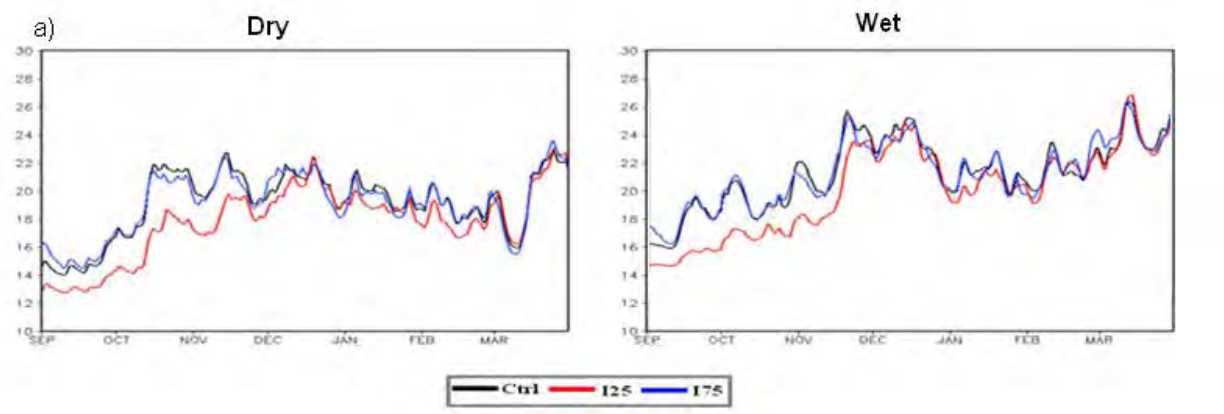

Figure 4.8 Temporal variations in the top-layer soil moisture (mm/day) for 1 September to 31 March of a) dry and b) wet years. The control simulation is represented in black, interactive wet soil moisture simulation is in blue and the dry soil moisture simulation is in red.

For the two different seasons, there is less deviation in top-layer soil moisture amounts between wet run and control simulation throughout the period of analysis (figure 4.8). However, the dry run is distinctively dissimilar from the control (and wet run) during the early part of the season till around end of December. Less deviation in the top soil moisture is observed between the different initialisation experiments in late summer, although the dry run experiment still deviates to lower top-layer soil moisture levels than the other two simulations particularly for dry runs (figure 4.8a). Towards the end of March, the three simulations seem to be similar or approaching same top soil moisture levels. This can aid in explaining the soil moisture retention capabilities of the model throughout the season. There is greater sensitivity to the dry soil moisture perturbation simulations during early summer whilst slight deviations occur with wet soil moisture perturbations.

From January, persistence of the dry run's lower top-layer soil moisture levels is shown to persist more for the dry seasons (figure 4.8a) as compared to the wet seasons (figure 4.8b). The

temporal evolution of the soil moisture gives useful information which cannot be easily detected from the spatial maps. The soil moisture variation though is reassuring in that it shows that RegCM3 does not merely present its internal variability (Giorgi and Bi, 2000; Kgatuke et al., 2008 and Crẽtat et al., 2011). This probably creeps in after mid-season period (December or January) were some mixed responses start to occur. Thus an idea of how long the soil moisture retention period can be detected from these responses with the dry perturbation seemly persisting for longer. Pal and Eltahir, (2002) found out that dry soil moisture conditions result in stronger persistence of drought or drier condition during a dry season compared to the wet season over USA. Fischer et al. (2007) concur with their findings but applied over the 2003 Europe heat wave. It is also interesting to note that the mean conditions tend to be almost similar to the variability of 1991/92 but with slightly higher magnitude by a factor of about 1.5mm/day. The converse is not so true for the mean soil moisture of the wet runs which is almost similar to 1995/96 and 1998/99 (not shown here) trends.

4.3.2 Spatio-temporal Analysis of Mean Precipitation for dry versus wet seasons.

Figure 4.9 shows the mean total precipitation spatial maps for the a) dry and b) wet perturbations using dry seasons on the left as well as c) dry and d) wet perturbations for the moist seasons on the right column. The mean states of the interactive dry soil moisture perturbations generally show a slight decrease in precipitation over most of the region (figure 4.9a, c). Marked decrease is only found over Angola. There is no response over the western coastal areas with some slight increases in total precipitation over some parts of the southwestern areas and Lesotho and the Drakensberg Mountains. As shall be discussed in more detail later, the southwestern areas receive more of their precipitation during the austral winter such that during the summer period any semblance of moisture introduced might result in moistening of the already dry soils.

The wet soil moisture perturbations for the dry seasons show some slight increases occurring over the northeastern half of the region (fig. 4.9b) and marked increase of positive anomalies are observed over the sub-tropics of between 2-4mm/day and is statistically significant at 95% confidence level. The southwestern areas are again not showing any response with the other sections depicting negative precipitation responses especially over Kalahari and the Namib

Deserts. As for the wet soil moisture perturbations with the wetter seasons, the portion over the southern parts of the region shows that decreases in precipitation is more widespread in southeastern areas through Botswana, northeastern Namibia and southern Angola (fig. 4.9d).Some statistically significant increases in precipitation at 95% confidence level occur from the sub-tropics around central Zimbabwe into Zambia and eastern Angola.

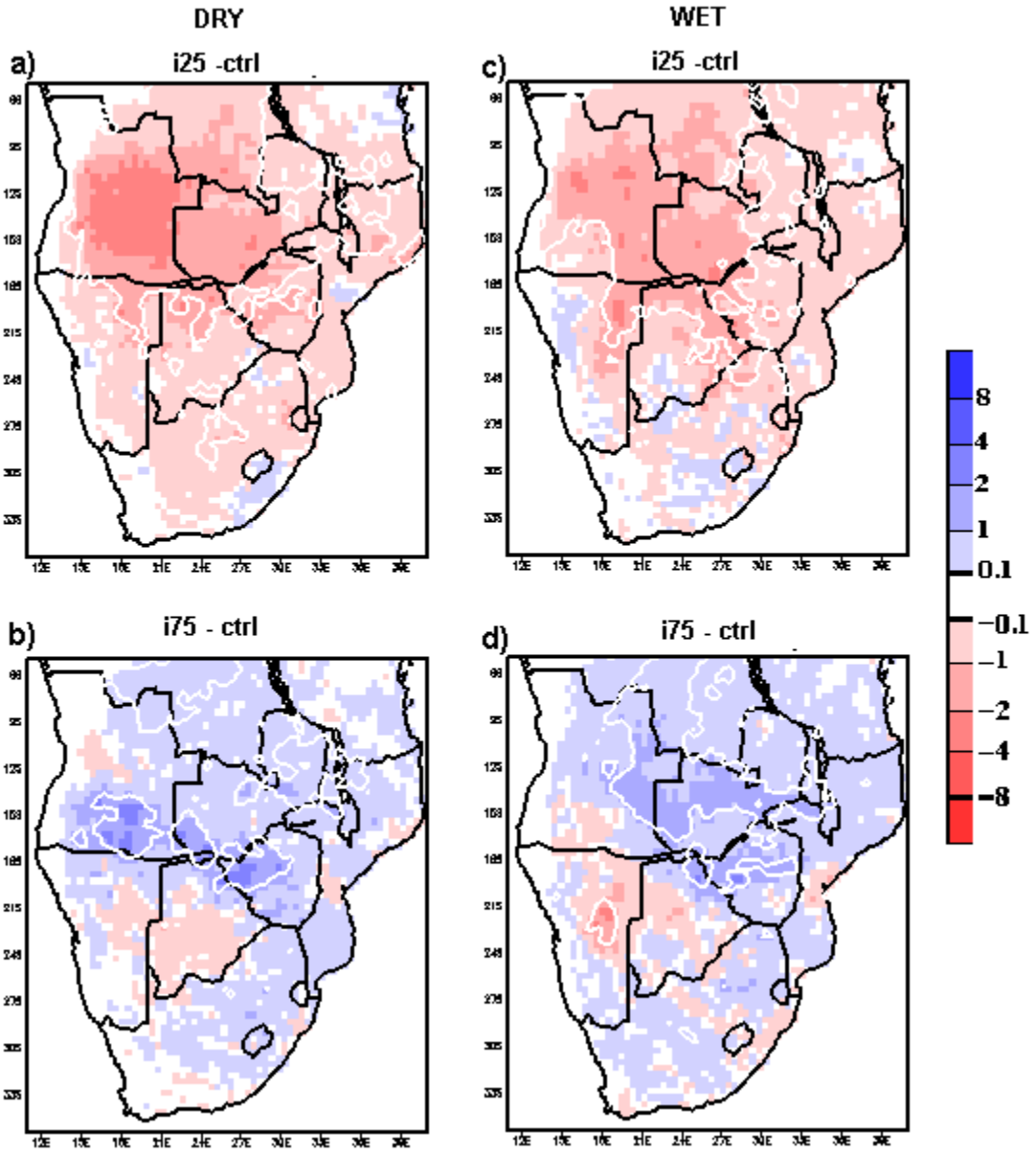

Figure 4.9 Mean Total Precipitation for the dry years on the left column with a) dry perturbation minus control; b) wet perturbation minus control; and for the wet seasons on the right column c) dry perturbation minus control; d) wet perturbation minus control. White lines enclose areas that are statistically significant at 95% confidence level.

Generally, the mean precipitation responses to dry soil moisture perturbations result in decrease over much of the region for either the dry or wet seasons. Stronger responses are observed during drier seasons than the wet seasons whilst mixed responses in total precipitation occur over the southwestern parts of the region. The northern areas depict a positive response to the wet soil moisture perturbations. The mean precipitation anomalies generally show slight responses to soil moisture feedbacks as some of the signal is probably cancelled out within the mean. The feedback mechanism is not quantified here and it should be pointed out as well that there are other small-scale or local forcings that can lead to the responses shown here. Jack (2013) used an RCM and a Lagrangian model to identify some land surface moisture sources. The study found that a major moisture source is located over South Africa. Coupled with the El Niño effect and other large-scale forcings it then aids us to explain the mixed responses of precipitation that occur over southern parts of the region with a wet soil moisture perturbation. This clearly shows that soil moisture-rainfall feedback mechanism is not linear and more complex with other climate forcings contributing to precipitation moderation.

The spatial extent of the mean total precipitation does not fully give us insight into how the precipitation evolves over time with the soil moisture initialisation. Thus a temporal representation of the mean total precipitation responses for the control, dry soil moisture and wet soil moisture runs are analysed (fig 4.10). Comparison of the mean precipitation shows that it is highly variable throughout the seasons. The responses are somewhat clearer during the early part of the summer season after initialisation with wet soil moisture perturbations having a slightly higher soil moisture magnitude and a distinct lower soil moisture amount for the dry run. By December, perturbations in the wet seasons tend to fizzle out and mixed responses are observed from thereon (fig. 4.10b). Whereas for dry seasons a strong or marked decrease in mean precipitation is depicted until late January when the initial perturbations decrease and mixed responses occur then the three experimental responses are totally similar by end of February.

The seasonal variation of the precipitation responses due to soil moisture initialisation depicts strong and persistent response during a dry season as compared to the wet season. This supports earlier findings in other parts of the world where dry soil moisture conditions enhanced a dry

spell or drought persistence during a dry year (Pal and Eltahir, 2002; Fischer et al., 2007). The responses to soil moisture obtained also help us to support the fact that the RegCM3 is presenting its internal shift. One can also infer that after the gradual phasing out of the soil moisture perturbations there are other factors that play a part in modulating the precipitation and intra-seasonal dry spells (one spell is depicted to be around mid-January for both seasons) as indicated by the sudden drop in rainfall amounts (fig. 4.10).

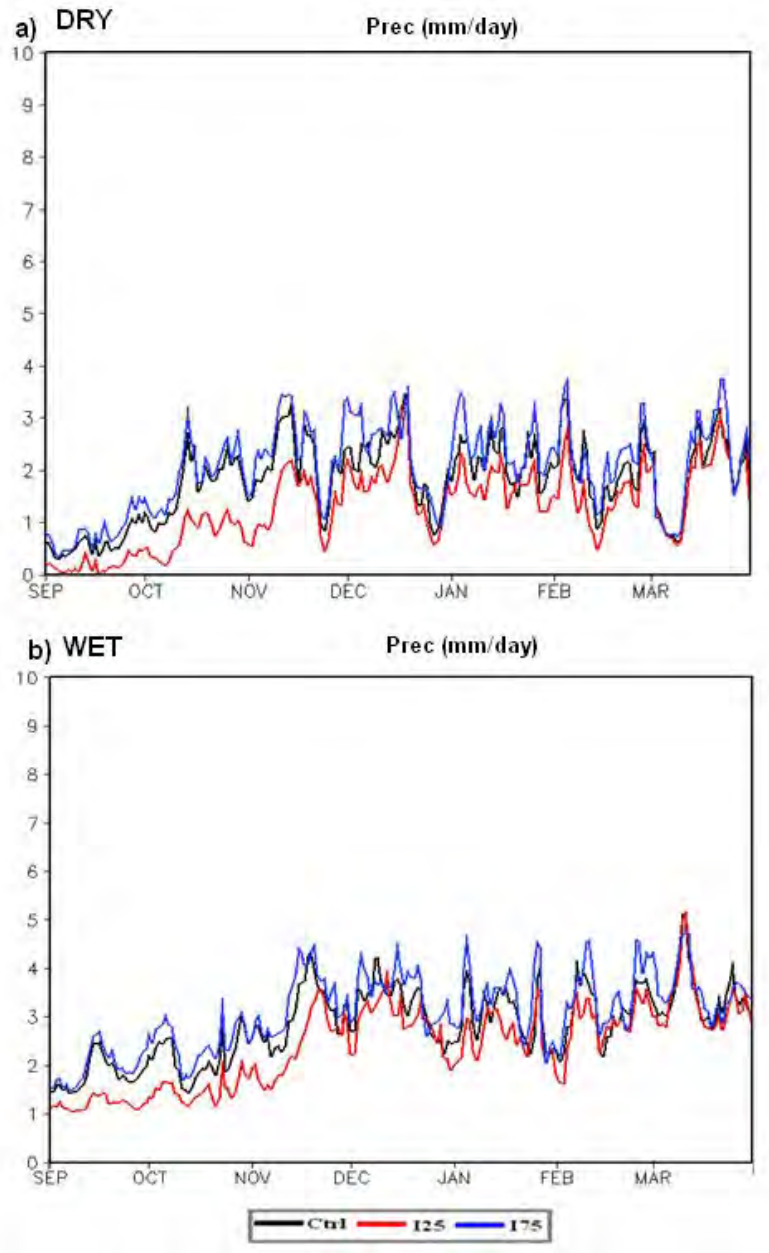

Figure 4.10 Temporal variations in the mean total precipitation (mm/day) for the control, dry and wet soil moisture perturbations for the a) dry season and b) wet season. The control simulation is represented in black, interactive dry soil moisture simulation is in red and the wet soil moisture simulation is in blue.

4.3.3 Spatio-temporal Analysis of Mean Surface Temperature for dry versus wet seasons.

Figure 4.11 shows the mean surface temperature responses to dry and wet soil moisture perturbation with respect to the control simulation for dry seasons on left column; a) dry run; b) wet run and for wet seasons on the right column with c) dry run and d) wet run. The ground temperature responses (fig. 4.11) to soil moisture tend to be clearer as compared to the precipitation responses (figs. 4.9 and 4.10). For dry soil moisture initialisation during the dry seasons, there is a spatially cohesive increase in air over most of the region with strong increases over northwestern Zambia and eastern Angola (fig. 4.11a). Some slightly negative responses occur over the western coastal areas. The wet soil moisture perturbation also depicts a spatially cohesive decrease in surface temperature over most of the region except for the western coast of Namibia.

As for the wet season, the dry soil moisture perturbation still shows positive responses over most of the region except for the southwestern areas were mixed responses to surface temperature occur (fig. 4.11). Some portions depicting no response to the wet soil moisture perturbation occur over central South Africa with generally a decrease in ground temperature over much of the region (fig. 4.11d). The area with no response to the wet soil moisture perturbation cannot be clearly explained. However, one can infer this to be a possible effect from the wet precipitation biases that were observed over that area (fig. 4.2). The area can be too wet such that any more moisture will not enhance precipitation increases or dampen the ground temperature further when moist or near-saturation conditions already exist. Such can be the limitation of biases; however there are other forcings than can affect the temperature fields such as altitude, cloud cover and radiative energy fluxes.

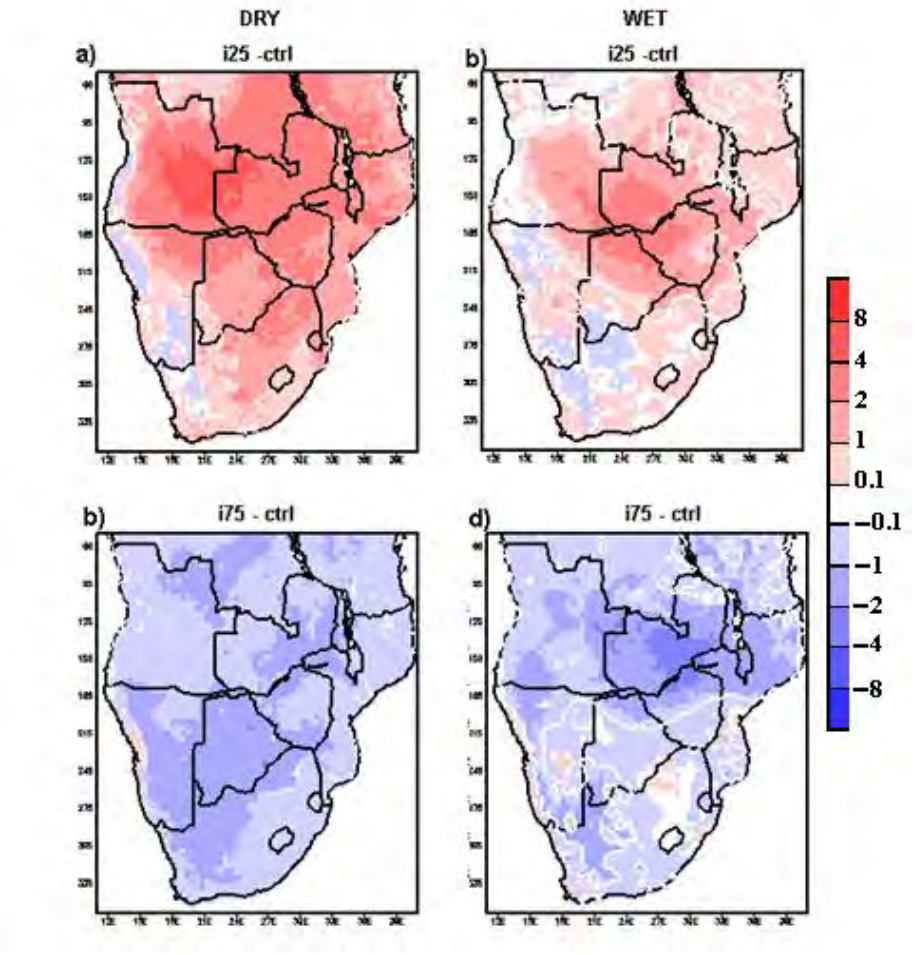

Figure 4.11 Mean Surface Temperature (°C) for the dry seasons on the left column with a) dry perturbation minus control; b) wet perturbation minus control; and for the wet seasons on the right column c) dry minus control; d) wet minus control. For temperature fields, blue indicate decrease or negative responses whilst red is for an increase or positive response. White lines enclose areas that are statistically significant at 95% confidence level.

The temporal evolution of mean surface temperature clearly shows distinct responses for the 25% or 75% soil moisture initialisation in comparison with the control simulation for both dry and wet seasons (fig. 4.12). The magnitude is distinctively higher for the dry soil moisture initialisation until late into the summer season. This seasonal behaviour of the ground temperature also aids in explaining why there is such spatially cohesive responses observed in surface temperature to the dry soil moisture perturbations. The strong responses to dry soil moisture initialisation are evident in the marked magnitudes from the control or wet simulations during the early summer period (fig. 4.12).

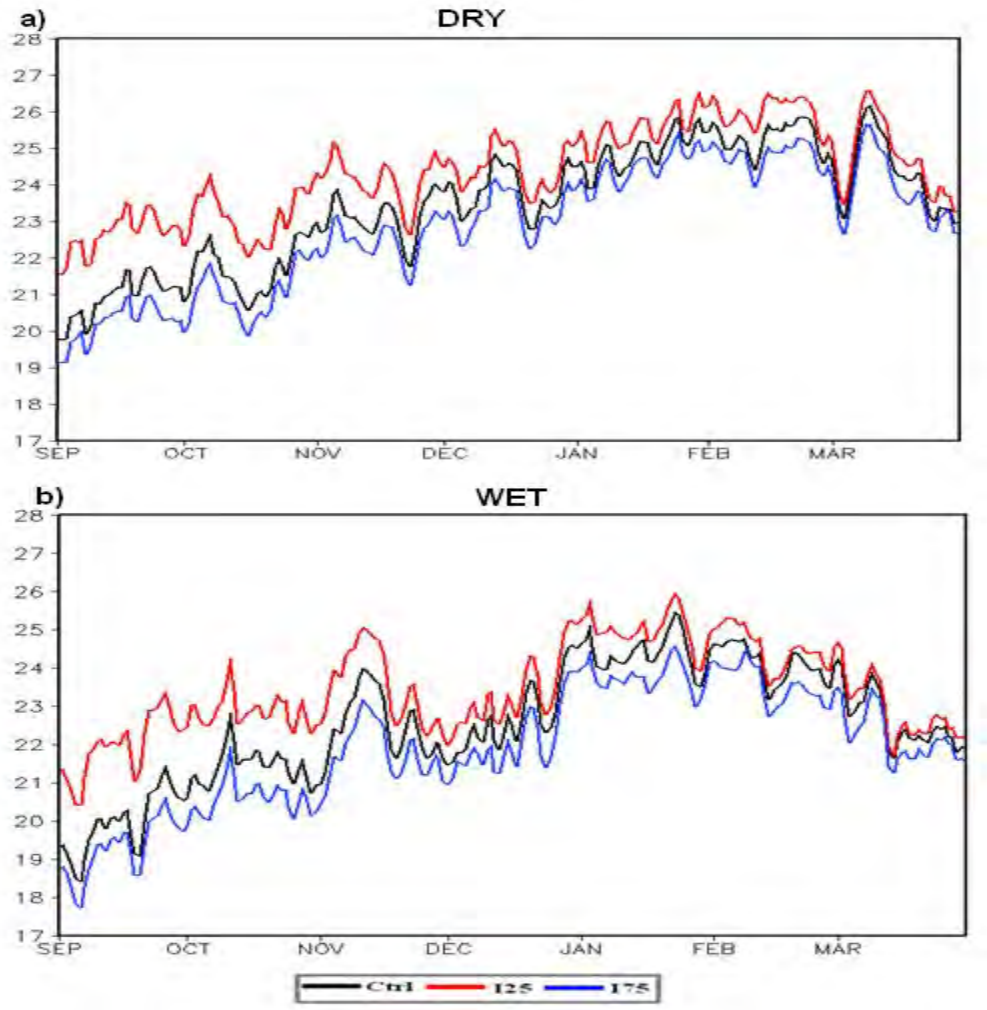

Figure 4.12 Temporal variations in the mean surface temperature (°C) for the control, dry and wet soil moisture perturbations for the a) dry season and b) wet season. The control simulation is represented in black, interactive dry soil moisture simulation is in red and the wet soil moisture simulation is in blue.

4.3.4 Summary of spatio-temporal analysis of the dry versus wet seasons

The spatio-temporal analysis of the dry seasons (1991/92; 1994/95 and 1997/98) and wet seasons (1995/96, 1996/97 and 1998/99) using the mean fields of soil moisture, total precipitation and surface temperature gives an insight into the role of soil moisture for the two important parameters within the regional climate community. Weak and mixed responses are observed with total precipitation. There is a clearly a positive response to soil moisture for surface temperature (also reflected in soil moisture) and it persists longer than the rainfall signals especially in dry seasons. Although not quantified through mean conditions used here, there is some discernible

role of soil moisture over southern Africa. The responses cannot be outrightly concluded to be positive feedback mechanism as there are some parts of the region such as the southwestern areas that do not show any response with rainfall changes and maintained a decrease in surface temperature for both soil moisture experiments. This is also evidenced in the top-layer soil moisture spatial responses (figures not shown here for brevity). Although the areas of interest for further studies are being identified, there is need to explore in more detail the soil moisture perturbations and also look at other surface variables that are influenced by soil moisture. Thus from the 6 years simulated, the detailed analysis will focus on 1991/92 (driest season) and 1995/96 (wettest season).

4.4 Sensitivity Analysis of the Driest and Wettest Season

4.4.1 Total Precipitation

Figure 4.13 shows total precipitation anomalies for interactive experiments from the control for 1991/92 (left column) and 1995/96 (right column). There is reduced total precipitation over the subcontinent during the 1991/92 summer season for the dry soil moisture perturbation. Marked decreases of more than 4mm/day occur over Angola (figure 4.13a). Few isolated areas show an increase in total precipitation anomalies over southeastern South Africa, Lesotho and southwestern Botswana. Summer of 1995/96 exhibits vast parts of the region under reduced rainfall for the dry soil moisture run (figure 4.13b) but of a lesser magnitude than for 1991/92 season (figure 4.13a). A large portion of the southern parts of the subcontinent display slight increases in total precipitation anomalies particularly over South Africa, southern Botswana and Namibia. Statistical significant decreases in total precipitation anomalies at 95% confidence level occur over the northern parts of the subcontinent.

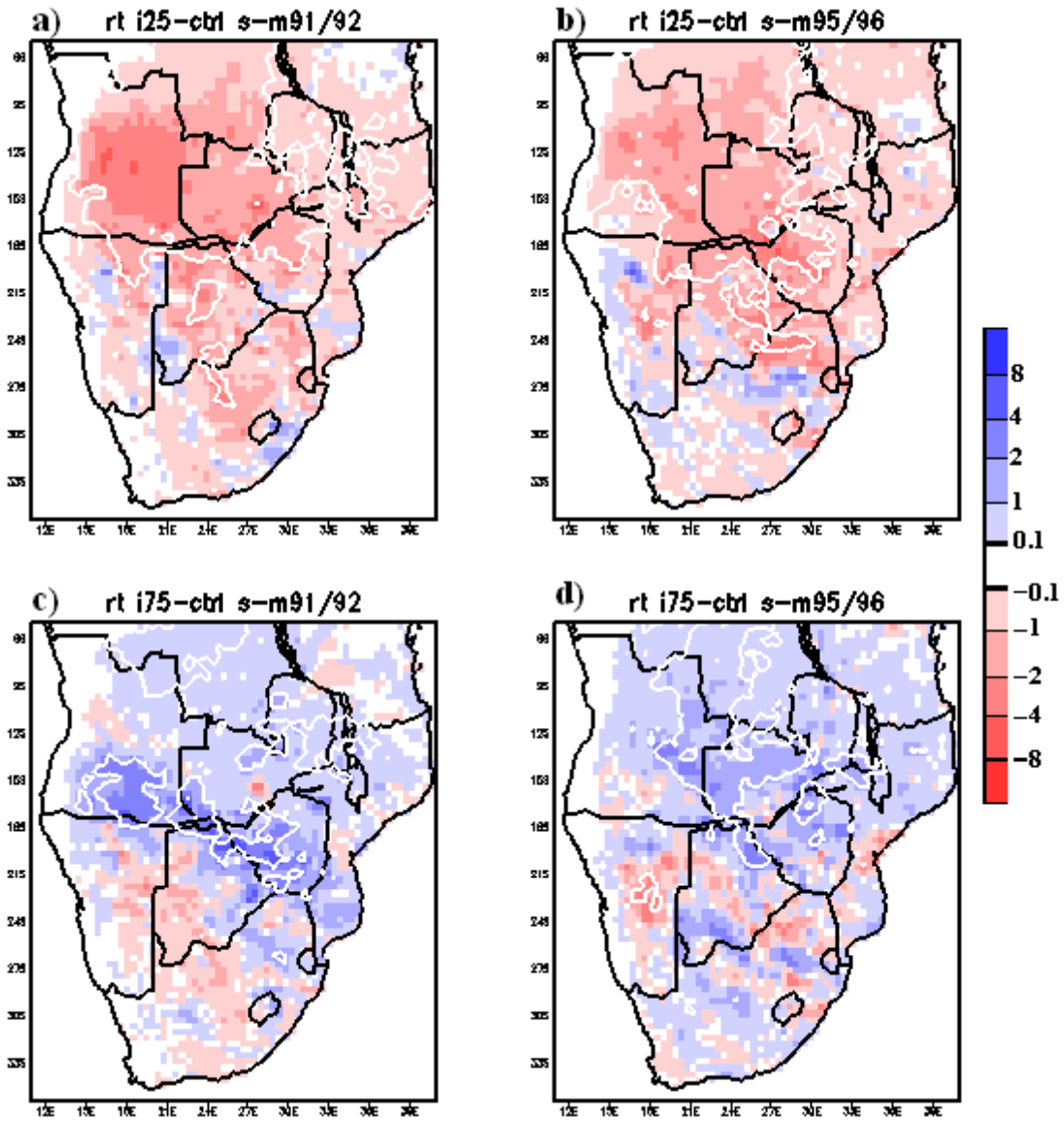

Figure 4.13 Total precipitation anomalies for interactive experiments for 1 September to 31 March 1991/1992 for a) dry run and b) wet run as well as for c) dry run and d) wet run for 1 September to 31 March 1995/1996. White lines enclose areas that are statistically significant at 95% confidence level.

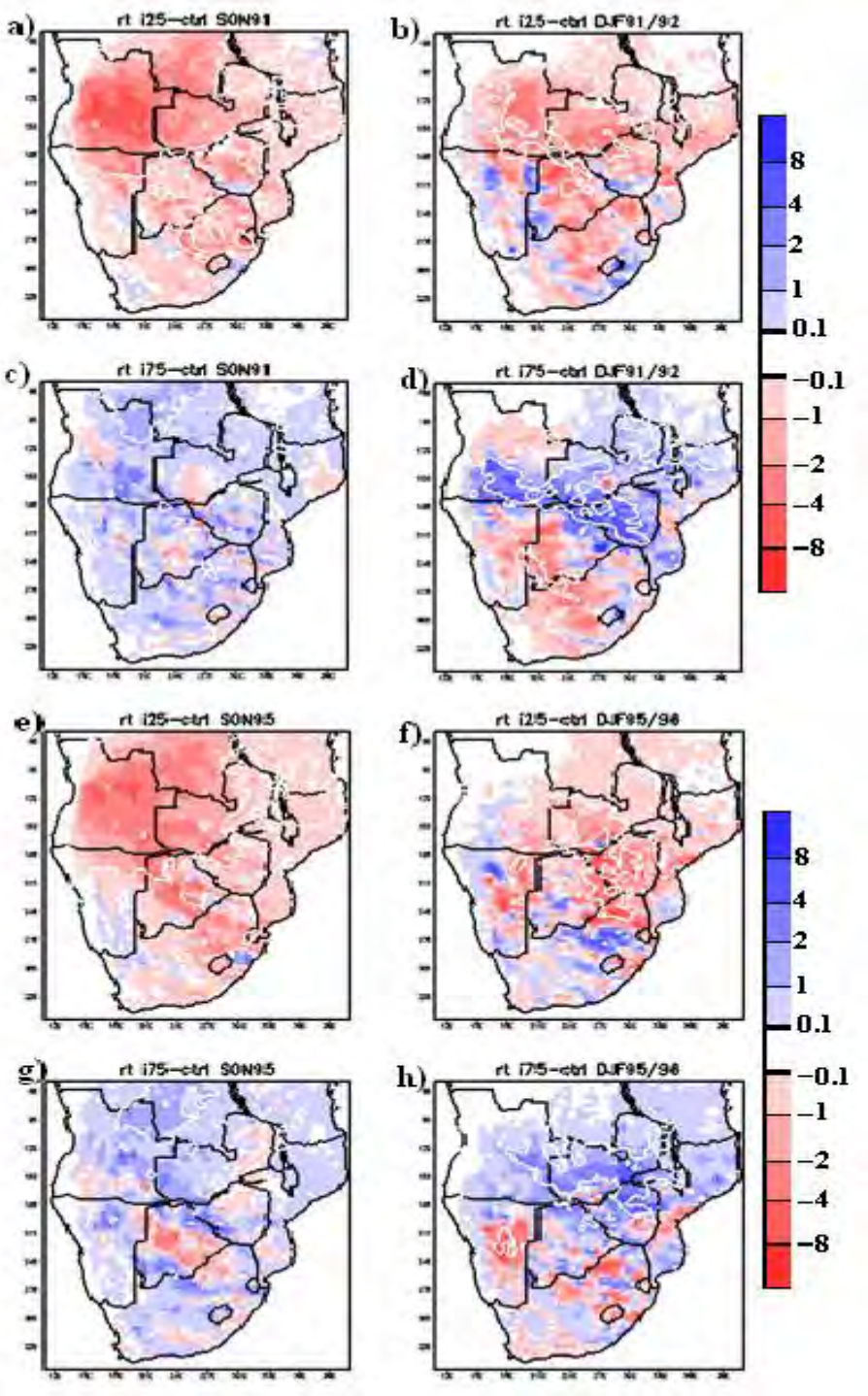

Figure 4.14 Anomalies of total precipitation (mm/day) for early summer, September to November, SON (left column) of 1991 and 1995 as well late summer, December to January, DJF (right column) of 1991/1992 and 1995/96. These are for all experiments of interactive dry perturbation (first and third rows) and interactive wet perturbation (second and bottom rows). White lines enclose areas that are statistically significant at 95% confidence level.

Anomalous wet soil moisture simulation for summer 1991/92 shows increases in total precipitation anomalies over most of the region except for the southwestern parts where some slight decreases in precipitation occur (figure 4.13c). Marked increases with precipitation of more than 8mm/day occur over the central parts of the subcontinent covering southwestern Angola, southern Botswana and southwestern Zimbabwe (figure 4.13c). This is quite higher than the mean state (fig. 4.9c). Wet run for 1995/96 season (figure 4.13d) depicts more widespread increases in positive total precipitation anomalies over southern Africa as compared to 1991/92 (figure 4.13c). Marked increases in total precipitation over the northern areas and in southwestern Botswana (figure 4.13d). However small portions over the southern parts of the region, northeastern Namibia, central Botswana and northern South Africa exhibit decreases in total rainfall anomalies.

For both seasons, no major changes in precipitation occur over the coastal areas, falling within the transitional zone between decreases and increases of rainfall. A very small portion of the region is showing statistically significant increases in precipitation for anomalous wet soil moisture conditions. At longer time scales (seven months simulations compared to the one month simulation, Tadross et al., 2010), total rainfall responses to soil moisture perturbations exhibit cohesiveness in spatial distribution, with dry runs resulting in reduced rainfall over the region and wet runs leading to increase in rainfall over most of the region(figure 4.13). Dry soil moisture perturbation experiment results in stronger responses for reduction in total rainfall during drier 1991/92 than wetter 1995/96 season (figures 4.13a and 4.13b). However, the converse is not so apparent for wet soil moisture perturbations (figures 4.13c and 4.13d).

Figure 4.14 depicts spatial distribution anomalies of total precipitation (mm/day) for early summer, September to November, SON of 1991 and 1995 (left column) as well late summer, December to January, DJF of 1991/92 and 1995/96 (right column). These are for all experiments of interactive dry soil moisture perturbation (first and third rows) and interactive wet soil moisture perturbation (second and last rows). Interactive dry soil moisture anomaly of SON 1991 exhibits a decrease in total precipitation over most of the region with marked decreases

occurring over Angola (figure 4.14a). Although still exhibiting generally a decrease in total precipitation in late summer 1991/92 (figure 4.14b), there is a marked increase in total precipitation in some portions over the south of the region. Areas depicting statistically significance at 95% confidence level are mostly confined to the north of the subcontinent particularly the area of marked decrease in precipitation over Angola (figures 4.13a and 4.13b).

For the wet soil moisture initialisation experiment, SON 1991 shows slight to moderate increases in total precipitation over the subcontinent with some isolated portions of reduced rainfall (figure 4.14c). DJF 1991/92 (figure 4.14d) depicts increases in total precipitation being confined to central and northeastern parts of the region. Although not statistically significant, negatives anomalies occur over the southwestern areas. No major change occurs over Western Cape and northwestern portions of the region (figure 4.14). This occurs in all the experimental setups of 1991/92 regardless of the anomalous forcing. This gives an insight into an area that would require further sub-regional analysis as the same straits were observed with the mean conditions of the 6 seasons analysed earlier (figure 4.9). Very little portions of the region show statistical significance at 95% confidence level for total precipitation anomalies.

As for anomalous dry soil moisture simulation of SON 1995 (figure 4.14e), there is negative total precipitation for the whole region except for the southeastern and southwestern portions where some slight increases in total precipitation occurs. The areas that are statistically significant at 95% confidence level are confined to the northern parts of the region. As for DJF 1995/96 (figure 4.14f), most of the region exhibits a reduction in rainfall except for the southwestern part of the subcontinent especially over South Africa, Botswana and Namibia. As compared to early summer (SON95), the area under reduced precipitation is diminished although the greater part of west and south areas depict increases in total rainfall. Very small and isolated portions of the region are statistically significant at 95% confidence level.

Figure 4.14g displays anomalous wet soil moisture condition of early summer 1995 which depicts a general increase in total precipitation anomalies over most of the continent except for most of Botswana, northern Zimbabwe, Swaziland and northeastern half of South Africa where decreases in total precipitation occur. Late summer of 1995/96 (figure 4.14h) still shows an

increase in rainfall over much of the region for the wet soil moisture run. However, compared to early summer, there has been an extension in area and magnitude over most of the south of the region where decreases in total precipitation are shown. Notable reduction in total precipitation of more than 8mm/day occurs over central Namibia and southeastern Zimbabwe (figure 4.14h). Whereas notable and significant increases in total precipitation anomalies only occur over northern Zimbabwe, Zambia and southeastern Angola.

In general, the persistence of drier conditions under the anomalous dry soil moisture perturbations occurs more strongly during the dry 1991/92 summer season as compared to the wet 1995/96 season (figure 4.14). This suggests that a dry year is more responsive to soil moisture perturbations than a wet year. This concurs with earlier findings that droughts persist under anomalous dry soil moisture conditions (Namias, 1988; Matarira, 1990a; Eltahir and Pal, 1996; Pal and Eltahir, 2001; Fischer et al., 2007; Kim and Hong, 2007). In anomalous wet soil moisture perturbations, early summer tends to show positive response to total precipitation over the bulk of the subcontinent for both seasons (figures. 4.14c and 4.14g). Late summer period (figures. 4.14d and 4.14h), tends to have mixed responses especially over southern parts of the region. Most of the positive responses in total precipitation are confined to the northern parts of the region. In comparison to the mean seasonal anomalies (figure 4.13), the dry (wet) soil moisture run of early summer 1991/92 (figures 4.14a and 4.14c) mainly contribute towards the mean spatial distribution of the dry (wet) run for 1991/92 than the late summer dry (wet) run pattern. Whereas, the mean spatial distribution of seasonal rainfall anomalies for 1995/96 (figure 4.13b and 4.13d) is very similar to that of late summer 1995/96 (figure 4.14f) for the dry soil moisture initialisation. However, for the wet soil moisture simulation for 1995/96 (figure 4.13d), the mean season spatial distribution's inclination to either early or late summer of 1995/96 (figures 4.14g and 4.14h) is not apparent. Thus, one can infer that the wet soil moisture initialisation experiment is less responsive or does not influence spatio-temporal rainfall patterns in a wet season whilst the converse can be true in a dry season. In addition, the influence of this anomalous forcing is more apparent during early summer for the anomalously dry soil moisture initialisation. To substantiate the latter, a look at the temporal responses of the total rainfall to the soil moisture perturbations in comparison to the control simulation is essential. It should be

noted that although there is some differences in magnitude, this is the general response that is observed for the other seasons not presented here.

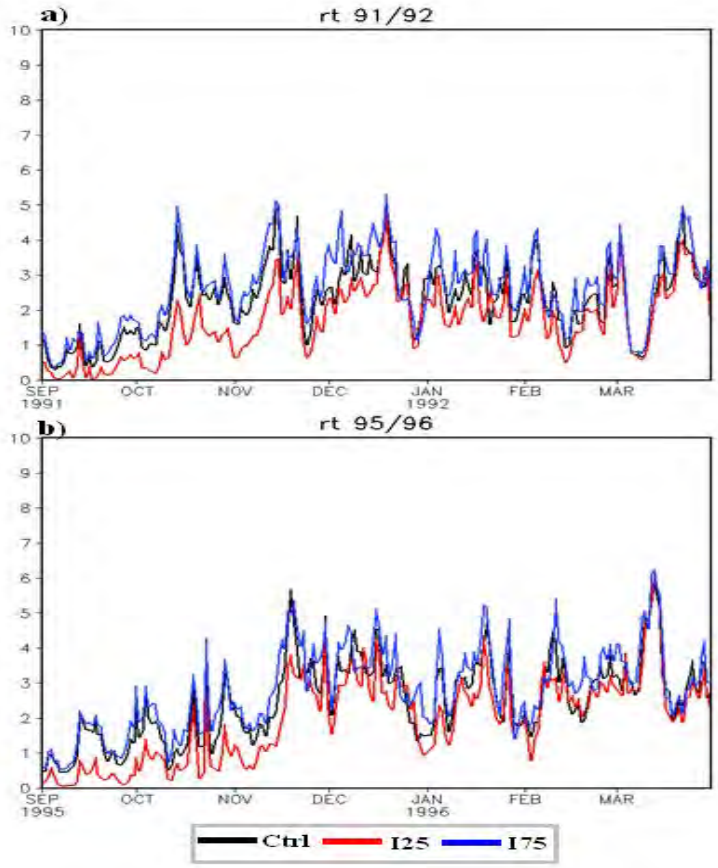

Figure 4.15 Temporal variations in the total precipitation for 1 September to 31 March of a) 1991/92 and b) 1995/96 seasons. The control simulation is represented in black, interactive dry soil moisture simulation is in red and the wet soil moisture simulation is in blue.

Figure 4.15 displays the temporal variations in the total precipitation from 1 September to 31 March of a) 1991/92 and b) 1995/96 season. Both time series show highly variable total precipitation for all the experiments. The variation follows a similar pattern for the three different simulations with the maximum and minimum values of precipitation coinciding at their occurrence throughout the season. The dry soil moisture perturbation has the uniquely lower precipitation than the control simulation for most of the period of study particularly during the early season. This substantiates the fact that anomalous dry forcing shows stronger coupling between the dry surface and the atmosphere. This can be associated with enhancing anticyclonic circulation development which leads to rainfall reduction and warm weather which under

persistence or extreme catastrophe can lead to heat waves (Tyson and Preston-Whyte, 2000; Fischer et al., 2007). Whilst, the wet soil moisture perturbation experiment shows the highest peaks of all (fig. 4.15). From end of February 1992 (fig. 4.15a), the three experiments tend to follow similar pattern in agreement with the top-layer soil moisture (fig. 4.8) and the mean seasonal total precipitation (fig. 4.9) temporal distribution. From early February 1996 (fig. 4.15b), total precipitation shows similar traits for the three simulations or overshooting or intermingling between the simulations. This can help explain the spatially mixed responses of total rainfall to the soil moisture perturbations during late summer which can be inferred as a dissipation in the initial soil moisture perturbation that affect mostly early summer precipitation. This is similar to the temporal trends observed with the mean seasonal total precipitation analysed earlier (fig. 4.8).

4.4.2 Surface Temperature

Figure 4.16 displays surface temperature (°C) anomalies for interactive soil moisture perturbation experiments of 1 September to 31 March 1991/92 and 1995/96 seasons respectively. The surface temperature shows some consistency in its distribution that is in accordance with the dry or wet soil moisture perturbation (figure 4.16). Anomalous dry soil moisture initialisation shows generally an increase in surface temperature over most of southern Africa except for the southwestern areas.

The intra-seasonal analysis shows almost similar spatial distribution of surface temperatures, figure 4.17. However, for dry soil moisture perturbation, early summer, SON1991 (figure 4.17a) shows stronger responses in positive surface temperature than SON1995 (figure 4.17e) especially over southeastern Angola, western Zambia and southern DRC. Similar stronger responses in surface temperatures occur in late summer (DJF) but with broadened area of negative surface temperature anomalies over the south of the region in DJF 1995/96 (figure 4.17f) relative to DJF 1991/92 (figure 4.17b). Southeastern Angola and southern Zambia display extensive increases greater than 8°C. Southwestern areas of the region show similar responses in the decrease of surface temperature for the intra-seasonal maps (figure 4.17) like in the seasonal means for dry soil moisture simulation anomalies analysed earlier (figures 4.16a and 4.16b). This is mostly dry

or semi-arid regions which could imply that any form of perturbation moistens the soils and thus lead to temperatures being suppressed.

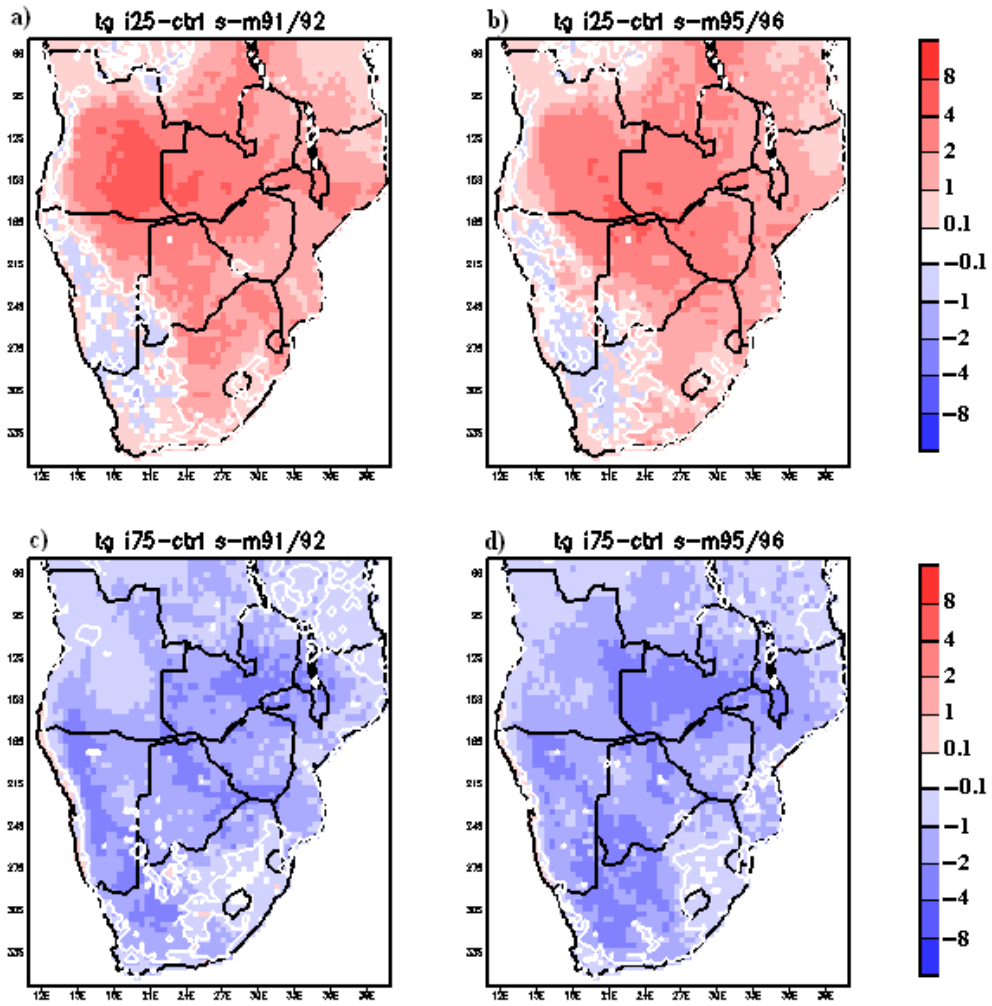

Figure 4.16 Surface Temperature (°C) anomalies for interactive experiments for 1 September to 31 March 1991/1992 of a) dry and b) wet perturbations and for 1 September to 31 March 1995/1996 of c) dry and d) wet perturbations. White lines enclose areas that are statistically significant at 95% confidence level.

Anomalous wet soil moisture conditions depict negative surface temperature anomalies from the control simulation for early summers i.e. SON91 and SON95 (figures 4.17c and 4.17g). Strong negative surface temperature responses occur over Namibia, Botswana and western South Africa within the 4°C to 8°C range. The vast portion of southern area still shows significant decreases in surface temperature anomalies. Late summer (DJF91/92 and DJF 95/96) still depict decreases in surface temperature for most of the subcontinent with notable responses occurring over western

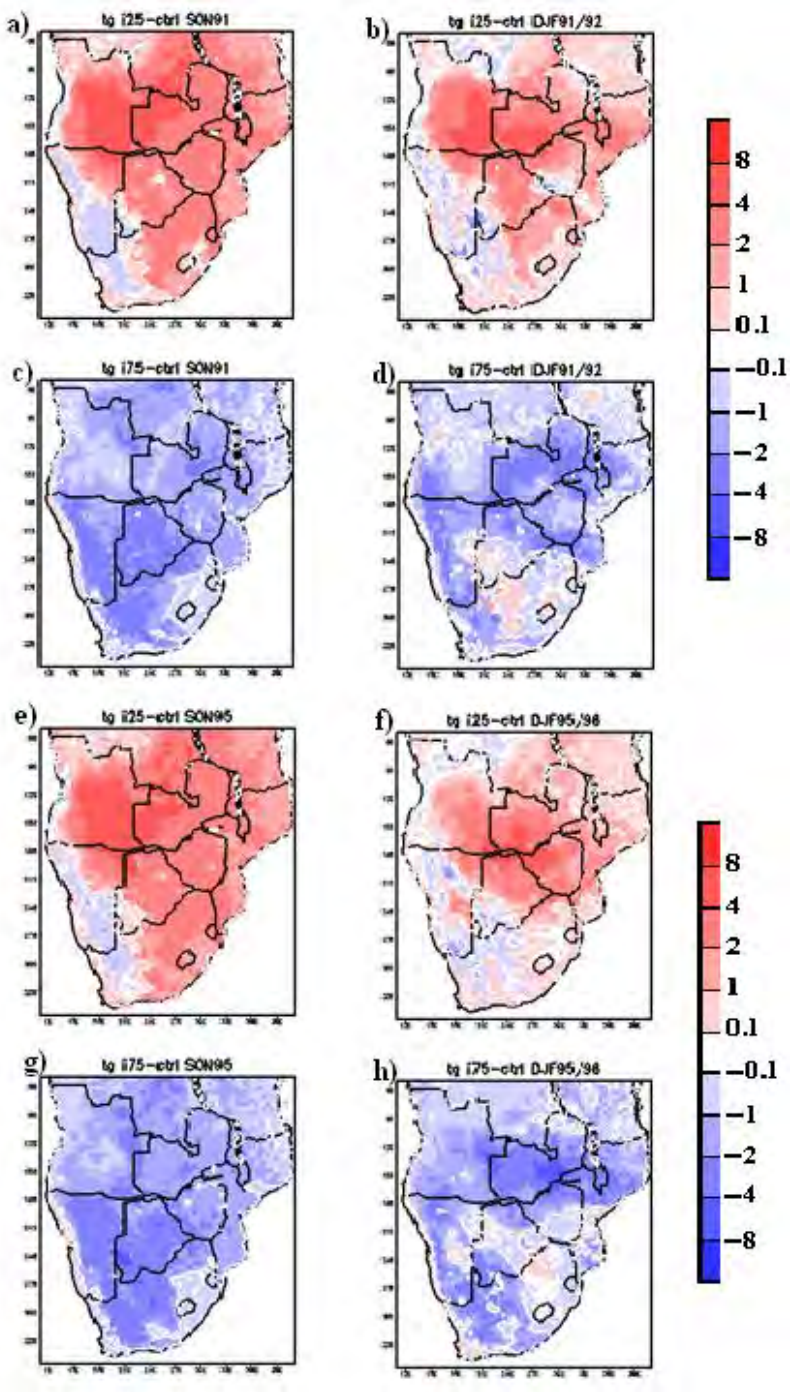

Figure 4.17 Spatial distribution anomalies of Surface Temperature (°C) for early summer, September to November, SON (left column) of 1991 and 1995 as well as late summer, December to January, DJF (right column) of 1991/1992 and 1995/96. These are for all experiments of interactive dry perturbation (first and third rows) and interactive wet perturbation (second and bottom rows). White lines enclose areas that are statistically significant at 95% confidence level.

and central areas (figures 4.17d and 4.17h). Although not statistically significant, some portions of the region show positive responses in surface temperature especially over northern South Africa and parts of Botswana. For all the anomalous soil moisture initializations, there is no distinct change in the spatial surface temperature distribution with the progression of the season in comparison to the mean seasonal pattern (figures 4.16c and 4.16d). Southwestern areas show negative temperature response for either dry or wet perturbations. A greater part of the region falls within the area that is statistically significant at 95% confidence level.

In anomalous dry soil moisture initialization, there is generally an increase in surface temperature across the subcontinent region except for the southwestern areas where slight decreases in temperature occur although not statistically significant. Whereas, for anomalous wet soil moisture initialization of late summer (DJF) period, decrease in surface temperature occur over the bulk of southern Africa except over northern South Africa and parts of Botswana where some slight increases take place. Stronger responses in surface temperatures to soil moisture perturbations occur for dry soil moisture simulation particularly during early summer period. There is more retention of the soil moisture memory with the stronger responses of the dry soil moisture perturbation as compared to the wet soil moisture perturbation experiments. Pal and Eltahir (2001) show that under dry soil moisture initialisation, dry conditions persist or worsen the severity of drought like situations.

There is generally a distinct response to soil moisture perturbation in surface temperatures over the region and the degree of sensitivity during the dry soil moisture conditions for any part of the season. Temperature tends to exhibit some direct and clear responses to the soil moisture perturbations with the vast part of the region displaying the positive feedback mechanism as described by Pal and Eltahir, (1996); Eltahir, (1998); Schär et al., (1999); Pal and Eltahir, (2001, 2003) and Jaeger and Seneviratne, (2011). Over southern Africa, Mackellar (2007) using a different RCM, MM5 also found that near surface temperature displays relatively high spatial correlations to the initial soil moisture anomaly but only in the early months of the simulations and the magnitude of the temperature response was small. Thus the choice of RCM and parameterization could also be a factor due to model's sensitivity to the perturbations.

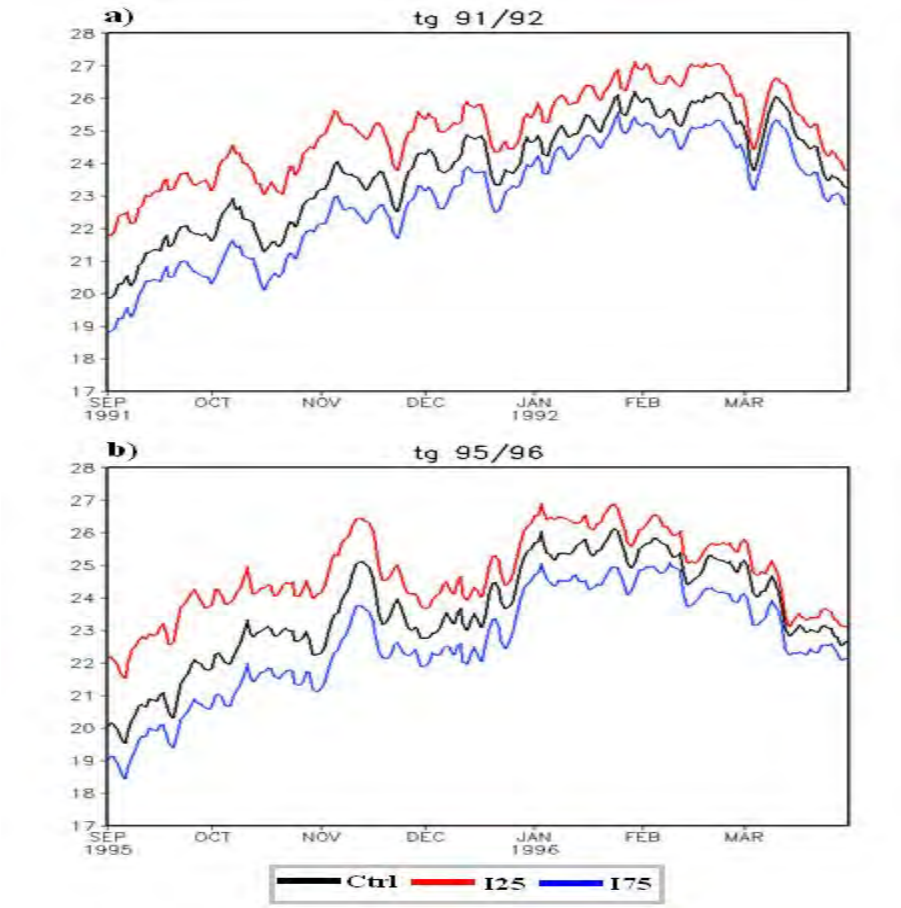

Figure 4.18 Temporal variations in the surface temperature (°C) for 1 September to 31 March of a) 1991/92 and b) 1995/96. The control simulation is represented in black, interactive dry soil moisture simulation is in red and the wet soil moisture simulation is in blue.

In contrast to the more coherent spatial distribution of surface temperature over the region, mean temporal distribution depicts highly variable surface temperature over southern Africa (figure 4.18). However, some consistency with the spatial distribution analysis and positive feedback mechanism to soil moisture is maintained as anomalously dry soil moisture initialisation result in higher surface temperatures throughout the summer seasons (figures 4.18a and 4.18b). Wet soil moisture perturbations simulate lowest mean surface temperature responses over the subcontinent. The magnitude difference in the soil moisture perturbations from the control simulations is consistent throughout the summer seasons but with higher deviations during early summer. This is consistent with the observed stronger magnitude responses in the spatial cohesive patterns of surface temperature during early summer, figure 4.17 (left column). Thus knowledge of the temperature's spatio-temporal biases during the summer period can give some

insight or degree of measure on the soil moisture levels required for moisture retention in late summer. This can be based on the magnitude of response to the soil moisture initialisation and soil moisture retention capabilities of different areas over southern Africa. Thus, can be useful in soil moisture estimation or in climate prediction (Koster and Suarez 2001; Koster et al., 2004a, 2004b, 2006; Seneviratne et al., 2006b, 2010; Vidale et al., 2007). The RCM experiments show that soil moisture-atmosphere interactions have significant effects on temperature extremes and slightly on precipitation extremes (Jaeger and Seneviratne, 2011).

4.4.3 Sensible Heat Flux

Figure 4.19 displays the sensible heat flux anomalies of the interactive soil moisture perturbations from the respective control simulations of 1991/92 and 1995/96. Dry soil moisture perturbation simulations for both seasons show an increase in sensible heat flux over most of the region except for the southwestern parts covering most of Namibia, western South Africa and southwestern Angola where some slight decreases in sensible heat fluxes occur (figures 4.19a and 4.19c). Notable increases of over 50 W/m^2 occur in western Zambia and central Angola in both seasons although slightly higher and more extensive in 1991/92. This would be expected as this season is drier and has higher surface temperature anomalies (figures 4.16a and 4.16c) resulting in more heating of the ground and within the PBL which would lead to an increase in the sensible heat flux.

Figures 4.19 b and 4.19d show that for wet soil moisture perturbation experiments, there is a general decrease in sensible heat flux anomalies over the bulk of the subcontinent except for small portions of the southeastern South Africa, western Botswana and eastern Namibia where there is an increase in sensible heat flux for 1995/96 season. Although, there is a small difference in spatial distribution and magnitude between the two seasons, areas that are statistically significant vary and are more widespread for the dry 1991/92. There are very small portions showing strong responses greater than 30 W/m^2 in both seasons. Notable but small isolated areas occur over Zimbabwe (figure 4.19b) and over eastern Angola, southern Zambia and northern Zimbabwe (figure 4.19d). For all the different perturbations, the western coastal areas covering

southwestern Angola, western Namibia and parts of western South Africa show a decrease in sensible heat flux.

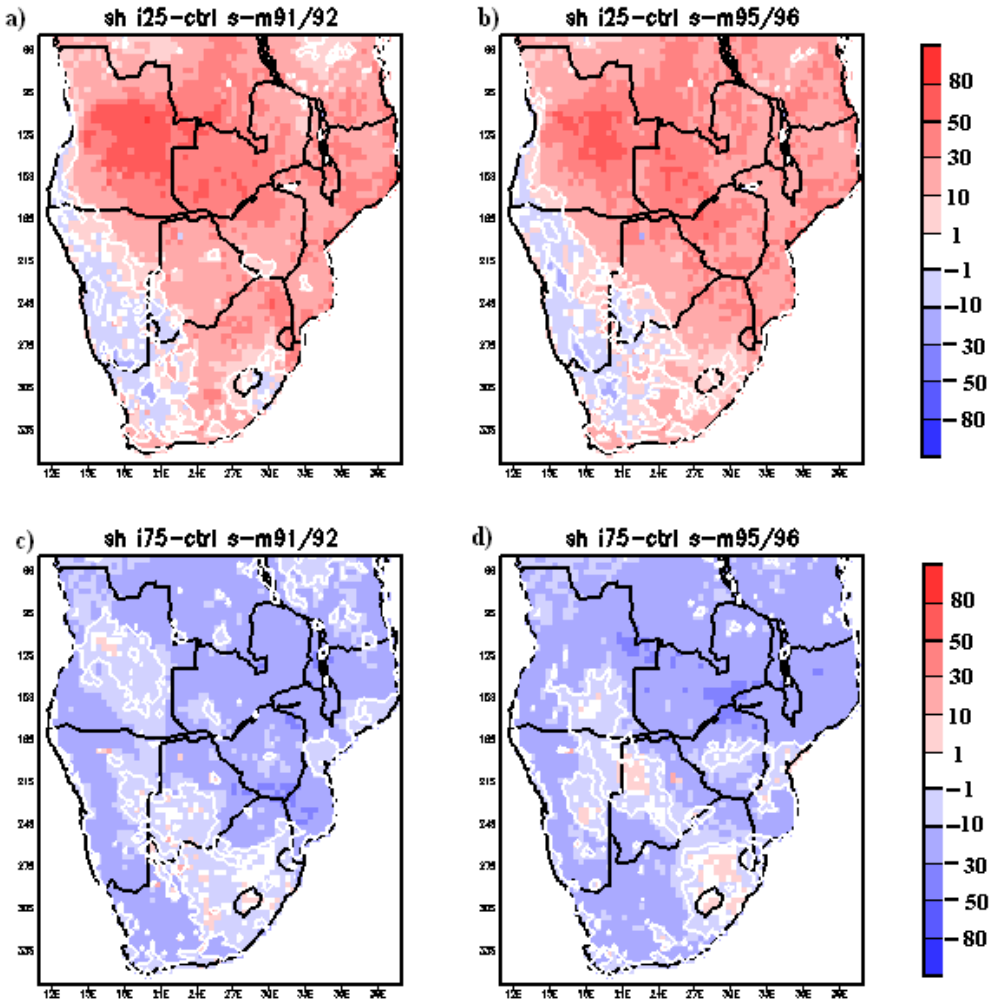

Figure 4.19 Sensible heat flux (W/m^2) anomalies for interactive experiments of 1 September to 31 March 1991/1992 of a) dry and b) wet perturbations as well as for 1 September to 31 March 1995/1996 of c) dry and d) wet perturbations. White lines enclose areas that are statistically significant at 95% confidence level.

Figure 4.20 shows the spatial distribution of the sensible heat flux anomalies for the early and late summer period of 1991/92 and 1995/96 seasons. The anomalously dry soil moisture initialization exhibits that for early summer (figures 4.20a and 4.20e), there is an increase in sensible heat flux over much of the region except for the southwestern parts of the subcontinent where some slight decrease in sensible heat flux occurs. A stronger response in the sensible heat fluxes is observed in the early summer period (SON) than late summer (DJF). However, the

persistence into late summer is stronger for the drier 1991/92 than 1995/96 season. Marked increases of greater than 80 W/m^2 occur over most of Angola, southern DRC and western Zambia (figure 4.20a) and northeastern Angola as well as southwestern DRC (figure 4.20e). Parts of the region showing a decrease in sensible heat flux is more widespread during the DJF period (figures 4.20b and 4.20f). An area displaying positive anomalies is confined to the northern and central parts of southern Africa especially over northern Botswana, Zimbabwe, Zambia, northern Mozambique and eastern half of Angola. The early summer period distribution (figures 4.20a and 4.20e) is influential in the determination of mean seasonal spatial distributions (figures 4.19a and 4.19b).

Wet soil moisture initialization experiments show an increase in sensible heat fluxes over much of southern Africa. Early summer period display a very small portion with positive anomalies over southeastern South Africa (figures 4.20c and 4.20g). There is an expansion of the area under positive sensible heat flux anomalies in the late summer period, (figures 4.20d and h) covering most of eastern half South Africa, southern Botswana, eastern Namibia, central Angola and southern Tanzania (figure 4.19d). In DJF 1995/96, the increase in sensible heat fluxes occurs mostly over southern parts of the region including eastern South Africa, southern Zimbabwe, central Mozambique, central Botswana and eastern half Namibia. Late summer 1991/92 shows negative anomalies (greater than 30 W/m^2) over northern Zambia, southern Zimbabwe and central Mozambique (figure 4.20d) whereas in DJF 1995/96 the negative anomalies occur over northern Zimbabwe and central Zambia (figure 4.20h). For the anomalously wet soil moisture simulations, although the dry 1991/92 sub-seasons (figures 4.20c and 4.20d) depict slightly stronger responses in magnitudes there are no distinct differences in spatial distribution especially during early summer of1991/92 and 1995/96. For the sub-seasons (figure 4.20), there are no major differences in sensible heat fluxes over the western coastal areas stretching from southwestern Angola down to western South Africa. Once again, the early summer spatial patterns pan out to be the major contributor towards the mean spatial distribution (figure 4.19)for the seasons especially for the wet soil moisture perturbations.

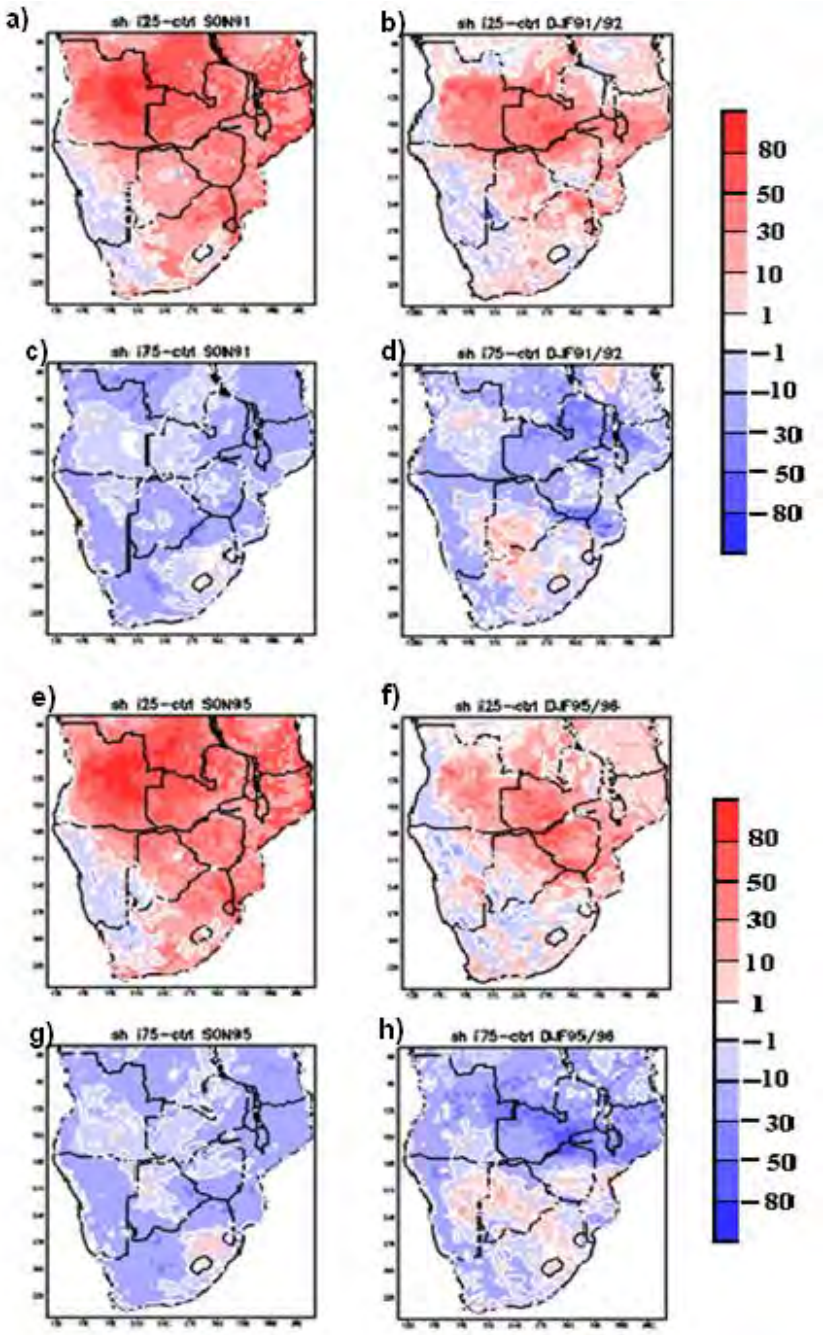

Figure 4.20 Spatial distribution anomalies of sensible heat flux (W/m^2) for early summer, September to November, SON (left column) of 1991 and 1995 as well late summer, December to January, DJF (right column) of 1991/1992 and 1995/96. These are for all experiments of interactive dry perturbation (first and third rows) and interactive wet perturbation (second and bottom rows). White lines enclose areas that are statistically significant at 95% confidence level.

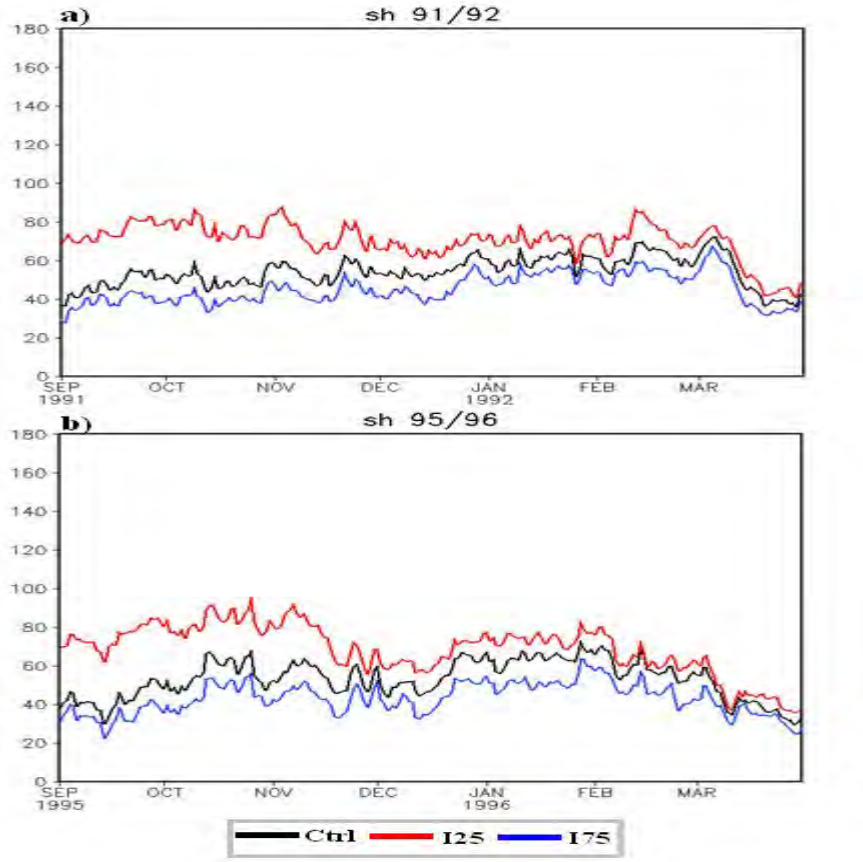

Figure 4.21 Temporal variations in the sensible heat flux (W/m^2) of 1 September to 31 March for a) 1991/92 and b) 1995/96 season. The control simulation is represented in black, interactive dry soil moisture simulation is in red and the wet soil moisture simulation is in blue.

Similarly to the surface temperature's temporal distributions (figure 4.18), the dry soil moisture initialization simulation have the highest sensible heat flux throughout the season (figure 4.21a) whilst the wet soil moisture perturbation shows the least sensible heat flux (figure 4.21b). The three simulations vary from 40 to 70 W/m^2 in sensible heat flux for most of the 1991/92 season (figure 4.21a). Although slightly varying by about ± 10 W/m^2, 1991/92 tends to be similar to the temporal variation of 1997/98 season (not shown here). From September 1995, the simulations are variable over a bigger range (at times being greater than 30 W/m^2) until mid-December 1995. The early summer period (SON) exhibits clearly the difference in the simulations with the dry soil moisture experiments distinctively higher than the control and wet soil moisture simulations (figures 4.21a and 4.21b). Late summer shows less variability and consistency in magnitude difference between the three simulations which also tend towards the same magnitude especially from mid-March for both seasons. However, the dry run is distinctively higher in sensible heat

flux magnitude for most of 1991/92 season. This also explains and supports the results discussed on the spatial distribution of sensible heat flux anomalies (figures 4.19 and 4.20) whereby the strong responses were displayed during early summer (figures 4.20a and 4.20e) and more distinctively in the dry 1991/92 season (figures 4.19a and 4.19b).

4.4.4 Latent Heat Flux

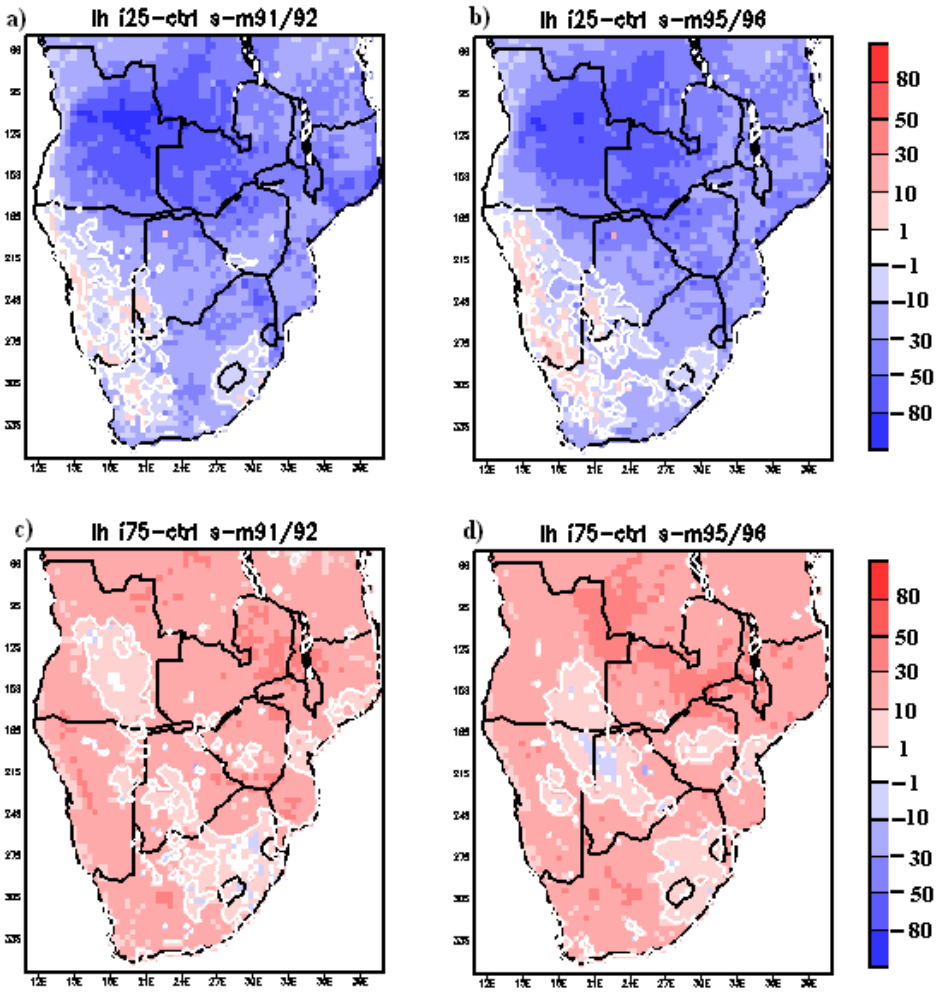

Figure 4.22 Latent heat flux (W/m^2) anomalies for interactive experiments for 1 September to 31 March 1991/1992 of a) dry and b) wet perturbations as well as for 1 September to 31 March 1995/1996 of c) dry and d) wet perturbations. White lines enclose areas that are statistically significant at 95% confidence level.

Figure 4.22 shows that the anomalous dry soil moisture conditions produce a decrease in latent heat flux over much of the region except for the southwestern areas where some slight increases

occur. Marked decreases in latent heat fluxes greater than 50 W/m^2 are simulated over central Angola, southwestern DRC and western Zambia (figures. 4.22a and 4.22b). Most of the region except for the southwestern area falls within the 95% confidence level. Conversely, the wet soil moisture initialisations (figures. 4.22c and 4.22d) generate positive latent heat flux anomalies over most of southern Africa with some patchy areas showing a decrease in latent heat flux. Notable increases of more than 30 W/m^2 occur over Zambia for the 1991/92 season (figure 4.22c) and is more widespread in 1995/96 season to cover northeastern Angola, southwestern DRC and central Zambia. Stronger responses in latent heat fluxes are associated with the anomalously dry soil moisture perturbations (figures 4.22a and 4.22b) than the wet soil moisture initialisation experiments (figures 4.22c and 4.22d). The coastal areas of Namibia and some portions in the southwest of the region depict an increase in latent heat flux for all the soil moisture perturbation simulations done. Again, most parts of the subcontinent show statistically significance at 95% confidence level.

On a sub-seasonal scale, dry soil moisture simulation (figure 4.23a) shows a decrease in latent heat flux over the region except for a small portion of southwestern areas during early summer of 1991/92. This persists into late summer (figure 4.23b) but with an increase in latent heat flux occurring over a greater part of the southwestern areas. 1995/96 season (figures 4.23e and 4.23f) depicts similar traits for dry soil moisture run of 1991/92 with a decrease in latent heat flux but weaker responses. However, more widespread increases in latent heat flux occur in late summer 1995/96 to cover most of the southwestern half of the region (figure 4.23f).

Wet soil moisture perturbations show generally an increase in latent heat fluxes over most of the region for both sub-seasons of the two years (figures 4.23c, 4.23d, 4.23g and 4.23h). Notable increases occur over northern Zambia, Malawi and northern Mozambique (greater than 80 W/m^2) in DJF 1991/92 (figure 4.23) but is constricted only to central Zambia and northern Zimbabwe (between 30 to 50 W/m^2) in late summer 1995/96 (figure 4.23f). The major differences in spatial distribution of latent heat flux occur over southern parts of the region during the late summer period where slight decreases are simulated. There is no clear signal to explain the mixed responses or inconsistency in latent heat flux especially over the southern parts of the subcontinent particularly during the late summer period. However, there is a persistence in

the increase of latent heat flux over the northern areas especially in late summer 1991/92 (figure 4.23d).

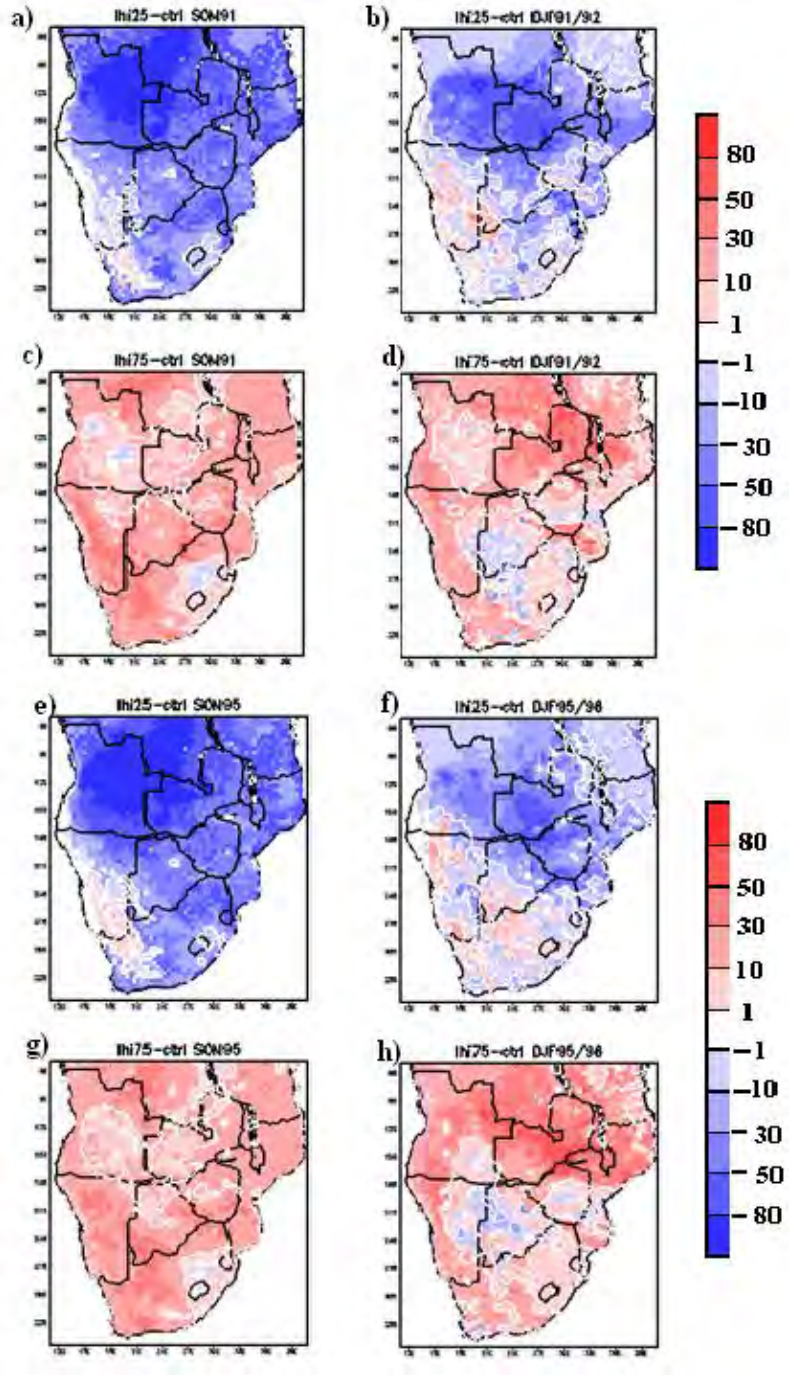

Figure 4.23 Spatial distribution anomalies of latent heat flux (W/m^2) for early summer, September to November, SON (left column) of 1991 and 1995 as well late summer, December to January, DJF (right column) of 1991/1992 and 1995/96. These are for all experiments of interactive dry perturbation (first and third rows) and interactive wet perturbation (second and bottom rows). White lines enclose areas that are statistically significant at 95% confidence level.

Summing it up, the early summer spatial distribution patterns (figures. 4.23a, 4.23b, 4.23e and 4.23g) ultimately tend to determine the mean spatial distribution for both seasons (figure 4.22). However, there is a general expected trend to decrease (increase) latent heat flux with anomalously dry (wet) soil moisture perturbations. These responses are in direct contrast to the sensible heat fluxes (figures 4.19 and 4.20). This is in agreement with the positive feedback mechanism theory where initial dry (wet) soil moisture conditions generally lead to an increase (decrease) in surface temperature which results in an increase (decrease) in sensible heat flux and thus a decrease (increase) in latent heat flux (Eltahir & Pal, 1996; Eltahir, 1998; Pal and Eltahir, 2001). Fischer et al. (2007) show the important role for partitioning of net radiation into latent and sensible heat fluxes, which is largely controlled by soil moisture. Thus lack of soil moisture strongly reduced latent heating and thereby amplified the surface temperature anomalies.

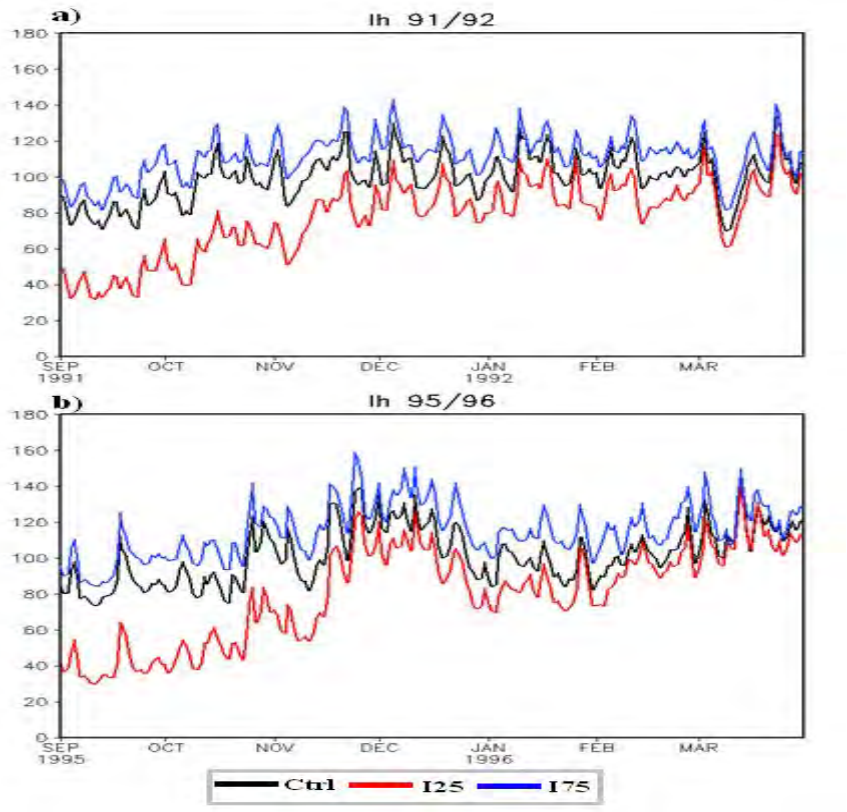

Figure 4.24 Temporal variations in the latent heat flux (W/m^2) for 1 September to 31March of a) 1991/92 and b) 1995/96. The control simulation is represented in black, interactive dry soil moisture simulation is in red and the wet soil moisture simulation is in blue.

On the temporal aspect, the anomalous dry soil moisture perturbation distinctively depicts the least amount in latent heat flux throughout the period for both seasons (figure 4.24). The wet soil moisture initialisation experiment shows the highest values for latent heat flux and at times are marginally similar to the control simulation towards the end of the season. As was observed with the sensible heat flux (figure 4.21) there are distinctive responses in temporal variation during early summer then small differences in magnitudes towards the latter part of the season(figure 4.24). The periods during which the three experiments are almost similar are longer in 1995/96 (figure 4.24b) than the 1991/92 season (figure 4.24a). This could help to explain the marginal responses to the soil moisture perturbations in the spatial distribution pattern of 1995/96 season (figure 4.22d) as well as why the early summer spatial pattern (figure 4.23, left column) ultimately determines the mean distribution for both seasons (figure 4.22). Thus, surface sensible and latent fluxes responses or partitioning do show the influence of anomalous soil moisture forcing (Shukla, 1999; Schär et al., 1999; Fischer et al. 2007).

The responses over the western areas where reduced temperatures and total precipation increases for either a dry or wet perturbation is worth discussing here. This is attributed to the fact that the southwestern areas receive most of their precipitation during the austral winter such that during the summer period any semblance of moisture regardless of whether it is a dry/wet perturbation does introduce moisture into these semi-arid/desert areas of southern Africa which are usually dry during this period (figures 4.1a and 4.2a). Thus, any additional moisture introduced will result in positive feedback mechanism occurrence (This was also reviewed over European studies by Seneviratne et al. 2010). The perturbation experiments over the western areas showed that higher soil moisture lead to increase in evapotranspiration (through the latent heat, fig 4.22) and increase in precipitation leading to surface temperature being reduced. Whereas for any perturbation at the wilting point (25% field capacity within the model's BATS scheme) might imply actually introducing soil moisture to an ultimately dry environment. Given such a scenario it would also enhance the evapotranspiration (increase in latent heat) which would reduce the temperature of this subregion. Thus, whenever temperature increases the total energy available for latent heat flux (fig. 4.22), less energy will be available for sensible heating (fig. 4.20). Several modeling studies suggested that under specific conditions convective instability and/or cloud formation may be stronger over dry soils thus leading to lowered surface temperatures (Giorgi et al. 1996; Findell & Eltahir, 2003; Hohenegger, 2009).

4.4.5 Incident Solar Radiation

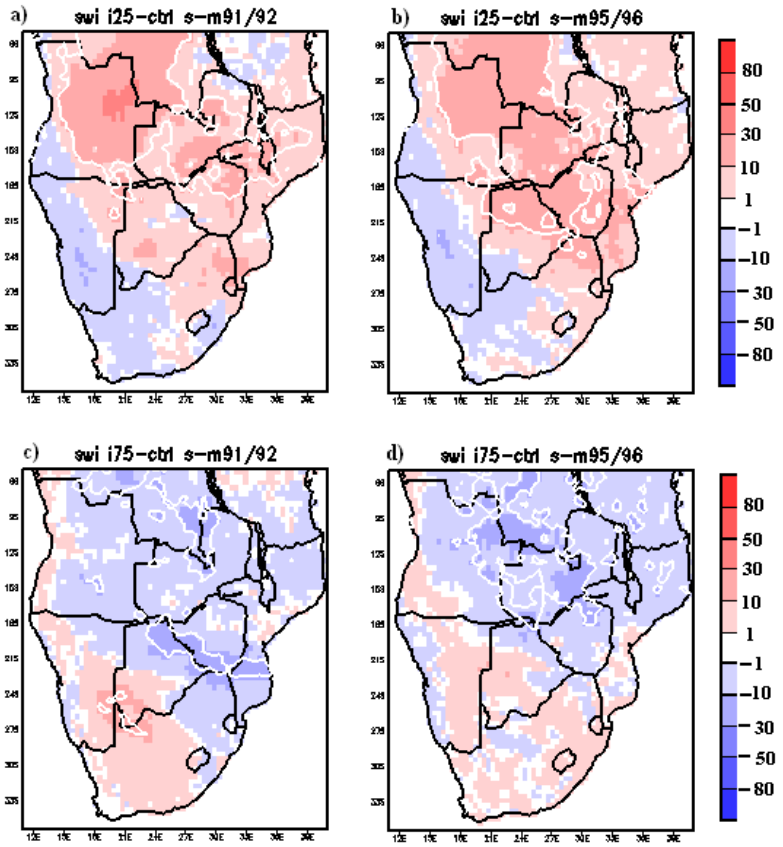

Figure 4.25 Incident solar radiation anomalies (W/m^2) for interactive experiments of 1 September to 31 March 1991/1992 of a) dry and b) wet perturbations as well as for 1 September to 31 March 1995/1996 of c) dry and d) wet perturbations. White lines enclose areas that are statistically significant at 95% confidence level.

The dry soil moisture perturbation simulations for both years show an increase in incident solar radiation over most of the region except for the southwestern areas with slight decreases (figure 4.25). Increases in incident solar radiation occurs mostly over eastern Angola and southwestern DRC in 1991/92 but spreading to include central Zambia, northeastern Botswana and western Zimbabwe in 1995/96. This implies either clear skies or less cloud development or a fluffy type of cloud prevails (Tyson and Preston-Whyte, 2000; Barry and Chorley, 2009). Strongest response in incident solar radiation occurs over eastern Angola in 1991/92 (figure 4.25a). A small area of statistically significance at 95% confidence is confined to the northern portions of the subcontinent in 1991/92 (figure 4.23a) and also encompasses the central areas around northern Botswana and Zimbabwe in 1995/96 (figure 4.23b).

In contrast, wet soil moisture perturbations represent a decrease in incident solar radiation over most of the region except for the southwestern areas of the subcontinent during 1991/92 season (figure 4.25c). 1995/96 shows decrease in radiation confined to the northern half of the subcontinent with slight increases occurring over the southern parts (figure 4.25d). The reduction in incident solar radiation is associated with an increase in cloud cover or type of cloud over those regions and also to an increase in precipitation (Tyson and Preston-Whyte, 2000). Significant and notable decreases occur over parts of southern DRC, northeastern Botswana, southwestern Zimbabwe and central Mozambique in 1991/92 (figure 4.25c) whilst in 1995/96 these decreases occur over southern DRC, eastern Angola and central Zambia (figure 4.25d).

Southwestern parts of the region show contrasting responses than would be anticipated from positive feedbacks i.e. dry (wet) runs leading to reduction (increase) in incident solar radiation. However, the incident solar radiation responses are not consistent with other surface variables (surface temperature and heat fluxes) analysed earlier and also with the increase in precipitation (figure 4.13) where there is an increase in incident solar radiation (figure 4.25) and vice versa. It can be proposed that the dry soil moisture condition over the southwestern areas (especially southeastern Namibia, southwestern Botswana and northwestern South Africa) can induce a decrease in latent heat flux (evaporation) and an increase in sensible heat flux which provides a source of buoyant energy that can enhance convection and deepen low pressure systems (Giorgi et al. 1996; Tyson-Preston-Whyte, 2000; Petersen et al., 2009). Thus, with sufficient atmospheric moisture available, this process would increase precipitation over this sub-region.

On a sub-seasonal level, figure 4.26 shows incident solar radiation anomalies (W/m^2) for early summer, September to November of 1991 and 1995 as well as late summer, December to January of 1991/92 and 1995/96. The anomalous soil moisture conditions show a transition between early and late summer for both years. During the early summer, an increase in the incident solar radiation occurs over most of the subcontinent except for parts of the southwestern areas under the dry soil moisture perturbations. Notable increases of more than 80 W/m^2 occur over northeastern Angola and southwestern DRC (figures 4.26a and 4.26e). There is a reduction in the magnitude of positive solar radiation responses during late summer with more widespread

negative solar radiation over the southwestern areas especially for DJF1995/96. Thus, implying stronger persistence during the dry 1991/92 season under dry soil moisture perturbation.

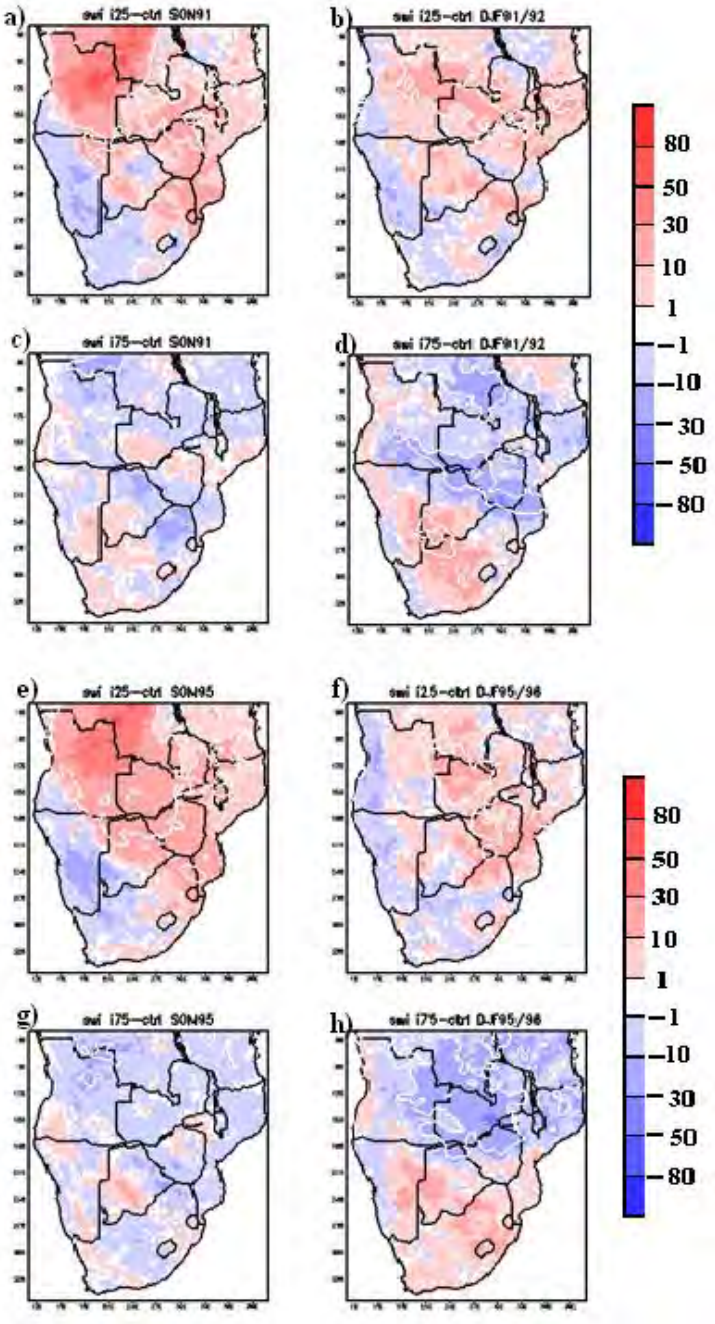

Figure 4.26 Incident solar radiation anomalies (W/m^2) for early summer, September to November, SON (left column) of 1991 and 1995 as well late summer, December to January, DJF (right column) of 1991/92 and 1995/96. These are for all experiments of interactive dry perturbation (first and third rows) and interactive wet perturbation (second and bottom rows). White lines enclose areas that are statistically significant at 95% confidence level.

On wet soil moisture initialisation, experiments show a slight decrease in incident solar radiation over most of the region for early summer (more extensive in SON95 than SON91) with some slight increases particularly over southeastern Namibia and southwestern Botswana for SON91 and over central Botswana for SON95 (figures 4.26c and 4.26g). Notable decrease in incident solar radiation which could imply cloud development occurs over southwestern DRC, northeastern Botswana and northern South Africa for early summer 1991/92 (figure 4.26c). During the end of summer, there is reduction in incident solar radiation over northern and central parts of the region for DJF1991/92 (figure 4.26d) whilst being confined to the northern parts of the region for DJF1995/96 (figure 4.26h). However, the southern parts of the subcontinent especially eastern Namibia, southwestern Botswana and central South Africa for DJF1991/92 (figure 4.26d) as well as eastern Namibia, western Botswana and northeastern South Africa for DJF1995/96 (figure 4.26h) depict an increase in incident solar radiation. This could be attributed to the model not having a strong or coherent response to soil moisture perturbations for incident solar radiation over the southern parts of the region. Different responses occur over the west coast with a decrease in radiation for late summer 1991/92 (figure 4.26d) whilst an increase occurs in 1995/96 (figure 4.26h).

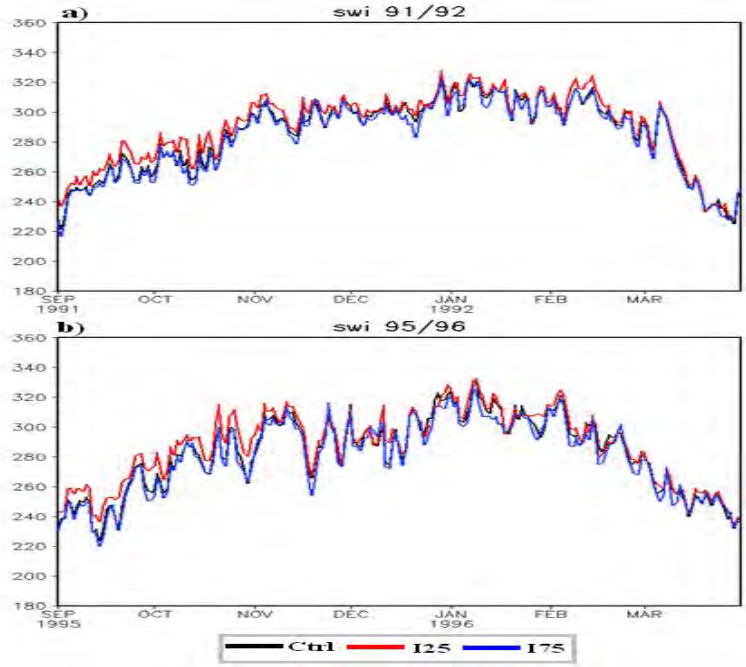

Figure 4.27 Temporal variations in the incident solar radiation (W/m^2) for 1 September to 31 March of a) 1991/92 and b) 1995/96. The control simulation is represented in black, interactive dry soil moisture simulation is in red and the wet soil moisture simulation is in blue.

Temporal variations in incident solar radiation presented in figure 4.27 depict slight variations during early summer for both seasons. The dry soil moisture perturbations show marginally higher magnitudes from the control and wet soil moisture perturbation simulations. A uniform and constant incident solar radiation period occurs from mid-November to end of December 1991(figure 4.27a). An interesting period to further analyse would be January 1996 where there is an interchange of incident solar radiation, with the control simulation being initially similar in variation with the dry soil moisture experiment and then later with the wet soil moisture simulation (figure 4.27b). Such incident solar radiation variations in association with cloud amount or type of cloud available could be attributed to changes in the synoptic forcing situation suggesting an anticyclonic circulation dominating when dry and control simulations coincide (Torrance, 1981). This can confirm the dry spells that occur sometime in January over the region (Torrance, 1981; Matarira and Flocas, 1989; Matarira and Jury 1992; Tyson and Preston-Whyte, 2000; Unganai and Mason, 2001; Usman and Reason, 2004).

4.4.6 Planetary boundary layer

Figure 4.28 shows the planetary boundary layer (m) anomalies to different soil moisture perturbations for 1991/92 and 1995/96 seasons. Dry soil moisture initialisation simulations exhibit an increase in PBL over most of the region except for southwestern areas encompassing western South Africa, southwestern Botswana and southwestern half of Namibia where slight decreases in PBL (less than 100m) occur (figures 4.28a and 4.28c). The difference between the seasons occurs in the PBL being over 600m in Angola for 1991/92 (figure 4.28a). Wet soil moisture perturbations depict a decrease in PBL over the whole region for 1991/92 season with most areas falling within statistically significant zones (figure 4.28a). 1995/96 season exhibits a significant decrease in PBL over most of the region except for southeastern South Africa, Swaziland, central Botswana and west coast of Namibia (figure 4.28b). Southwestern areas depict a decrease in PBL for both dry and wet simulations. Transitional zones falling between the infinitesimal positive and negative range occurs over southwestern Namibia and western South Africa.

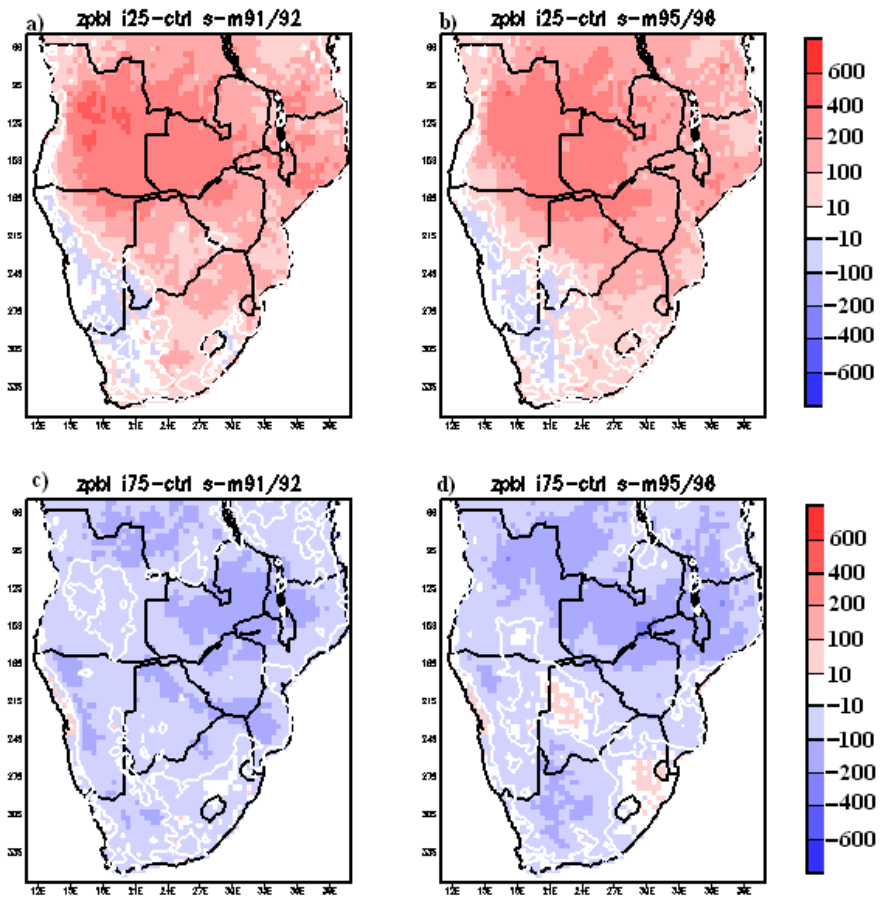

Figure 4.28 Planetary boundary layer height anomalies (m) for interactive experiments of 1 September to 31 March 1991/1992 of a) dry and b) wet perturbations as well as for 1 September to 31 March 1995/1996 of c) dry and d) wet perturbations. White lines enclose areas that are statistically significant at 95% confidence level.

Wet soil moisture conditions show a decrease in planetary boundary layer height over the whole region during 1991/92 season (figure 4.28c) but there is a reduction in PBL height over most of the subcontinent with a slight elevation in the PBL height over southwestern Botswana, Swaziland and southeastern South Africa (figure 4.28d). The area under reduction in PBL height is wider over the wet 1995/96 season than the dry 1991/92 season. Conspicuous areas falling within the transitional zones occur over South Africa in 1991/92 (figure 4.28c) and eastern Namibia, Botswana and South Africa in 1995/96 (figure 4.28d). For all the perturbations especially the anomalous dry soil moisture simulations, a greater portion of the region falls within the statistically significant at 95% confidence level.

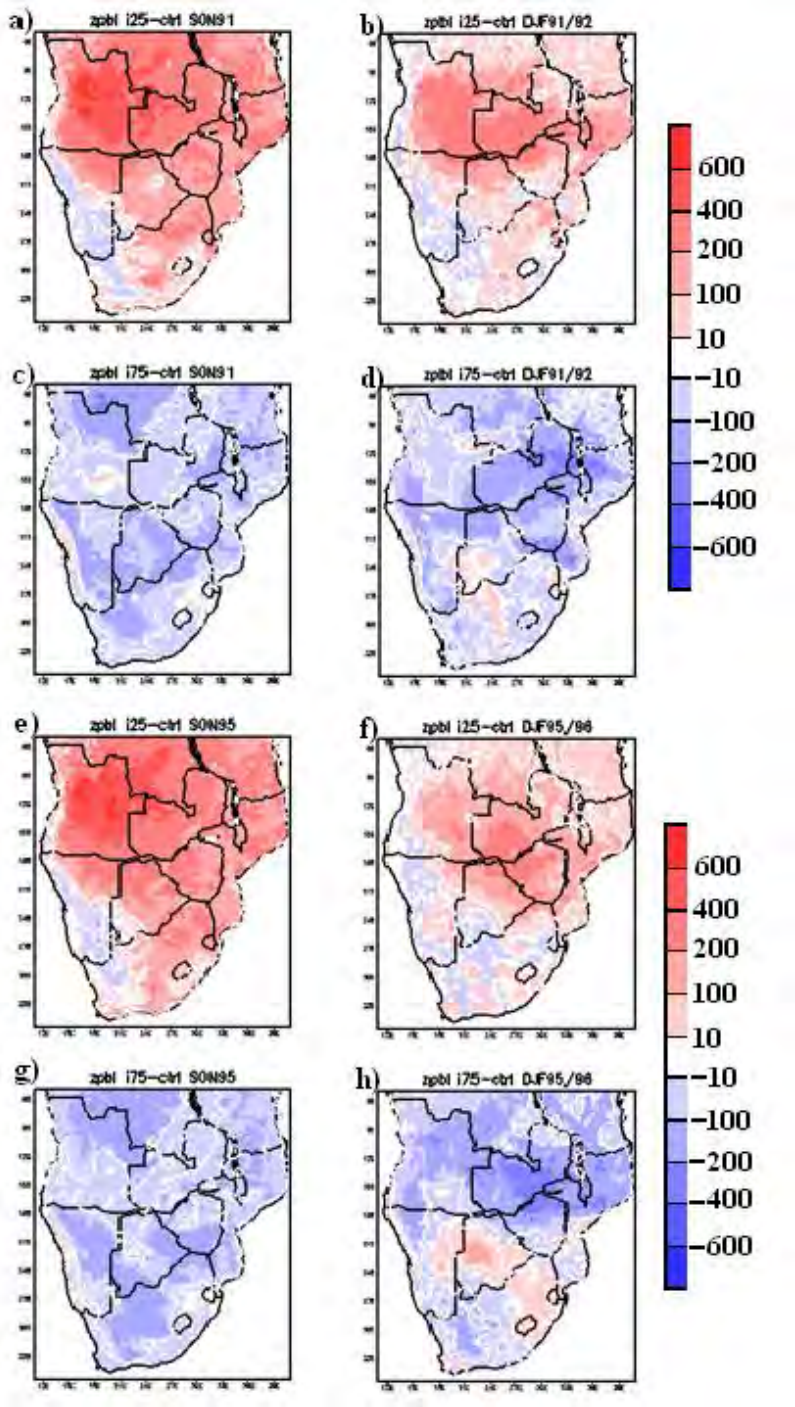

Figure 4.29 Anomalies of planetary boundary layer height (m) for early summer, September to November, SON (left column) of 1991 and 1995 as well late summer, December to January, DJF (right column) of 1991/92 and 1995/96. These are for all experiments of interactive dry perturbation (first and third rows) and interactive wet perturbation (second and bottom rows). White lines enclose areas that are statistically significant at 95% confidence level.

For dry soil moisture perturbations at sub-seasonal scale, both early summer periods (1991/92 and 1995/96) show an increase in planetary boundary layer height over most of the region except for the southwestern areas where slight decreases in PBL height occur(figures 4.29a and 4.29e). Notable increase of greater than 600m in PBL height occurs over northeastern Angola. Late summer periods still depict positive anomalies in PBL height although at lesser depths and over a smaller area than in early summer. Southern parts of the subcontinent show an expansion in the area with slight decreases in PBL height especially in DJF1995/96(figure 4.29c). Marked increases in PBL height (greater than 200mm) occur over eastern Angola, southern Zambia and northwestern Zimbabwe in DJF 1991/92(figure 4.29b) and slightly shifts southward to be over parts of southern Zambia, northern Botswana and northwestern Zimbabwe in DJF 1995/96 (figure 4.29f). There are stronger responses and broader area falling under positive anomalies of PBL in early and late summer of 1991/92 than 1995/96.

In early summer of both seasons, wet soil moisture perturbations exhibit a decrease in PBL over southern Africa except for the coastal areas of Namibia (figures 4.29c and 4.29g) and in a portion of southeastern Angola in SON 1991. Late summer does not show distinct changes in the general spatial distribution pattern. However, there is a change in areas of marked responses and an enlargement of the area with positive anomalies in PBL within the southern parts of the region especially in DJF 1995/96 (figure 4.29h). Significant increases in PBL occur over southern Botswana and central South Africa for DJF 1991/92 (figure 4.29d) as well as eastern Namibia, central Botswana and southeastern South Africa for DJF 1995/96 (figure 4.29h). Southern Zambia and northwestern Zimbabwe show some consistency in the PBL responses to the soil moisture perturbations during late summer period. In general, anomalous dry soil moisture initialisation situations lead to an increase in the PBL height whilst wet soil moisture perturbations result in a decrease in PBL. There is some coherency in the PBL height responses to the soil moisture perturbation for the bulk of the subcontinent. This concurs with the positive feedback mechanism based on PBL conditions as observed by Eltahir (1998), Pal and Eltahir (2001) and Jaeger and Seneviratne, (2011).

Figure 4.30 depicts temporal variations in the planetary boundary layer height (mm) for 1 September to 31 March of a) 1991/92 and b) 1995/96 season. The three experiments depict that

anomalously dry soil moisture conditions have the highest PBL magnitude as compared to the control and wet soil moisture perturbations that have the least levels throughout the seasons (figure 4.30). Notable is larger differences between the dry soil moisture initialisation and the control simulations. This is more prominent during the early part of the seasons. The distinct dry soil moisture run's highest PBL is maintained into late summer during the dry 1991/92 season. Similar findings show that dry or drought-like conditions persist longer during a dry season as compared to a wet season (Eltahir and Pal, 1996; Pal and Eltahir, 2001; Kim and Hong, 2007).

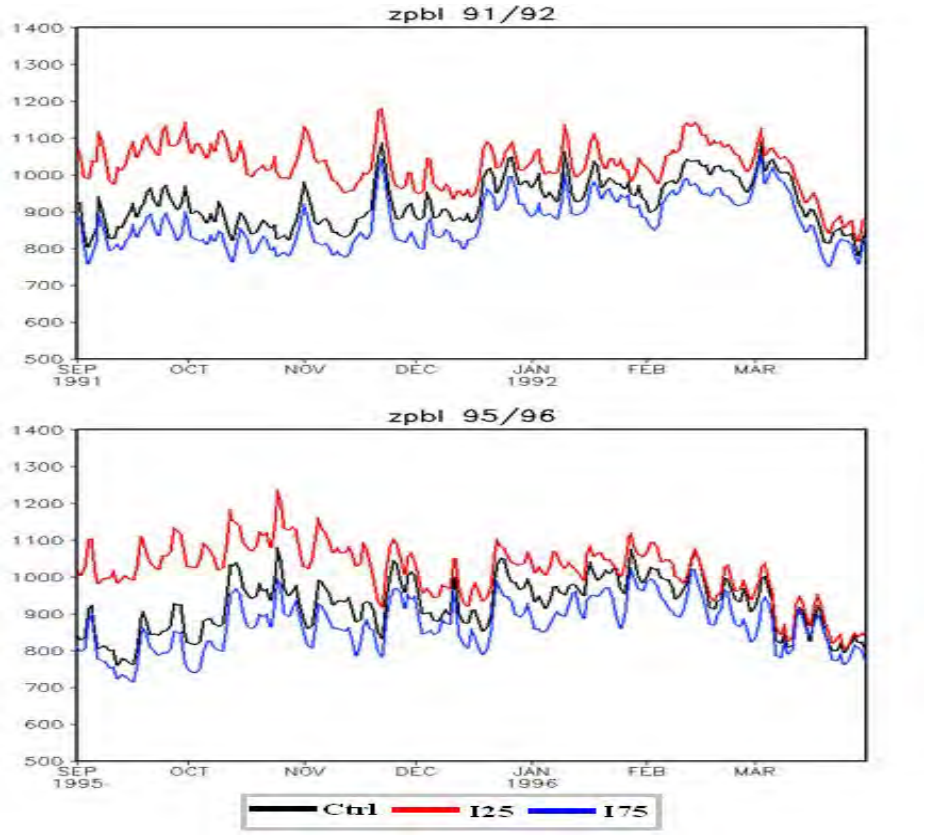

Figure 4.30 Temporal variations in the planetary boundary layer height (m) for 1 September to 31 March of a) 1991/92 and b) 1995/96 season. The control simulation is represented in black, interactive dry soil moisture simulation is in red and the wet soil moisture simulation is in blue.

4.5 Summary

This chapter described the regional atmospheric responses to the soil moisture perturbations over southern Africa during the summer rainfall season stretching from 1 September to 31 March the

subsequent year (1991/92, 1994/95 and 1997/98 as dry years and 1995/96, 1996/97 and 1998/99 for the wet years). The mean seasonal response to the forcing and the intra-seasonal responses disaggregated into early summer (SON) and late summer (DJF) have been considered. This gave an insight into responses of the local summer climate to soil moisture forcings by drying or moistening the land surface. Main findings are summarised as:

- There is a mechanism that exists between the soil moisture and most of the climate parameters analysed here. The attenuation of this soil moisture initialisation is around December to mid-January thus giving a soil moisture retention period of about 3-4months.

- Although some limitations were realised such as the wet/dry biases found over the northern and southeastern areas in most of the seasons analysed, RegCM3 was still able to reproduce the climate dynamics as in being able to capture the spatial distribution of precipitation and could thus be used for the sensitivity experiments with a lower margin of error.

- For both mean seasonal periods of analysis (September to March), RegCM3 model does capture the spatial distribution and simulates fairly well the magnitude of precipitation as compared to the CRU and GPCP datasets. Some wet biases are found over the northern and southeastern areas with a systematic dry bias over Angola.

- However, RegCM3 simulates well the spatial distribution and magnitude of air temperature over much of southern Africa. It simulates well surface temperatures over high terrain and Lowveld as well as the Limpopo valley.

- Whilst RegCM3 simulates variability in precipitation and temperature between the two summer seasons and to some degree captures the mean spatial distribution of interannual variation, it has a tendency to overestimate rainfall, which partly results in lower simulated surface temperatures.

- During early summer, there is greater sensitivity in the model's top-layer soil moisture with the dry perturbations showing distinctive magnitude whilst slight deviations occur with wet soil moisture perturbations.

- Total rainfall responses to soil moisture perturbations exhibit cohesiveness in spatial distribution particularly over central and northern areas, with dry runs resulting in reduced rainfall anomalies and wet runs leading to increases.

- The persistence of drier conditions in the anomalous dry soil moisture perturbations are reflected more strongly during the dry 1991/92 summer as compared to the wet 1995/96. Although varying in magnitude and spatial extent, similar responses are observed in dry 1994/95 and 1997/98 as well as wet 1996/97 and 1998/99 seasons. This strong persistence can also be attributed to other forcings such as the El Nino and exacerbates the drying conditions as well as large scale circulations.

- Anomalous wet soil moisture simulations for early summer tend to show positive responses to total precipitation for both seasons particularly over central and northern parts of the subcontinent. Late summer period, tend to have mixed responses although most of the consistent positive responses in total precipitation are confined to the northern parts of the region.

- Temporal responses to the dry soil moisture perturbation depict uniquely lower precipitation than the control simulation for most of the period of study particularly the early season. There are mixed responses of total rainfall to the soil moisture perturbations during late summer.

- Surface temperature anomalies show spatial consistency to respective perturbations. Anomalous dry soil moisture initialisation shows an increase in surface temperature over most of southern Africa except for the southwestern portions of the region. Anomalous wet soil moisture initialisation leads to cooling over the subcontinent.

- There is more retention of the soil moisture memory and stronger responses to surface temperature with the dry soil moisture perturbation as compared to the wet soil moisture perturbation particularly during early summer. This is depicted in all the summer simulations.

- Temporal distribution depicts highly variable surface temperature over southern Africa. However, some consistency with the spatial distribution analysis and positive feedback mechanism is maintained as dry soil moisture perturbation results in higher surface temperature magnitudes throughout the summer seasons especially during early summer.

- There is a consistent spatio-temporal response of principally a decrease (increase) in latent heat flux with anomalously dry (wet) soil moisture perturbations particularly over central and northern parts of the subcontinent. These responses are in direct contrast to the sensible heat fluxes and PBL.

- The dry soil moisture perturbation simulations for both dry and wet summers show an increase in incident solar radiation over most of the region except for the southwestern areas with slight decreases. Southwestern areas show contrasting responses i.e. dry (wet) runs lead to decrease (increase) in incident solar radiation. This is common in all the six summer simulations.

- The incident solar radiation responses are not spatially consistent with other surface variables (surface temperature and heat fluxes) and with the precipitation which shows an increase in rainfall where there is an increase in incident solar radiation and vice versa.

- The temporal variations in incident solar radiation depict slight deviations during the early part of summer for both seasons. Thus the weak and mixed incident solar radiation responses suggest that there is no direct interaction to soil moisture only. This also supports the fact that the soil moisture forcing mainly affects the lower atmosphere and partially contribute to type or amount of cloud which forms the cover (besides vegetation

and aerosols) responsible for the amount of solar radiation reaching the surface.

- From the summers' sensitivity experiments, a positive feedback mechanism exists where initial dry (wet) soil moisture conditions generally lead to an increase (decrease) in surface temperature which results in an increase (decrease) in sensible heat flux and PBL, thus lead to a decrease (increase) in latent heat flux or evapotranspiration. This is true for most of the region with the exception of the southwestern areas. However, weak or mixed responses occur with total precipitation and incident solar radiation.

Chapter 5

Synoptic Analysis and Mean January Climate Responses

5.1 Introduction

After the analysis of the spatial and temporal distribution associated with the different soil moisture perturbations; it becomes apparent to check on the synoptic situations that can lead to these responses. This would aid in identifying the large-scale circulations associated with these soil moisture initialisations. An analysis is done on the geopotential heights and moisture flux so as to identify the associated anomalies conditions to the spatial responses that were described in the previous chapter. In order to further understand the effects of soil moisture perturbations within the boundary layer, an analysis of the 700hPa geopotential heights was done. The 700hPa level is crucial when looking at atmospheric levels over southern Africa. It is one of the levels that are used quite often to characterize the circulation patterns in meteorology and climatology (Torrance, 1981; Tyson and Preston-Whyte 2000; Mackellar, 2007). The vertical profile of cloud liquid water depth and air temperature associated with the different soil moisture perturbations was also analysed.

In addition to synoptic analysis, assessment of how the frequency and intensity of precipitation varies with soil moisture perturbations over the region was done. This also includes a review of the daily cycles of the model's surface variables analysis to give some insight into how they vary for the three different simulations. Lin et al. (2000) proposes that the diurnal cycle is one of the prominent cycles in the water and energy exchanges within the climate system and can be considered to be an ideal test-bed for GCMs and RCMs as well as their parameterisations. Some of the results presented here are extracted from the preliminary simulations focussing on January[15], a very crucial month in agriculture and the rainfall season due to intra-seasonal

[15] More detailed analysis of January simulations on soil moisture, see Tadross et al. (2010) or visit www.wrc.co.za.

characteristics such as dry spells and shifts in the rain-bearing systems e.g. ITCZ (Torrance, 1981; Matarira and Jury 1992; Makarau, 1995; Buckle, 1996; Tyson and Preston-Whyte, 2000; Unganai and Mason, 2001; Usman and Reason, 2004). January is also identified as the middle of the rainy season. It is also the period where some mixed temporal responses in soil moisture perturbations have been observed for some of the surface variables analysed especially during late summer of 1995/96 and in mean for the wet seasons (including 1996/97 and 1998/99 seasons). So this month is very important as it comes after the equilibration period of the model's response to changes from the soil moisture initialization. However, these results do give a clear representation of how soil moisture perturbations affect the mean synoptic conditions across the region.

5.2 Geopotential Heights

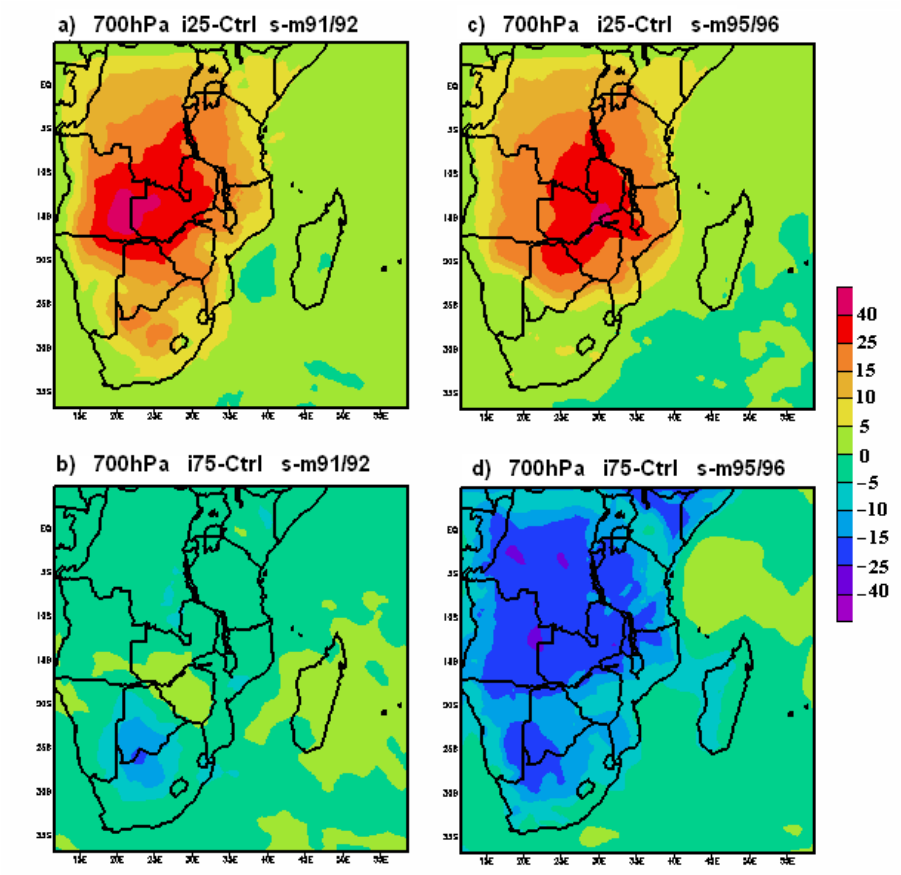

Figure 5.1 Geopotential height anomalies at 700hPa for the soil moisture perturbations from the control for 1 September to 31 March 1991/92 RegCM3 a) dry run b) wet run, and for 1 September to 31 March 1995/96 with c) dry run and d) wet run.

Figure 5.1 shows the 700hPa geopotential heights anomalies for both years and the different experimental set ups. Most of the region is under very high positive anomalies with greater than 25gpm over the central subcontinent for both dry soil moisture experiments of 1991/92 and 1995/96 seasons (figures 5.1a and 5.1c). These anomalies are greater and further west during the dry 1991/92 suggesting the spatial extent and intensity are dependent on the synoptic forcing. In contrast, the wet soil moisture initialisations induce negative anomalies over the region for the two seasons (figures 5.1b and 5.1d). The region of negative anomalies is more widespread and greater during the wet 1995/96. 1991/92 summer exhibits some portions of the region with slight positive geopotential anomalies (i.e. less than 5gpms) over Zimbabwe, southern Botswana, southeastern Angola and northwestern Namibia.

Early summer situation for the dry soil moisture perturbations depicts strengthening of geopotential heights over the region except for southern areas of Namibia and southeastern Lesotho in both seasons (figures 5.2a and 5.2e). Strong positive geopotential anomalies are simulated over Angola with more than 25gpms in SON1995 and just less than 25gpms for SON1992. The area falling within the strong positive anomalies (above 15gpm) is more widespread encompassing most of Angola, DRC, southwestern half of Zambia, northeastern Namibia, northern Botswana and northwestern Zimbabwe during early summer 1995(figure 5.2e). However, the area under the strong anomalies is constricted to Angola, DRC, western Zambia, northwestern Botswana and a portion of northeastern Namibia for SON 1991 (figure 5.2a).

Late summer exhibits positive geopotential heights although weakening and shrinking in area over the region for both seasons (figures 5.2b and 5.2f). The centre of strong positive anomalies greater than 15gpm occurs over eastern Angola and western Zambia in DJF 1991/92. There is persistence of the stronger geopotentials (greater than 15gpm) but the centre shifts eastwards to be over Angola and Zambia border in late summer 1991/92(figure 5.2b). DJF 1995/96 shows a greater drop in the geopotential heights from early summer (figure 5.2f). Although slightly weaker in magnitude, there is an expansion of area under negative geopotential anomalies over the southern parts of the region especially in DJF 1995/96. Southeastern Lesotho results in

negative geopotential height anomalies regardless of the soil moisture perturbation state. Basically, the geopotentials are showing that there is enhanced anticyclonic circulation over the region during early summer than later in the season for anomalous dry soil moisture experiments. Greater persistence of the anticyclonic circulation is observed during the drier 1991/92 season (figures 5.2a and 5.2b). Thus longer time-scale interactive soil moisture perturbations are useful in assessing the persistence and response in magnitude of anomalies.

Anomalous wet soil moisture conditions depict negative geopotential heights for the whole southern Africa region during early summer of the two seasons (figures 5.2c and 5.2g). Areas of marked geopotential height decreases (5 to 10gpms) occur over southwestern DRC, Botswana, central South Africa, southern Zimbabwe and central Mozambique in SON 1991 (figure 5.2c) whilst being constricted to patches over southwestern DRC, northeastern Angola, northeastern Namibia, northern and southwestern Botswana, as well as central South Africa in SON 1995 (figure 5.2g). Late summer still shows deepening in geopotential heights over the subcontinent for DJF 1991/92 (figure 5.2d). However, DJF 1995/96 (figure 5.2h) displays much of the region still under negative anomalies but slight geopotential increases do occur over the southeastern part of the region stretching from eastern Namibia, southeastern half of South Africa, Lesotho, Swaziland and southern Mozambique. Late summer presents areas of marked decrease in geopotential height shifting to northern parts of the region especially over DRC, Zambia and Zimbabwe. This area coincidentally falls within ITCZ preferential position during the DJF period (Torrance, 1981; Lindesay, 1998; Washington and Todd, 1998; Tyson and Preston-Whyte, 2000).

Generally, anomalous dry soil moisture initialisations are leading to strengthening of anticyclonic circulation which leads to subsidence and dry conditions whilst wet soil moisture initialisation leads to a decrease in geopotential height or deepening of low pressure systems which would enhance convergence. The dry soil moisture perturbations result in stronger and more persistent geopotential responses as compared to the wet soil moisture perturbations. The magnitude of response is higher during early summer (SON) than late summer (DJF) for both seasons analysed. Southwestern parts of the region are consistently showing slight geopotential decreases for all the perturbations of late summer.

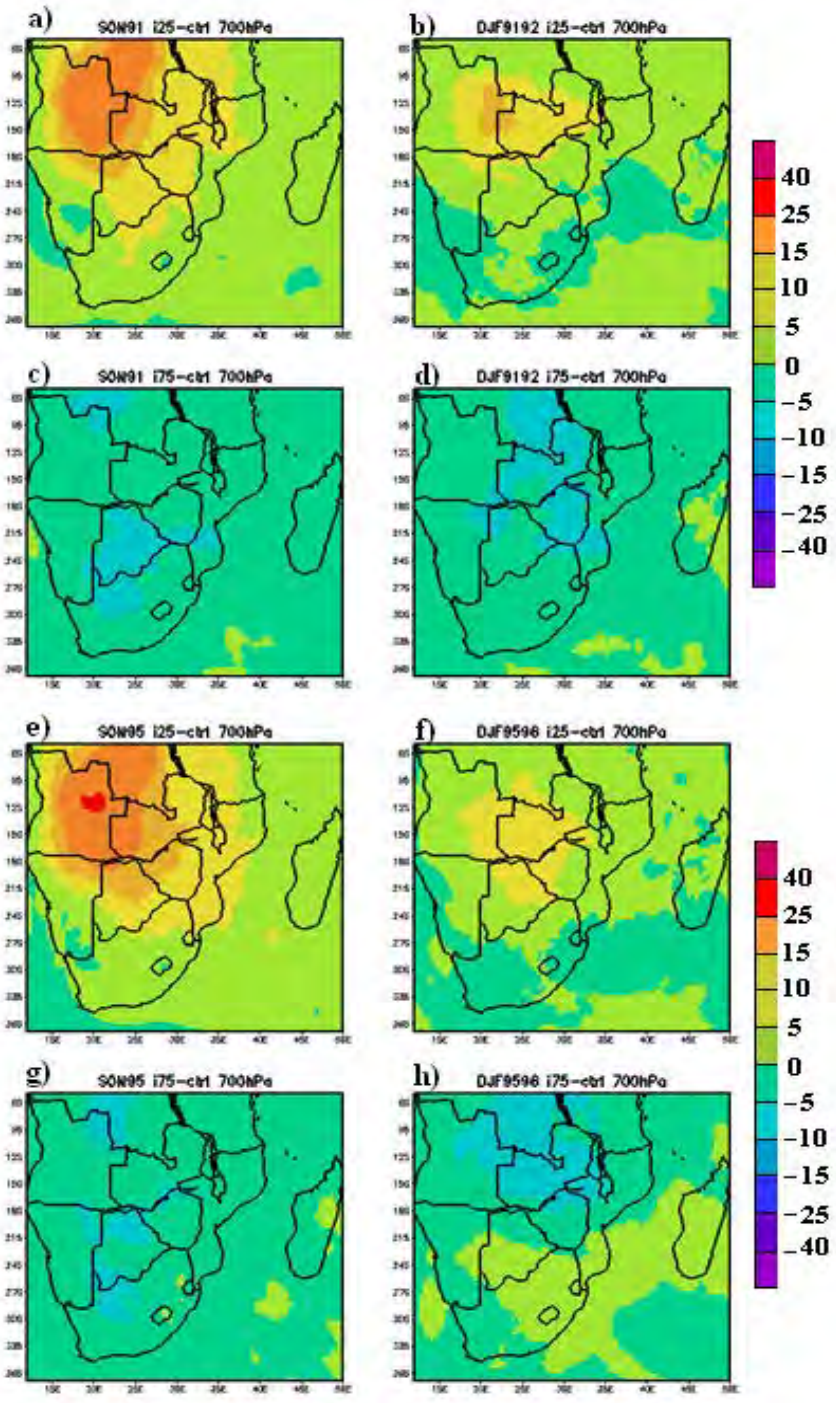

Figure 5.2 Geopotential anomalies (gpm) at 700hPa for the soil moisture perturbation simulation from the control simulation of early summer of 1991/92 and 1995/96 (left column) and later summer of 1991/92 and 1995/96 (right column).

These results demonstrate that the soil moisture perturbation has a greater effect on the circulation of the lower atmosphere when the perturbation is consistent with the synoptic forcing i.e. if there are dry (e.g. anticyclonic) large-scale changes then drier soil moisture initialisation will have a greater effect, whereas if the synoptic forcing is wetter, then a wet soil moisture initialisation will interact to prove the greatest change in circulation. In general, dry soil moisture perturbation simulations result in the strengthening of the anticyclonic activity which leads to conditions unfavourable for cloud development and rainfall activity. This would also lead to an increase in temperatures. Therefore, it contributes towards enhancing the severity and persistence of droughts and floods (Eltahir and Pal, 1996; Zheng and Eltahir, 1998; Pal and Eltahir, 2001; Kim and Hong, 2007). Wet soil moisture perturbation simulations result in weakening of anticyclones or deepening of low pressure systems (or cyclones). This leads to conditions quite favourable for cloud development and enhancement of rainfall activity. This will eventually emanate in surface temperatures dropping.

5.3 Moisture Fluxes

Generally, the sources of moisture flux are shown to be the adjacent Indian Ocean and less being advected inland from the tropics (figure 5.3a). Very little moisture is advected inland up the west coast as it is more of a southerly component. Inland, most of the moisture flux is in the easterlies passing over Zimbabwe, Zambia and Botswana. An anticyclonic circulation over northern South Africa pushes some of the moisture back into the Indian Ocean and some of this diverges into the cyclonic circulation in the Mozambique Channel before reaching the continental region. Intuitively, some source of moisture must be inland waters or soil moisture already retained from the already prescribed conditions (see figure 4.1). January 1996, representation of moisture flux in the control run gives more moisture from the northwesterlies down from the east coast and the easterlies from the Indian Ocean advecting more moisture inland than in January 1992 (figure 5.3b). The same scenario of southerlies up the cold west coast is maintained like in January 1992 particularly, the anticyclonic circulation over the northwest of Botswana where there is less moisture influx. Generally, there is more moisture influx inland in January 1996 than in January 1992. This is a very useful factor to consider on some of the weak responses to soil moisture perturbation in January 1996.

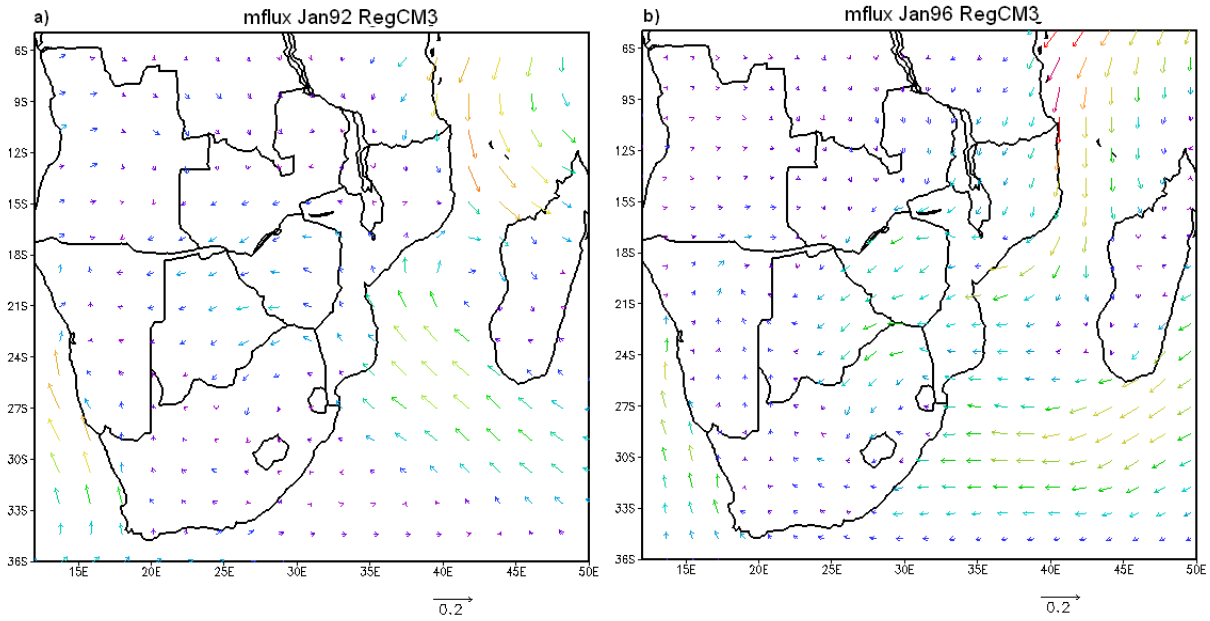

Figure 5.3 Direction and magnitude of moisture flux (g kg^{-1} ms^{-1}) for (a) January 1992 and (b) January 1996 in the RegCM3 at 2 metres above surface.

Direction and magnitude of moisture flux anomalies (g kg^{-1} ms^{-1}) for the soil moisture perturbation experiments show a marked increase in moisture influx inland from the northeast during the dry experiment(figures 5.4a and 5.4c). There is an increase in moisture flux from the Mozambique Channel in both dry soil moisture perturbations, which is probably an indication of an enhanced north-east monsoon due to increased heating and convection over land. However, offshore moisture flux occurs in some parts of the coast including the west. A pronounced cyclonic circulation occurs over central South Africa, northern Botswana and clear zones of convergence occur over some parts of the region. This could possibly result in an increase in convective type of precipitation.

In January 1992, there is a marked increase in moisture flux in a northwesterly direction over DRC, Zambia, Botswana and Zimbabwe for the wet soil moisture perturbation (figure 5.4b). There is increased onshore northeasterly moisture flow from the Indian Ocean. An anticyclonic circulation develops to the southeast of the region which drives the moisture flux from the southeast inland for the two mid-seasonal periods (figures5.4b and 5.4d). An increase in moisture flux occurs over northern South Africa, Zimbabwe and Botswana during January 1996 with the

wet soil moisture initialisation (figure 5.4d). There is a reduction in the moisture flux advection into the main land and an anticyclonic circulation develops over southern Namibia, western South Africa, and Angola.

For both Januaries moisture flux anomalies, the flow along the western shore is not changed resulting in some little or no change in moisture flux. There is a substantial change in moisture flux in Mozambique Channel which is more enhanced in January 1992 whilst January 1996 maintains an anticyclonic circulation. This maintains a northeasterly inflow from the Channel in January 1996. Anomalous soil moisture perturbations keep a reasonable amount of moisture flux inland regardless of source or fetch of the low level moisture.

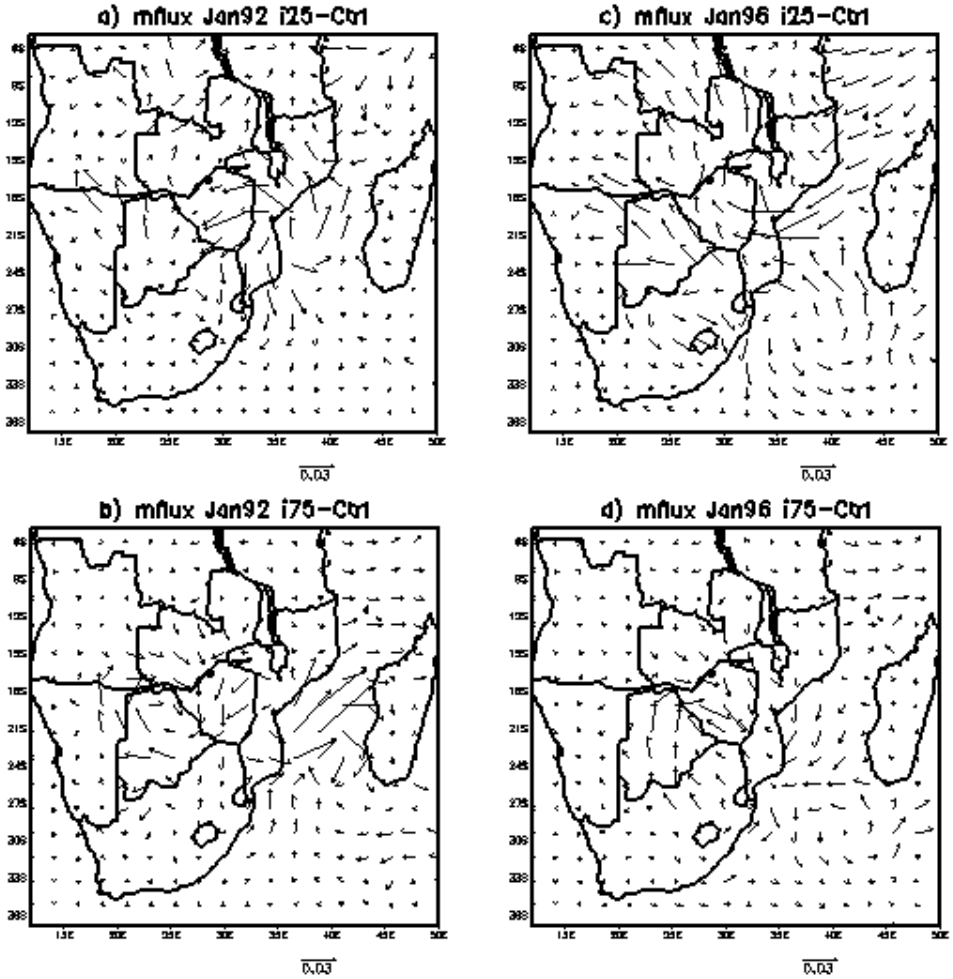

Figure 5.4 The direction and magnitude of 2m moisture fluxes anomalies (g kg^{-1} ms^{-1}) for January 1992, interactive a) dry run - control, b) wet run – control; January 1996, interactive c) dry run - control and d) wet - control.

5.4 Vertical Analysis

5.4.1 Cloud Liquid Water Path

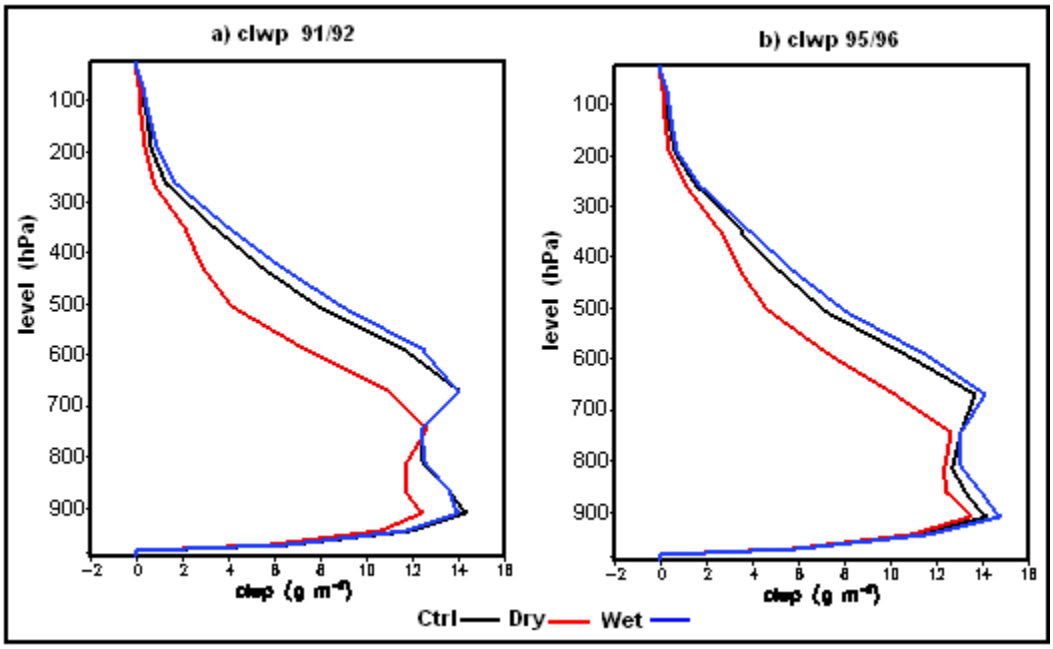

Figure 5.5 Vertical profiles for cloud liquid water path (g m^{-3}) for the perturbed and control simulations in (a) 1991/92 and (b) 1995/96 seasons. Black represents the control run, red is the dry run and blue for the wet run.

Figure 5.5 shows the vertical profiles of the mean CLWP (g m^{-3}) for 1991/92 and 1995/96 seasons. The control experiment shows almost a similar profile to that of the interactive wet simulation although the wet run has slightly more liquid water in the upper atmosphere (14g m^{-3}). In comparison to the control simulation, anomalous dry soil moisture experiments show more CLWP throughout the profile except near the surface and towards the top of the profile. The CLWP value is 16 g m^{-3} near 800hPa in 1995/96 (figure 5.5b) and has almost similar value in the middle atmosphere for 1991/92 (figure 5.5a). This can support the point that these experiments have more convective rainfall activity occurring due to moisture contents in the vertical profile. The similarity in the top of profile CLWP values could be attributed to most of the top cloud being thin cirrus ice cloud with less influence from optical depth (GES DISC, 2008).

The interactive dry anomalous soil moisture experiments have less CLWP than the control run throughout the profile. Importantly, the dry experiments exhibit the larger difference with the

control regarding the level at which the profiles have their maximum CLWP. This level indicates the height at which the cloud is most abundant. It appears that whilst both runs reach a maximum of CLWP at lower level (figure 5.5), the control run maintains larger amounts to higher levels (around 700hPa). This suggests that the amount and thickness of cloud is partly determined by the soil moisture initialisation, which is also in accordance with the results seen for changes in the incident solar radiation. In general, soil moisture perturbations show a small increase in CLWP for the anomalous wet soil moisture initialisation as compared to the control implying no major change in convection but major suppression in convective activity within the interactive dry soil moisture setup particularly during 1991/92.

5.4.2 Atmospheric Analysis of Air Temperature

The dry soil moisture perturbation simulations (figures5.6a and 5.6c) show positive air temperature anomalies across the region in the lower atmosphere. Highest positive anomalies of over 2°C are confined to the west of the region with negative anomalies occurring in the middle atmosphere. Negative anomalies that are less than -1.5°C occur in middle atmosphere in 1991/92 season (figure 5.6a) as compared to 1995/96 (figure 5.6c). Positive anomalies occur over most of region's cross-section for both seasons. The vertical distribution of the atmospheric temperature over the western areas depicts an unstable condition situation. Given the positive anomalies in the lower troposphere and with the presence of soil moisture in that region, warm light air will tend to rise resulting in precipitation. This is also aids in explaining the increase in precipitation observed over the southwestern areas (figure 4.13).

Figure 5.6 shows the vertical analyses of air temperature anomalies of the soil moisture perturbations from the control simulations for 1991/92 and 1995/96 seasons at latitude 18ºS in the central part of southern Africa region. Anomalous wet soil moisture conditions for 1991/92 results in a cross-section comprising of negative air temperature anomalies over the west and central areas but slight warming over the eastern areas and a small portion within the west for the lower atmosphere (figure 5.6b). Middle atmosphere depicts warming over most of the region with a warm pool of about 1.5°C occurring over the western areas. The western areas depict a

very stable atmosphere with cold dense air and warm light air above it creating an inversion layer.

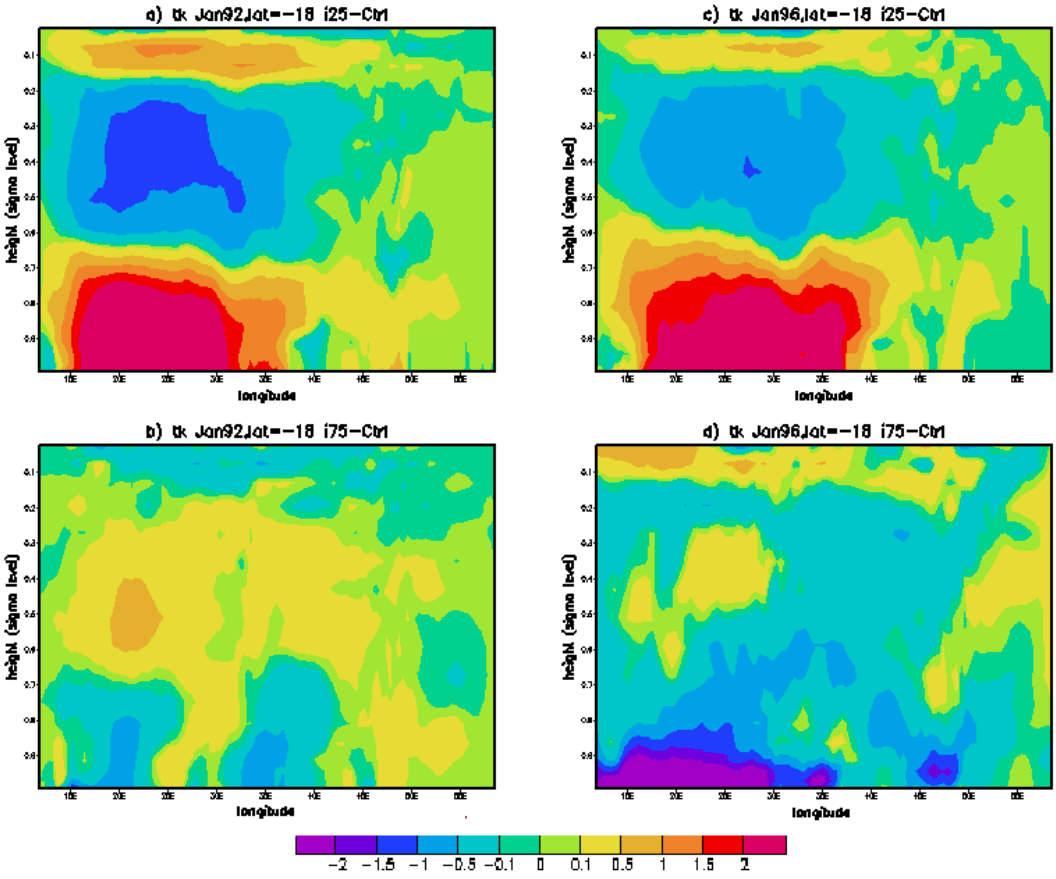

Figure 5.6 Vertical analyses of air temperature anomalies of the soil moisture perturbations from the control simulations for 1991/92 (left column) and 1995/96 (right column) seasons at latitude 18ºS in the central part of southern Africa region.

As for 1995/96, the air temperature shows cooling throughout most of the atmosphere except for the upper atmosphere whilst slight positive anomalies occur in the middle atmosphere over the western and eastern areas (figure 5.6d). The cooler air temperature anomalies would imply unstable conditions for the wet soil moisture perturbation simulation. The stability conditions established here through the overall atmosphere temperature characteristics do partially explain the incoherent rainfall response to soil moisture perturbation especially over the southern parts of the subcontinent. This supports existence of negative feedback mechanisms in some areas. Similar to the findings of Giorgi et al., (1996); Findell and Eltahir, (2003b) and Cook et al.,

(2006). Note that, similar patterns in the vertical distribution of atmospheric temperature occur for mid-latitude at 25°S (not shown here).

5.5 Mean January Climate Responses

Besides the moisture fluxes presented earlier, the following analysis presents some important results obtained from the preliminary January simulations (see Tadross et al., 2010). As mentioned earlier, January is a crucial month which is usually termed the mid-season month commonly associated with occurrence of long intraseasonal dry spells (Torrance, 1981; Matarira and Jury, 1992; Makarau, 1995; Unganai and Mason, 2001; Usman and Reason, 2004). In agriculture, this is a critical time in crop maturity or development and impacts on crop yield. Some distinctive results and sub-seasonal changes have been observed during January as discussed in the previous chapter. A diurnal variation analysis is vital in seeking more insight into the feedback mechanism and thus isolates physical mechanisms (Schär et al., 1999). The soil moisture sensitivity will be used to understand the implications of soil moisture conditions on the frequency and intensity of rainfall.

5.5.1 Diurnal Cycles

Figure 5.7 presents the area-averaged diurnal cycles of the selected surface variables over southern Africa using the universal time constant (Z/UTC). The diurnal cycle of precipitation shows peaks after midday for both years (figures 5.7a and 5.7d). This is expected as most of southern African rainfall is of convective form and falls during daytime into night time after the surface warms up (Torrance, 1981; Buckle, 1996; Tyson and Preston-Whyte, 2000). The average peak magnitude is higher for January 1996 for all experiments, which should be expected for the simulated wetter year than for January 1992. Interactive simulation for the wet run tends to be similar in pattern to the control whilst the interactive dry run has the lowest peak.

Figures 5.7b and 5.7e show that the peak in surface temperature occurs in the afternoon with the coldest temperature occurring at night. The diurnal pattern for the surface temperature depicts higher peaks for the interactive dry run which was shown to have a lower peak for the total

rainfall. This implies that drier surfaces result in higher surface temperatures. Coherently with rainfall patterns, the peaks decrease through from dry simulation to control and then wet simulations. The latter being the wettest in precipitation's diurnal patterns.

Evapotranspiration diurnal cycles show similar patterns to the total rainfall cycles with the maximum of evaporation rates increasing in the afternoon and the minimum occurring after midnight to 5am (figures5.7c and 5.7f). The dry runs show 2mm/day diurnal range from afternoon maximum to overnight drop in evapotranspiration. The highest peak in evapotranspiration rate is simulated with wet simulation experiments where the maxima are 10mm/day and 9mm/day for January 1992 and January 1996 respectively. In the control simulation the maximum is less by a 1mm/day from the wet run. However, there is no marked difference from the wet and control runs during the early and late hour periods.

In contrast, the anomalous dry soil moisture run depicts a larger maximum with sensible heat flux than the control experiment due to low evapotranspiration rate, low rainfall rates and high surface temperatures as shown in the earlier diurnal patterns (figures5.8a and 5.8d). The diurnal cycle for sensible heat flux shows similar patterns to the surface temperatures discussed earlier for all experiments. Wet soil moisture perturbation and control simulation show similar patterns except for slight differences around midday. Figures5.8 b and 5.8e show the diurnal cycles of incident solar radiation for January 1992 and January 1996 respectively. No marked difference in diurnal patterns occurs with incident solar radiation for all experiments as the maxima are similar with a marginal difference after midday. The highest peak occurs with the dry soil moisture perturbation which would at least imply the model is simulating less cloud or fluffy (or very thin) clouds and thus allowing more incoming solar radiation to reach the surface than for the other experiments. The diurnal variations of incident solar radiation could aid explain the mixed and weak responses on spatial and temporal distribution discussed earlier (figures 4.29 and 4.30).

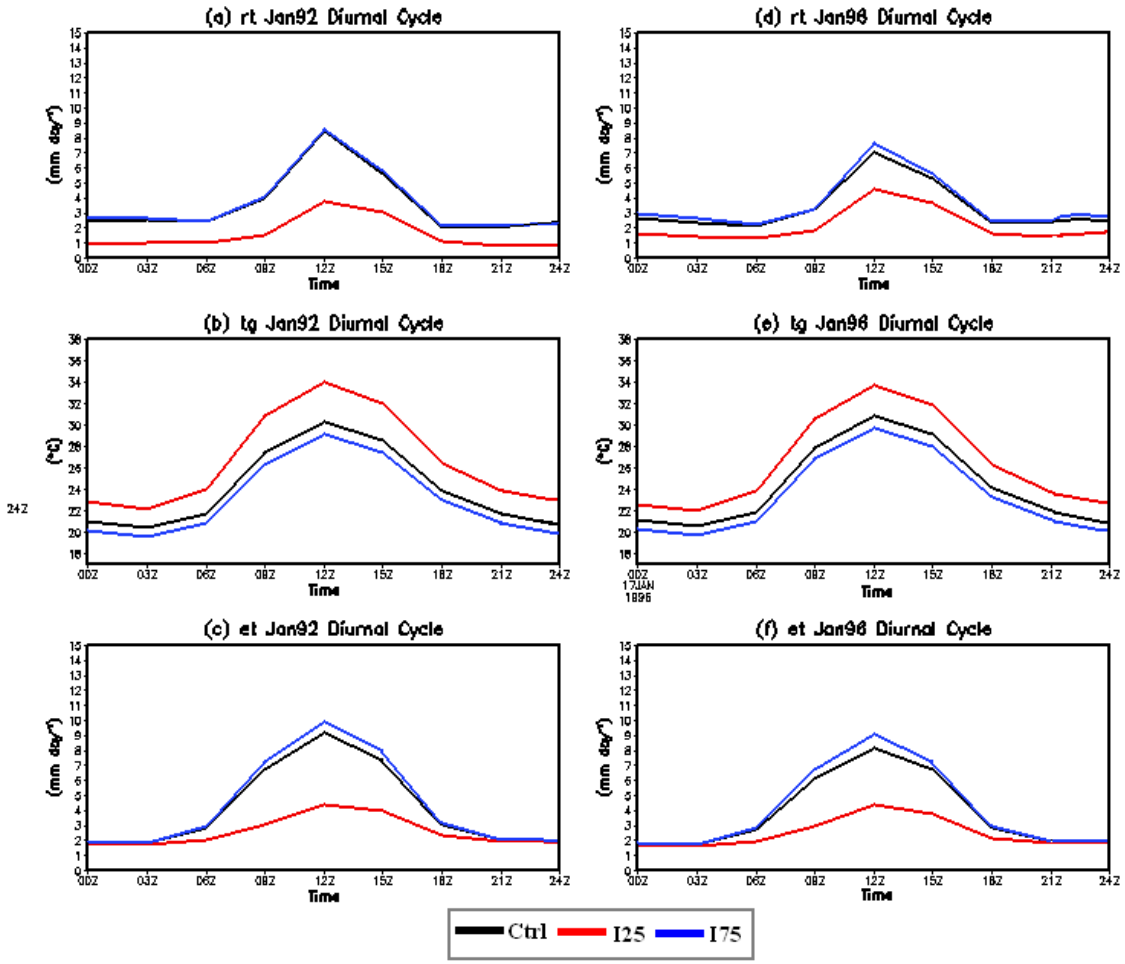

Figure 5.7 Diurnal cycles of (a) Total precipitation, (b) Surface Temperature (c) Evapotranspiration for January 1992 and (d) Total precipitation, (e) Surface Temperature and (f) Evapotranspiration for January 1996.

The planetary boundary layer diurnal cycle increases in height to reach a peak in the afternoon at around 12UTC (2pm) and slowly decreases until around 15UTC (5pm) then sharply diminishes till 16UTC (8pm) where the PBL height becomes constant thereafter. During the day, incident solar radiation results in the warming of the surface air which destabilizes the profile due to becoming hotter than air above. This leads to a daytime convective boundary layer (Tyson and Preston-Whyte, 2000; Pal and Eltahir, 2001; Barry and Chorley, 2009; Jaeger, and Seneviratne, 2011). Mixing in the boundary (mixed) layer occurs through turbulence and thus the height increases during the day. At night, there is no incident solar radiation so the surface begins to cool through outgoing longwave radiation. Less mixing occurs at night time and thus the layer

becomes stable. This was also observed byTyson and Preston-Whyte(2000); Pal and Eltahir(2001); Wallace and Hobbs(2006) and Barry and Chorley (2009).

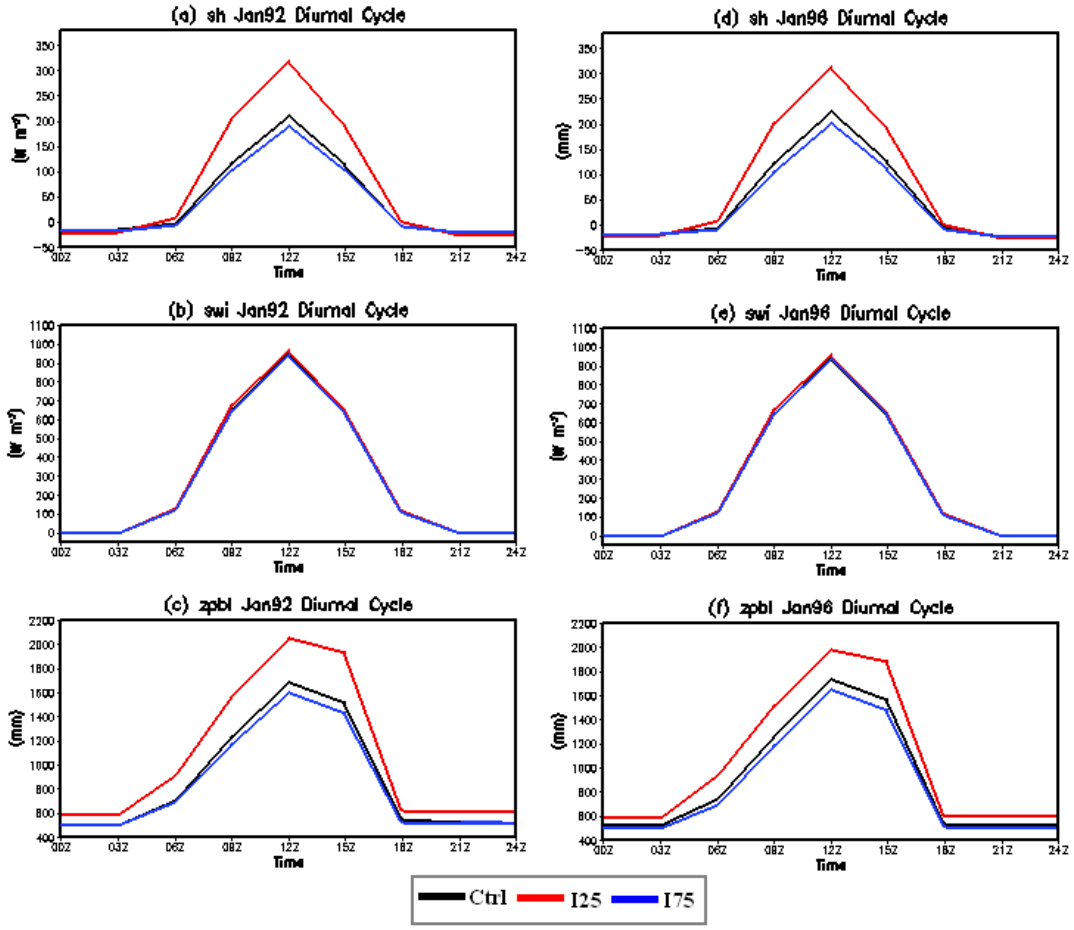

Figure 5.8 Diurnal cycles of (a) Sensible heat flux, (b) Incident solar radiation (c) Planetary boundary layer for January 1992 and (d) Sensible heat flux, (e) Incident solar radiation and (f) Planetary boundary layer for January 1996.

In the above diurnal patterns, the mixed layer is lower for wet soil moisture experiments and higher for interactive dry runs. According to Pal and Eltahir (2001), anomalously high soil moisture tends to reduce the PBL height thus increasing the moist static energy per unit mass air amongst other additional factors. Jaeger and Seneviratne (2011) concur that an increase in soil moisture leads to an increase in latent heat flux (similar to diurnal variation of evapotranspiration, figures 5.7c and 5.7f) and a decrease in sensible heat flux (figures 5.8a and 5.8 d) causing a lower and colder PBL (figures 5.8c and 5.8f) as indicated by the decreased air

temperature (figures 5.7b and 5.7e). Thus the diurnal variations of the surface parameters analysed seem to confirm the positive feedback mechanism for the bulk of the region. It is also evident that soil moisture does not substantially impact the overall daily variability. The effects are only clear in magnitudes. According to Sylla (*pers. Comm. 2013)* it is like excessive soil moisture induces intensification of the atmospheric hydrological cycle without modifying its variability. This can manifest as increase of frequency in some regions or large intensity in others.

5.5.2 Rain Days and Rainfall Intensity

Figure 5.9 shows the rain days and intensity for the control experiments of January 1992 and 1996. Rain days were considered to be any day receiving at least 2mm/day and intensity was then calculated from the total monthly rainfall between the rain days. The 2mm/day threshold was selected as the water level that would be satisfactory to the maize crop requirements and thus making this analysis become relevant to the agriculture sector over the southern Africa region (R Shultz, *pers. comm.* 2009). Unlike the meteorological definition which is a mere 0.2mm/day. January 1992 reveals the greater part of the region as having more than 18 rain days (Figure 5.9a). The largest number of rain days (more than 27 days) occurs over southern Zambia, northern Zimbabwe, southern coast of Mozambique and Lesotho. The southwestern areas show little or no precipitation with less than 3 rain days especially over Western Cape areas, as well as the semi-arid or desert areas of Botswana and Namibia.

Figure 5.9b displays rain days for the control simulation of January 1996. Most of Zimbabwe, Botswana, northern South Africa, central Zambia and northern Mozambique depict a very rainy situation with 21 or more rain days. The rest of the region has a gradual spread of increase in rain days from the west towards the east (figure5.9b). It has been recently observed that Emanuel scheme precipitates a lot especially in the tropics and sub-tropics (B. Sylla, 2011*pers. comm*.). This could aid in explaining the near 30 rain days observed in some sub-regions. However, the area with rain days is larger in January 1996 (figure 5.10b) than in January 1992 (figure 5.9a).

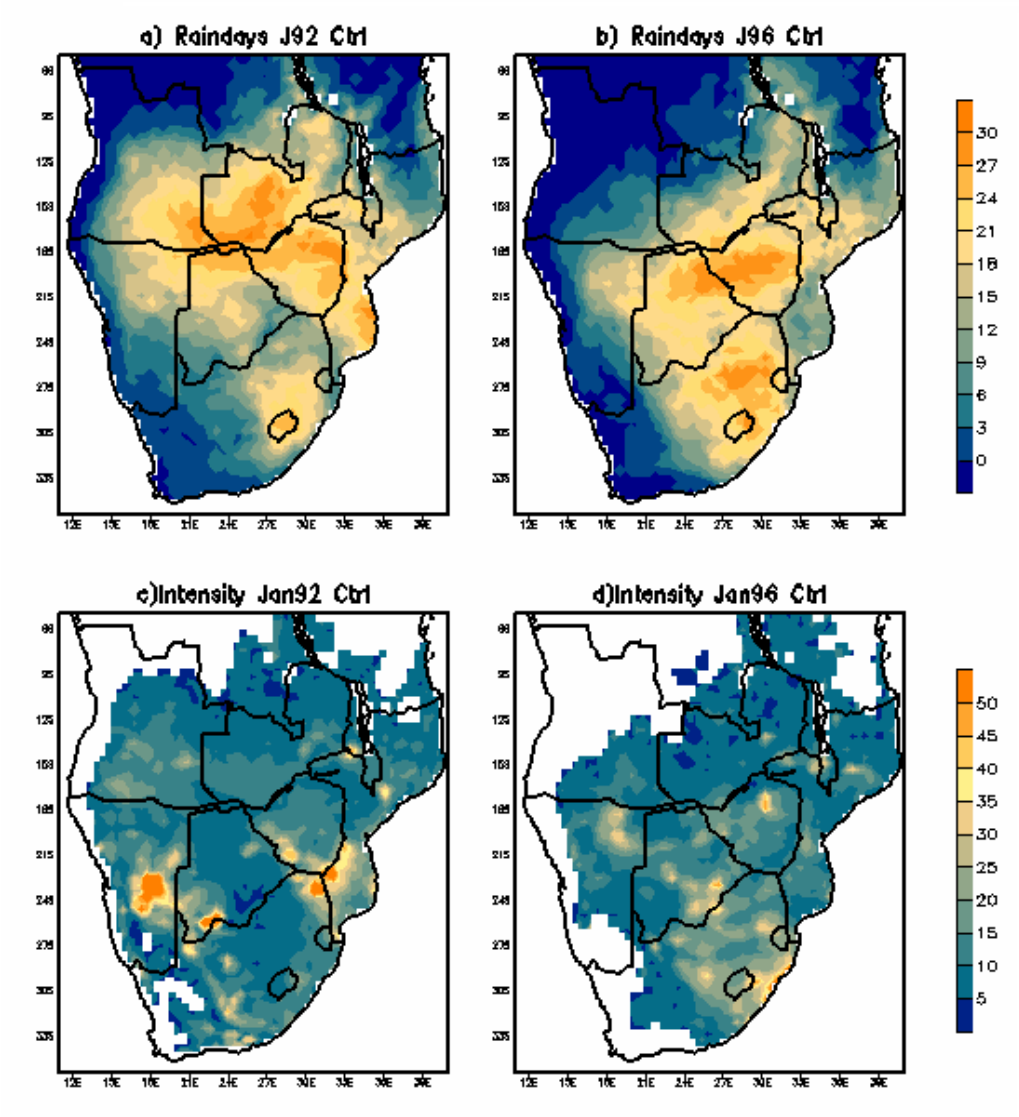

Figure 5.9 Rain days and Intensity (mm/day) for RegCM3 simulations; January 1992 a) Rain days, b) Intensity and January 1996 c) Rain days, b) Intensity. Rain day is considered to be 2mm/day.

Less intense rain is shown over the northern parts of the region and more intense rain being inclined towards the southern areas during January 1992(figure 5.9c). Some isolated intense storms are shown over Namibia, Botswana, southern Zimbabwe and northeastern South Africa implying that most of the precipitation occurred within a 3 day period (figure5.9c). Much of the area with high number of rain days (figure 5.9a) shows a less intense rainfall pattern (figure5.9c) that indicates a fair distribution of the rainfall throughout the month. In January 1996, intense rains (figure 5.9d) are mostly confined within the region of highest number of rain days (figure 5.9b) implying a regular distribution of daily rainfall throughout the month. However, over the

southeastern coast, there are about 24 to 27 rain days (figure 5.9b) and intense falls of about 50mm/day (figure5.9d) signalling that some heavy falls could have occurred on some of the days. Note that, in some areas the intensity could not be calculated as rain days less than 2mm/day threshold were not considered. Thus with zero rain days the intensity cannot be calculated.

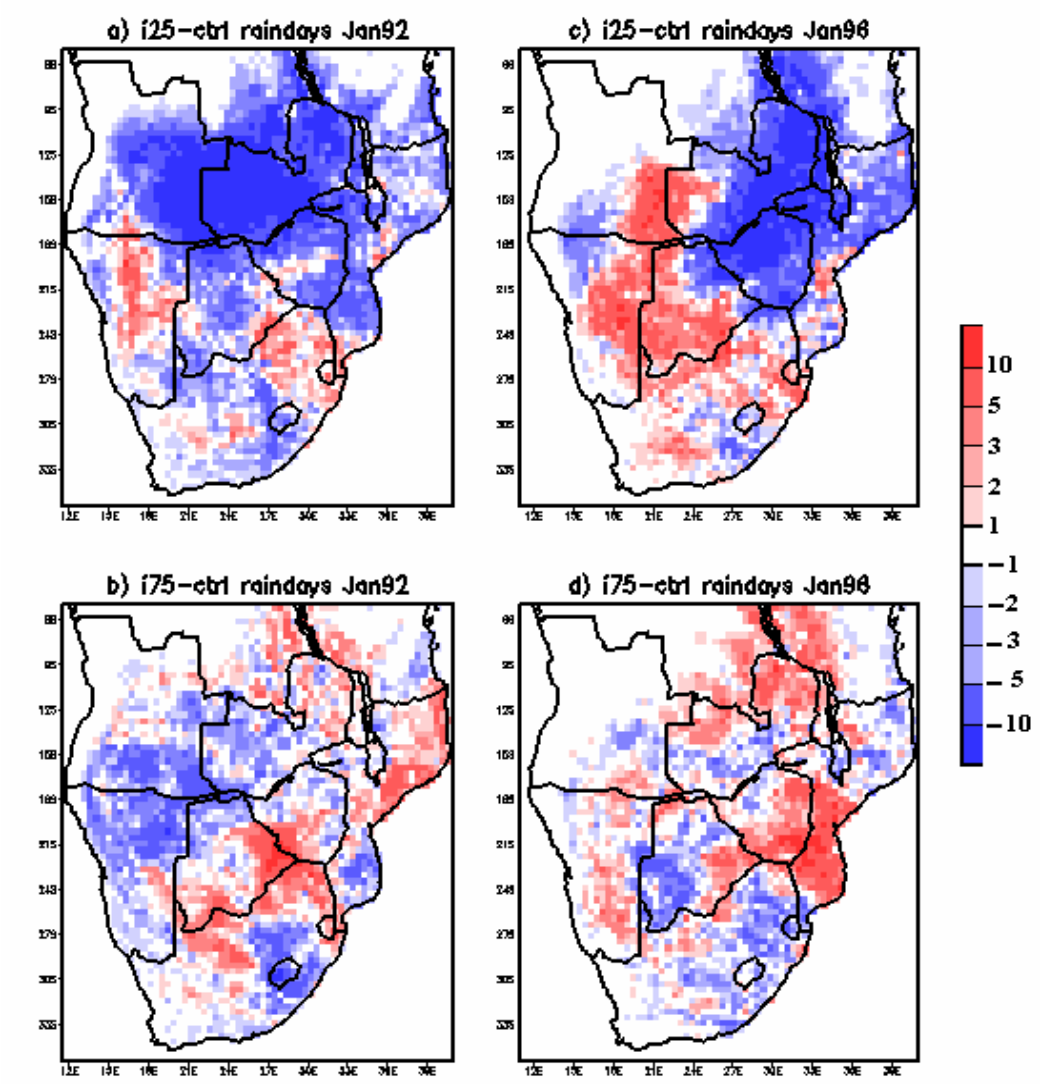

Figure 5.10 Total rain days anomalies between the interactive experiments from the control simulation for January 1992 a) dry - control, b) wet – control and 1996 c) dry - control and d) wet – control. Rain day is considered to have at least 2mm/day.

Figure 5.10 displays total rain days anomalies in RegCM3 between the interactive experiments from the control simulation for January 1992 and 1996. Anomalous dry soil moisture conditions

for January 1992 (figure 5.10a) depicts a decrease in rain days over the region with marked reduction of more than 10 rain days occurring over eastern Angola and southern Zambia whilst over Malawi and southern Mozambique isolated minor decreases (below 5 days) occur. However, increases of up to 10 rain days are simulated over northern Namibia and eastern South Africa. The dry soil moisture perturbation for January 1996 (figure5.10c) has a NE-SW inclined distribution with a marked decrease over the northeastern parts of the subcontinent and an increase over most of the southwestern region. Positive anomalies of more than 5 days are over southeastern Angola, northeastern Namibia and western Botswana whilst decreases of more than 10 rain days occur over northern Zimbabwe and eastern Zambia. In general, distribution pattern in rain days follows a west to east for increase to decrease in dry soil moisture runs (figures5.10a and 5.10c).

For both wet runs of January 1992 and 1996 (figures5.10b and 5.10d), there is no distinctive response between the years. However, there is more of an increase in rain days with an NW-SE inclination and isolated areas of decrease in rain days. For all simulations, there is a vast area falling within the transitional zone (i.e. between decreases and increases from -1 to 1). These are eastern Tanzania, western coastal areas, isolated areas as well as northwestern and southwestern parts of the region. This could imply that within the model the number of rain days in these areas is not affected by the forms of soil moisture perturbations. Basically, even with the changes in soil moisture initializations the precipitation will remain below 2mm/day. Southeastern South Africa and Lesotho show a decrease for all forms of soil moisture perturbations, indicating that dynamical changes resulting from these experiments result in a shift of rainfall producing systems away from these regions.

Figure 5.11 displays January 1992 and January 1996 intensity anomalies (mm/day) between the interactive soil moisture simulations from the control simulation. There is no clear response in the rainfall intensity distribution pattern over the region in any of the simulations. At first glance, the dry experiments tend to show a decrease in the intensity over the bulk of the region with a NW-SE gradient (figures5.11a and 5.11c) especially over western parts of the region (figure 5.11a) and eastern parts of the region (figure5.11c). The converse for increase in intensity applies for the wet soil moisture perturbation experiments (figures5.11b and 5.11d) especially over

Botswana and southwestern South Africa (figure 5.11b) as well as Zimbabwe (figure 5.11d). However, there are also vast areas, as mentioned in the rain days' section, which lie within the transitional zones. Portions of southeastern South Africa and Lesotho maintain a decrease in rainfall intensity for all soil moisture perturbations. This is a contrast to January 1992 when the synoptic forcing is characterised by large-scale subsidence, more so than during 1996. Although this requires further investigation it might imply that spatial organisation of changes in rainfall intensity may be heavily dependent on the synoptic forcing of the regional climate.

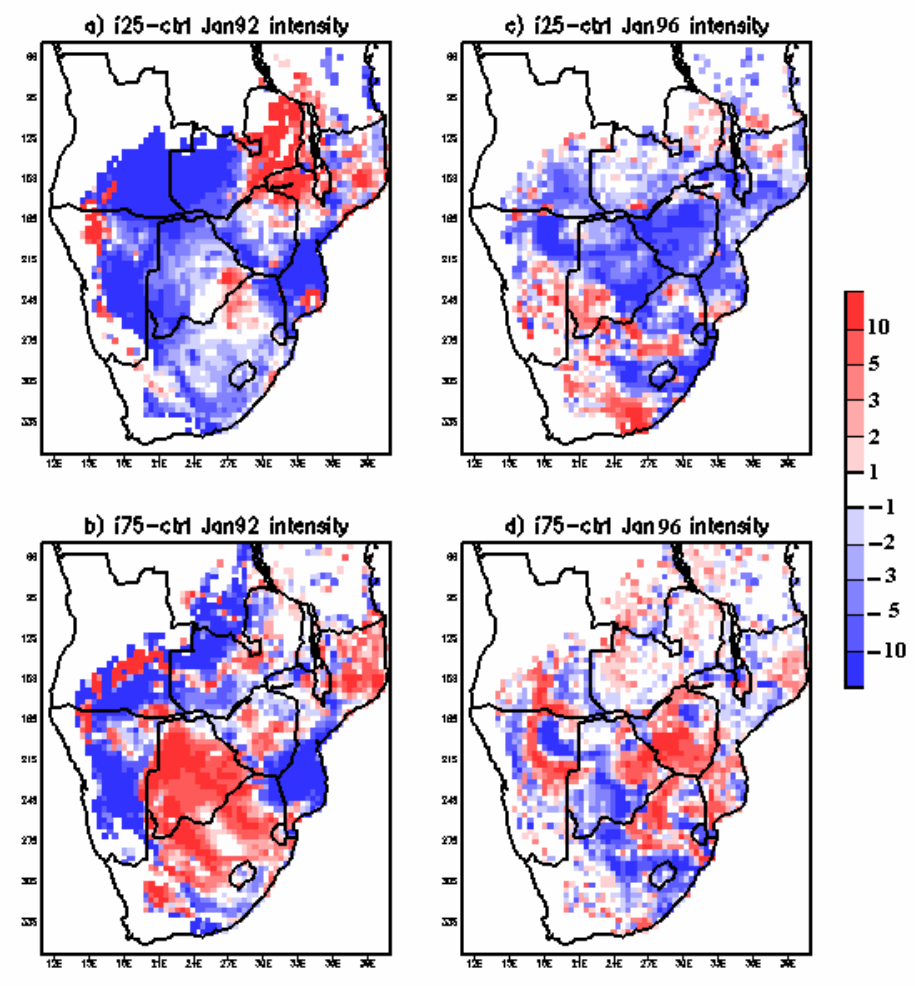

Figure 5.11 Intensity anomalies (mm/day) between the interactive experiments minus the control simulation for January 1992 a) dry - control, b) wet – control and 1996 c) dry - control and d) wet – control.

5.6 Summary

This chapter covered synoptic analysis of the situation associated with the soil moisture perturbations. An atmospheric analysis was also done on air temperature and cloud liquid water path profiles. This brought out some useful information about other forcings that may lead to the responses observed in the summer simulations analysed. A focus on the January month also aided in explaining some other factors such as diurnal variations, rain days and intensity.
The main findings are summarised as:

- The 700hPa geopotentials show that there is enhanced anticyclonic circulation over the region during early summer than later in the season for anomalous dry soil moisture experiments. Greater persistence of the anticyclonic circulation is observed during the dry 1991/92. Wet soil moisture initialisation leads to a decrease in geopotential height.

- Anomalous dry soil moisture simulations result in the strengthening of the anticyclonic activity which leads to conditions unfavourable for cloud development and rainfall activity. Wet soil moisture perturbations result in decrease of geopotentials implying a weakening of anticyclones or deepening of low pressure systems.

- Anomalous wet soil moisture simulations lead to conditions quite favourable for cloud development and enhancement of rainfall activity with increase in low level moisture convergence. This would also lead to decreases in surface temperatures, solar incident radiation resulting in depressed sensible heat flux whilst enhancing latent heat flux and lowering the PBL. The response is stronger in the dry 1991/92 season. This is more spatially cohesive over northern areas of the subcontinent.

- There is more moisture influx inland in January 1996 than in drier January 1992. Thus weaker responses are observed for soil moisture perturbation in January 1996 and this may be attributed to available moisture reserves being adequate such that additional moisture won't augment change. For both seasons, coastal flow over the west is not changed resulting in some little or no change in moisture flux. Anomalous soil moisture perturbations depict low level moisture convergence over the central parts of the region.

- The anomalous dry soil moisture experiments have uniquely less cloud liquid water path (CLWP) than the control and wet simulations throughout the vertical profile with a bigger magnitude difference in 1991/92. Importantly, the level at which the profiles have their maximum CLWP, which indicates the levels at which cloud is most abundant, is most different between the control simulations and interactive dry soil moisture runs. Wet soil moisture runs result in slight difference of CLWP from the control suggesting no major change in convection but major suppression in convective activity within the interactive dry soil moisture setup particularly for the dry 1991/92 season.

- Vertical integration of the atmosphere demonstrates that dry soil moisture simulations show increases in air temperature across the region in the lower atmosphere with negative anomalies occurring in the middle atmosphere. The vertical distribution of the atmospheric temperature over the western areas depicts unstable conditions.

- In the lower atmosphere, the cooler air temperature for the wet soil moisture perturbation in comparison to the control simulation would imply stable conditions especially over the western areas. The stability situations established here through the overall atmosphere temperature characteristics do partially explain the incoherent rainfall response to soil moisture perturbation. This also supports existence of negative feedback mechanisms in some areas especially over the southwestern region.

- Diurnal patterns of the surface variables analysed simulate a natural cycle associated with southern Africa climate with the maximum occurring after midday. It is also evident that soil moisture does not substantially impact the overall daily variability but its magnitude.

- Diurnal cycle patterns tend to show positive response mechanism for the respective soil moisture perturbations. Thus, distinct high (low) peaks are observed for the dry (wet) soil moisture initialisation with the surface temperature, sensible heat flux, incident solar radiation and planetary boundary layer (rainfall and evapotranspiration) variables.

- There is no clear response shown in the rain days and rainfall intensity distribution pattern over the region for all the different simulations. Intensity distribution in comparison to the number of rain days implies a fair distribution of rainfall for most of the month.

Chapter 6

SOM Characterisation of Synoptic Patterns in Summer Climate

6.1 Introduction

Self-organizing maps (SOMs) are used in this chapter to assess the possible changes in circulation patterns in response to soil moisture perturbations. A SOM is trained with the NCAR/NCEP re-analysis 2 data over the summer period from 1September to 31 March of 1991/92 and 1995/96 at a daily time-scale. In order to adequately represent the circulation and moisture sources over the region, variables chosen for mapping are the geopotential heights at 500hPa and 850hPa, and precipitable water in the atmosphere at 700hPa. The SOM is then used to identify the differences between the control and the soil moisture perturbation simulations with respect to distribution and frequency of occurrence of synoptic circulation patterns.

The main reason to choose the above mentioned variables is that the two geopotential height levels are commonly used over southern Africa to characterize circulation patterns in meteorology and climatology (Torrance, 1981; Buckle, 1996; Lindesay, 1998; Tyson and Preston-Whyte, 2000; Mackellar, 2007). These levels adequately reflect most systems such as baroclinic mid-latitude, baroclinic sub-tropical and tropical systems (Tyson, 1986; Tyson and Preston-Whyte, 2000). As for precipitable water it gives a good indication of the amount of condensable water vapour within the atmosphere column. This can be associated with moisture features over the region and position of the ITCZ (Mackellar et al., 2010). It is important to note that the re-analysis data was standardized before training. It is an effective method to utilize when there is a bias in the means of the input data. All the data at each grid point and time-step was standardized in terms of the long-term variable mean and standard deviation (Hudson, 1998; Mackellar, 2007; Mackellar et al., 2009).

The size of the SOM array determines the degree of generalization**.** After a trial error approach of different SOM arrays, a SOM of 12 nodes which adequately represented the synoptic circulation patterns was chosen. Sang et al. (2008) support this choice and point that climatologists categorize 12 types of circulation patterns as adequate. This is a 4 x 3 array (i.e. 4 in the x-direction and 3 in the y-direction) and the weights of the nodes were initialized using random initialisation. More details on options available on the SOM package and references have been discussed in chapter 3 (e.g. Kohonen, 1995; Hewitson and Crane, 2002). SOM package has also been incorporated into the open source statistical code called R. This was the package used to produce these SOM figures. A rectangular topology was used for visualization of array nodes; initial learning rate was set to 0.05 and an initial training radius of 3. From the respective SOMs training with the reanalysis data, the nodes can be displayed graphically in what has been called meta-maps (Main, 1997).

6.2 Circulation Types

The SOM representation is such that adjacent nodes are associated with similar synoptic states whilst very different synoptic states are located in opposite corners. Each map on the node array or meta-map represents a node of the SOM and the contoured data on each map are the weights linked with the node. Each day of the NCEP/NCAR lateral boundary conditions for 1991/92 and 1995/96 seasons are mapped to a particular SOM node in the 4 x 3 SOM. The nodes are then related to the same day of the RegCM3 anomalous soil moisture simulations. Thus the mean response to atmospheric conditions to the soil moisture perturbations can be evaluated for each SOM node or each synoptic type.

6.2.1 850hPa Geopotential heights

Figure 6.1 shows the different circulation patterns identified by the SOM for NCEP/NCAR 850hPa geopotential height (gpm) reanalysis data anomaliesduring the summer season. The SOM illustrates two clear different synoptic patterns. The first with conditions favourable for vertical uplift in the tropics occur on the top left (e.g. nodes 1, 2) represented by the sub-tropical low pressure system over the northern parts of the region whilst some weak sub-tropical ridge

occurs around the middle of the domain. And a second pattern where a weak anticyclonic circulation over Namibia/Botswana and Indian Ocean strengthens from left to right and top to bottom with the strongest high pressure systems occurring to the bottom right (nodes 8, 12) implying warm and dry subsiding air. The trough to the southeast of the region (node 1) deepens as one traverse in space to the bottom right to become a closed low pressure system (node 12). The sub-tropical ridge is evident over the domain within the SOM space and shifts northwards in the neighbouring transitional states.

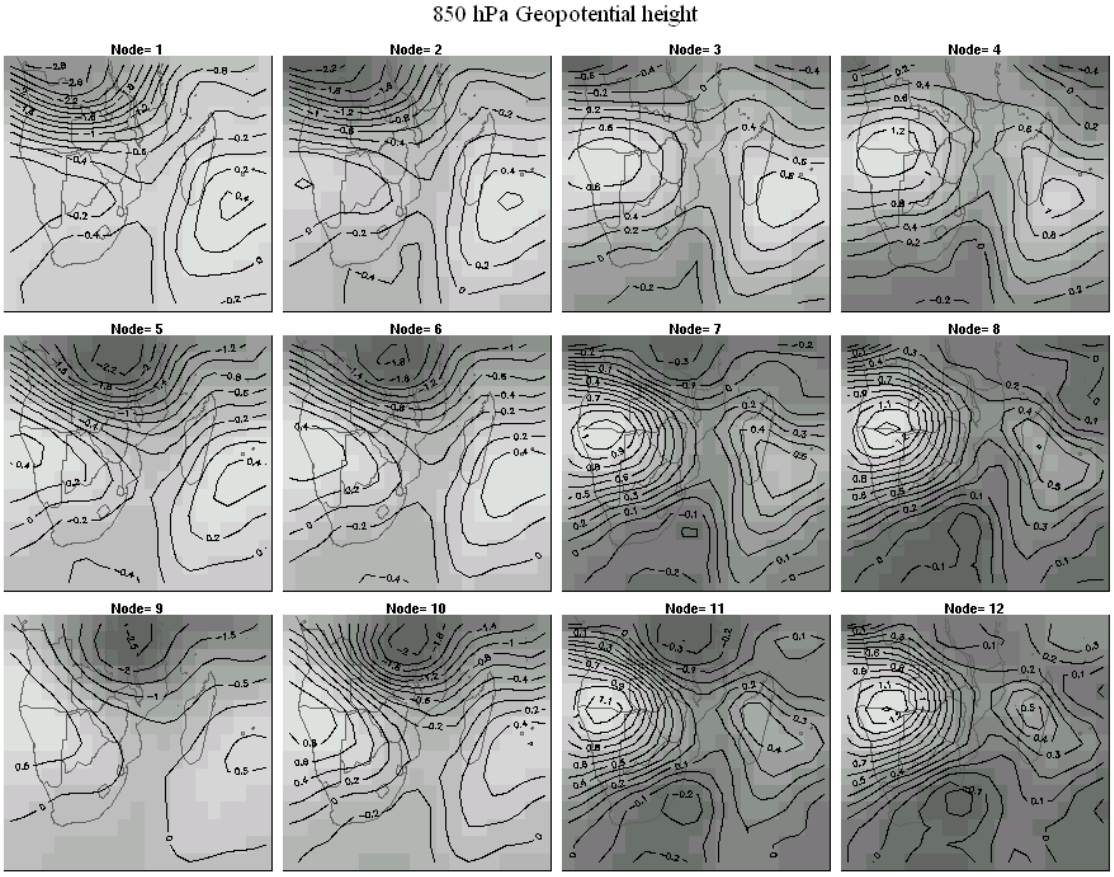

Figure 6.1 A 3x4 SOM of daily average NCEP/NCAR 850hPa geopotential height (gpm) anomalies from 1 September to 31 March 1991/92 and 1995/96.

6.2.2 500 hPa Geopotential Heights

Figure 6.2 shows the patterns identified by the SOM for NCEP/NCAR 500hPa geopotential height (gpm) reanalysis data anomalies. Transformation from left to right in the SOM space depicts broadening and an increase in strength of the Indian Ocean anticyclone whilst the

depression over the northwestern parts of the domain fills up and a trough deepens over to the south of the region. The easterly wave covers most of the domain in the top row of the SOM although confined to the northern portions whilst a westerly wave is observed over the southern parts in the bottom right of the meta-map. These easterlies overlying a surface low pressure over Angola/DRC are synoptic characteristics favourable for convergence which may lead to convective precipitation if there is sufficient moisture available or advected especially over the top left corner of the SOM (node 1). As one traverses towards the bottom right corner of the SOM, there is anticyclonic circulations which imply enhanced subsistence of dry air and thus lead to dry or drought-like conditions being mapped over the most frequent synoptic state (node 12).

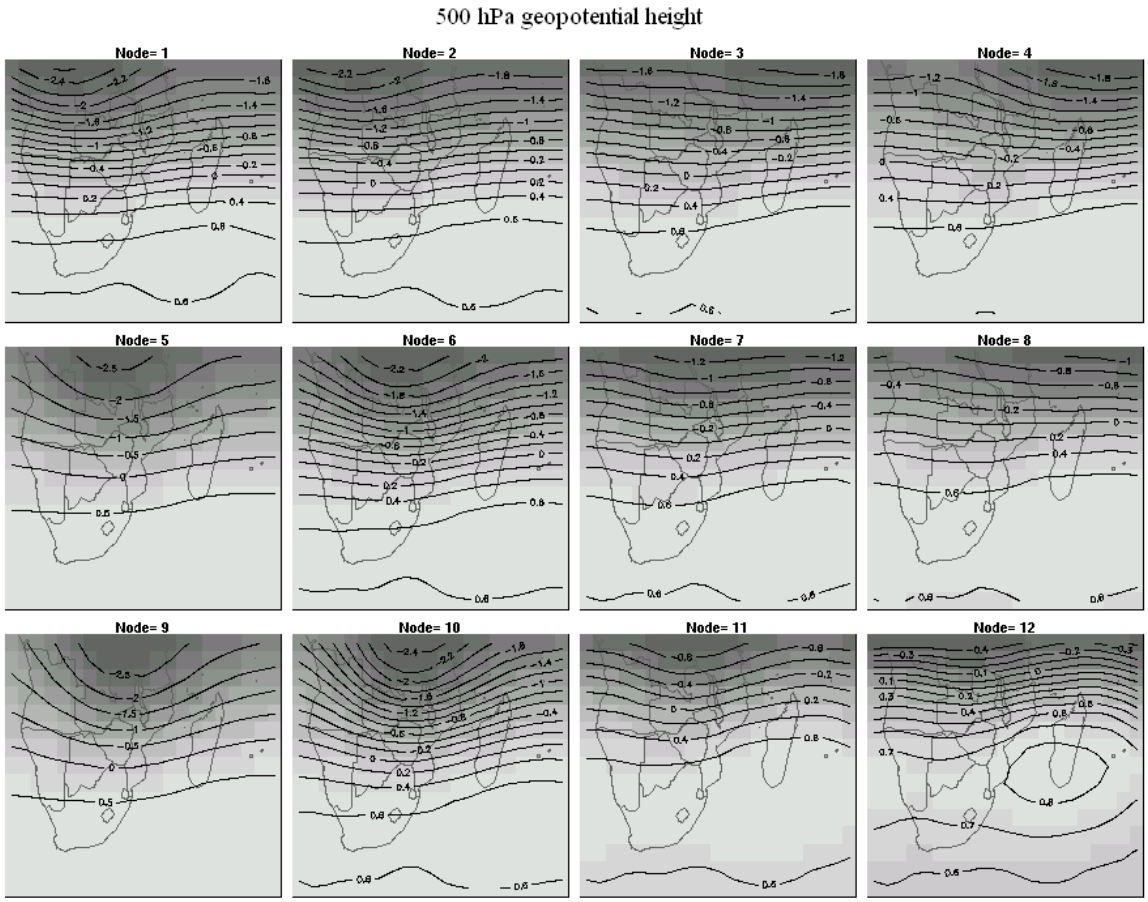

Figure 6.2 A 3x4 SOM of daily average NCEP/NCAR 500 geopotential height (gpm) anomalies from 1 September to 31 March 1991/92 and 1995/96.

6.2.3 700 hPa Total Precipitable Water

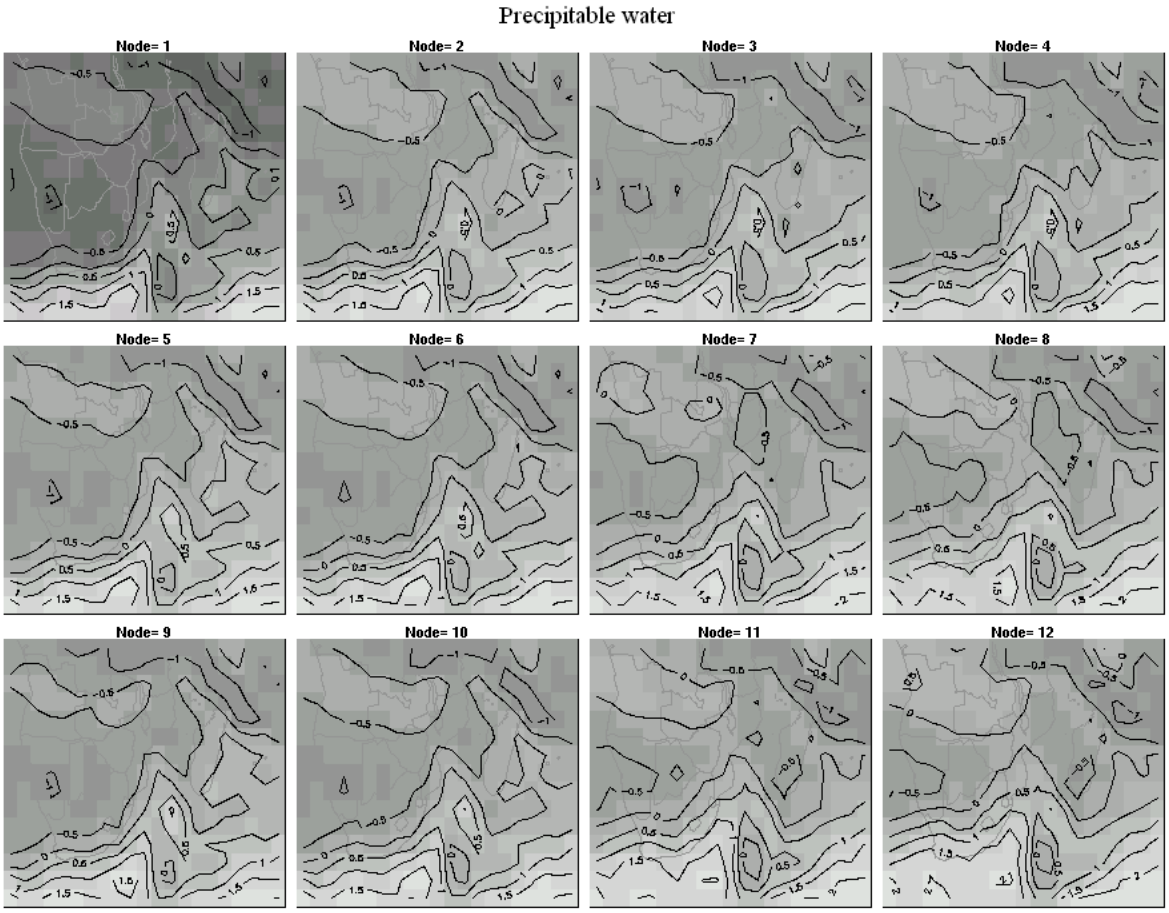

Figure 6.3 A 3x4 SOM of daily average NCEP 700hPa precipitable water (kgm^{-2}) anomalies from 1 September to 31 March 1991/92 and 1995/96.

Moisture conditions as represented by the total precipitable water (kgm^{-2}) anomalies at 700hPa SOM (figure 6.3) which shows that there are two different patterns, one in the top left corner with wetter conditions over the southeastern half of domain than that on the bottom right area of the SOM space characterized by dry conditions. Maximum precipitable water is associated with the trough and low pressure system (node 1). Moisture covers most of the central, northeastern and southeastern parts of the subcontinent. The moisture covers up the east coast and most of Mozambique Channel on the left side of the meta-map. The moisture gradually decreases to be confined towards the south of the domain in the bottom right of SOM array (nodes 8, 11 and 12). There is less moisture over the west and east of the domain in areas that are linked with the

850hPa anticyclone centres (figure 6.1). This is typical of late winter/spring circulation patterns and moisture distribution over southern Africa (Torrance, 1981; Buckle, 1996; Lindesay, 1998; Tyson and Preston-Whyte, 2000).

6.3 Seasonal Evolution through the SOM Array

There is a variation in systems' strength and lifetime (such as anticyclones and tropical depressions) from top left to bottom right in the SOM array. The seasonal progression conditions are analysed by looking at the time of the year the synoptic forcing (nodes) occur (Mackellar, et al., 2010). Figure 6.4 displays the median dates of occurrence for each node of the simulated seasons of 1991/92 and 1995/96. Node 12 (bottom right) occurs in early October and moving along the row to the left node 11, node 10, and node 9 occur later in the season. Traversing down the rows and columns clearly depicts the seasonal evolutions. Nodes 1 and 9 occur during the late part of the summer season (February into March) which depicts a low pressure system over the northern areas which can be associated with the southern tip of the ITCZ at this time of the season (Torrance, 1981; Lindesay, 1998; Buckle, 1996; Tyson and Preston-Whyte, 2000). Nodes 11 and 12 which occur during spring time depict a persistent high pressure system over the subcontinent and the moisture is confined to the southern parts of the region. This can be related to the passage of mid-latitude frontal systems during this time (Buckle, 1996; Lindesay, 1998; Tyson and Preston-Whyte, 2000). Middle row falls within the transitional phase as the median dates are within mid-summer.

6.4.0 Frequency of Occurrence

The NCEP/NCAR reanalysis data boundary conditions show that node 12 has the highest frequency of 25.1% occurrence which is 107 days from both seasons (Table 6.1). The frequency of occurrence of SOM mapping for both simulated seasons shows preference to node 12, node 4, node1 and node 9 in descending order respectively. This implies that the model favours circulation conditions with a surface tropical ridge of high pressure and a low pressure system to the southeast of the region as well as mid-level anticyclonic circulation over Indian Ocean inhibiting favourable conditions development through subsidence of warm and dry air (node 12).

These conditions are prominent in frequency of occurrence towards the right bottom parts of the SOM array. Node 4 is the second in highest number of dailies with 61 days mapping into it. This node depicts synoptic features almost similar to node 12 and median date of the node occurring falling in mid-season particularly for summer 1995/96. On left side, Node 1 (54days) and node 9 (42days), represent a deep low pressure system over to the north and weak sub-tropical ridge with more moisture occurring towards the end of rainfall season.

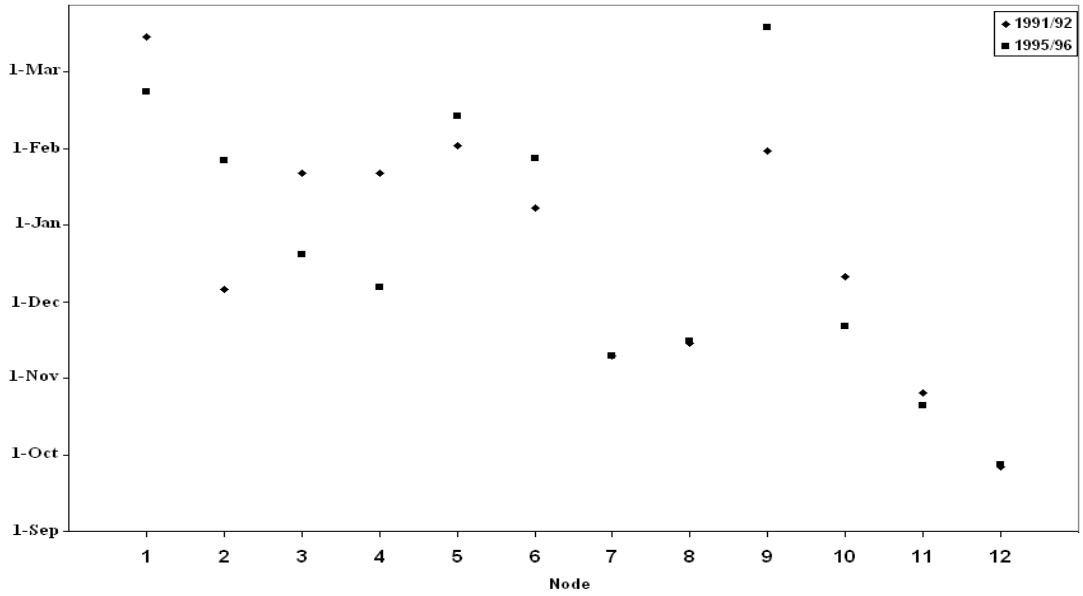

Figure 6.4 Median dates of occurrence of each of the SOM node for simulated seasons of 1 September to 31 March of 1991/92 and 1995/96.

Upon separating the two seasons, the temporal characteristics of the synoptic states illustrate the number of days mapping into each node for the two seasons (figure 6.5). Differences in the synoptic patterns of the simulated periods are then presented by the frequency of occurrence of SOM node during each period. Node 12 which has the highest frequency of occurrence illustrates that almost similar days are mapped from the two seasons (53 and 54 days for 1991/92 and 1995/96 respectively (figure 6.5). The dry synoptic conditions of node 12 associated with its early summer occurrence have been described. SOM nodes with notable high but different frequencies of occurrence are shown by nodes 1, 2 and 3. These nodes which are associated with a deep low pressure system over northwest of the domain, weak sub-tropical ridge in the centre, a trough to the south with 500hPa easterly waves and precipitable water over the southeastern half of the domain occur more often in 1995/96 than 1991/92. These nodes 1, 2 and 3 occur

during mid-season into late summer implying its influence on precipitation during this time of season. Nodes 4 and 9 occur more frequently in 1991/92 than 1995/96 but under different synoptic characteristics inclining towards stable conditions in node 4 and unstable conditions in node 9. The least common frequency synoptic characteristics fall within the transitional middle row nodes. Thus, spatial distribution within the nodes can be used to show the sensitivity responses of model's surface variables to the soil moisture perturbations through the associated prominent synoptic patterns within the nodes.

Table 6.1 Total days and frequency of occurrence of each SOM node for both simulated seasons.

Node	1	2	3	4	5	6	7	8	9	10	11	12
Days	54	27	32	61	25	14	16	14	42	17	17	107
Freq (%)	12.7	6.3	7.5	14.3	5.9	3.3	3.8	3.3	9.9	4.0	4.0	.25.1

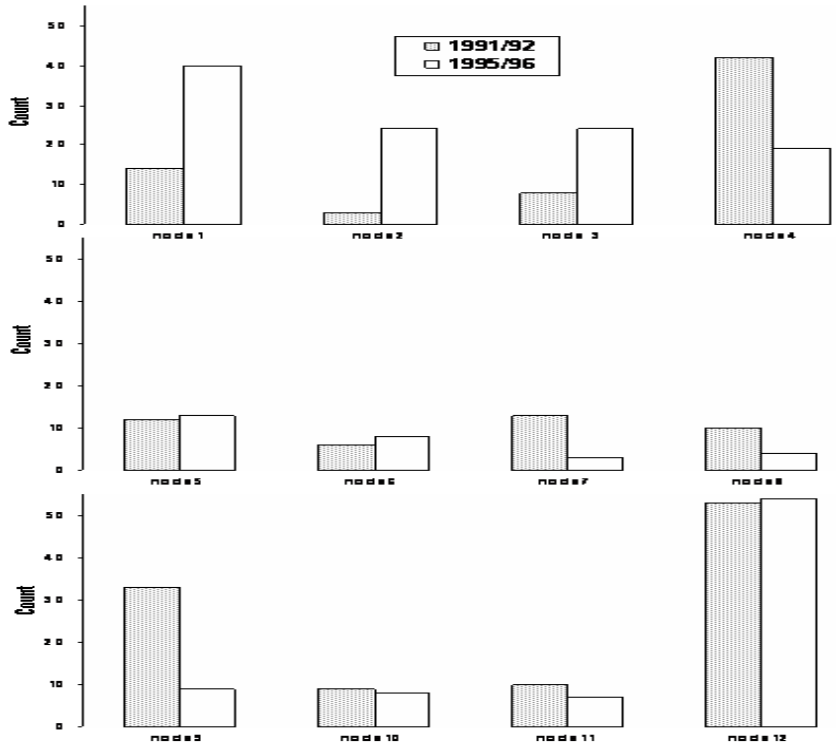

Figure 6.5 Frequency of occurrence (days) for the simulated seasons, 1 September to 31 March 1991/92 (the grey shading bars) and 1995/96 (plain white bars) for each of the SOM nodes.

6.5.0 RegCM3 Simulations Mapping onto the Synoptic States

After applying the SOM to the NCEP/NCAR lateral boundary conditions for each day, the corresponding days of the control, the dry and wet soil moisture simulations were mapped to each node so that the impact of varying soil moisture could be determined under different synoptic conditions. As each node is associated with different synoptic patterns, an anomalous response of the soil moisture perturbations from the control for each of these synoptic patterns can be produced. This can be done for all the model's surface variables analysed in chapter 4 on summer simulations. However, the results shown here would suffice in explaining the findings and avoid repeating discussion of all the surface variables with related or directly contrasting spatial responses. Thus, the model's planetary boundary layer is presented.

6.5.1 Planetary Boundary Layer Anomalies

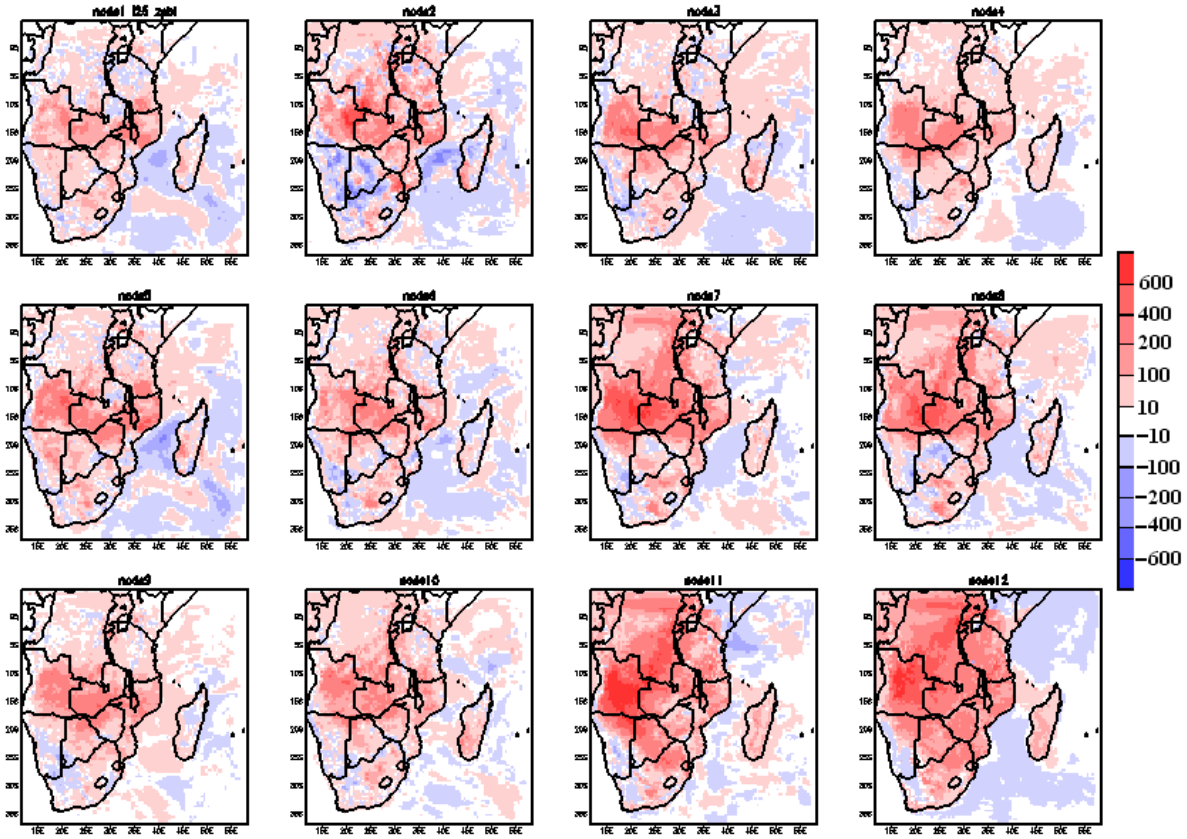

Figure 6.6 Planetary boundary layer (m) anomalies for the 4x3 nodes from the daily RegCM3 simulation of dry soil moisture perturbation – control of September 1991 to March 1992. Red shading indicates positive planetary boundary layer anomalies and blue shading indicates negative planetary boundary layer anomalies.

Figure 6.6 shows the 4x3 nodes for planetary boundaries anomalies (m) of 1 September 1991 to 31 March 1992 using the RegCM3 daily simulations (dry soil moisture perturbation-control run) mapping into the respective nodes for days identified through the SOM classification of the NCEP/NCAR reanalysis data. The effects of the synoptic circulation characteristics of wet to dry conditions are projected through the spatial responses observed as one traverses from top left corner to bottom right corner of the nodes array. There is an increase in depth and spatial cohesiveness of PBL over most of the region except for the southwestern areas as one moves from the top left of the meta-map (node 1, representing wetter synoptic states) to the bottom right corner of the array (nodes 11 and 12 for dry synoptic states). There is also a reduction in area under which negative PBL anomalies occur to the south and north of the region (particularly in node 2) as you move from the top left corner of the meta-map.

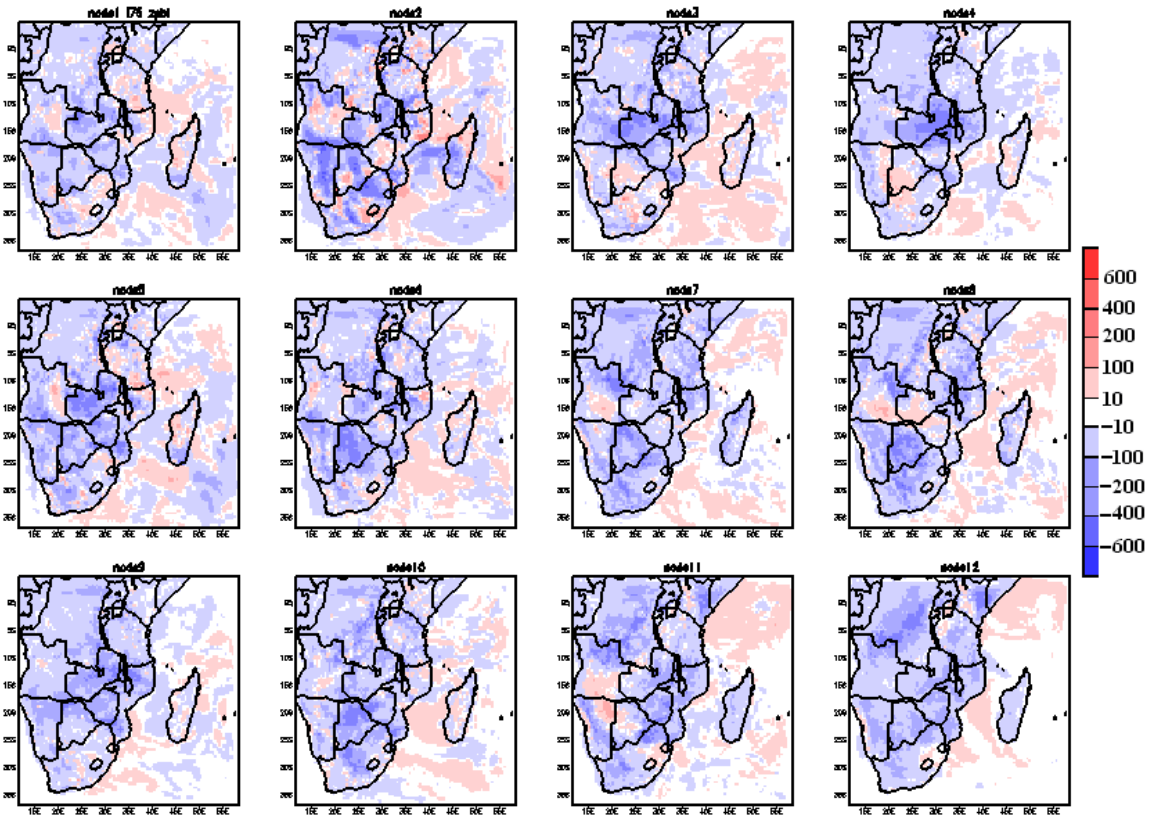

Figure 6.7 Planetary boundary layer anomalies (m) for the 4x3 nodes from the daily RegCM3 simulation of wet soil moisture perturbation – control of September 1991 to March 1992. Red shading indicates positive planetary boundary layer anomalies and blue shading indicates negative planetary boundary layer anomalies.

Wet soil moisture perturbation daily simulations (figure 6.7) show a general decrease in PBL height anomalies over the region for most of the mapping in the 4x3 node array. Node 12 (under dry synoptic states) shows weak decreases but spatially cohesive PBL anomalies over the region. As we move up and to the left within the nodes, some portions of the region especially over the southern parts show an increase in PBL heights. Nodes 1 and 2 also depict increases in PBL height (under a wet synoptic forcing) over the northern parts of the region. There are strong PBL height decreases occurring over the central parts of the region in the top row of the array.

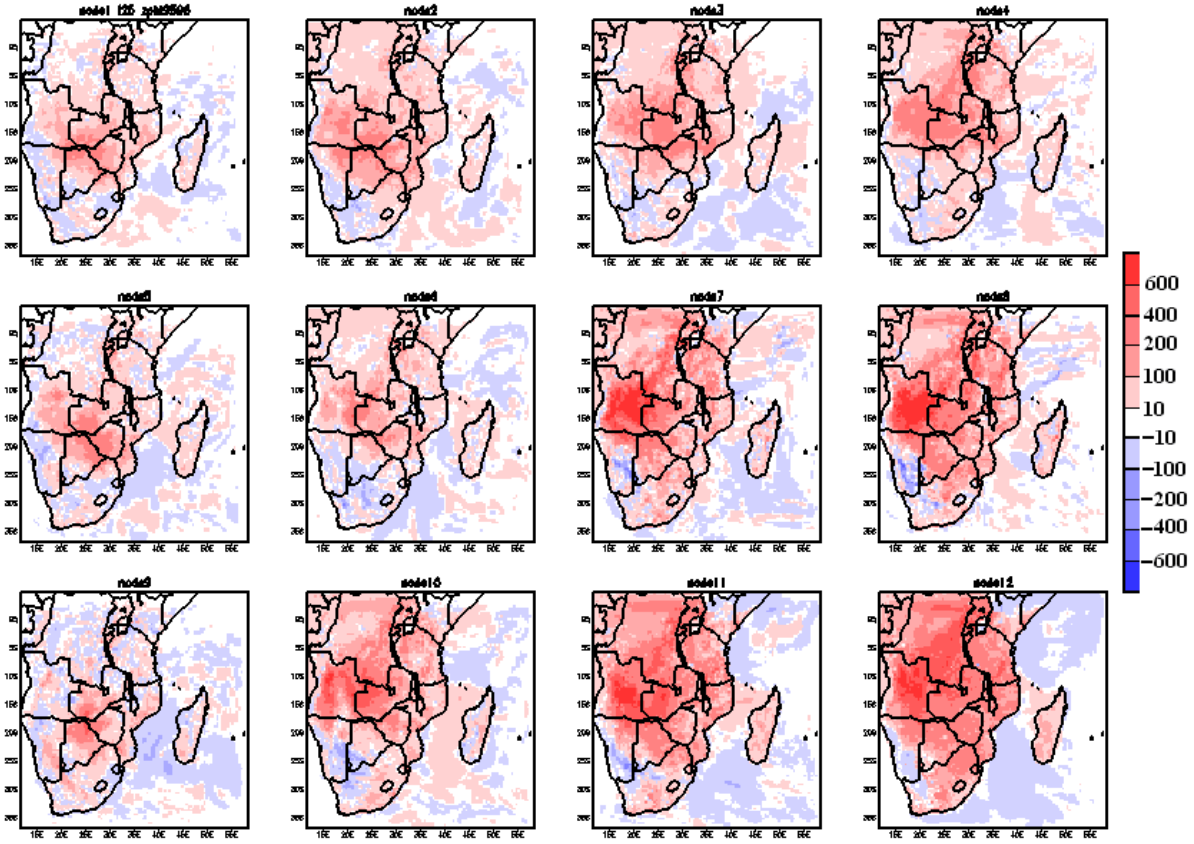

Figure 6.8 Planetary boundary layer anomalies (m) for the 4x3 nodes from the daily RegCM3 simulation of dry soil moisture perturbation – control of September 1995 to March 1996. Red shading indicates positive planetary boundary layer anomalies and blue shading indicates negative planetary boundary layer anomalies.

For anomalous dry soil moisture perturbation, 1995/96 season depicts PBL decreases over the northern and southwestern areas of the region with the central portions showing a weak elevation in PBL height on the left side of the array representing wetter synoptic states(figure 6.8). Moving to the right in the array displays an increase in depth of the positive PBL anomalies especially

over central parts of the region particularly in Angola where greater than 600m rises are represented (nodes 7, 8, 11 and 12). However, southwestern areas maintain the negative PBL heights throughout the nodes array. Spatial homogeneity across the region is also enhanced over the right side of this meta-map where dry synoptic circulation patterns prevail. The anomalous wet soil moisture perturbation for 1995/96 season shows more negative PBL anomalies in the meta-map than for 1991/92 (figure 6.9). Nodes 11 and 12 show a decrease in PBL height over most of the region. An area of a positive PBL height increase from the southeastern parts of the region to the western parts as you move to left and up in the meta-map. Nodes 1, 2 and 5 exhibit a vast part of the southwestern areas with positive PBL height anomalies (figure 6.9). Deepest PBL height anomalies 400m occur over Zambia in the above mentioned nodes.

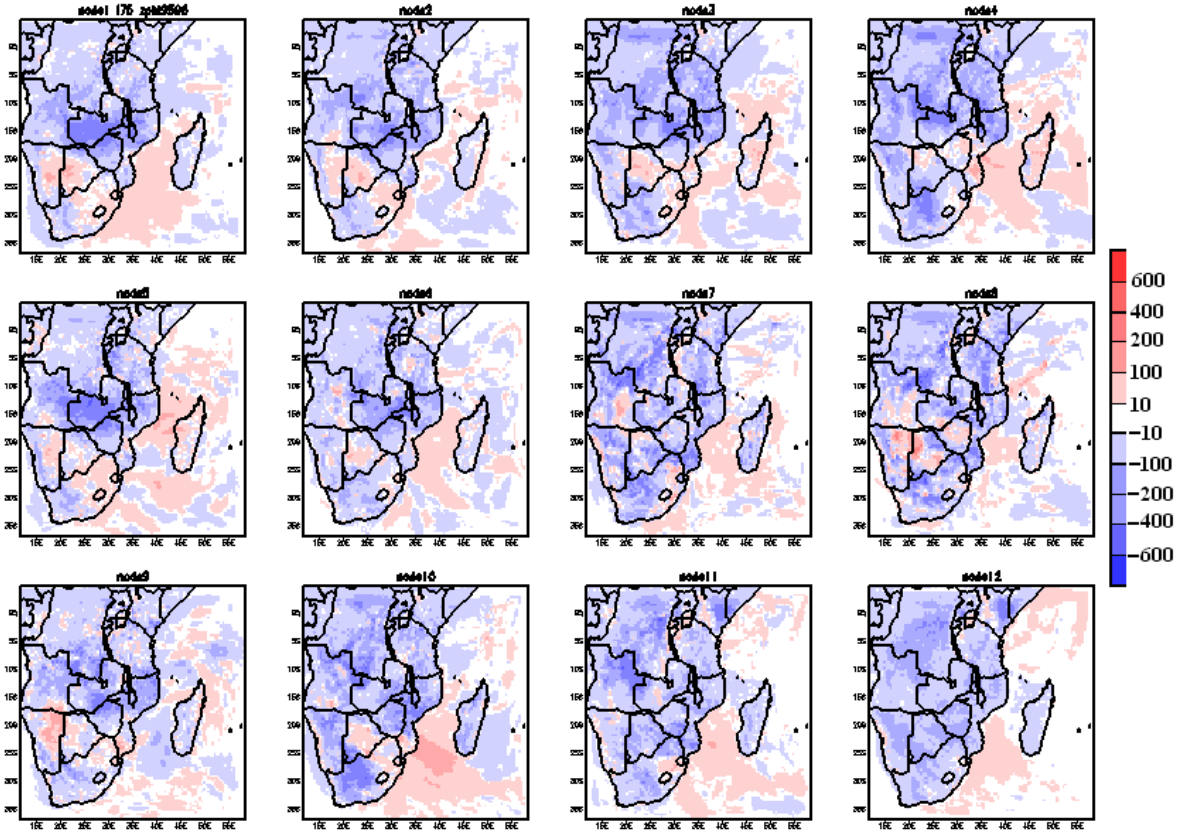

Figure 6.9 Planetary boundary layer anomalies (m) for the 4x3 nodes from the daily RegCM3 simulation of wet soil moisture perturbation – control of September 1995 to March 1996. Red shading indicates positive planetary boundary layer anomalies and blue shading indicates negative planetary boundary layer anomalies.

Thus, the effects of soil moisture perturbations on the synoptic circulation show an increase in magnitude and spatial cohesiveness across the node array from top left to bottom right in

accordance with the wet to dry synoptic characteristics spread. Viewing from bottom right particularly for the dry soil moisture perturbation depicts a seasonal evolution that can be related to soil moisture memory in that the persistence of the spatial cohesiveness lessens as the season progresses. This is shown through the spatial consistency of elevated PBL that is observed in nodes 12 (figures 6.6 and 6.8) which occurs in early summer whilst there is a heterogeneous map with a decrease, transition zones and positive PBL heights in nodes 1(figures 6.6 and 6.8) which occurs in late summer. Thus, the SOM does show the seasonal transition with responses to soil moisture initialisation showing stronger responses during early summer and favouring dry synoptic states or being influenced by the late winter/spring synoptic characteristics.

From the PBL anomalies shown here, the responses to soil moisture variation are stronger under dry conditions as represented by the bottom right hand-side of the SOM. This is represented through the spatially cohesiveness and strong magnitude response to all synoptic forcings. Wet synoptic conditions depict responses that are weak in magnitude and spatial consistency. Tadross et al. (2010) propose that it indicates the impacts of biosphere-atmosphere coupling are stronger when the synoptic scale forcing is for dry conditions. PBL shows strong responses to the soil moisture perturbations under all synoptic forces as shown by the differences over the continental region besides those observed over the ocean. Similar responses are observed for surface temperature, sensible and latent heat fluxes (Appendix B). Spatially mixed responses (noise-like signals) occur for the total rainfall (Appendix B) which would imply that rainfall patterns are strongly influenced by large-scale synoptic circulations than the soil moisture perturbations. This would aid in explaining the non-linear responses to soil moisture initialisation given the complex nature of rainfall. Mackellar et al. (2010) and Tadross et al. (2010) observed similar traits in vegetation atmosphere experiments and using different RCMs at finer resolutions.

6.5 Summary

Self-organising map has broadened the techniques by which synoptic climatology may be approached and classifies data on a non-linear basis. This chapter evaluated effects of synoptic patterns on the summer climate perturbation on a daily scale using SOM. The major findings are summarised as:

- Top left corner of the SOM occurs during the late part of the summer season which shows deep low pressure system over the northern areas which can be associated with the southern tip of the ITCZ at this time of the season. Thus, the left side of SOM generally represents the wet synoptic states which occur during mid into late summer for both 1991/92 and 1995/96.

- The dominant synoptic states (bottom right of the SOM) occur during early summer and are associated with a surface tropical ridge of high pressure with a low pressure system to the southeast of the region as well as mid-level anticyclonic circulation over Indian Ocean but also having low level moisture to the south of the domain.

- The effects of soil moisture perturbations on the synoptic circulation show an increase in magnitude and spatial cohesiveness across the SOM from top left to bottom right in accordance with the wet to dry synoptic characteristics spread.

- Viewing from bottom right particularly for the dry perturbation depicts a seasonal evolution that can be related to soil moisture memory in that the persistence of the spatial cohesiveness lessens as the season progresses.

- The SOM does somewhat show the transition to the model's equilibrium state with responses to soil moisture initialisation showing stronger responses during early summer and favouring dry synoptic states or being influenced by the late winter/spring synoptic characteristics.

- Planetary boundary layer shows strong responses to the soil moisture perturbations under all synoptic forces as shown by the differences over the continental region besides those observed over the ocean. Similar responses are observed for surface temperature, sensible and latent heat fluxes.

- Spatially mixed responses (noise-like signals) occur for the total rainfall which would imply that rainfall patterns are strongly influenced by large-scale synoptic circulations rather than a direct influence of the soil moisture perturbations.

- Over the southwestern area, there are no distinctive responses to dry/wet soil moisture perturbations across the synoptic states for the all the RegCM3 model surface variables.

Chapter 7

Sub-regional Analysis of Summer Climate Simulations

7.1 Introduction

Some important results have been presented in the previous chapters. Most of these showed some consistency or coherence in responses over the northern parts of the domain under study. Southern areas depicted most of the inconsistencies and thus prompted a closer look at some of these areas. An area average analysis is done for some surface variables discussed in the previous chapters. Two parameters of evaporative fraction and moist static energy are appended. These are derived from the simulated variables and thus give one a different way of presenting and condensing the results output. Figure 7.1 shows areas selected for the sub-regional analysis of summer climate simulations to soil moisture perturbations. Selected areas are the southwestern areas i.e. Southwestern Botswana, southern Namibia and western South Africa which will be represented as the *West*, Lesotho, Swaziland, southern Mozambique and southeastern South Africa which is represented as the *South* and western Mozambique, central Malawi, southern Zambia, Zimbabwe and northeastern Botswana shown here as *Central* **(**see Table 7.1). Analysis of the whole region of study and its mean values shall be discussed as the *Domain*.

7.2 RegCM3 Top-layer Soil Moisture

Figure 7.2 displays the RegCM3 simulated top-layer soil moisture anomalies (mm/day) for the selected zones over *Central , South* and *West* for the soil moisture perturbations from the control simulations of the respective early and late summer time periods of 1991/92 and 1995/96. Over the *Central* and *South*, the top-layer soil moisture anomalies depict the anticipated responses with dry soil moisture perturbations from the control leading to a reduction in top-layer soil moisture whilst the wet soil moisture perturbations lead to an increase in top-layer moisture (figure 7.2). The magnitude of change in the response of top-layer soil moisture anomalies is

stronger for the dry simulation and higher during early summer for both initialisations over the *Central* area. The top-layer soil moisture responses over the *Central* zone are consistent with the positive soil moisture-atmosphere feedback mechanism as observed in earlier studies (Delworth and Manabe, 1988a, 1988b; Eltahir, 1998; Findell and Eltahir, 1999; Schär 1999; Pal and Eltahir, 2001; Seneviratne, 2006a; Alfieri et al., 2008). The *South* zone has higher magnitude change of responses for the wet soil moisture perturbation than the dry soil moisture run. However, higher top-layer soil moisture levels still occur during early summer, SON. Over the *West*, there is increase in top-layer soil moisture for both perturbations. This reiterates earlier explanations that it is a predominantly dry zone during this summer period (Lindesay, 1998; Tyson and Preston-Whyte, 2000) implying that any influx of moisture would lead to an increase of the top-layer soil moisture conditions.

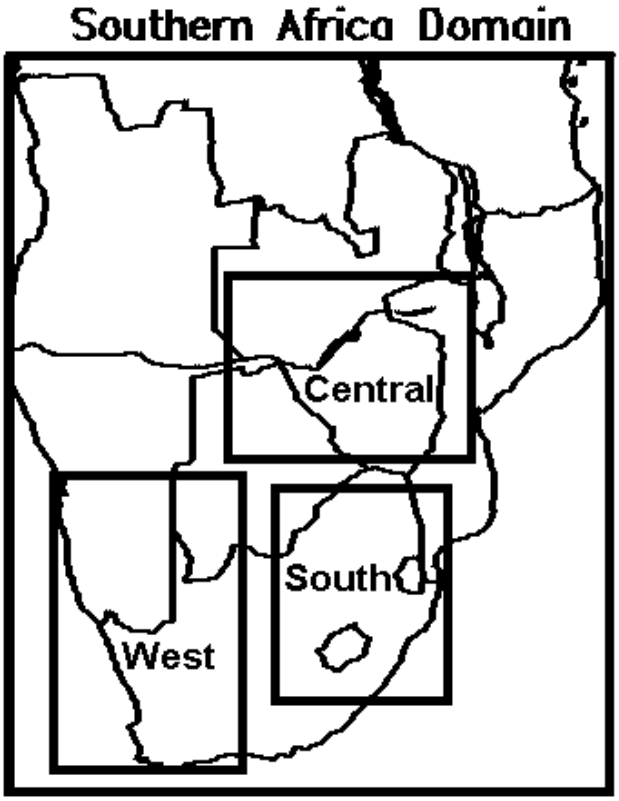

Figure 7.1 Zones selected for the sub-regional analysis of summer climate simulations to soil moisture perturbations. There is the *Domain, Central, South* and *West* areas.

Table 7.1 Zones selected for the sub-regional analysis to soil moisture perturbations.

Zone	Areas
Central	western Mozambique, central Malawi, southern Zambia, Zimbabwe and northeastern Botswana
South	Lesotho, Swaziland, southern Mozambique and southeastern South Africa
West	Southwestern Botswana, southern Namibia and western South Africa

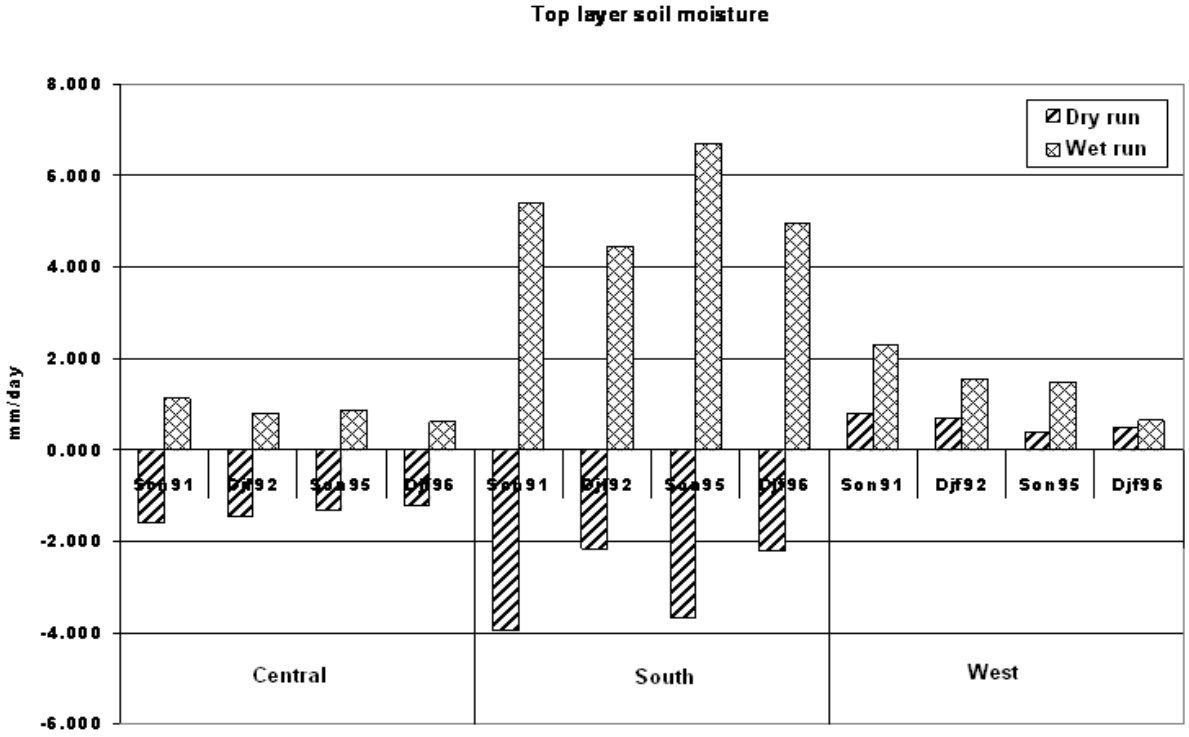

Figure 7.2 Top-layer soil moisture anomalies (mm/day) for the selected zones over *Central , South* and *West* for the soil moisture perturbation experiments from the control simulations of the respective early and late summer time periods of 1991/92 and 1995/96.

7.3 Total Precipitation

Central area depicts an increase in total rainfall (mm/day) for the wet soil moisture perturbation and a reduction for the dry soil moisture run (figure 7.3). The distinct magnitude response in total rainfall is stronger for the dry soil moisture simulation. Minor differences between the

anomalous perturbations and control simulation occur during late summer of 1991/92. This can be related to the model's capabilities of soil moisture memory retention as discussed on temporal distribution of total rainfall (figure 4.15) and how long the model's atmosphere takes before reaching equilibrium in soil moisture circulation. The *Central* area has positive soil moisture-precipitation feedback responses with a dry (wet) soil moisture perturbation resulting in precipitation decreases (increases).

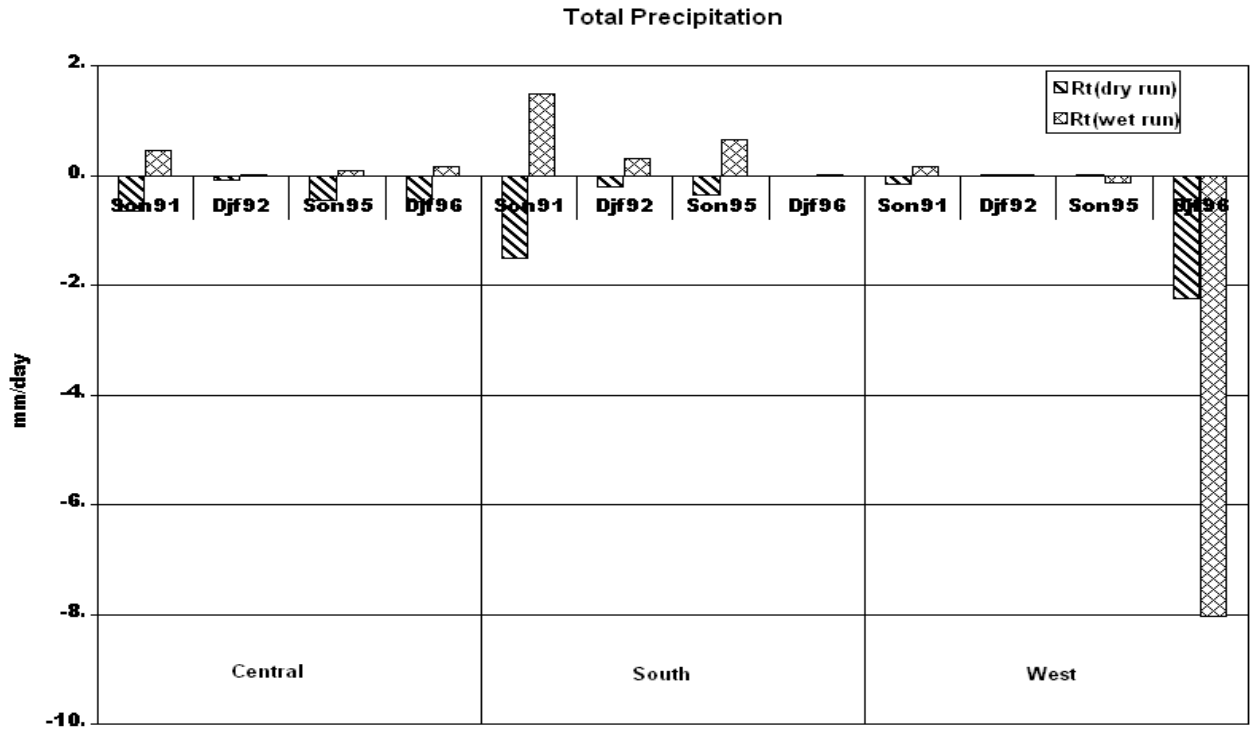

Figure 7.3 Total rainfall anomalies (mm/day) for the selected zones over *Central , South* and *West* for the soil moisture perturbation experiments from the control simulations of the respective early and late summer time periods of 1991/92 and 1995/96.

As for the *South* area, a positive feedback response to the perturbations occurs with a reduction in total precipitation anomalies for dry soil moisture simulations and an increase for the wet soil moisture runs (figure 7.3). Distinctively high responses in precipitation anomalies occur for early summer period. Negligible differences between the dry soil moisture initialisation and the control is observed during late summer 1995/96. This is in agreement with the mean temporal pattern of total rainfall which showed the perturbations and control having almost similar values

in late summer (figure 4.15). There is a stronger persistence into late summer in 1991/92 season than 1995/96 over the *South* area.

The *West* area exhibits some inconsistent responses in total rainfall to the soil moisture perturbations (figure 7.3). Early summer 1991/92 depicts a decrease in total rainfall for the dry soil moisture simulation with increase in rainfall for the wet soil moisture run whereas late summer shows minor increases in total rainfall for both perturbations. A contrasting response to those observed for other zones occurs for 1995/96 with early summer depicting minor increases for dry soil moisture run and slight decreases for the wet run. Late summer, DJF95/96 shows marked decreases in rainfall for both perturbations although there is evidence of top-layer soil moisture anomalies (figure 7.2). These are incoherent responses to the perturbations that were observed over this area for most of the variables analysed in this study. This would imply that other dynamic forcings affect the precipitation variation over the *west* area.

7.4 Surface and Air temperatures

Figure 7.4 displays surface and air temperature (°C) for the selected zones over the *Central*, *South* and *West* for the soil moisture perturbation experiments from the control simulations of the respective early and late summer periods of 1991/92 and 1995/96. Generally, one would expect surface temperature to be higher than the air temperature which is simulated at 2m above the ground. However, there is a decrease in temperature from the surface to the 2m level in the dry soil moisture perturbations during late summer 1991/92 over the *Central* area (figure 7.4). This is also observed over the *West* for early summer in both seasons and DJF 1995/96.

Despite the noted temperature variations in the vertical, there is consistency in the positive soil moisture-temperature responses to the soil moisture perturbations for the three zones (figure 7.4). Anomalous dry soil moisture simulation leads to warming whilst wet soils result in cooling. The difference is observed in the magnitude of change to the responses over *Central* and *South* presenting higher response for dry soil moisture runs than wet soil moisture initialisation whilst the opposite occurs over the *West* where stronger responses are observed for the wet soil moisture perturbations.

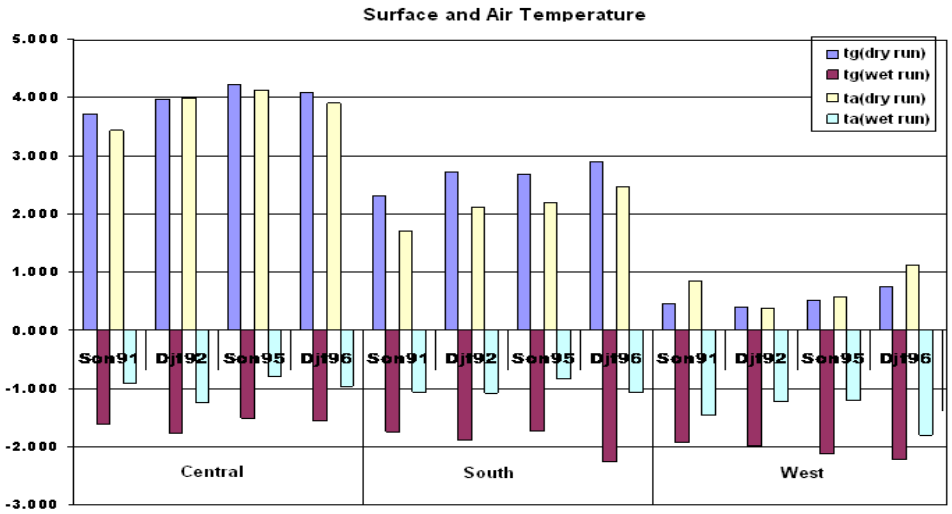

Figure 7.4 Surface (tg) and air (ta) temperature (°C) for the selected zones over *Central , South* and *West* for the soil moisture perturbation experiments from the control simulations of the respective early and late summer time periods of 1991/92 and 1995/96.

7.5 Heat fluxes and Incident Solar Radiation

Latent and sensible heat flux anomalies produce positive responses to both soil moisture perturbations difference from the control simulations for all the three areas (figure 7.5). Anomalous dry soil moisture initialisation exhibit a decrease (increase) in latent (sensible) heat fluxes whilst wet soil moisture initialisation shows an increase (decrease) in latent (sensible) heat. Stronger responses in heat fluxes for the dry run occur over the *Central* area with gradual decrease in response through the *South* down to the *West* area. For wet soil moisture run, the stronger responses are biased toward the *West* area. These responses are consistent with the temperature anomalies (figure 7.4). One would expect an increase in temperature associated with dry soil moisture perturbations would lead to a rise in saturated vapour pressure and ultimately an increase in evaporation. Thus an increase in sensible heat flux occurs whilst the evaporative cooling effect pans out in a decrease in latent heat flux. This again proves how the partitioning of energy fluxes is directly related to soil moisture perturbations (Shukla, 1999; Schär et al., 1999; Fischer et al. 2007).

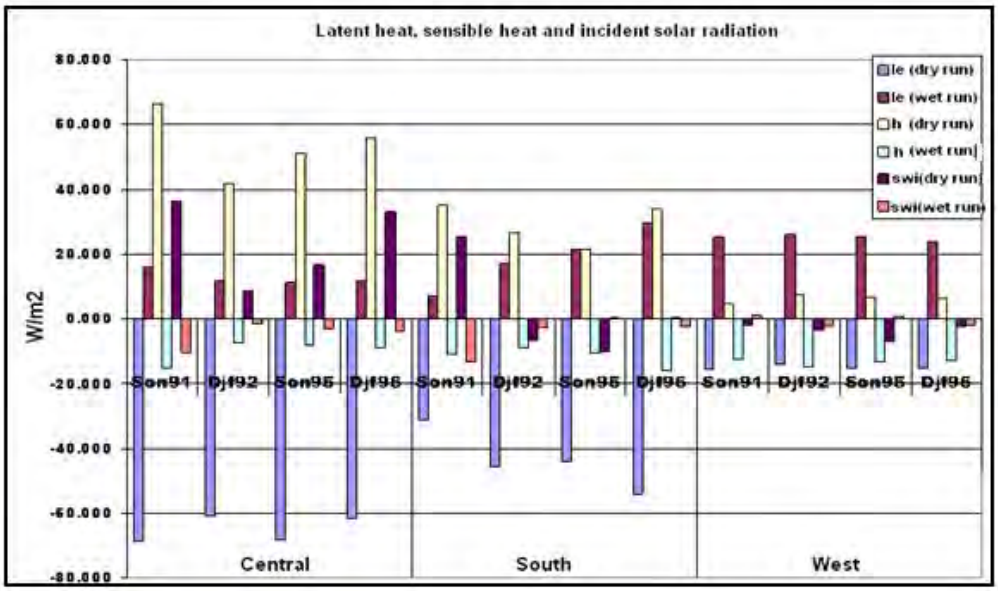

Figure 7.5 Latent heat (le) and sensible heat (h) fluxes as well as incident solar radiation (swi), (W/m^2) for the selected zones over *Central, South* and *West* for the soil moisture perturbation experiments from the control simulations of the respective early and late summer time periods of 1991/92 and 1995/96.

As for the incident solar radiation, only the *Central* area is showing some consistency in the mean response with dry soil moisture perturbations leading to an increase in incident solar radiation whilst wet soil moisture perturbation depict a decrease in the radiation (figure 7.5). Mixed responses in the radiation occur over the *South* and *West* areas. There are decreases in incident solar radiation for both perturbations, a reduction in radiation for the dry soil moisture run and an increase for the wet soil moisture simulation. As was observed in earlier chapters, the incident solar radiation shows ambiguous responses to the perturbations in contrast to what one would expect particularly over the southern parts of the subcontinent. As for the *Central* area the basic theory would be an increase in soil moisture conditions leads to increase in moisture in the atmosphere which would result in more cloud development or thick clouds thus implying reduced incoming solar radiation reaching the surface (Tyson and Preston-Whyte, 2000; Barry and Chorley, 2009). However, there are other dynamic forcings involved rendering incident solar radiation a weak respondent variable to surface soil moisture initialisations in the *South* and *West* areas. One would also need to consider that the reflectivity of the simulated clouds which would

imply less solar radiation reaching the surface as a factor amongst other forcings for the indirect relation to soil moisture perturbations.

7.6 Planetary boundary layer

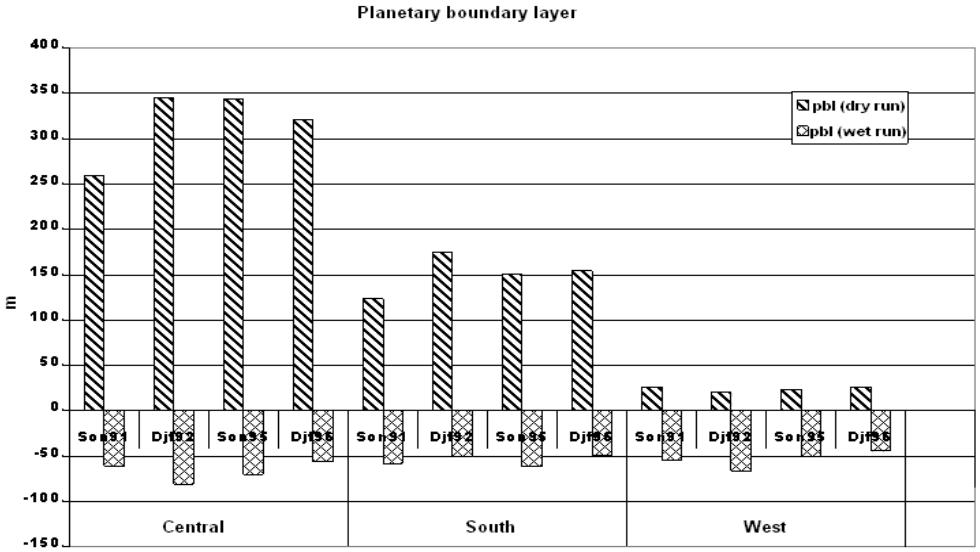

Figure 7.6 Planetary boundary layer (m) for the selected zones over *Central , South* and *West* for the soil moisture perturbation experiments from the control simulations of the respective early and late summer time periods of 1991/92 and 1995/96.

Planetary boundary layer (m) has turned out to be another model's variable with consistent responses to the soil moisture perturbations (figure 7.6). Dry soil moisture perturbations depict an elevation in PBL height for all the selected areas with stronger responses occurring over the *Central* zone. This is coherent with temperature and sensible heat flux responses discussed above. As explained earlier, a high sensible heat flux tends to increase turbulent mixing which increases the PBL growth rate and hence the height of the PBL (Eltahir 1998, Pal and Eltahir 2001; Jaeger and Seneviratne, 2011). Betts et al. (1994) whilst discussing the 1993 extreme rainfall event in USA emphasised the role of boundary layer in providing the required instability for deep convection. Wet soil moisture perturbations show a decrease in PBL height which is analogous with a decrease in surface temperature and sensible heat flux anomalies.

7.7 Evaporative Fraction

Figure 7.7a shows evaporative fraction (EF) of the control (black), dry (red) and wet (blue) soil moisture perturbation simulations for summer season of 1991/92. The seasonal variations are presented for the *Domain* of study, and the selected zones, *Central, South* and *West*. The seasonal variation of evaporative fraction is a reflection of the climate of the area, in particular of rainfall and soil moisture (Farah et al., 2004). The mean temporal distribution exhibited by *Domain* shows weakly varying EF throughout the season for the wet soil moisture run and control simulation. The dry soil moisture run has an EF of 0.3 in September and gradually rises to about 0.6 by March. EF depicts lowest values of EF for dry soil moisture initialisation whilst the highest values occur for wet soil moisture perturbation. Some reduction in EF occurs in January which may be attributed to the reduction in soil moisture as was observed with seasonal variation of the top-layer soil moisture (figure 4.11) and possible drop in rainfall. This is in agreement with Gentine et al. (2007) findings that EF decreases when soil water decreases or when solar energy increases.

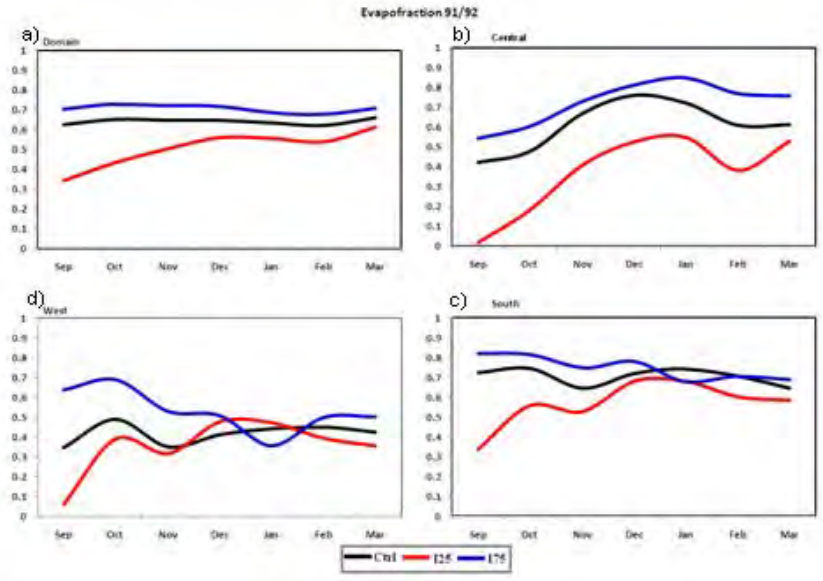

Figure 7.7 Evaporative Fraction of the control (black), dry (red) and wet (blue) soil moisture perturbation simulations for summer season of 1991/1992. (a) Domain, (b) Central, (c) South and (d) West.

Over the *Central* area, the EF at the beginning is virtually zero for the dry soil moisture simulation, with distinctively higher EF values for control and wet soil moisture runs. Control simulation shows a peak in December with the perturbations showing a month lag and only peak in mid-January 1992 and immediately begins to drop (figure 7.7b). As for other two areas of analysis, *South* and *West*(figures 7.7c and 7.7d), early summer depict some consistent responses with high EF values for wet run of about 0.7 and low values for the dry run with virtually zero in the *West* zone. Inconsistencies or mixed responses in the surface variables are apparent with the EF during late summer 1992. Work has been done showing how EF from remote sensing and ground measurements can be used to estimate evapotranspiration (Lhomme and Elguero, 1999; Wang et al., 2006; Gentine et al., 2007).

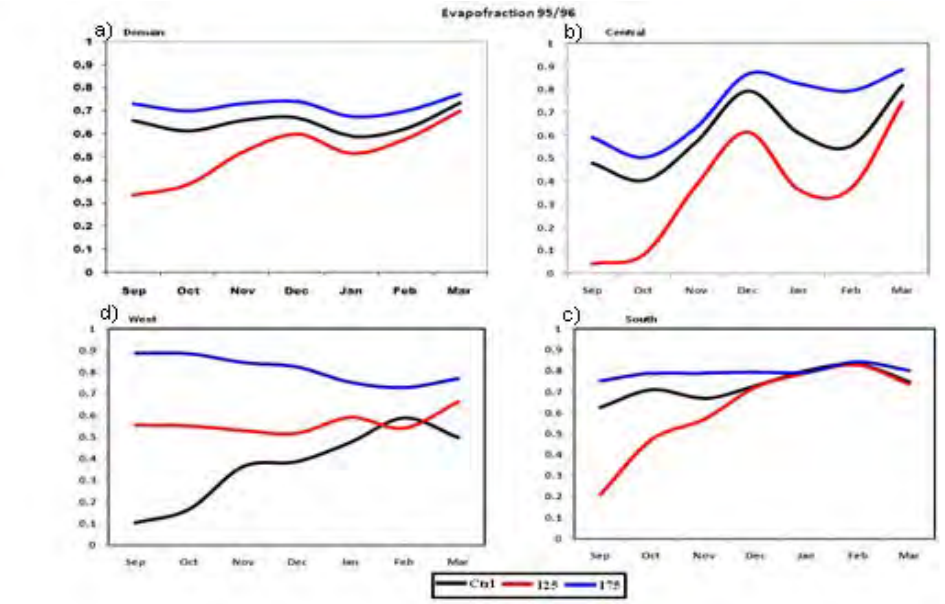

Figure 7.8 Evaporative Fraction of the control (black), dry (red) and wet (blue) soil moisture perturbation simulations for summer season of 1995/1996. (a) Domain, (b) Central, (c) South and (d) West.

The mixed responses that are observed for late summer over *South* and *West* areas complicate the suggested methodologies that follow the surface radiation principles or the parameterization of the surface energy-balance. The virtual zero responses indicate that evaporative fraction responds to soil moisture condition when a certain critical level of moisture and soil water potential is reached (Farah et al., 2004). Thus when EF is zero it implies that all of available energy is partitioned into sensible heat flux, (equation 3.2). Anomalous dry soil moisture would reduce all

latent heat flux to almost zero and thereby enlarge the sensible heat flux. The important role of partitioning of net radiation into latent and sensible heat fluxes, which is mainly controlled by soil moisture has already been highlighted in this study and from earlier studies (Shukla, 1999; Schär et al., 1999; Fischer et al., 2007).

1995/96 summer shows some distinction in seasonal variation magnitude of the evaporative fraction (figure 7.8).For the *domain*, EF under the dry soil moisture simulation starts off distinctively lower than the control and wet soil moisture run (figure 7.8a). However, all three are peaking in December with a dip in January 1996 and then tend to increase thereafter. This variability is similar to that observed for top-layer soil moisture conditions (figure 4.11) which increases in December and decreases in January. Thus, confirming soil moisture as one of the environmental factors that influence EF (Lhomme and Elguero, 1999; Farah et al., 2004; Gentile et al., 2007). Typical of the southern Africa's rainfall is the intraseasonal dry spells experienced mostly around January (Makarau, 1995; Makarau and Jury, 1997; Matarira and Jury 1992; Unganai and Mason; 2002; Usman and Reason, 2004). This suggests that the EF can possibly be utilised to identify these spells.

Central area presents responses in EF similar to those of the *Domain* (figure 7.8a) although with steep gradients towards an increase in EF during December and sharp decrease into January (figure 7.8b). The distinct responses in EF do show clearly the variation due to the different soil moisture perturbations thus estimation of the evapotranspiration rates can be done for this area. *South* zone (figure 7.8c) shows the uniquely EF values for the three simulations during early summer becoming similar from December into January 1996. *South* zone distinctively exhibit the different simulations but the control simulation has the lowest EF value and crosscut each other with the dry run during late summer. This response does bring out the fact that besides soil moisture there are other local forcings or environmental factors that also influence the evaporative fraction in the sub-tropics to mid-latitude areas.

Overall, evaporative fraction shows more coherent variation during 1995/96 (figure 7.8) compared to 1991/92 (figure 7.7) where some mixed responses were observed. Some virtual zero EF values also occur in dry 1991/92 indicating that evaporative fraction responds to soil moisture

condition when a certain threshold of moisture level is reached. This also confirms the important role of energy flux partitioning which is mainly influenced by soil moisture perturbations. Stronger responses in EF to the soil moisture perturbations occur in wet 1995/96 than in dry 1991/92. *South* and *West* zone also brings out that there are other factors that influence the EF besides soil moisture within the sub-tropics to mid-latitude areas. However, the seasonal variation of EF is a good reflection of the climate of these areas due to soil moisture as consistent responses occur over the *Central* Zone. In relation to the mean EF response as depicted by the *Domain*, the *South* and *West* areas' mixed EF responses also suggest a different soil moisture feedback mechanism prevails over these zones. These findings also apply to Bowen ratio as it is related to EF (equation 3.2).

7.8 Moist Static energy

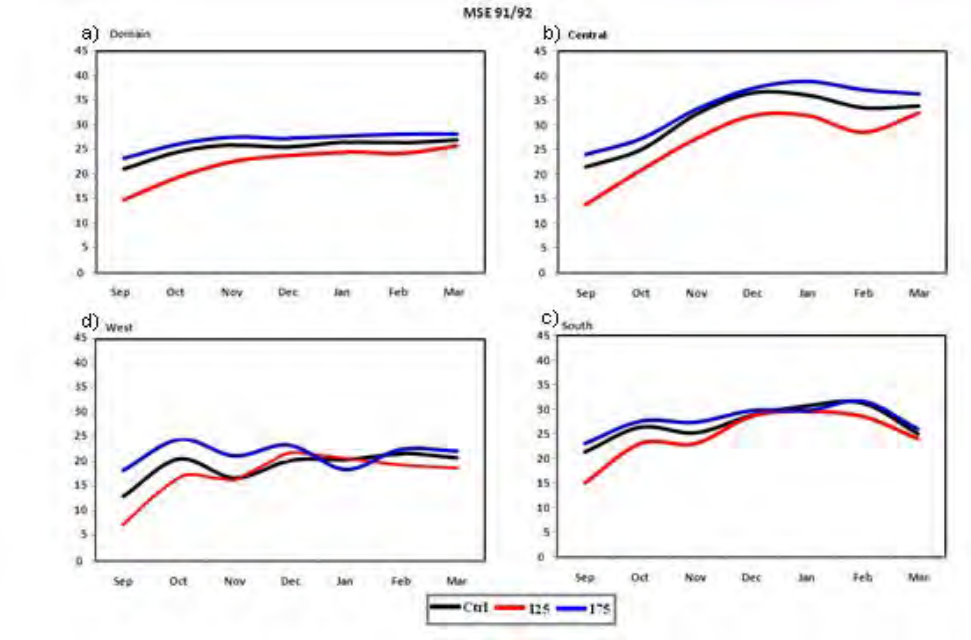

Figure 7.9 Moist static energy (kJ/kg) of the control (black), dry (red) and wet (blue) soil moisture perturbation simulations for summer season of 1991/1992. . (a) Domain, (b) Central, (c) South and (d) West.

Figure 7.9 presents moist static energy (MSE) of the control, dry and wet soil moisture perturbation simulations for summer season of 1991/92. The wet soil moisture run depicts the highest moist static energy over the *Domain* averaging between 25-30 kJ/kg whilst the dry soil moisture run has the least MSE (figure 7.9a). There is a constant MSE for most of the season. However, the dry run has distinctively lower MSE than the other two simulations during early

summer (SON), (figure 7.9a). Available MSE is analogous to potential temperature and both are used to determine stability of the atmosphere (Pal et al., 2007). Thus, the *Domain*'s mean conditions show that wet soil moisture simulation leads to unstable and favourable situation for convective developments whilst the dry run with less available MSE suppresses any meaningful convective activity.

The *Central* (figure 7.9c) zone shows higher values of MSE than the mean values for the region as shown in the *Domain* (figure 7.9a). The MSE for the wet soil moisture simulation which is in close proximity with the control simulation show a gradual increase to values greater than 30kJ/kg from end of October with a gradual decrease after December 1991. The gradual decrease implies model's climate is stabilising and may also be associated with the intra-seasonal dry spells as discussed earlier. The dry soil moisture perturbation is uniquely lower in MSE than the other two simulations. Moving to the *South* zone (figure 7.9b) shows variations in the available MSE with the pattern of highest values for wet soil moisture run and the least values for dry run maintained until after December 1991 where the three simulations exhibit similar MSE of about 30 kJ/kg. Thereafter, only the dry run will have lower MSE than the other simulations from mid-January 1992. The wet soil moisture perturbation shows a weak response in MSE in comparison to the control. As for the *West* area, the mixed responses in the variation of the MSE for the three simulations occur from early November 1991 (figure 7.9d). Clear pattern is only observed at the beginning and towards the end of the season for the *West* zone.

Figure 7.10 shows 1995/96 summer season responses to MSE of the control, dry and wet soil moisture simulations. The *Domain* shows distinctive responses for the simulations with uniquely lowest MSE for dry soil moisture perturbation during early summer (figure 7.10a). The wet run has the highest MSE throughout the season of between 25-30kJ/kg. Quite similar in magnitude simulated for 1991/92 season (figure 7.9a) although with differences in variation. 1995/96 (figure 7.10a) depicts a slight increase in MSE during October and the simulations tend to a similar magnitude at the end of period of study whilst the simulations remain different throughout 1991/92's *Domain* (figure 7.9a). *Central* zone shows distinctive and higher MSE responses for simulations throughout the season although they merge towards the end(figure 7.10b). A sharp increase in MSE trend of about 15kJ/kg occurs from October to mid-December

1995 followed by a 10kJ/kg fall till mid-January 1996. Marked differences in response occur during late summer of 1995/96 although dry soil moisture run is outstandingly lower in response throughout the season. *Domain* and *Central* zone show a pattern depicting that wet soil moisture perturbation lead to higher MSE which tends to destabilize the atmospheric conditions whilst dry soil moisture perturbation results in lower MSE and a stabilizing effect on the atmosphere than the control simulation ((figures 7.10a and 7.10b).

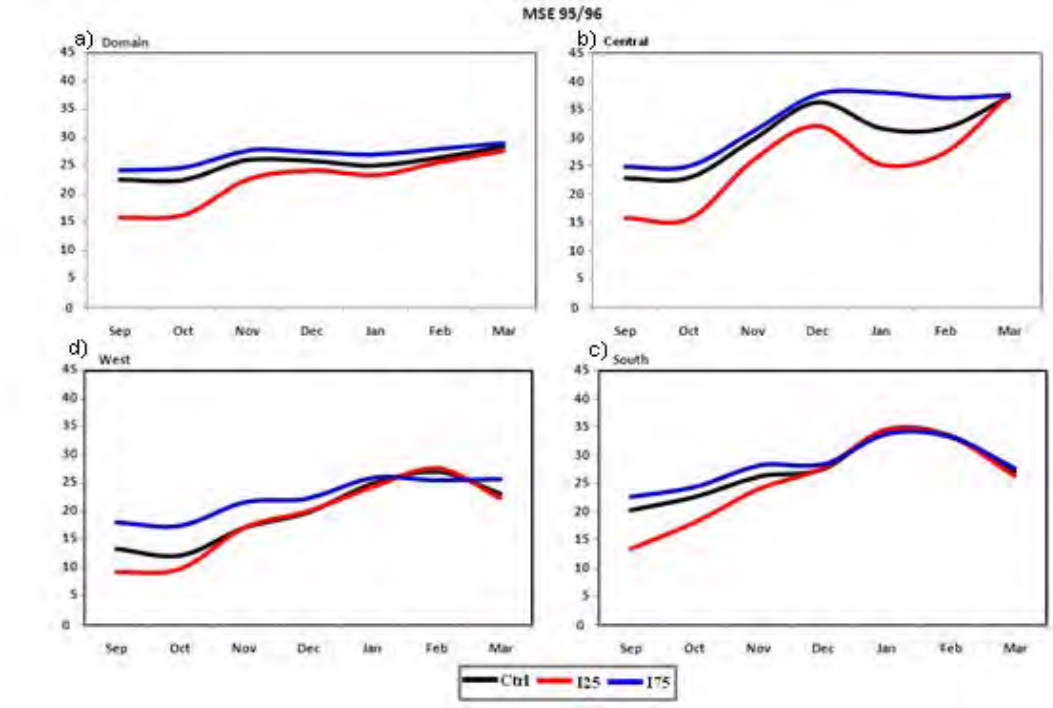

Figure 7.10 Moist static energy (kJ/kg) of the control (black), dry (red) and wet (blue) soil moisture perturbation simulations for summer season of 1995/1996. (a) Domain, (b) Central, (c) South and (d) West.

In the *South* zone, 1995/96 season presents distinctive MSE responses for the perturbations and control simulation during early summer (figure 7.10c). From mid-December, the soil moisture perturbations depict very weak MSE response and are similar to the control simulation for the rest of the season. Similarities are observed to 1991/92 *South* zone during early summer (figure 7.9c) but the dry soil moisture perturbation has a unique response during late summer 1991/92 in contrast to a weak response in 1995/96. This elaborates the soil moisture initialisation influences and retention capabilities as well as the stability persistence between dry and wet years (but also between different parts of southern Africa. This is more prolonged during 1991/92 (figure 7.9).

Area average analysis of the *West* zone shows that wet soil moisture initialisation results in high MSE for most of the season whilst the dry soil moisture and control simulations have similar responses from mid-October 1995 (figure 7.10d). Mid-January exhibit a twist in the response as the wet soil moisture simulation, MSE response becomes less than dry soil moisture and control simulations before interchanging again by late February. This means that the dry soil moisture run becomes less stable than wet soil moisture simulation. As such it can be explained that the wet run was associated with surface cooling and the possible stabilization of the boundary layer resulting in reduction in MSE (Cook et al. 2006; Seth and Giorgi 1997). Over the *West* area, similar mixed responses were observed during 1991/92 season but earlier (i.e. mid-December) and with a different variation (figure 7.9d). Thus the *West* zone brings out the notion that soil moisture perturbations lead to mixed responses in the MSE particularly during late summer but wet soil moisture initialisation does have a stronger retention capability period especially in 1991/92 (figures 7.9d and 7.10d).

The mixed or weak responses which occur over the *South* and *West* zones can also be attributed to the sub-tropics or mid-latitude zones being in southern hemisphere where land/ocean ratio has a stronger influence than in the northern hemisphere. Giorgi et al. (1996) explanation of the convective activity being enhanced during dry soil moisture initialisation can be considered in these zones. Whilst Cook et al. (2006) explanation of wet soil moisture simulations enhancing surface cooling which may lead to stability through subsidence does substantiate the decreased MSE responses observed over the *West* area. Also, any semblance of moisture regardless of whether it is a dry/wet perturbation does introduce moisture into these semi-arid/desert areas of southern Africa which are usually dry during this period.

Seasonal variation of MSE (analogous to potential temperature) gives useful insight to its relation to soil moisture dynamics. Geography (position and/or altitude) also influence the atmospheric response and particularly with mixed responses observed over the *West* area. Note that, the MSE responses are almost similar to the EF. This can be expected as De Ridder (1999) showed equivalent potential temperature increases with EF under most circumstances. However, the relationship was derived using a simple 1-D slab model in the boundary layer. Thus important dynamics on the influence of land surfaces on the potential for deep convection was

neglected so as to attain the expression relating equivalent potential temperature to the surface EF.

7.9 Summary

This chapter looked at the sub-region areas mainly over the southern parts of the subcontinent that displayed mixed responses in contrast to the broad spatial cohesive pattern in the variable anomalies discussed in previous chapters. These mixed response signals in the various synoptic states especially over top left of the SOM and the southwestern area's unique response to the perturbations prompted some further analysis at sub-regional scale. This was done to get a better understanding of the soil moisture-atmosphere interactions over southwestern parts of the subcontinent which are not showing spatial cohesive responses like the northern parts of the region.

The major findings are summarised as:

- Over the *Central* and *South* areas, the top-layer soil moisture anomalies depict a dry soil moisture simulation leading to a reduction in moisture whilst the wet soil moisture perturbations result in an increase. However, there is an increase in simulated top-layer soil moisture for both perturbations over the *West* area.

- There is a positive response to the forcing with reduction in total precipitation for dry soil moisture perturbation and an increase in rainfall for anomalous wet soil moisture over the *Central* and *South* areas. The *West* area exhibits some inconsistent responses in total rainfall to the soil moisture perturbations.

- Early summer 1991/92 depicts a decrease in total rainfall for the dry soil moisture simulation with increase in rainfall for the wet soil moisture run whereas late summer shows minor increases in total rainfall for both perturbations. A contrasting response in the *West* to those observed for other areas occurs in 1995/96. Late summer presents marked decreases in rainfall for both perturbations although there is an increase in top-layer soil moisture for all perturbations.

- There is consistency in the positive temperature responses to the soil moisture perturbations for the three zones. Anomalous dry soil moisture simulation leads to warming whilst wet soil results in cooling. Over the *West*, the air temperature is higher than the ground temperature for all but late summer of 1991/92 for the dry soil moisture perturbations. An inversion layer is established in the lower atmosphere.

- There are consistent responses to perturbations for the heat fluxes and PBL.A high sensible (low latent) heat flux leads to an increase in PBL under dry soil moisture perturbations over all the zones. Wet soil moisture perturbations show a decrease in PBL height which is related with a decrease (increase) in sensible (latent) heat flux anomalies.

- As for incident solar radiation, only the *Central* area is showing some consistency to the mean seasonal response with dry soil moisture perturbations leading to an increase in incident radiation whilst wet soil moisture perturbation depict a reduction in the radiation. Mixed responses in incoming radiation occur over the *South* and *West* areas.

- Evaporative fraction shows more coherent variation during 1995/96 compared to 1991/92 where some mixed responses were observed. Some virtual zero EF values occur in dry 1991/92 indicating that evaporative fraction responds to soil moisture condition when a certain threshold of moisture level is reached. Stronger responses in EF to the soil moisture perturbations occur in wet 1995/96 than in dry 1991/92.

- *Central* area has consistent EF seasonal responses. *South* and *West* zones mixed response suggest that there are other factors that influence the EF besides soil moisture in sub-tropics to mid-latitudes. However, the EF seasonal variation of EF is a good reflection of the climate of the zones due to soil moisture conditions. The *South* and *West* areas mixed EF responses also suggest a different soil moisture feedback mechanism prevails especially over the *West*.

- For the *Central* area, wet soil moisture simulation leads to unstable and favourable situation for convective developments whilst the dry soil moisture run with less MSE suppresses any meaningful convective activity. Distinctive MSE responses in early summer and mixed responses (*South* and *West* areas) for late summer elaborates the soil moisture initialisation influences and the retention capabilities as well as the stability persistence between dry and wet years but also between different parts of the region. This is more prolonged during the dry 1991/92 season.

- Soil moisture perturbations do influence the partitioning of energy into latent and sensible heat fluxes for RegCM3.

- Geography (position and/or altitude) and climatology also influence the atmospheric response and particularly with mixed or weak responses observed over *South* and *West* areas within the sub-tropics to mid-latitude areas.

Chapter 8

Conclusion

8.1 Overview and Summary

8.1.1 Introduction

This study has considered the role of soil moisture-atmosphere interactions on climate variability over southern Africa using a regional climate model, RegCM3. The research aimed to increase our perspective of the responses of the local climate to soil moisture forcings by drying or moistening the land surface. The sensitivity and response capabilities to soil moisture perturbations of the model were investigated through a set of experiments. This included analysis of soil moisture retention capabilities on both inter-annual and seasonal timescales so as to understand how antecedent soil moisture conditions influence the summer climate variability. The study also aimed to understand the implications of soil moisture conditions on frequency and intensity of rainfall. Thereafter, the study sought out the large-scale atmospheric forcings under which the regional climate significantly responds to perturbations in soil moisture. Lastly, the research analysed identified regions where characteristics of seasonal climate may be influenced differently by soil moisture and has a substantial impact on surface climate variables.

To investigate these underlying processes of soil moisture-atmosphere interactions, a series of experiments utilizing wet, dry and normal soil moisture conditions were designed. The main simulation experiments were designed such that the model was initialised with 25% and 75% soil moisture field capacity which are prescribed as the wilting and saturating threshold values within the (BATS) land surface model scheme (Dickinson et al., 1993; Seth and Giorgi, 1998; Pal and Eltahir, 2001). Preliminary soil moisture perturbation experiments focussed on January for dry and wet years with the respective control simulation being driven by the initial boundary

conditions as formerly described in the methodology chapter. These simulations were used to assess the existing soil moisture-atmosphere interactions over southern Africa (Mdoka 2005; Tadross et al., 2010). Results of the soil moisture-atmosphere feedback mechanism over southern Africa's research are available in the successfully completed Water Research Commission's project report (see Tadross et al. 2010). After assessing the January soil moisture feedbacks, longer simulations were performed on a seasonal time-scale from September to March of the subsequent year. Simulations were done with August being the spin-up month. September which is part of spring time was incorporated to check on the role of antecedent soil moisture conditions for the subsequent summer rainfall season. These simulations enhance the knowledge on the soil moisture-atmosphere feedbacks, persistence of antecedent soil moisture conditions and magnitude of temporal responses for the variables that were analysed. Use of SOM analysis also helped in addressing the influence of soil moisture conditions on synoptic circulations within the troposphere.

8.1.2 Summer Climate Simulations

RegCM3 model does capture well the spatial distribution of mean precipitation as compared to the CRU and GPCP datasets. The model does reproduce the magnitude of precipitation over most of southwestern half of the regions although some wet biases occur from the southeastern areas up to DRC. A systematic cold bias is observed over Angola. The model is also capable to simulate well the west-east gradient to the south of the subcontinent as well as the terrain-based (orography) responses. This is also the case during early part of the summer season, SON with an improved reproduction of both the magnitude and spatial distribution. In the late summer (DJF) period, although the model still captures the spatial distribution, the wet biases are more widespread over the eastern half of the region. Thus RegCM3 forced with NCEP/NCAR Reanalysis 2 data and using Emanuel convection scheme overestimates precipitation over the tropics and high ground; but does exceptionally well in capturing the magnitude and spatial distribution over the southwestern areas and over the adjacent Oceans. However, RegCM3 model simulates well the spatial distribution of air temperature over southern Africa. The model reproduces the magnitude of temperature over Lowveld/Limpopo valley, Kalahari and Namib Desert, high terrain such as the Drakensburg Mountains and west coastal areas. It captures well

the spatial distribution over the region for both early- and late-summer periods. Whilst for late summer, DJF, the model reproduces the maxima of temperature over Kalahari and Namib Deserts and captures the minima over Lesotho. However, some slight cold biases are found over the western half of the region with some warm biases over the west coastal areas. The sections below will address the primary goal which is on the interactions of soil moisture with the large-scale atmospheric circulation during the summer rainfall season and show how antecedent soil moisture conditions influence the summer climate variability including soil moisture retention capabilities.

The RegCM3 model does well to capture spatial distribution of simulated total soil moisture and magnitude as compared to the observed IPF soil moisture data over the region but it underestimates over the northern subcontinent. The spatial responses to soil moisture perturbations show consistency for most of the surface variables especially over the northern parts of the region. Some inconsistency or mixed responses occurred over the south especially the southwestern areas of the subcontinent. Stronger and positive responses occurred with the dry soil moisture perturbations particularly during the dry seasons and this was clearly shown in a close-up look on 1991/92 season. Most of the model's variables analysed display these characteristics but to a lesser extent for total rainfall and incident solar radiation. Generally, area-average temporal distribution analysis shows a positive feedback to the soil moisture perturbations which might be caused by stronger responses that were observed especially over the northern parts of the subcontinent.

In general, dry soil moisture perturbations lead to spatially cohesive decrease in surface temperature, sensible heat flux and planetary boundary layer whereas wet soil moisture perturbations result in an increase of the three surface variables over most of the region except the southwestern areas. There is a stronger response and persistence occurring during dry seasons than in the wet summer rainfall seasons especially with the dry soil moisture perturbation experiments. This is confirmed by the spatially consistent responses during early summers that are similar to the mean distribution whilst late summers show some inconsistencies over the southwestern areas. Temporal variations of the surface temperature, sensible heat flux and planetary boundary layer give distinct responses throughout most of the season with the dry soil

moisture simulation uniquely different in magnitude. This supports the spatially stronger responses of the dry soil moisture simulations. As for incident solar radiation, similar characteristics but weak and inconsistent responses are observed particularly to the southwest but the time series shows almost similar variation and magnitude for all experiments throughout the season. The soil moisture perturbations are showing an influence of geography (i.e. position and altitude) as most spatial consistent responses are confined to the central and northern areas (tropics) whilst the southwestern and southern areas (sub-tropical to mid-latitudes) depict mixed responses. Similar responses but either weak positive or negative were observed in earlier studies with different RCMs and methodologies (New et al., 2003; Cook et al., 2006; Mackellar, 2007).

There is generally a distinct response to soil moisture perturbation in surface temperatures over the region and a marked degree of sensitivity during the anomalously dry soil moisture simulation for any part of the season. Temperature tends to exhibit some direct and clear responses to the soil moisture perturbations with the vast part of the region displaying the positive feedback mechanism as described by Eltahir, (1998). Although not presented here, similar responses have been observed for all the other summer simulations' soil moisture perturbations. Mackellar et al., (2009) using a different RCM, MM5 found that near-surface temperature displays relatively high spatial correlations to the initial soil moisture anomaly but only in the early months of the simulations and the magnitude of the temperature response was small. Thus, the choice of RCM and parameterization could also be a factor due to model's sensitivity to the perturbations.

There is a consistent spatio-temporal response of principally a decrease (increase) in latent heat flux with anomalously dry (wet) soil moisture perturbations. These responses are in direct contrast to the sensible heat fluxes. However, this is in agreement with the positive feedback response theory where initial dry (wet) soil moisture conditions generally lead to an increase (decrease) in surface temperature which results in an increase (decrease) in sensible heat flux and thus a decrease (increase) in latent heat flux (also applies to evapotranspiration). Fischer et al. (2007) experiments of the 2003 simulated heat wave over Europe showed the vital role of separating net surface radiation into latent and sensible heat fluxes, which to a large extent is controlled by soil moisture. This was also emphasized by Eltahir (1998) and Schär et al. (1999)

which show symmetric relation with enhanced net radiation under anomalous wet soil moisture conditions and vice versa.

As explained above, a decrease in soil moisture leads to a decrease in latent heat (evapotranspiration) and an increase in sensible heat flux (also Bowen ratio). This causes a deeper, warmer and drier planetary boundary layer as indicated by the increased surface temperature within the RegCM3. Similar observations were made by Tyson and Preston-Whyte, (2000); Pal and Eltahir, (2001); Hohenegger, (2009); Jaeger and Seneviratne, (2011). The dry soil moisture perturbations, also lead to an increase in incident solar radiation which would imply a clear sky or less cloud cover and a reduction in precipitation. This is more prevalent over the northern parts of the region where consistent responses were commonly observed with mixed responses occurring over the southern parts of the subcontinent especially the southwestern areas and this applies to all the summer simulation perturbations The responses concur with findings from other parts of the world for example; Eltahir and Pal, (1996); Eltahir (1998); Pal and Eltahir, (2001); Kim and Hong, (2007); Jaeger and Seneviratne, (2011).

Although other forcings are also at play on the sensitivity factor in the feedback mechanism, there is a persistence of the stronger responses that occur for dry soil moisture perturbations especially in drier or drought-like conditions. There is an apparent signal especially in the low latitude (barotropic conditions) with contrasting mixed responses or no effect occurring in the mid-latitude (baroclinic conditions) areas particularly the southwestern areas of the region. Over southern Africa, similar analysis on boundary layer processes and mechanisms were done by Matarira (1990a, 1990b); Matarira and Jury (1992) and Mackellar (2007). Mackellar (2007) concurs over mid-latitude with the conclusion that soil moisture–atmosphere responses are geographically based.

The drought persistence or enhancing of dry conditions under dry soil moisture initialisation was also observed over West Africa (Zheng and Eltahir, 1998) and in USA (Pal and Eltahir, 2001). If one was to infer a linear relationship between soil moisture, ENSO and drought; from this study we have shown that dry soil moisture conditions induce anticyclonic circulation which then manifest into subsiding, warming and drying of the air leading to the dry conditions persisting.

Whilst with the El Niño phase it also manifests into having the descending limb of the Walker circulation over the southern Africa thus resulting in warm and dry air that exacerbate the dry or drought conditions. However, it is beyond the scope of this study to quantify the causal effect of either the ENSO on soil moisture and further studies would be required to understand the the physical mechanisms relating soil moisture, ENSO to dry or drought conditions. Richard et al. (2001) noted that some ENSO events are not accompanied by droughts over southern Africa. Other climate factors like moisture trajectories (e.g. Jack, 2013); aerosols (e.g. Tummon et al., 2010); vegetation (e.g. Mackellar et al., 2009) and the influence of adjacent Oceans (Indian Ocean, e.g. Richard et al., 2000 and Atlantic Ocean, e.g. Vigaud et al., 2009) in modulating the climate variability of southern Africa need to be incorporated in a holistic approach to their specific roles.

8.1.3 Synoptic Analysis and Mean January Climate Responses

Diurnal patterns of the surface variables analysed simulate a natural cycle associated with southern Africa climate with highest peaks being attained after midday (Torrance, 1981; Buckle, 1996; Lindesay, 1998; Tyson and Preston-Whyte, 2000). Diurnal cycle patterns show positive response characteristics for the respective soil moisture perturbations. Thus, high (low) peaks are observed for the dry (wet) soil moisture initialisation with the surface temperature, sensible heat flux, incident solar radiation and planetary boundary layer (rainfall and evapotranspiration) variables. Distinct magnitude change in responses is observed with dry soil moisture perturbations as compared to wet soil moisture anomalies which are almost similar to the control simulations for all variables analysed. In general, the diurnal cycle patterns support the existence of positive feedbacks and give an insight into the strength of the variables' response to these mechanisms under the anomalous soil moisture conditions. It is also evident that soil moisture does not substantially impact the overall daily variability but its magnitude.

Spatial distribution pattern in rain days' anomalies follows a west-east gradient during dry soil moisture simulations whilst there is no distinctive response during wet simulations. For all simulations, there is a vast area within the transitional zone (i.e. between decreases and increases) in both rain days and rainfall intensity. This could imply that within the model the

number of rain days in these areas is not affected by these levels of soil moisture perturbations induced. This addresses the second objective on the implications of soil moisture conditions on frequency and intensity of rainfall. Southeastern South Africa and Lesotho show a decrease in rain days for all forms of soil moisture perturbations, indicating that dynamical changes resulting from these experiments result in a shift of rainfall producing systems away from these regions. There is no clear response shown in the rainfall intensity distribution pattern over the region for all the different experimental simulations. Intensity distribution in comparison to the number of rain days implies a fair distribution of rainfall for most of the month. Although this requires further investigation it implies that spatial organisation of changes in rainfall intensity may be heavily dependent on the synoptic forcing of the regional climate.

Vertical integration of the atmosphere demonstrates that dry soil moisture simulations show increases in air temperature across the region in the lower atmosphere with negative anomalies occurring in the middle atmosphere. The cooler air temperature is observed for the wet soil moisture perturbation than the control simulation which would imply stable conditions for the wet soil moisture perturbation. The stability situations established here through the overall atmosphere temperature characteristics do partially explain the incoherent rainfall response to soil moisture perturbation. This also supports existence of negative feedback mechanisms in some areas especially over the southwest. Soil moisture perturbations have mostly affected the lower troposphere. This further shows how and the vertical extent of soil moisture interactions with the atmosphere during the summer rainfall season.

As for the geopotential height analysis, the dry soil moisture perturbations result in stronger geopotential responses as compared to the wet soil moisture perturbations. This aids in explaining the stronger and persistent positive (negative) responses for surface temperature, sensible heat and PBL (latent heat) observed for dry soil moisture perturbation of the analysed variables during early summer. Southwestern parts of the region are consistently showing slight geopotential decreases for all the perturbations of late summer. This is consistent with unresponsive characteristics noted over southwestern areas of the region which are typically dry during this season rendering any dry or wet perturbation a forcing that would increase moisture levels.

Finally the responses observed here can also be attributed to anomalous dry soil moisture initialisations leading to strengthening of anticyclonic circulation which means more subsidence of dry air and unfavourable conditions for cloud development or rainfall activity. This leads to increases in surface temperature, sensible heat flux and PBL whilst decreases occur for latent heat flux and incident solar radiation. The converse is true with anomalous wet soil moisture initialisation resulting in a decrease in geopotential height or deepening of low pressure (cyclonic) systems which would enhance convergence and increase in precipitation (Eltahir; 1998; Tyson and Preston-Whyte 2000). This explains how the soil moisture perturbations relate with the large-scale atmospheric circulation during the summer rainfall season. The response is stronger in the dry soil moisture conditions than during the wet soil moisture period. These consistent responses are more prevalent over the northern parts of the subcontinent. Again, given this scenario, El Nino years are also the drier years and that probably imply amplification of the persistence period via the strengthening of the anticyclonic circulation. However, not much has been documented yet that has verified this; for example, studying of the co-relation between the ENSO signal or Nino 3.2 region and the soil moisture index or conditions over southern Africa.

8.1.4 SOM Analysis of Synoptic Patterns in Summer Climate

Self-organising map, SOM has broadened the techniques by which synoptic climatology may be approached and classifies data on a non-linear basis. SOM technique was utilised to substantiate some of the primary objective findings and also address the third objective seeking out the large-scale atmospheric forcings under which the regional climate substantially responds to soil moisture perturbations. One of the synoptic patterns clearly identified through this technique occurs during the late part of the summer season which depicts deep low pressure over the northern areas which can be associated with the southern tip of the ITCZ at this time of the season (Torrance, 1981; Buckle, 1996; Lindesay, 1998; Tyson and Preston-Whyte, 2000). This is the period when pressure rises begin to occur within the subcontinent as shown by the weak subtropical ridge from the Atlantic Ocean, overlaid by mid-tropospheric easterlies and adequate low-level moisture over much of the domain within the SOM array. Thus, the left side of SOM

generally represents the wet synoptic states which occur during mid into late summer for both 1991/92 and 1995/96.

The highest frequency of occurrence in the NCEP/NCAR reanalysis 2 data classifies into the bottom right of the SOM. This implies that dominant synoptic states show a surface tropical ridge of high pressure and a low pressure system to the southeast of the region as well as mid-level anticyclonic circulation over Indian Ocean but also having low-level moisture off to the south of the domain. The synoptic characteristics are observed to occur during early summer in the seasonal evolution analysis of the SOM array. Thus, the right side of the SOM generally represents the dry synoptic states which occur during early October. These are typical of southern Africa's late winter/spring circulation patterns and low-level moisture distribution (Torrance, 1981; Buckle, 1996; Lindesay, 1998; Tyson and Preston-Whyte, 2000).

The effects of soil moisture perturbations on the synoptic circulation show an increase in magnitude and spatial cohesiveness across the SOM from top left to bottom right in accordance with the wet to dry synoptic characteristics spread. Viewing from bottom right particularly for the dry soil moisture perturbation depicts a seasonal evolution that can be related to soil moisture memory in that the persistence of the spatial cohesiveness lessens as the season progresses. This is shown through the coherent elevated planetary boundary layer (warming of surface temperature) that is observed in the bottom right of the SOM which occurs in early summer whilst there is a heterogeneous map with shallower PBL (cooling), transition zones and higher PBL (warming) in the top left side of the SOM which occur in late summer. The SOM does show the seasonal transition with responses to soil moisture initialisation showing stronger responses during early summer and favouring dry synoptic states or being influenced by the late winter/spring synoptic characteristics. Dry synoptic conditions show the degree of strong coupling in the soil moisture-atmosphere interaction (Pal and Eltahir, 2001, 2003).

Planetary boundary layer, PBL (similarly surface temperature, latent and sensible heat fluxes) shows strong responses to the soil moisture perturbations under all synoptic forcings but rainfall characteristics are strongly influenced by large-scale synoptic circulations. Over the southwestern area, there are no distinctive responses to dry/wet soil moisture perturbations

across all the synoptic states. This concurs with earlier observations made over this dry and semi-arid part of southern Africa (Cook et al., 2006; Mackellar, 2007; Tadross et al., 2010). In this area, the existing soil moisture conditions should be lower than the moisture levels of the three soil layers within the BATS scheme coupled to the RegCM3 model. Thus, any perturbation will enhance the moisture levels leading to negative PBL (also decrease in surface temperature and sensible heat flux) responses observed for all the dry soil moisture initialisations.

Soil moisture perturbations has a greater effect on the circulation of the lower atmosphere when the perturbation is consistent with the synoptic forcing i.e. if there are dry (e.g. anticyclonic) large-scale changes then drier soil moisture initialisation will have a greater effect, whereas if the synoptic forcing is wetter, then a wet soil moisture initialisation will interact to prove the greatest change in circulation. This has been observed in similar studies but focussing on vegetation to atmosphere interactions (Tadross et al., 2010; Mackellar et al., 2010). Thus SOM technique helps in further understanding the interactions of soil moisture with the large-scale atmospheric circulation during summer and seeks out the large-scale atmospheric forcings under which the regional climate substantially responds to soil moisture perturbations

8.1.5 Sub-regional Analysis of the Summer Climate Simulations

Finally, this section discussed identified regions where characteristics of seasonal climate varied due to soil moisture and had substantial impact on chosen climate variables. From the selected zones, analysis of simulated top-layer soil moisture show decreases for dry soil moisture perturbation over the *Central* and *South* areas whilst increases in top-layer soil moisture levels occur for wet soil moisture perturbation. The *West* area depicts increases in top-layer soil moisture for both perturbations. This would explain the similar responses that were observed over the southwestern areas for most surface variables discussed.

There is consistency in the positive temperature responses to the soil moisture perturbations for the three zones. Anomalous dry soil moisture simulation leads to warming whilst wet soil moisture run results in cooling. Over the *West*, the air temperature (2m above ground) is higher than the ground temperature for all but late summer 1991/92 for the dry soil moisture

perturbations. This signifies the stabilizing factor the temperature responses are showing over that area for the dry run by establishing an inversion in the lower atmosphere. This can be anticipated especially over the semi-arid or desert or mountain areas falling within that *West* zone. In southern Africa, surface inversions are greatest over the interior of Namibia and Botswana due to low relative humidity and low cloud cover (Tyson and Preston-Whyte, 2000). The daytime surface inversions that occur over Namib coast are caused by the modification and stabilization of the lower atmosphere by the cold Benguela Current. In western South Africa which is mountainous terrain, cold air drainage in katabatic flow causes the accumulation of cold air in valleys to form valley inversions (Tyson and Preston-Whyte, 2000; Barry and Chorley, 2009; Petersen et al., 2010).

Incident solar radiation produced some interesting responses to soil moisture perturbations. For the *Central* area, the basic theory would be an increase in soil moisture conditions lead to an increase in moisture in the atmosphere (Eltahir, 1998) which would result in more cloud development or thick clouds and/or precipitation thus implying reduced incoming solar radiation reaching the surface. However, besides soil moisture affecting the lower troposphere, there are other dynamic forcings involved rendering incident solar radiation a weak respondent variable to surface soil moisture initialisations in the *South* and *West* areas. One would also need to consider that the reflection and absorption from the clouds which would imply less solar radiation reaching the surface as a factor leading to the mixed incident solar radiation responses to soil moisture perturbations. However, these inconsistent responses suggest that the incident solar radiation is not directly interacting with the surface perturbations only.

Dry soil moisture perturbations depict an increase in PBL height for all the selected areas with stronger responses occurring over the *Central* area. This is consistent with temperature and sensible heat flux responses discussed above. As explained earlier, high sensible heat flux tends to increase turbulent mixing which increases the PBL growth rate and hence the height of the PBL (Eltahir, 1998; Pal and Eltahir 2001; Jaeger and Seneviratne, 2011). Wet soil moisture perturbations show a decrease in PBL height which is analogous with a decrease in surface temperature and sensible heat flux anomalies.

Evaporative fraction (EF) shows more coherent variation during 1995/96 compared to 1991/92 where some mixed responses were observed. Stronger responses in EF to the soil moisture perturbations occur in wet 1995/96 than in dry 1991/92. *South* and *West* zones also depict that there is some local forcing or other environmental factors that influence the EF besides soil moisture. However, the seasonal variation of EF is a good reflection of the climate of the zones due to soil moisture with consistent responses occurring only over the *Central* area. The *South* and *West* areas' mixed EF responses suggest a different soil moisture feedback mechanism or unique partitioning of the energy fluxes and/or other forcings prevail over these zones. These findings do also inversely apply to Bowen ratio which is related to EF (Farah et al., 2004).

EF is observed to drop around January in the perturbations; this is typical of the southern Africa's rainfall which experiences intraseasonal dry spells mostly around January (Matarira and Jury 1992; Makarau, 1995; Makarau and Jury, 1997; Unganai and Mason; 2002; Usman and Reason, 2004). Some virtual zero EF values were also shown in the dry 1991/92 seasons indicating that evaporative fraction responds to soil moisture conditions when a certain threshold of moisture level is reached. Thus when EF is zero it implies that all of available energy is partitioned into sensible heat flux. So, anomalous dry soil moisture would reduce latent heat flux to almost zero and thereby enlarge the sensible heat flux towards maximum for virtual zero EF to be reached. Therefore, role of partitioning of net radiation into latent and sensible heat fluxes is very vital and is mostly controlled by soil moisture conditions as previously ascertained by Schär et al. (1999); Shukla (1999); Cook et al. (2007) and Fischer et al. (2007).

Regional variation of available moist static energy (MSE) is also a good reflection of the climate of the zones due to soil moisture conditions. Over the *Central* area, wet soil moisture perturbation leads to unstable and favourable situation for convective development whilst the dry soil moisture simulation has less available MSE which could suppress any meaningful convective activity. Distinctive MSE temporal responses in early summer and mixed responses for late summer (*South* and *West* areas) elaborate the influence of soil moisture initialisation and soil moisture retention capabilities. This shows persistence of the responses between dry and wet years as well as sensitivities of different parts of the region. This is more prolonged and stronger in magnitude of response during the dry 1991/92 season. Seasonal variation of MSE (analogous

to potential temperature) gives useful insight to its relation to soil moisture dynamics. Geography (i.e. position and altitude) and climatology also influence the atmospheric response, particularly with mixed responses observed over the *South* and *West* areas. The land/ocean ratio over southern hemisphere should be noted on its influence in the mid-latitude inland areas which should be stronger than in the northern hemisphere. Note that, the MSE responses are almost similar to the EF. One can use the knowledge of some of these thermodynamic variables' characteristics as an indicator of soil moisture responses within the various zones for either hydrometeorological, agrometeorological or climatological modeling or predictions (Pal and Eltahir 2001; Farah et al., 2004; Jaeger and Seneviratne, 2011).

Finally, consistent strong responses are observed for surface variables analysed except for rainfall (very weak) over the *Central* area (tropics) with a positive feedback mechanism. Stronger and persistent responses in the variables analysed occur during early summer and is more enhanced in dry soil moisture perturbation especially in a dry year. *South* and *West* (sub-tropics to mid-latitude areas) show mixed responses to the perturbations with only surface temperature, heat fluxes and PBL exhibiting consistency. Both negative and positive feedback mechanisms to the soil moisture forcing occur over these areas. This is also evidenced by the intraseasonal interchange of the wet soil moisture perturbation response from a higher to lower available MSE than the dry soil moisture perturbation during the season which would then imply a change from unstable to stable conditions and thus, subsidence which could then suppress moisture convergence. New et al. (2003) and Cook et al. (2006) have demonstrated the negative feedback phenomenon over southern Africa. However, in some areas over southern Africa a weak feedback which can be either positive or negative depending on geographical and climatological setting has been detected (Cook et al. 2006; Mackellar, 2007). However, these studies do not reveal the strong positive feedback that this study shows over the central and northern parts of the regions but concur on the mixed responses that occur over the southern parts of the subcontinent. The influence of geography (position and altitude) and climatology has also been proposed in this study particularly over the *West* and *South* areas.

8.3 Caveats or Limitations

There are some important issues that have not been fully explored in this study besides the obvious factors of time constraints, computer climate modeling time or server/storage space demands and sometimes malfunctions or bugs within RegCM3 model leading to crashing of the computer.

Firstly, southern Africa region is very sensitive to a change of physical schemes (Crẽtat et al., 2012), lateral boundary forcings (Sylla et al., 2012) and aerosol radiative forcings (Tummon et al., 2010) which could affect the radiative feedbacks discussed in this study. Thus understanding of the nature of the biases can aid in improving climate model simulations and avoid the translation of errors to model's applications (Sylla et al., 2012).

One of the biggest challenges in climate modelling over southern Africa tends to be the simulation of rainfall. Previous studies over southern Africa have shown some substantial wet and dry biases over particular areas of the region (Tadross et al., 2005; Engelbrecht et al., 2009, Mackellar et al., 2009, Tummon et al., 2010; Sylla et al., 2010, 2012; Jack, 2013). Most of the CORDEX Africa projects have also noted these significant biases (Nikulin et al., 2012; Endris et al., 2013; Gbobaniyi et al., 2013 and Kalognomou et al., 2013). Such biases may probably be due to the model set up such as convection parameterization (Crẽtat et al., 2012); boundary conditions, simulated circulation anomalies, and moisture transport (Sylla et al., 2010, 2012; Nikulin et al., 2012; Zhang et al., 2013; Jack 2013). Kalognomou, (2013) concur and highlighted the following potential sources of bias in each of the CORDEX models: the internal solvers of the models themselves, the physics packages like the PBL, and cumulus schemes as well as their subschemes like trigger, closure, and entrainment functions. Additionally, the representation of the land surface processes and circulations will also have an influence on the model's rainfall bias.

Optimisation of the RCMs requires very robust testing of the whole model package. In seeking to improve the model's simulation of the real climatology, the challenges emanate from the model's package itself, choice of domain, convection scheme and moderation of some parameter values

(Seth & Giorgi, 1998; Crẽtat et al., 2012; Giorgi et al., 2012; Sylla et al., 2012). Sylla et al., (2012) honestly stated that "*Choice of domain, convection scheme and some parameter values also contributed to this improvement, although it is difficult to clearly identify the contributions of these different elements……*"

In the sensitivity tests over four CORDEX domains using the new RegCM4 model, Giorgi et al. (2012) also show that the model has consistent level of performance in different climatic regimes across the domains although some systematic model biases persist. RegCM4 model shows a significant sensitivity to different parameterizations and parameter settings which can thus be used to optimize model performance over different domains. However, Giorgi et al. (2012) quickly stress that the settings appear to perform generally well over most of these domains, there is still no single parameter setting that performs best in all domains tested; thus conducting a customisation exercise for our very sensitive southern Africa region before carrying out specific model applications will be required. The preliminary simulations the researcher has done with RegCM4 do not show much improvement on biases and rainfall from the RegCM3 runs. As such some intensive customisation process is required and therefore was not recommendable to change to RegCM4 due to time constraints.

The observations or reanalysis data is another big concern in climate modelling. Validating of a model's performance can be misleading if one uses erroneous observations or analyses data. Some of these data have systematic errors due a number of factors amongst the common ones being the sparse data, assimilation methods, model physics and resolution. Thus the observational climate data products with their limitations could lead to erroneous wet or dry biases (Nikulin et al., 2012 & Zhang et al., 2013). Although it has its own limitations, there is a need to consider the new reanalyses datasets such as the European Center for Medium Range Weather Forecast (ECMWF) ERA Interim reanalyses (Dee et al., 2011& Uppala et al., 2008) which is now commonly used as a boundary forcing field especially in most CORDEX projects (Nikulin et al., 2012; Gbobaniyi et al., 2013; Endris et al., 2013 and Kalognomou et al., 2013). Recent reanalysis datasets have improved through the use of four dimensional data assimilation, use of forecast models, ensemble data assimilation increase in the horizontal and vertical resolution, temporal resolution as well as fully coupled ocean-atmosphere data assimilation

(Zhang et al., 2013). Thus, future studies' model validation can be improved through the use of these latest reanalysis datasets.

There is limited background of earlier studies over southern Africa that can be used to objectively validate the findings in this study. The few studies over the region are being done using different RCMs with different parameterizations, model physics (convective schemes), resolution and model biases but also using different land surface models to simulate the soil moisture-atmosphere interactions. Robust comparisons with other studies over southern Africa (New et al. 2003; Cook et al. 2006 and Mackellar et al., 2009) is complicated as the simulations are based on different domains, different years/events or period of analysis and different resolutions. The results can be comparable objectively if the factors mentioned above and in-depth knowledge of the physical mechanism of the feedback process, hydrological cycle process, large-scale dynamics, diurnal cycles and period of simulations are uniformly considered for the different models that have been used in land surface-atmosphere interactions. Better representation of model simulations requires a good choice of the domain as there exist some boundary condition problems. Seth and Giorgi (1998) point to the fact that precipitation and moisture transport are affected by the choice of the limited area domain. For sensitivity studies to internal forcings, domains much larger than the area of interest should be utilized (Seth and Giorgi, 1998). A large domain should be selected to include the large-scale responses to the soil moisture (Pal and Eltahir, 2002). A better part of this study's time was spent incorporating the factors mentioned above. However, using different methods and models, similar results are observed especially over the south of the subcontinent (New et al., 2003; Cook et al., 2006; Mackellar, 2007).

Most of the studies on soil moisture and atmosphere interactions are primarily based on global and regional model simulations. Particularly over southern Africa, there is not much observational data based analysis due to lack of long-term soil moisture measurements. The available soil moisture that exist in-situ is discontinuous and limited to a few areas e.g. IPF soil moisture data[16]. There are some correctional measurements that are being addressed and

[16] This SHARE project focusing on southern Africa soil moisture observation data will be completed in 2012. www.ukzn.ac.za/sahg/share.

validation would be required before the data is fully usable (Ceballos et al., 2005; IPF, 2008). Therefore, the soil moisture data over southern Africa is still deemed insufficient to address land-atmosphere interactions at regional scale. There are no standard measurement techniques and protocols which further complicates the use of soil moisture network data due to difference in measurement depths and units; sampling interval and precision (Dorigo, 2011). Land surface assimilation products use approaches that constrain off-line land surface model simulations from observations due to long-term land surface variables and therefore, provide a unique opportunity to statistically assess land-atmosphere coupling (Zhang and Dong, 2009).

This study used seven months long simulations (September to March) for the six summer seasons to study the soil moisture atmosphere feedback mechanism. Although that might give credibility to the findings, it is not clear if it is adequate to fully attain the complete radiative feedback mechanism within the model used. Although this requires more computing time and storage capacity, longer time-scales of simulations should be considered for these soil moisture perturbation experiments. Longer time-scale simulations would be required for a critical study of the radiative processes in the soil moisture-rainfall feedback and to check if the model can simulate closer to the real climatology. Without the radiative feedback processes the initial soil moisture anomaly has little effect on the seasonal rainfall (Zheng and Eltahir, 1998; Schär et al., 1999; Pal and Eltahir, 2002). It is worth noting that a too wet model may interfere with the way the feedback process actually operates possibly due to too much remnants of moisture available and might require a longer period to equilibrate the moisture within the model's atmosphere. In a non-linear system, bias towards wet soil moisture conditions can result in an erroneous solution such as the weak response observed with some of the wet soil moisture perturbation experiments in this study.

The soil moisture-rainfall feedback is also dependent on the convective parameterization and varies from one region to another (Mdoka, 2005). To fully understand the complete radiative feedback mechanism, Schär et al. (1999) proposes a detailed analysis of the convection schemes which should include an investigation of the mean diurnal cycle to isolate the physical mechanism underlying the soil moisture-rainfall feedback. This is confirmed by Tadross et al. (2005b) that the diurnal cycle and frequency of rainfall over southern Africa are dependent on

the choice of convection scheme. Further, they show that the choice of PBL is also important for simulating the diurnal cycle of incident solar radiation, all of which are important for correctly simulating the hydrological cycle. This study could only focus on the mean diurnal cycle patterns using the Emanuel convection scheme to only ascertain the soil moisture-atmosphere feedback mechanism that exists. Mackellar et al. (2009) also state the importance of convection scheme but did not find major difference in responses when using different convective schemes with MM5 model.

In this study, RegCM3 is coupled with a land surface model (LSM), Biosphere Atmosphere Transfer Scheme (BATS; Dickinson et al., 1993). Recent study by Steiner et al. (2009) showed that coupling of the NCAR Community Land Model (CLM3; Sellers et al., 1997) to the RegCM3 atmosphere substantially improves the simulation of mean climate over West Africa. Some of the findings include soil texture boundary condition with the hydrologic treatment of the soil column leading to greater infiltration, less water storage in the soil, evapotranspiration components of water cycle which return less total water to the atmosphere than BATS. Winter et al., (2009) coupled RegCM3 with Integrated Biosphere Simulator (IBIS; Foley et al., 1996) which introduced several advantages including vegetation dynamics, the explicit modeling of soil/plant biogeochemistry, additional soil layers, an improved method for initialization of soil moisture and temperature. Diro et al., (2012) recently carried out sensitivity experiments to investigate RegCM4's sensitivity to LSMs (CLM and BATS) over Central America and found out that BATs has a more realistic simulation of the occurrence of the mid-summer drought over that region. Their study also showed that the use of CLM instead of BATS leads to a warmer and drier land surface and a better representation of the seasonal mean spatial pattern of precipitation. This shows that there are more dynamic models which can now be coupled with RCMs to improve on the atmosphere-land surface interactions. This improvement reinforces the concept that changes in land surface conditions can cause substantial changes in the atmospheric circulation (Steiner et al., 2009). However, there is a need for validation of these couplings with LSMs over southern Africa to assess these findings as there are also some advantages of using BATS which are observed in both studies and the findings from this study.

There is a need for a robust look at large-scale dynamics such as circulation patterns and moisture trajectories to aid in the soil moisture-rainfall feedbacks analysis especially in the whole vertical troposphere extent or boundary layer. Recent findings by Jack (2013) identifying the moisture sources inland of southern Africa could be useful and should be incorporated in the RCMs when studying the soil moisture dynamics. More findings can be obtained from assessing the sensitivity within a particular window or area of interest over southern Africa (i.e. selected area within the region where the soil moisture perturbations will be introduced) whilst maintaining prescribed boundary conditions elsewhere in the region. This can help to better understand the local effects from remote influence and assess the capabilities of the model at finer resolutions. This improves in identifying the major processes responsible for the soil moisture-atmosphere feedback in those small areas of interest i.e. separate the local forcings such as the instability in the vertical distribution of atmospheric temperature and humidity (characterized by CAPE) and the increase of the MSE in the PBL from large-scale atmospheric forcings such as those generated by monsoon circulations within the tropics, frontal systems in mid-latitudes or orographic lifting (Washington And Todd, 1998; Tyson and Preston-Whyte, 2000; Pal et al., 2007; J. Pal, *pers comm.*).

Finally, there was little evaluation of the feedback mechanisms due to varied soil moisture levels. This is in regard to model's remnants of moisture available and might require a longer period to equilibrate the soil moisture within the different BATS model's three soil-layer structure. Moreover, a holistic approach would require multi-year simulation and incorporate the atmospheric responses to vegetation and aerosols to fully understand the exact contribution factor of soil moisture. Experiments have also been carried out to examine the moisture trajectories, vegetation or aerosols effect to atmosphere over southern Africa and West Africa including sensitivity tests of the regional climate models, RegCM3, MM5 and WRF (Drew, 2004; Abiodun et al., 2008; Mackellar, 2007; Mackellar et al., 2009; Tummon et al., 2010; Jack, 2013; I. Oliviera and G. Maure, *pers. comm.*) but not much has been done to delineate the contributory effect of soil moisture, vegetation and aerosols to climate variability over southern Africa (Tadross et al., 2010). Thus, more research is still imminent over the region in so far as land-atmosphere as well as ocean-land-atmosphere interactions are concerned.

8. 4 Recommendations for future work

Longer time-scales simulations are required for a critical study of the radiative processes in the soil moisture-rainfall feedback and to check if the model can simulate closer to the real climatology. There is need to increase the size of the analysis' dataset by either employing a multi-year simulation or by simulating more periods or events of interest than the three years. To help resolve the variability of model's atmosphere, experiments should also be selected for normal years rather than just extreme dry and wet years, El Niño and La Niña years (assuming stability of the ENSO teleconnections in the future i.e. if ENSO phases do not become locked into one state; Hewitson, *pers. comm.*). Thus a wide range of different characteristics can be explored.

Thus more fine-tuning process of model's physics and sensitivity experiments of the model to soil moisture conditions should be done. Increasing the number of studies with different RCMs would aid in determining if the models are producing the most realistic response. The soil moisture-rainfall feedbacks over southern Africa should be reviewed in an inter-comparison analysis of the regional climate models that are being used over the region e.g. RegCM3, MM5, PRECIS and WRF (Weather and Research Forecast). This would require use of the same domain choice and lateral resolution in the different RCMs. Over southern Africa, there is need to validate the sensitivity of coupling the RCMs to the different LSMs such as CLM3 and IBIS which improves the land surface-atmosphere interactions in other parts of the world (see Steiner et al., 2009; Winter et al., 2009).

Similar experiments to the present study (which assumed a homogeneous soil layer) but with varying soil moisture within the BATS' top-layer, root-layer and deep-layer soils can be helpful in assessing each layer's contribution to the model's atmosphere response. The change in the soil moisture perturbations or field capacities (e.g. 10%, 25%. 50%, 75%, 90%) should also be considered to check the model's sensitivity levels (i.e. thresholds) especially towards the wetter soil moisture perturbation where the response was weaker as compared to the drier one. The southwestern area requires further studies to assess the threshold at which soil moisture perturbations result in a contrasting response since at the wilting point of the BATS scheme, moisture was still in abundance over that region.

Besides allowing interactive soil moisture initialisation which is the practical way in climate predictions, perturbations can also be done with fixed soil moisture levels to evaluate the atmosphere's response in a non-interactive land surface. This was attempted in this study but got erratic responses or noise signals which required fixing model's subroutine programming code errors. This could not be rectified in time for the results to be part of this thesis. Further research could also assess the sensitivity within a window of interest whilst maintaining default conditions elsewhere. This can aid in better understanding of the local effects and assess on the capabilities of the model at finer resolutions. Thus improve in better identifying the key processes that are responsible for the soil moisture-atmosphere feedbacks i.e. separate the local forcings from large-scale atmospheric forcings.

There is also need for research into impacts of climate change on soil moisture and its feedback to the atmosphere for southern Africa. Seneviratne et al., (2006a, 2010) and Vidale et al., (2007) explored land-atmosphere coupling over Europe and suggested that projected changes in future summer climate rely on soil moisture-atmosphere interactions. Sensitivities to temperature, precipitation, evaporation, radiation effects and to climate change scenarios should be tested. Incorporation of realistic soil moisture dynamics over the region into climate change predictions would be useful. This would lead to more plausible regional-scale future climate change predictions for southern Africa. Thus, the necessity for more investigation of the couplings in the regional climate system is imperative if we are to understand the dynamics of the regional climate.

However, the findings from this study should provide valuable information to fill some gaps in the knowledge of soil moisture conditions within the region's hydrological cycle process for the benefit of the community through better livelihoods and socio-economic development. The soil moisture-atmosphere interactions knowledge can enable meteorologists or hydrologists or agrometeorologists or decision makers or town planners etc. address events like fires, floods, drought or dry spells (as they relate to antecedent soil moisture conditions),to identify risk or prone areas and thus make sound decisions to curb their severity or persistence. Some of the knowledge could be useful for improving seasonal climate forecasts, climate change projections,

water management and agricultural planning over southern Africa through better use of initialisation conditions from surface variables analysed in this research that could then be incorporated in global/climate; hydrological or crop models. The uncertainty or inconsistency responses noted in the study (e.g. southwestern areas) could also aid in academic research to focus on these zones and thus improve land surface-atmosphere coupling knowledge for the region.

8.5 Conclusion

Augmenting other global, regional and local forcings, anomalously dry (wet) conditions have positive feedbacks with similar dry (wet) synoptic forcings of the regional climate. Stronger responses to antecedent soil moisture perturbations occur during early summer and more so for the dry soil moisture initialisation. Anomalous dry synoptic forcing persists for longer and intensifies the changes in the regional circulation especially during a drought or dry period. Dry soil induces an anticyclonic atmospheric circulation anomaly whilst wet soils enhance weak anticyclonic or cyclonic circulation especially over the northern parts of the region. The spatial organisation of changes in rain days and rainfall intensity may be heavily dependent on the synoptic forcing of the regional climate rather than the soil moisture perturbation.

Soil moisture perturbations mostly affect the lower troposphere. Surface variables analysed especially ground temperature show strong responses to the soil moisture perturbations under all synoptic forcings and is clearly linked to sensible and latent heat fluxes within the boundary layer. Thus, soil moisture perturbation affects the energy budget and its partitioning into latent and sensible heat flux within RegCM3 model. Rainfall characteristics are strongly influenced by large-scale synoptic circulations rather than a direct effect from soil moisture perturbations over southern Africa. However, a weak feedback with mixed responses that also depends on geography and climatology exists over the southwestern parts of the region.

References

Abiodun B.J. J.S. Pal, E.A. Afiesimama, W.J. Gutoswki and A Adedoyin, 2008: Simulation of the West African monsoon using RegCM3, Part II: impacts of deforestation and desertification. *Theor. Appl. Climatol.***93**: 245-261.

Adler, R., F., Huffman, G.J., A. Chang, R. Ferraro, P. Xie, J. Janowiak, B. Rudolf, U. Schneider, S. Curtis, D. Bolvin, A. Gruber, J. Susskind, P. Arkin, and E. Nelkin, 2003: The version-2 Global Precipitation Climatology Project (GPCP) monthly precipitation analysis (1979-Present), *J. Hydrometeor.*, **4**, 1147-1167.

Alfieri L, P Claps, P. D'Odorico, F Laio and T.M. Over, 2008: An analysis of the soil moisture feedback on convective and stratiform precipitation. *J. Hydrometeorol.,***9**(2): 280-291, doi: 10.1175/2007JHM863.1

Anthes, R.A, 1977: A cumulus parameterization scheme utilizing a one-dimensional cloud model, *Mon. Wea. Rev.* **105**: 270-286.

Atlas R.N., Wolfson and J. Terry, 1993: The effect of SST and soil moisture anomalies on GLA model simulations of the 1988 U.S. summer drought. *J. Climate*, **6**, 2034-2048.

Barry R. And R. Chorley, 2009: Atmosphere, weather and climate. Routledge; 9 edition 536**pp.**

Beljaars A.C.M.P., P. Virtebo, M.J. Miller and A.K. Betts, 1996: The anomalous rainfall over the United States during July 1993: Sensitivity to land surface parameterization and soil moisture anomalies. *Mon. Wea. Rev.,* **124**, 362-382.

Betts A.K., J.H. Ball, A.C.M. Beljaars, M.J. Miller and P. Virtebo, 1994: Coupling between land surface, boundary-layer parameterizations and rainfall on local and regional scales: Lessons from the wet summer of 1993, in *Fifth Conference on Global Change Studies*. *Amer. Meteorol. Soc.,* 174-181.

Betts A.K., J. H. Ball, A. C. M. Beljaars, M. J. Miller, and P. A. Virtebo, 1996: The land surface-atmosphere interaction: A review based on observational and global modeling perspectives. *J. Geophys. Res.,* **101, 7209**-7226.

Bromwich D.H. and R.L. Fogt, 2004: Strong trends in the skill of the ERA-40 and NCEP-NCAR reanalyses in the high and midlatitudes of the southern hemisphere, 1958-2001. *J. Climate,***17**: 4603-4619.

Buckle C, 1996: Weather and climate in Africa. Longman, Harlow 312**pp.**

Ceballos, A., K. Scipal, W. Wagner, J. Martinez-Fernandez, 2005: Validation and downscaling of ERS Scatterometer derived soil moisture data over the central part of the Duero Basin, Spain, *Hydrological Processes*, **19**, 1549-1566, doi:10.1002/hyp.5585

Charney J, G.P.H. Stone and W.J. Quirk, 1977: Drought in the Sahara: A biogeophysical feedback mechanism. *Science*, **187**, 434-435.

Chen F. and R. *Avissar*, 1994: The impact of land-surface wetness heterogeneity on mesoscale heat fluxes, *J. Appl. Meteorol.***33**, 1323–1340.

Cheng Q., C. Ko, Y. Yuan, Y. Ge, S. Zhang (2006) GIS modeling for predicting river runoff volume in ungauged drainages in the Greater Toronto Area, Canada. *Computers & Geosciences***32**: 1108-1119.

Cook B.I., G.B. Bonan and S. Levis, 2006: Soil moisture feedbacks to precipitation over southern Africa. *J. Climate,* **19**, 4198-4206.

Cook C., C.J.C. Reason and B.C. Hewitson, 2004: Wet and dry spells within particularly wet and dry summers in the South African summer rainfall region. *Clim. Res.* **26**:17-31.

Crane R.G. and B.C. Hewitson, 1998: Doubled CO_2 precipitation changes for the Susquehanna Basin: Downscaling from the Genesis general circulation model. *Int. J. Climatol.***18**: 65-76.

Crétat J., C. Marcon, B. Pohl and Y Richard, 2011: Quantifying internal variability in a regional climate model: a case study for southern Africa. *Clim Dyn.* **37**: 1335-1356, doi: 10.1007/s00382-011-1021-5.

Crétat J., B. Pohl, Y Richard and P. Drobinski, 2012: Uncertainties in simulating regional climate of southern Africa: sensitivity to physical parameterizations using WRF. *Clim Dyn.* **38**: 613-634. Doi 10.1007/s00382-011-1055-8.

Cunnington C., and P.R. Rowntree, 1986: Simulations of the Saharan atmosphere-dependence on moisture and albedo. *Quart. J. Roy. Meteor. Soc.*, **112**: 971-999.

D'Odorico, P. and A. Porporato, , 2004: Preferential states in soil moisture and climate dynamics. *Proc. Natnl. Acad. Sci. U.S.A.*, **101**: 8848-8851, 10.1073/pnas.0401428101.

Deardoff J.W., 1978: Efficient prediction of ground surface temperature and moisture with inclusion of a layer of vegetation. *J. Geophys. Res.,***83**, 1889-1903.

Delworth T., and S. Manabe, 1988a: The influence of potential evaporation on the variabilities of simulated soil wetness and climate. *J. Climate*, **1**, 183-203

Delworth T., and S. Manabe, 1988b: The influence of soil wetness on near-surface atmospheric variability. *J.Climate,***2**, 1447-1462.

Delworth T., and S. Manabe, 1993: Climate variability and land-surface processes. *Advances in Water Resources,* **16**: 3-20.

De Ridder K., 1999: The impact of surface evaporative fraction on boundary layer equivalent potential temperature. *Phys. Chem. Earth (B),* **24**(6): 615-618.

Dickinson R.E., P.J Kennedy, A. Henderson-Sellers and, M Wilson, 1986: Biosphere-Atmosphere Transfer Scheme (BATS) for the NCAR Community Climate Model, *Tech. Rep. TN-275+STR*, NCAR, Boulder, Colorado.

Dickinson R.E., R. M. Errico, F. Giorgi, and G. T. Bates, 1989: A regional climate model for the western United States. *Climatic Change,* **15**: 383–422.

Dickinson, R.E., A. Henderson-Sellers and P.J Kennedy, 1993: Biosphere-Atmosphere Transfer Scheme (BATS) version 1E as coupled to the NCAR Community Climate Model, *Tech. Rep.TN-275+STR*, NCAR, Boulder, Colorado. **pp**72.

Dorigo W. And co-authors, 2011: A new international network for in situ soil moisture data. Eos,Vol. 92, No. 17, 141-142.

Drew G, 2004: Modelling vegetation dynamics and their feedbacks over southern Africa in response to climate change forcing. *PhD Thesis. University of Cape Town*. Cape Town, South Africa, 253**pp.**

Eltahir E.A.B. and J. Pal, 1996: Relationship between surface conditions and subsequent rainfall in convective storms. *J. Geophys. Res.,* **101**, D21, 26, 237-245.

Eltahir E.A.B. 1998. A soil moisture-rainfall feedback mechanism. 1. Theory and Observations. *Water Resourc. Res.***34:** 765-776.

Emanuel K.A., 1991: A scheme for representing cumulus convection in large-scale models, *J. Atmos. Sci.*, **48**(21), 2313-2335.

Emanuel K.A., and M. Zivkovic-Rotman, 1999: Development and evaluation of a convection scheme for use in climate models, *J. Atmos. Sci.*, **56**, 1766-1782.

Endris H.S and co-authors, 2013: Assessment of the performance of CORDEX regional climate models in simulating east African rainfall. J. Climate, **21**: 8453-8475.

Engelbrecht F.A., J.L. McGregor and C.J. Engelbrecht, 2009: Dynamics of the conformal-cubic atmospheric model projected climate-change signal over southern Africa. *Int. J. Climatol.* **29:** 1013−1033.

Entekhabi D., I. Rodriguez-Iturbe, and R.L. Bras, 1992: Variability in Large-Scale Water Balance with Land Surface-Atmosphere Interaction. *J. Climate*, **5**, 798–813.

Farah H.O., W.G.M. Bastiaanssen and R.A. Feddes, 2004: Evaluation of the temporal variability of the evaporative fraction in a tropical watershed. *Int. J.Appl. Earth. Obs. Geoinfo.,* **5**:129-140.

Fauchereau N., M. Trzaska, M. Rouault and Y. Richard, 2003: Rainfall Variability and Changes in Southern Africa during the 20th Century in the Global Warming Context. *Natural Hazards* **29**: 139-154.

Fennessy M. J., and J. Shukla, 1999: Impact of initial soil wetness on seasonal atmospheric prediction. *J. Climate,* **12,** 3167–3180.

Findell and E.A.B. Eltahir, 1999: Analysis of the pathways relating soil moisture and subsequent rainfall in Illinois. *J. Geophys. Res.***104** (D24): 31, 565-31, 574.

Fischer E.M., S.I. Seneviratne, P. L. Vidale, D. Lüthi, and C. Schär, 2007: Soil moisture atmosphere interactions during the 2003 European summer heat wave, *J. Climate*, **20**: 5081-5098. DOI: 10.1175/JCLI4288.1.

Fritsch J.M. and C.F. Chappell, 1980: Numerical prediction of convectively driven mesoscale pressure systems. Part I: Convective paramerization, *J. Atmos. Sci*. **33**: 725-735.

Foley J., I. Prentice, N. Ramankutty, S. Levis, D. Pollard, S. Sitch and A. Haxeltine, 1996: An integrated biosphere model of land surface processes, terrestrial carbon balance, and vegetation dynamics. *Global Biogeochem. Cycles*, **10**(4), 603–628, doi:10.1029/96GB02692.

Gbobaniyi E. And co-authors, 2013: Climatology, annual cycle and interannual variability of precipitation and temperature in CORDEX simulations over West Africa. *Int. J. Climatol.*, doi: 10.1002/joc.3834.

Gentine P., D. Entekhabi, A. Chehbouni, G. Boulet and B. Duchemin, 2007: Analysis of evaporative fraction diurnal behaviour. *Agricultural and Forest Meteorol.,***143** (2007) 13–29.

Giorgi F., 1990: Simulation of regional climate using a limited area model nested in a general circulation model. *J. Climate*, **3**: 941–963.

Giorgi F., L.O. Mearns, C. Shields and L. Mayer, 1996: A regional model study of the importance of local versus remote controls of the 1988 drought and the 1993 flood over the central United States. *J. Climate*, **9**, 1150-1162.

Giorgi F. and X. Bi, 2000: A study of internal variability of a regional climate model. *J Geophys Res* **105:** 503–529.

Giorgi F., R. Francisco and J.S. Pal, 2003: Effects of a subgrid-scale topography and land use scheme on the simulation of surface climate and hydrology. Part 1: Effects of temperature and water vapour disaggregation, *J. Hydrometeorol.*, **4**, 317-333.

Giorgi F, Coppola E, Solmon F, Mariotti L and others 2012: RegCM4: Model description and preliminary tests over multiple CORDEX domains. *Clim Res.,* **52**:7–29.

Gbobaniyi E. And co-authors, 2013: Climatology, annual cycle and interannual variability of precipitation and temperature in CORDEX simulations over West Africa. *Int. J. Climatol.*, doi: 10.1002/joc.3834.

Goddard L. and N.E. Graham, 1999: Importance of the Indian Ocean for simulating rainfall anomalies over eastern and southern Africa. *J. Geophys. Res.***104**: 19099-19116.

Goddard L., S.J. Mason, S.E. Zebiak, C.F. Ropelewski, R. Bashed and M.A. Cane, 2001: Current approaches to seasonal-to-interannual climate predictions. *Int. J. Climatol.* **21**:1111-1152.

Grell G.A., 1993: Prognostic evaluation of assumptions used by cumulus parameterizations, *Mon. Weath. Rev*. **121**: 764-787.

Grimm A.M, J.S. Pal and F. Giorgi, 2007: Connection between spring conditions and peak summer monsoon rainfall in south America: Role of soil moisture, surface temperature and topography in eastern Brazil. *J. Climate*, **20**, 5929-5945.

Haagenson P., S. Chen and D. Gill, 1989: Penn State/NCAR Mesoscale Model users manual-Version **8,** *NCAR Tech. Rep***.,** 39**pp.**

Haga H, Y. Matsumoto, J. Matsutani, M. Fujita, K. Nishida and Y. Sakamoto, 2005: Flow paths, rainfall properties and antecedent soil moisture controlling lags to peak discharge in a granitic unchanneled catchment. *Water Resour. Res.*, **41**, W12410, doi: 10.1029/2005WR004236.

Hewitson B.C., 1994: Neural computing: applications in geography. *Kluwer Academic Publishers*, 194 **pp**.

Hewitson B.C. and R.G. Crane, 1996: Climate downscaling: techniques and application. *Clim Res*. **7**: 85-95.

Hewitson B.C. and R.G. Crane, 2002: Self–organizing maps: applications to synoptic climatology. *Clim Res***8**: 13-26.

Hewitson B.C., 2004: Spatially cohesive changes in precipitation over South Africa, *9th International Conference on Statistical Climatology*, Cape Town, South Africa.

Hewitson B.C., J. Darron, R.G. Crane, M.F. Zermoglio and C. Jack, 2013: Interrogating empirical-downscaling. *Climatic Change*, doi: 10.1007/s10584-013-1021-z.

Holtslag A.A.M., E.I.F. de Bruijn, and H.L. Pan, 1990: A high resolution airmass transformation model for short-range weather forecasting. *Mon. Wea. Rev.*, **118**: 1561–1575.

Hohenegger C., P. Brockhaus, C.S. Bretherton, C. Schär, 2009: The Soil Moisture–Precipitation Feedback in Simulations with Explicit and Parameterized Convection. *J. Climate*, **22**, 5003–5020.

Hudson D.A., Antarctic sea-ice extent, southern hemisphere circulation and South African rainfall. *PhD Thesis, University of Cape Town*, South Africa, 308**pp**.

Hulme M., R. Doherty, T. Ngara, M. New and D. Lister, 2001: African climate change: 1900–2100. *Clim. Res*. **17**:145-168.

Huffman, G.J., R.F. Adler, D.T. Bolvin, G. Gu, 2009: Improving the Global Precipitation Record: GPCP Version 2.1. *Geophys. Res. Lett.*, **36**, L17808, doi:10.1029/2009GL040000.

IPCC Fourth Assessment Report: Climate Change 2007, **pp**104.

Idso S, R. Jackson, R. Kimball and F. Nakayama, 1975: The dependence of bare soil albedo on soil water content. *J. Appl. Meteor*., **14**: 109-113.

Jack C., 2013: The moisture sources and development of a Lagrangian model over southern Africa. *PhD Thesis. University of Cape Town*. Cape Town, South Africa, 160**pp.**

Jaeger, E.B., and S.I. Seneviratne, 2011: Impact of soil moisture-atmosphere coupling on European climate extremes and trends in a regional climate model. **36**(9-10), 1919-1939, doi: 10.1007/s00382-010-0780-8.

Jury M.R., 1992: A climatic dipole governing the interannual variability of convection over the SW Indian Ocean and SE Africa region. *Trends in Geophysical Research*. **1**: 165-172.

Jury M. 1996: Regional Teleconnection patterns associated with Summer Rainfall over South Africa, Namibia and Zimbabwe. *Int. J. Climatol.,***16**: 135-153.

Jury M.R. and B. Pathack, 1993: Composite climatic patterns associated with the extreme modes of summer rainfall over southern Africa: 1975-1984. *Theor. Appl. Climatol.* **47:** 137-145.

Kållberg P., 1997: An overview of ERA-40 analyses, ECMWF, Reading, U.K.

Kalnay E., and Co-authors, 1996: The NCEP/NCAR 40-Year Reanalysis Project. *Bull. Amer. Meteor. Soc.*, **77**: 437-471.

Kalognomou E. And co-authors, 2013: A diagnostic evaluation of precipitation in CORDEX models over southern Africa. J. Climate, **26**: 9477-9506.

Kgatuke M.M., W.A. Landman, A. Beraki and M.P. Mbedzi, 2008: The internal variability of the RegCM3 over South Africa. *Int J. Climatol.* **28**: 505−520.

Kiehl J.T., J.J. Hack, G.B. Bonan, B.A. Boville, B.P. Breigleb, D. Williamson and P. Rasch, 1996: Description of the near community climate model (CCM3), *Tech.Rep. NCAR/TN-420+STR*, National Center for Atmospheric Research.

Kim, J. and S. Hong, 2007: Impact of Soil Moisture Anomalies on Summer Rainfall over East Asia: A Regional Climate Model Study. *J. Climate.***20**: 5732-5743.

Kistler, R., and Co-authors, 2001: The NCEP/NCAR 50-Year Reanalysis: Monthly means CD-ROM and documentation. *Bull. Amer. Meteor. Soc*. **82**: 247-267.

Kohonen, T., 1995: Self-Organising Maps. *Springer, Berlin.* 362 **pp**

Koster, R.D. and Co-authors, 2000: Variance and predictability of precipitation at seasonal-to-interannual timescales. *J. Hydrometeorol*., **1**: 26-46.

Koster, R.D. and M.J. Suarez, 2001: Soil moisture memory in climate models. *J. Hydrometeorol*., **2**(6): 558-570.

Koster, R.D., and M.J. Suarez, 2004: Suggestions in the observational record of land–atmosphere feedback operating at seasonal time scales. *J. Hydrometeor.,* **5,** 567–572.

Koster, R.D. and Co-authors, 2004a: Regions of strong coupling between soil moisture and precipitation. *Science*, **305**: 1138-1140.

Koster, R.D. and Co-authors, 2004b: Realistic initialization of land surface states: Impacts on subseasonal forecast skill. *J. Hydrometeorol.,* **5**: 1049-1063.

Koster, R. Dand Co-authors, 2006: GLACE: The Global Land-Atmosphere Coupling Experiment. Part 1: Overview, *J. Hydrometeorol*., **7**(4): 590-610.

Kunstmann H. and G. Jung, 2003: Investigation of feedback mechanisms between soil moisture, landuse and precipitation in West Africa. *Water Resources Systems-Water Availability and Global, IAHS* Publ. **280**: 149-159.

Landman W.A. and S.J. Mason, 1999: Change in the association between Indian Ocean sea surface temperatures and summer rainfall over South Africa and Namibia. *Int. J. Climatol.,***19**: 1477-1492.

Landman W.A., S.J Mason, P.D. Tyson and W.J. Tennant, 2001: Retroactive skill of multi-tiered forecasts of summer rainfall over southern Africa. *Int. J. Climatol*. **21**:1-19.

Landman, W. A., and A. Beraki, 2010: Multi-model forecast skill for mid-summer rainfall over southern Africa. *International Journal of Climatology*, DOI: 10.1002/joc.2273.

Lhomme J.P and E. Elguero, 1999: Examination of evaporative fraction diurnal behaviour using a soil vegetation model coupled with a mixed-layer model. *Hydrol. Earth System Sciences,***3**(2): 259-270.

Lin, X, Randall D.A and Fowler L.D, 2000: Diurnal variability of the hydrologic cycle and radiative fluxes comparisons between observations and a GCM. *J. Climate*, **13(**23):4159-4179.

Lindesay J.A., 1998: Climates of the Southern Continents: Present, Past and Future. *John Wiley and Sons Ltd.* 5-62, 265-292**pp**.

Loveland, T. R., B. Reed, D. O. Ohlen, J. Zhu, , L. Yang, and J. Merchant, 2000: Development of a global land cover characteristics database and IGBP DISCover from 1-km AVHRR data, *Int. J. Remote Sensing*, **21**(6/7), 1303-1330.

Mackellar N. 2007: Simulating the effects of land-surface change on southern Africa's climate. Africa. *PhD Thesis, University of Cape Town*, South Africa, 110**pp**.

Mackellar N, M.A Tadross and B.C. Hewitson, 2009: Effects of vegetation map change in MM5 simulations of southern Africa's summer climate. *Int. J. Climatol.,***29**: 885-898.

Mackellar N, M. Tadross and B. Hewitson, 2010: Synoptic-based evaluation of climatic response to vegetation change over southern Africa. *Int. J. Climatol.,* **30**: 774-789.

Mahanama, S.P.P., and R.D. Koster, 2003: Intercomparison of soil moisture memory in two land surface models. *J. Hydrometeorol*., **4**: 1134-1146.

Mahanama, S.P.P., and R.D. Koster, 2005: AGCM biases in evaporation regime: Impacts on soil moisture memory and land-atmosphere feedback. *J. Hydrometeorol*., **6**: 656-669.

Makarau A., 1995: Intra-seasonal oscillatory modes of Southern Africa summer circulation. *PhD Thesis. University of Cape Town*. Cape Town, South Africa, 321**pp.**

Makarau A. and Jury M. 1997: Seasonal Cycle of Convective Spells over Southern Africa during Austral Summer. *Int. J. Climatol.***17:** 1317-1332.

Marshall G.J, 2003: Trends in the southern annular mode from observations and reanalyses. *Int. J. Climatol*. **16**: 4134-4143.

Mason S.J., J.A Lindesay and P.D. Tyson, 1994: Simulating drought over southern Africa using seas surface temperature variations. *Water SA***20**: 15-22.

Mason S.J. and L. Goddard, 2001: Probabilistic precipitation anomalies associated with ENSO. *Bull. of the Amer. Met. Soc.* **71**:300-309.

Matarira C.H. and A.A. Flocas, 1989: **"**Spatial and Temporal rainfall variability over southeastern central Africa during extremely dry and wet years**"** *J. Meteorol.* **14**: 3-9.

Matarira, C.H., 1990a: Drought over Zimbabwe in a Regional and Global Context. *Int. J. Meteorol.***10**: 609-625.

Matarira C. H., 1990b: Frequency and tracks of anticyclones and their effect on rainfall patterns over Zimbabwe. *Theor. Appl. Climatol.*, **42**, 53-66.

Matarira, C.H. and M.R Jury, 1992: Contrasting Meteorological Structure of intra-seasonal wet and dry spells in Zimbabwe, *Int. J. Climatol.* **12**: 165-176.

Mdoka M., 2003: The rainfall characteristics over Zimbabwe. *The Annual South African Society for Atmospheric Sciences (SASAS) Conference.* Pretoria, South Africa.

Mdoka M.L., 2005: Climatic Trends and Soil Moisture Feedbacks over Zimbabwe. *MSc Thesis, University of Cape Town*, South Africa, 123**pp**.

Mei R. and G. Wang, 2011: Summer land-atmosphere coupling strength in the United States: Comparison among observations, reanalysis data and numerical models. *J. Hydrometereol*. doi: 10.101175/JHM-D-11-075.1

Mitchell T.D and P.D. Jones, 2005: An improved method of constructing a database of monthly climate observations and associated high-resolution grids. *Int J. Climatol.* **25:** 693-712, doi: 10.1002/joc.1181.

Mintz, Y., 1984: The sensitivity of numerically simulated climates to land-surface boundary conditions. *The Global Climate,* J. Houghton, Ed., Cambridge University Press, 79–105.

Moufouma W and D.P. Rowell, 2009: Impact of soil moisture initialisation and lateral boundary conditions on regional climate model simulations of the West African Monsoon. *Clim Dyn*. **35:** 213-229, doi: 10.1007/s00382-009-0638-0.

Mulenga H.M., 1998: Southern Africa climatic anomalies, summer rainfall and the Angola low. *Phd Thesis. University of Cape Town*. Cape Town, South Africa.

Namias, J. 1988: Spring and summer 1988 drought over the contiguous United States: Causes and prediction. *J. Climate*, **4**, 54-65.

New M., M. Hulme and P.D. Jones, 1999: Representing twentieth-century space-time climate variability. Part I: Development of 1961-90 mean monthly terrestrial climatology. *J. Climate* **12:** 829-856.

New M., M. Hulme and P. Jones, 2000: Representing twentieth-century space-time climate variability. Part II: Development of 1901-1996 monthly grids of terrestrial surface climate. *J. Climate* **13**: 2217-2238.

New M., R. Washington, C. Jack and B. Hewitson, 2003: Sensitivity of southern Africa to soil-moisture. *Clivar Exchanges***8**(2/3):45-47.

Nichols W.E and R.H. Cuenca, 1993: Evaluation of the evaporative fraction for the parameterization of the surface energy balance. *Water Resourc. Res.***29**(11), 3681-3690.

Nicholson S.E., 1986: The spatial coherence of African rainfall anomalies: interhemispheric teleconnections. *J. Clim Appl. Met.***25**: 1365-1381.

Nicholson S.E., 2001: Climatic and environmental change in Africa during the last two centuries. *Clim. Res.* **17**:123-144.

Nikulin G and co-authors, 2012: Precipitation climatology in an ensemble of CORDEX-Africa regional climate simulations. *J. Climate,* **25**: 6057-6078, doi: 10.1175/JCLI-D-11-00375.1

Ogallo L.A., 1993: Dynamics of east African climate. *Proc. Indian Acad. Sci. (Earth Planet Sci.)***102**: 203-217.

Oglesby, R.J. 1991: Springtime soil moisture, natural climatic variability, and North American summertime drought. *J. Climate*, **5**, 66-92.

Paegle J., J. Nogues-Paegle and K.C. Mo, 1996: Dependence of simulated precipitation on surface evaporation during the 1993 United States summer floods. *Mon. Wea. Rev.*, **124**, 345-361.

Pal, J.S and Coauthors, 2007: The ICTP RegCM3 and RegCNET: Regional Climate Modeling for the Developing World. *Bull. of the Amer. Met. Soc*. **88**(9):1395-1409.

Pal, J.S, E. E. Small, and E. A. B. Eltahir, 2000: Simulation of regional scale water and energy budgets: Representation of subgrid cloud and precipitation processes within RegCM. *J. Geophys. Res*., **105**, 29 579–29 594

Pal J.S. and E.A.B Eltahir, 2001: Pathways relating soil moisture conditions to future summer rainfall within a model of the land-atmosphere system. *J. Climate***14**: 1227-1242.

Pal J.S. and E.A.B Eltahir, 2002: Teleconnections of soil moisture and rainfall during the 1993 Midwest summer flood. *Geophys. Res. Lett*. **29**, doi:10.129/2002GL1048/5.

Pal J.S. and E.B. Eltahir, 2003: A feedback mechanism between soil-moisture distribution and storm tracks. *Quart. J. Roy Met. Soc*.**129**: 2279-2297.

Petersen J.F., D. Sack and R.E. Gabler, 2010: Fundamentals of physical geography. *Belmont CA, Brooke/Cole-Cengage*, 479**pp.**

Reason C.J.C. and H. Mulenga, 1999: Relationships between South African rainfall and SST anomalies in the southwest Indian Ocean. *Int. J. Climatol*. **19**: 1651-1673.

Reason C. J. C., A. Jagadheesha and M. Tadross, 2003: A model investigation of inter-annual winter rainfall variability over southwestern South Africa and associated ocean-atmosphere interaction. *South African Journal of Science***99**: 75-80.

Richard Y, S. Trzaska, P. Roucou and M. Rouault, 2000: Modification of the southern African summer rainfall. Part 1: Relationships with air-sea interaction processes. *Clim. Dyn.***16**: 235-265.

Richard Y., N. Fauchereau, I. Poccard, M. Rouault and S. Trzaska, 2001: 20th century droughts in southern Africa – spatial and temporal variability, teleconnections with oceanic and atmospheric conditions. *Int. J. Climatol*. **21**:873-895.

Rocha A.M.C., 1992: The influence of global sea surface temperatures on southern African summer climate. *PhD Thesis*, *University of Melbourne*, Australia, 248**pp**

Rocha A. and I. Simmonds, 1997a: Interannual variability of south eastern African summer rainfall. Part I: relationships with air-sea interaction processes. *Int. J. Climatol.* **17**:235-265.

Rocha A. and I. Simmonds, 1997b: Interannual variability of south eastern African summer rainfall. Part II: modelling the impact of sea surface temperatures on rainfall and circulation. *Int. J. Climatol.* **17**:267-290.

Ropelewski C.F. and M.S. Halpert, 1987: Global and regional scale precipitation patterns associated with the El Niño/Southern Oscillation. *Mon. Weath. Rev.***115**: 1606-1626.

Ropelewski C.F. and M.S. Halpert, 1989: Precipitation patterns Associated with the high indices phase of the Southern Oscillation. *J. Climate* **2:** 268 – 284.

Rowell D. P. and R.G. Jones, 2006: Causes and uncertainty of future summer drying over Europe. *Clim. Dyn.* **27**:281–299. doi: 10.1007/s00382-006-0125-9.

Rowntree P. R., and J. A. Bolton, 1983: Simulation of the atmospheric response to soil moisture anomalies over Europe. *Quart. J. Roy. Meteor. Soc.,* **109,** 501–526.
Schär C., D. Lüthi, U Beyerle and E. Heise, 1999: The soil-precipitation feedback: A process study with a regional climate model. *J. Climate*, **12**: 1487-1494.

Seth A. and F. Giorgi, 1998: the effects of domain choice on summer precipitation simulation and sensitivity in a regional climate model. *J. Climate,* **11***:* 2698-2712.

Seneviratne S. I., D. Lüthi, M. Litschi, and C. Schär, 2006a: Land atmosphere coupling and climate change in Europe, *Nature*, **443**(7108): 205– 209, doi:10.1038/nature05095.

Seneviratne S.I, R.D. Koster, Z. Guo, P.A. Dirmeyer, E Kowalczyk, D. Lawrence, P. Liu, C Lu, D. Mocko, K.W. Oleson and D Verseghy, 2006b: Soil moisture memory in AGCM simulations: Analysis of Global Land-Atmosphere Coupling Experiment (GLACE) Data. *J. Hydrometeorol.,***7**: 1090-1111.

Seneviratne S.I., T. Corti. E.L. Davin, M. Hirshi, E.B. Jaeger, I. Lehner, B. Orlowsky and A.J. Teuling 2010: Investigating soil moisture-climate interactions in a changing climate: A review. *Earth-Science Reviews* **99**, 125-161.

Shukla, J., and Y. Mintz, 1982: Influence of Land-surface evapotranspiration on the Earth's climate. *Science*, **215**, 1498-1501.

Steiner A.L, J.S. Pal, S.A. Rauscher, J.L. Bell, N.S. Diffenbaugh, A. Boone, L. Sloan and F. Giorgi, 2009: Land surface coupling in regional climate simulations of the west African monsoon. *Clim. Dyn.***33**(6): 869-892. Doi: 10.1007/s00382-009-0543-6.

Stern M.E. and J.S.Malkus, 1953: The flow of a stable atmosphere over a heated island. *J. Meteorol*., **10**, 105-120.

Storch V.H. and F. Zwiers, 1999: Statistical analysis in climate research. *Cambridge Univ. Press*., 484**pp**.

Sylla M.B., E. Coppola, L. Mariotti, F. Giorgi, P.M. Ruti, A. Dell' Aquila, X. Bi 2010: Multiyear simulation of the African climate using a regional climate model (RegCM3) with the high resolution ERA-interim reanalysis. *Clim Dyn.,* **35**: 231–247.

Sylla M.B, F. Giorgi, and F. Stordal, 2012: Large-scale origins of rainfall and temperature bias in high-resolution simulations over Southern Africa. *Climate Res.,* **52**, 193–211.

Sylla M.B, F. Giorgi, E. Coppola, and L. Mariotti, 2013: Uncertainties in daily rainfall over Africa: Assessment of gridded observation products and evaluation of a regional climate model simulation. *Int. J. Climatol*., **33**, 1805–1817, doi:10.1002/joc.3551.

Tadross M.A., B.C. Hewitson and M.T. Usman, 2005a: The interannual variability of the onset of the maize growing season over South Africa and Zimbabwe. *J. Climate,***18**, 3356–3372.

Tadross M.A, W.J. Gutowski, B.C Hewitson, M. New and C. Jack, 2005b: MM5 simulations of internal change and diurnal cycle of southern African regional climate. *Theor. Appl. Climatol.,***86**: 63-80.

Tadross M., I. Oliveira, M. Mdoka, F.Tummon, G. Maure, N. MacKellar, N. Browne, O. Crespo, S. Hachigonta and B. Hewitson, 2010: Water Research Commission Project: Modelling the influence of vegetation, soil moisture and aerosols on early summer Southern African climate.*WRCReport No. 1681/1/10*, pp79.

Tangang, F.T., B.Tang, A.H. Monahan, and W.W. Hsieh, 1998: Forecasting ENSO events: a neural network - extended EOF approach. *J. Climate*, **11:** 29-41.

Taylor C.M, 2000: The influence of antecedent rainfall on Sahelian surface evaporation. *Hydrol Processes*, **14**:245-1259.

Taylor C.M. and D.B Clark, 2000: The diurnal cycle and African easterly waves: a land surface perspective. *Quart. J. Roy. Meteorol. Soc*., **127**:845-868.

Taylor C.M. and co-authors, 2011: New perspectives on land-atmosphere feedbacks from the African Monsoon Multidisciplinary Analysis. *Atmospheric Science Letters* **12**: 38-44

Tennant W.J. and B.C. Hewitson, 2002: Intra-seasonal rainfall characteristics and their importance to the seasonal prediction problem. *Int. J. Climatol.* **22**: 1033-1048.

Teuling, A. J., S. I. Seneviratne, C. Williams, and P. A. Troch (2006), Observed timescales of evapotranspiration response to soil moisture, *Geophys. Res. Lett.*, **33**, L23403, doi: 10.1029/ 2006GL028178.

Torma, Cs., E. Coppola, F. Giorgi, J. Bartholy and R. Pongrácz, 2011: Validation of a high resolution version of the regional climate model RegCM3 over the Carpathian Basin. *J. Hydrometeorol.*. 12. (No 1.), pp 84-100.

Torrance J.D. 1981: Climate handbook of Zimbabwe. *Zimbabwe Meteorological Services*, Harare, Zimbabwe. 222**pp**.

Troccoli A. and P Kållberg, 2004: Precipitation correction in the ERA-40 reanalysis. *ERA-40 Project Report Series***13**. **pp** 6.

Tummon F., F. Solomon, C. Liousse and M. Tadross, 2010: Simulation of the direct and semidirect aerosol effects on the southern Africa regional climate during the biomass burning season. *J. Geophys. Res.,* **115***,* D19206, doi 10.1029/2009/JD013738.

Tyson, P.D, 1986: Climatic change and variability in southern Africa, *Oxford University Press*, Cape Town.

Tyson, P.D. and R.A. Preston-Whyte, 2000: The weather and climate of southern Africa, *Oxford University Press*, Cape Town, 396**pp**.

Unganai L.S, 2002: Prediction of summer rainfall over Zimbabwe from ocean-atmosphere parameters. *PhD Thesis*. University of Witwatersrand, South Africa

Unganai, L.S. and S.J. Mason, 2001: Spatial characterisation of Zimbabwe summer rainfall during the period 1920-1996, South Africa. *J. Science***97**, 425-431

Unganai L.S. and S.J. Mason, 2002: Long-range predictability of Zimbabwe summer rainfall. *Int. J. Climatol., 22*: 1091-1103.

Uppala S., and co-Authors, 2005: The ERA-40 reanalysis. *Quart. J. Roy. Meteor. Soc*., **130**, 2961-3012.

Usman T.U. and C.J.C Reason, 2004: Dry spell frequencies and their variability over southern Africa. *Clim. Res*. **26:** 199-211.

Vidale P.L., D. Luthi, R. Wegmann, C. Schär 2007: European summer climate variability in a heterogeneous multi-model ensemble. *Clim. Change***81**:209–232.

Vigaud N., Y. Richard, M. Rouault and N. Fauchereau, 2009: Moisture transport between the South Atlantic Ocean and southern Africa: relationships with summer rainfall and associated dynamics. *Clim Dyn.* **32**: 113−123.

Viterbo, P., 1996, The representation of surface processes in general circulation models, European Centre for Medium-Range Weather Forecasts, Reading, UK, **pp**201.

Von Storch H and F.R. Zwiers 1999: Statistical Analysis in Climate Research. *Cambridge University Press,* 484 **pp**

Wagner W., K. Scipal, C. Pathe, D. Gerten, W. Lucht and B. Rudolf, 2003: Evaluation of the agreement between the first global remotely sensed soil moisture data with model and precipitation data, *J. Geophys. Res*.,**108**, No. D19, 4611, doi:10.1029/2003JD003663.

Walawege R.P, 2002: An examination of the spatially extensive heavy Precipitation Events over South Africa and the Associated Moisture Trajectories. *MSc Thesis. University of Cape Town*, Cape Town, South Africa.

Walker J. And P.R. Rowntree, 1977: The effect of soil moisture on circulation and rainfall in a tropical model, *Quart. J. Res. Meteorol. Soc*., **103**:29-46.

Wallace J.M and P.V. Hobbs, 2006: Atmospheric Science: an introductory survey. *Elsevier*, 483**pp**.

Washington R. and M. Todd, 1998: Tropical-Temperate links in southern African and Southwest Indian Ocean Satellite–derived Daily Rainfall. *Int. J. Climatol.* **19**: 1601-1616

Wetzel P.J., S. Argentini and A. Boone, 1996: Role of land surface in controlling daytime cloud amount: Two case studies in the GCIP-SW area. *J. Geophy. Res.,* **101**:D3: 7359-7370.

Wilks D.S. 2006: Statistical methods in the atmospheric sciences. *Elsevier*, 627**pp**.

Williams, C. J. R., and D. R. Kniveton, 2012: Atmospheric-land surface interactions and their influence on extreme rainfall and potential abrupt climate change over Southern Africa. *Climatic Change*, **112**: 981–996.

Winter J.M., E.A.B. Eltahir and J.S. Pal, 2009: Coupling of integrated biosphere simulator to regional climate model version 3. *J. Climate,* **22**(10): 2743-2757.

Wu W. and R.E. Dickinson, 2004: Time scales of layered soil moisture memory in the context of land-atmosphere interaction. *J. Climate*, **17**(14): 2752-2764.

Xie P. and P.A. Arkin, 1996: Analysis of global monthly precipitation using gauge observation, satellite estimates and numerical model predictions, *J. Climate*, **9**: 840-858.

Yeh T.C., R. T. Wetherald and S. Manabe, 1984: The effect of soil moisture on the short-term climate and hydrology change: A numerical experiment. *Mon. WeatherRev.*, **112:** 474–490

Zhang J. and W. Dong, 2009: Soil moisture influence on summertime surface air temperature over East Asia. *Theor. Appl. Climatol*. DOI 10.1007/s00704-009-0236-4.

Zhang, Q., H. Körnich, and K. Holmgren, 2013: How well do reanalyses represent the Southern African precipitation? *Clim Dyn*., **40**: 951–962.

Zheng X. and E.A.B Eltahir, 1998: A soil moisture-rainfall feedback mechanism. 2. Numerical Experiments. *Water Resourc. Res.,* **34:** 777-785.

Zwiers F.W and von Storch, 1995: Taking serial correlation into account in tests of the mean. *J. Climate*, 8:336-351.

Appendix A

Appendix A-1: Model Validation - Soil Moisture

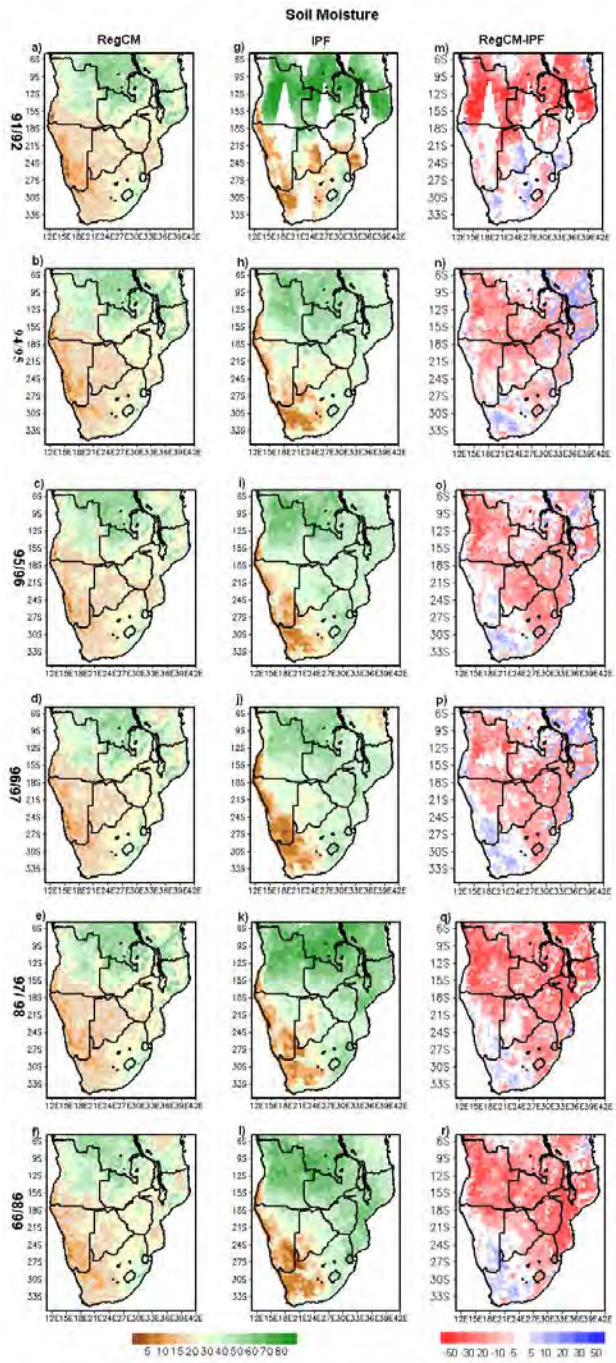

Figure A1. Comparisons of the RegCM3 soil moisture (mm/day) to the IPF total soil moisture data for the six simulations, RegCM3 (1st column), CRU (2nd column) and Bias (3rd column).

Appendix A-2: Model Validation - Total Precipitation

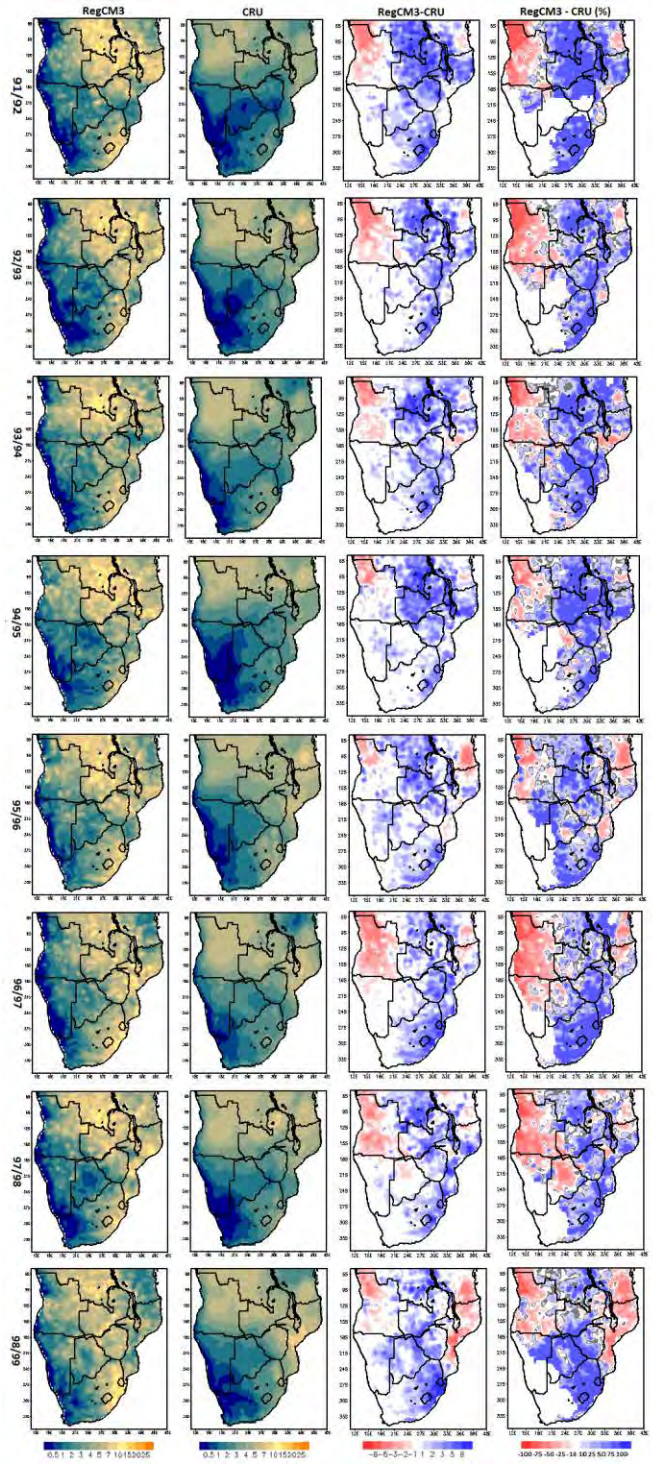

Figure A2. Comparisons of the mean precipitation (mm/day) for the RegCM3 to CRU dataset for the six simulations, RegCM3 (1st column), CRU (2nd column), Bias (3rd column) and %Bias (4th column).

Appendix A-3: Model Validation Air Temperature

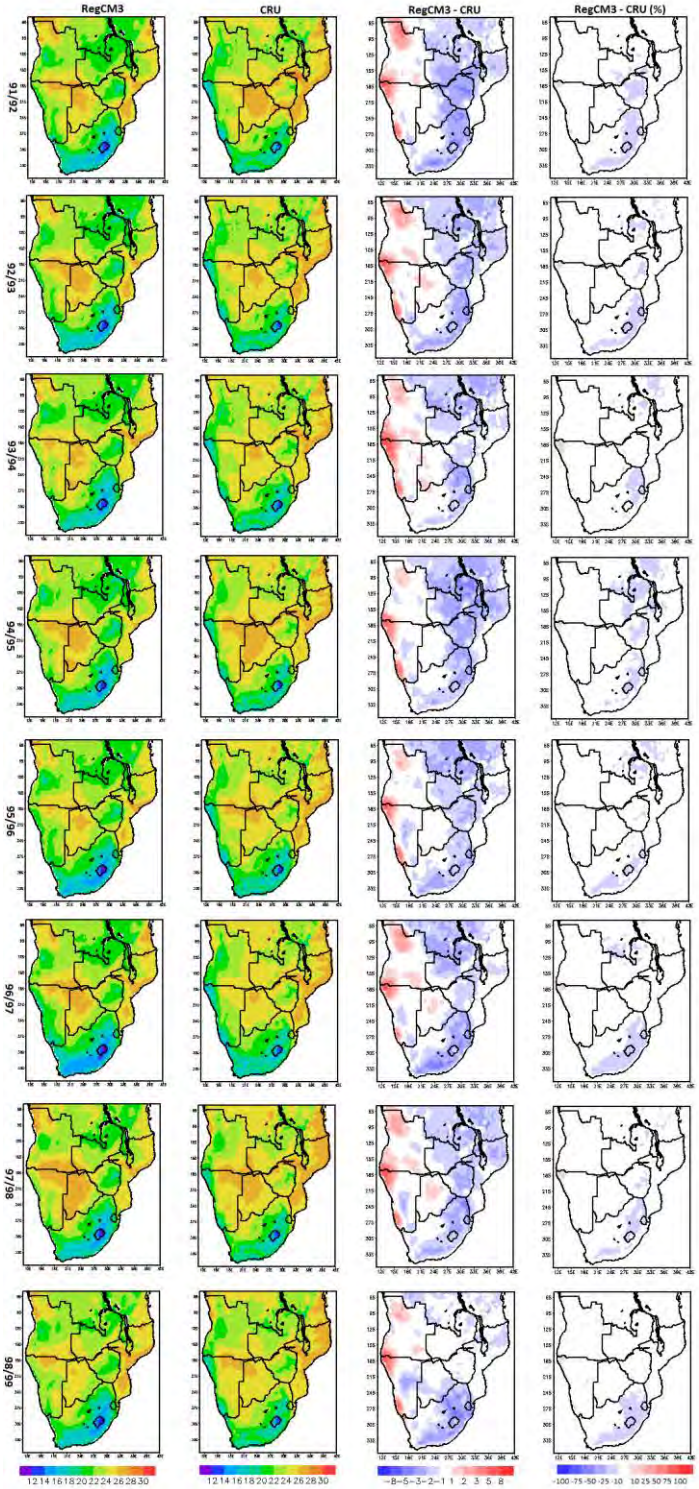

Figure A3. Comparisons of the mean air temperature (°C) for RegCM3 to CRU data for the six simulations, RegCM3 (1st column), CRU (2nd column), Bias (3rd column) and %Bias (4th column).

Appendix B

Appendix B-1: Total Rainfall

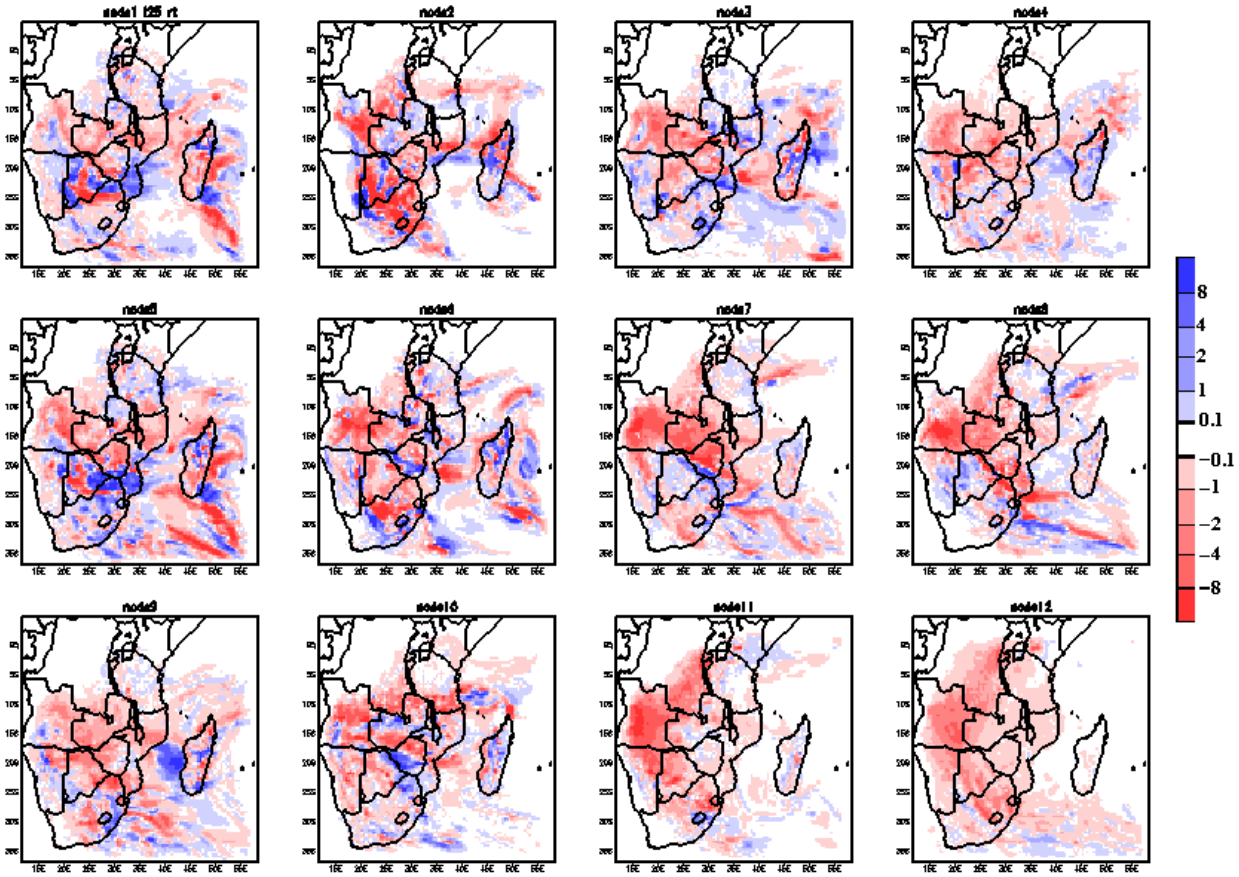

Figure B1. Total rainfall (mm) anomalies for the 4x3 nodes from the daily RegCM3 simulation of interactive at 25% field capacity of September 1991 to March 1992. Blue shading indicates increase in rainfall and red shading indicates decrease in rainfall.

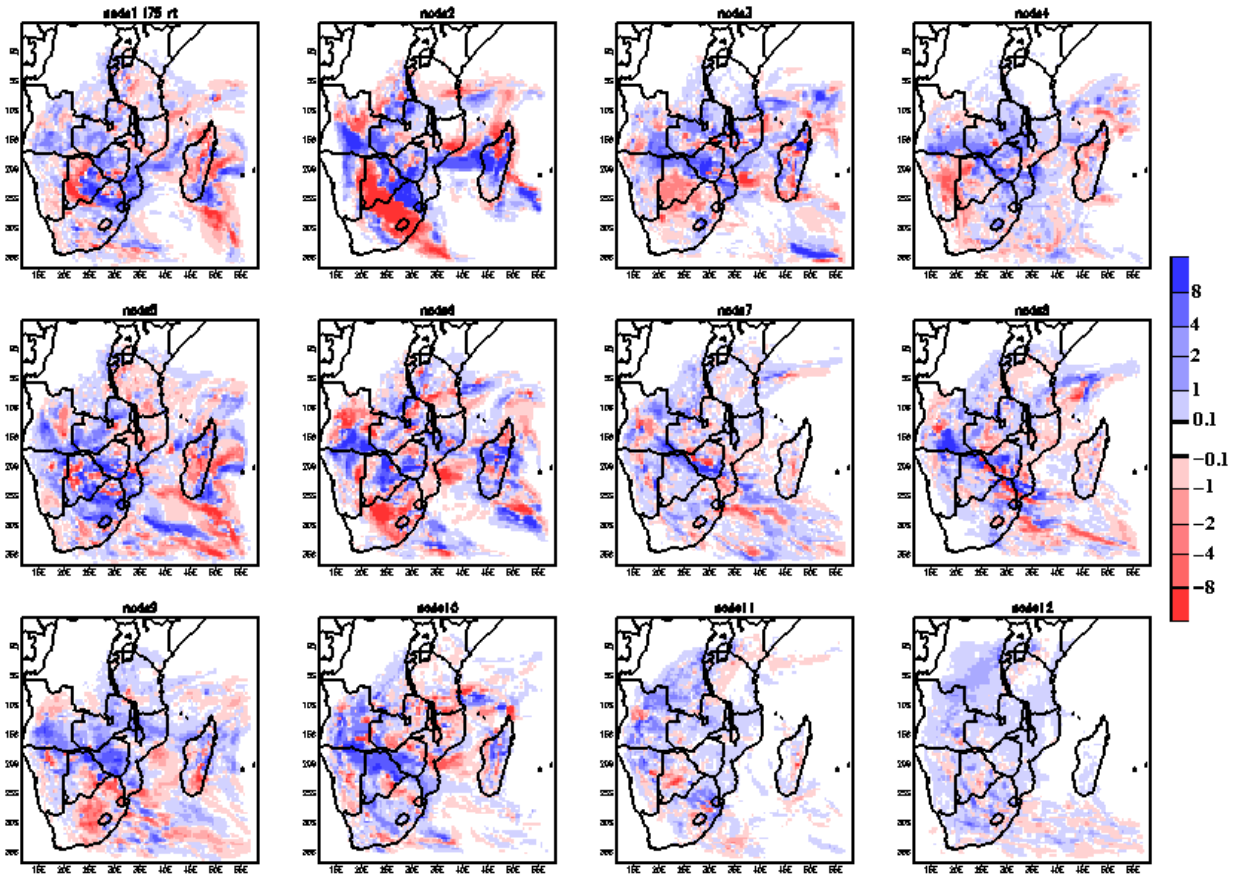

Figure B2. Total rainfall (mm) anomalies for the 4x3 nodes from the daily RegCM3 simulation of interactive at 75% field capacity of September 1991 to March 1992. Blue shading indicates increase inrainfall and red shading indicates decrease in rainfall.

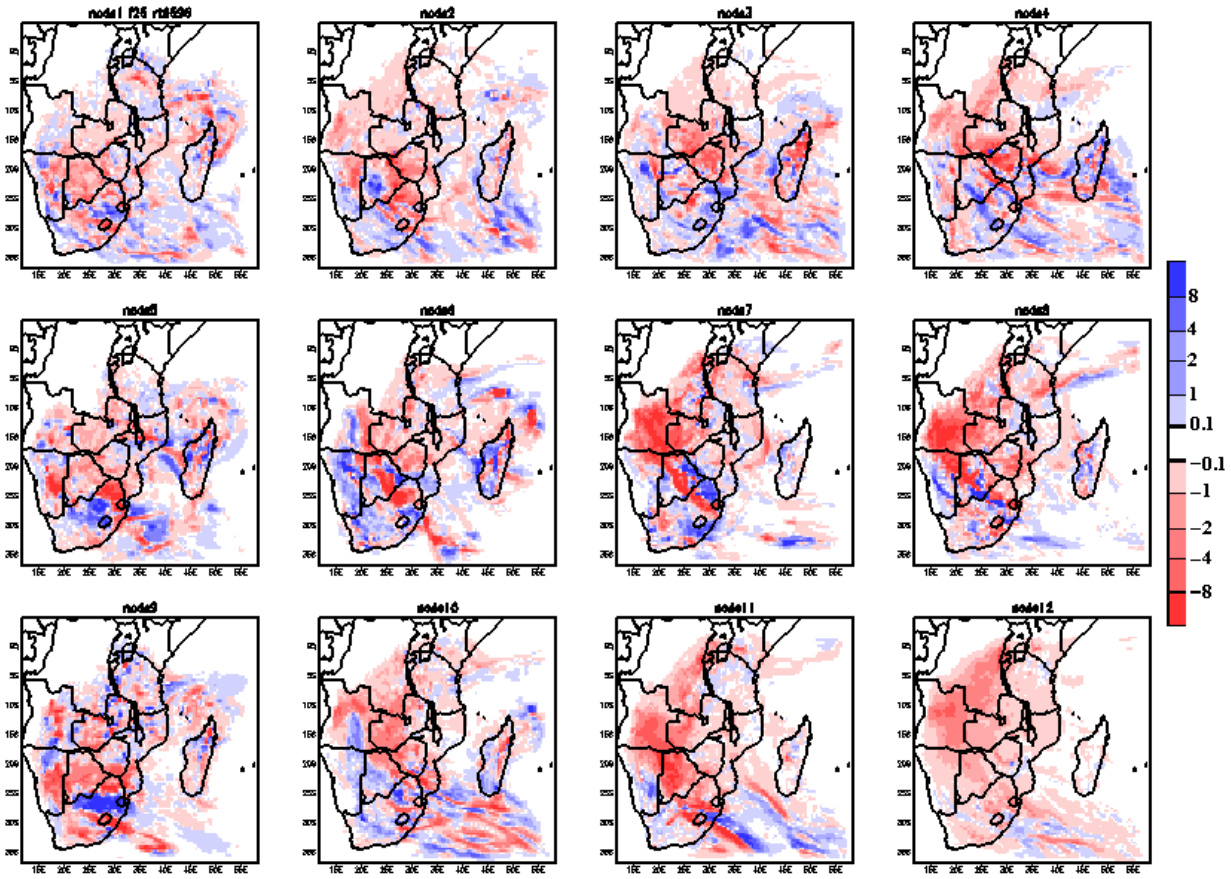

Figure B3. Total rainfall (mm) anomalies for the 4x3 nodes from the daily RegCM3 simulation of interactive at 25% field capacity of September 1995 to March 1996. Blue shading indicates increase inrainfall and red shading indicates decrease in rainfall.

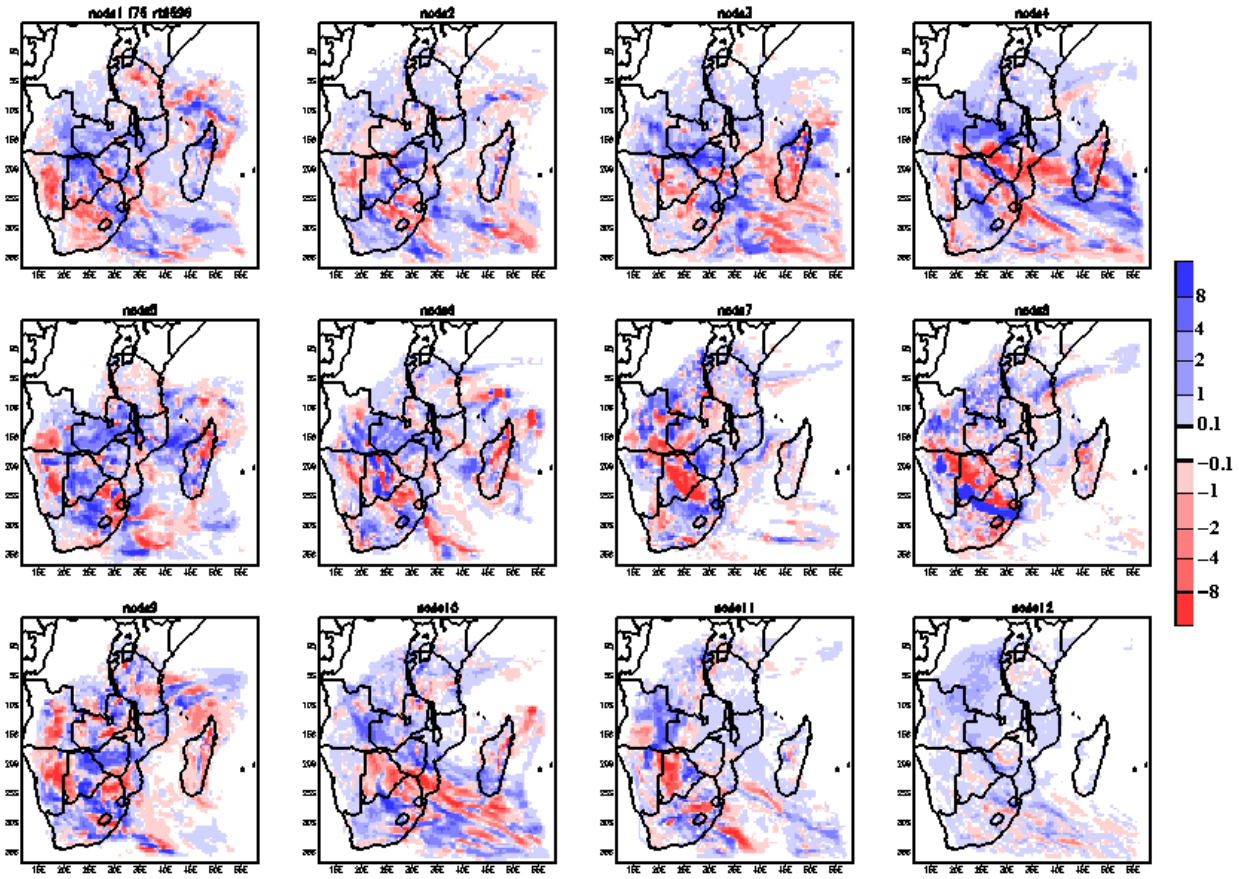

Figure B4. Total rainfall (mm) anomalies for the 4x3 nodes from the daily RegCM3 simulation of interactive at 75% field capacity of September 1991 to March 1992. Blue shading indicates positive temperature anomalies and red shading indicates negative temperatures.

Appendix B-2: Surface Temperature

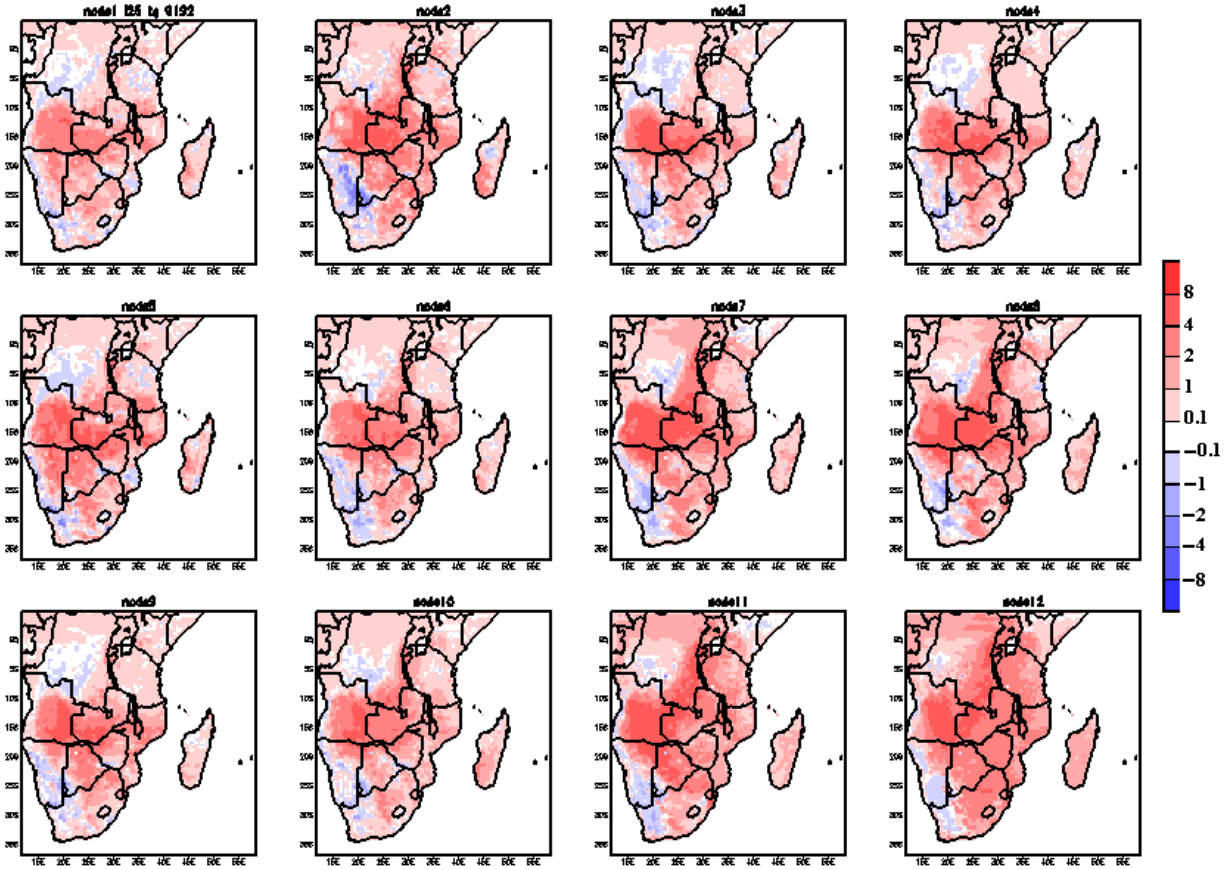

Figure B5. Surface temperature (°C) anomalies for the 4x3 nodes from the daily RegCM3 simulation of interactive at 25% field capacity of September 1991 to March 1992. Red shading indicates positive temperature anomalies and blue shading indicates negative temperatures.

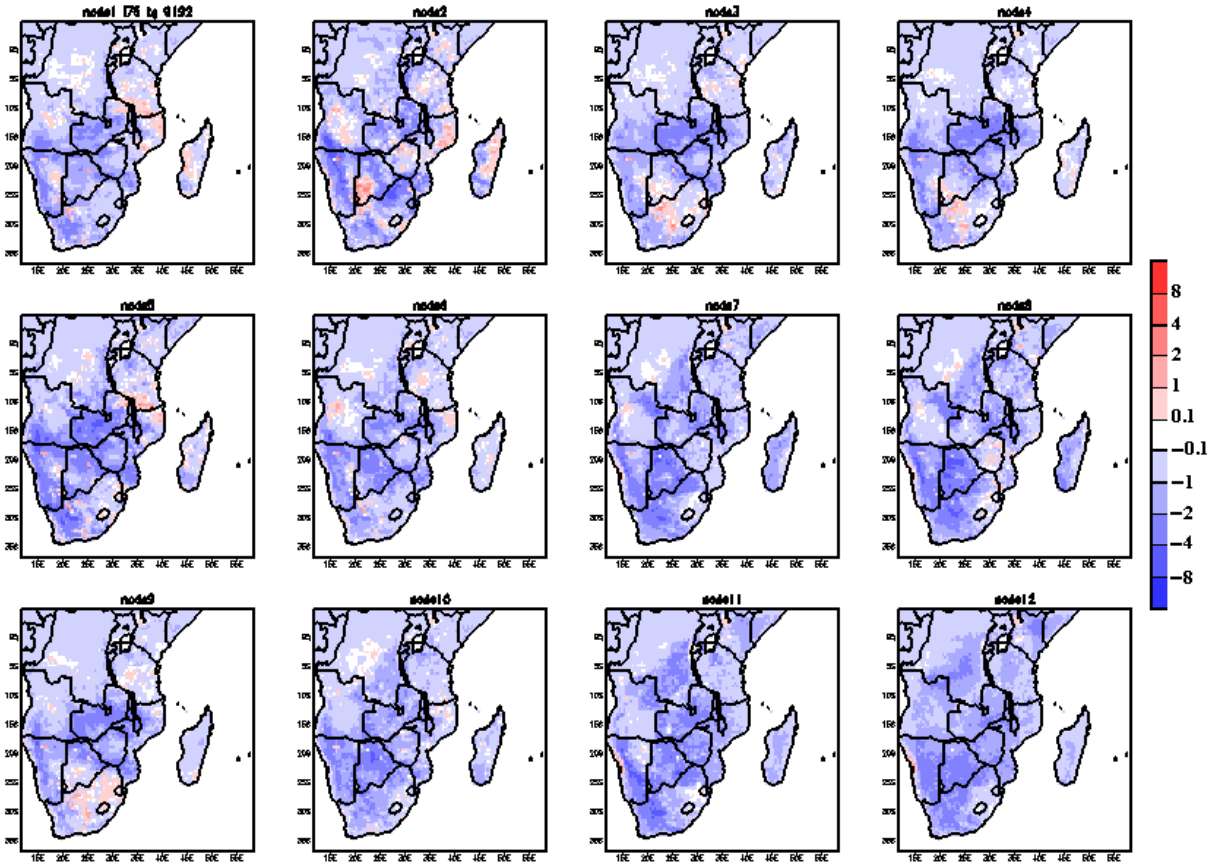

Figure B6. Surface temperature (°C) anomalies for the 4x3 nodes from the daily RegCM3 simulation of interactive at 75% field capacity of September 1991 to March 1992. Red shading indicates positive temperature anomalies and blue shading indicates negative temperatures.

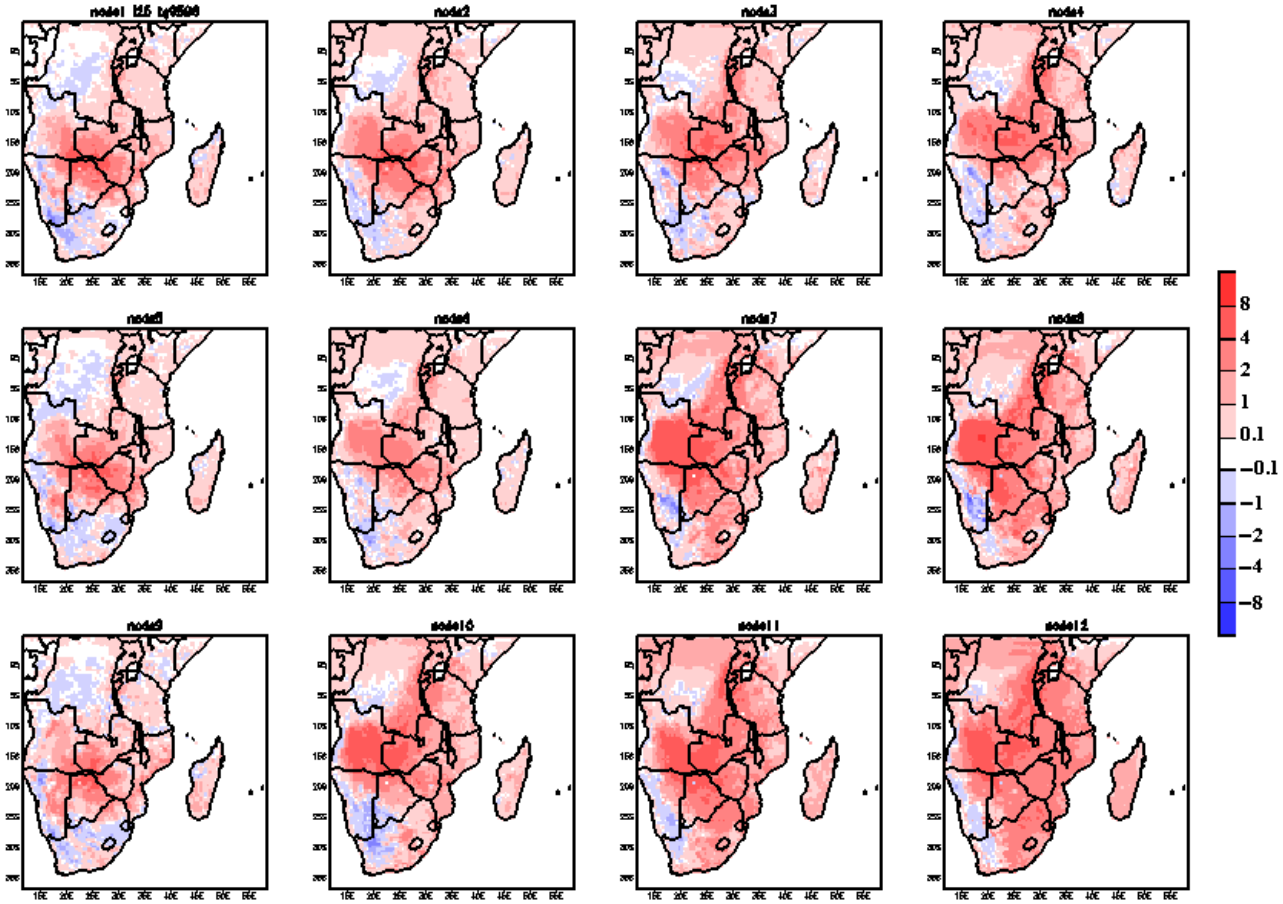

Figure B7. Surface temperature (°C) anomalies for the 4x3 nodes from the daily RegCM3 simulation of interactive at 25% field capacity of September 1995 to March 1996. Red shading indicates positive temperature anomalies and blue shading indicates negative temperatures. Red shading indicates positive temperature anomalies and blue shading indicates negative temperatures.

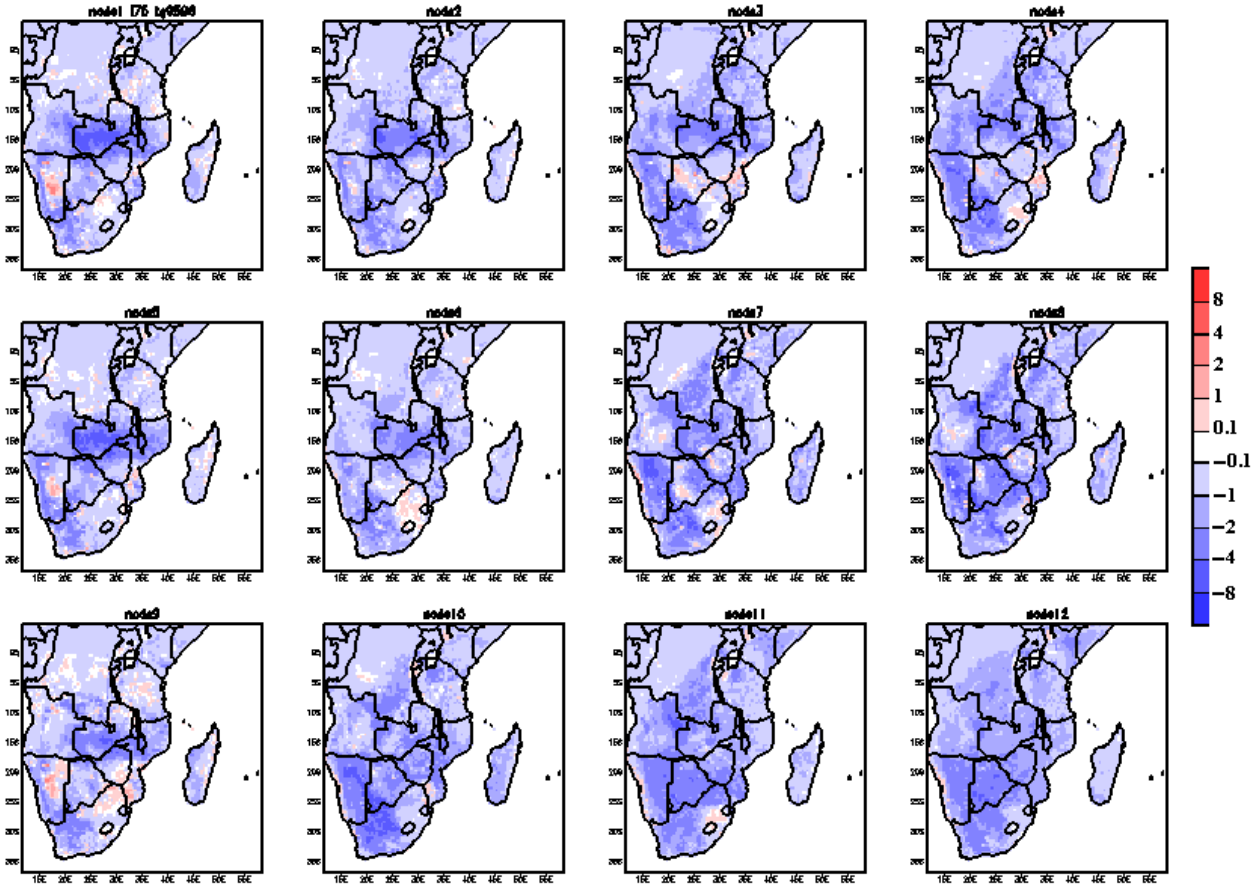

Figure B8. Surface temperature (°C) anomalies for the 4x3 nodes from the daily RegCM3 simulation of interactive at 75% field capacity of September 1995 to March 1996. Red shading indicates positive temperature anomalies and blue shading indicates negative temperatures.

Appendix B-3: Sensible Heat Flux

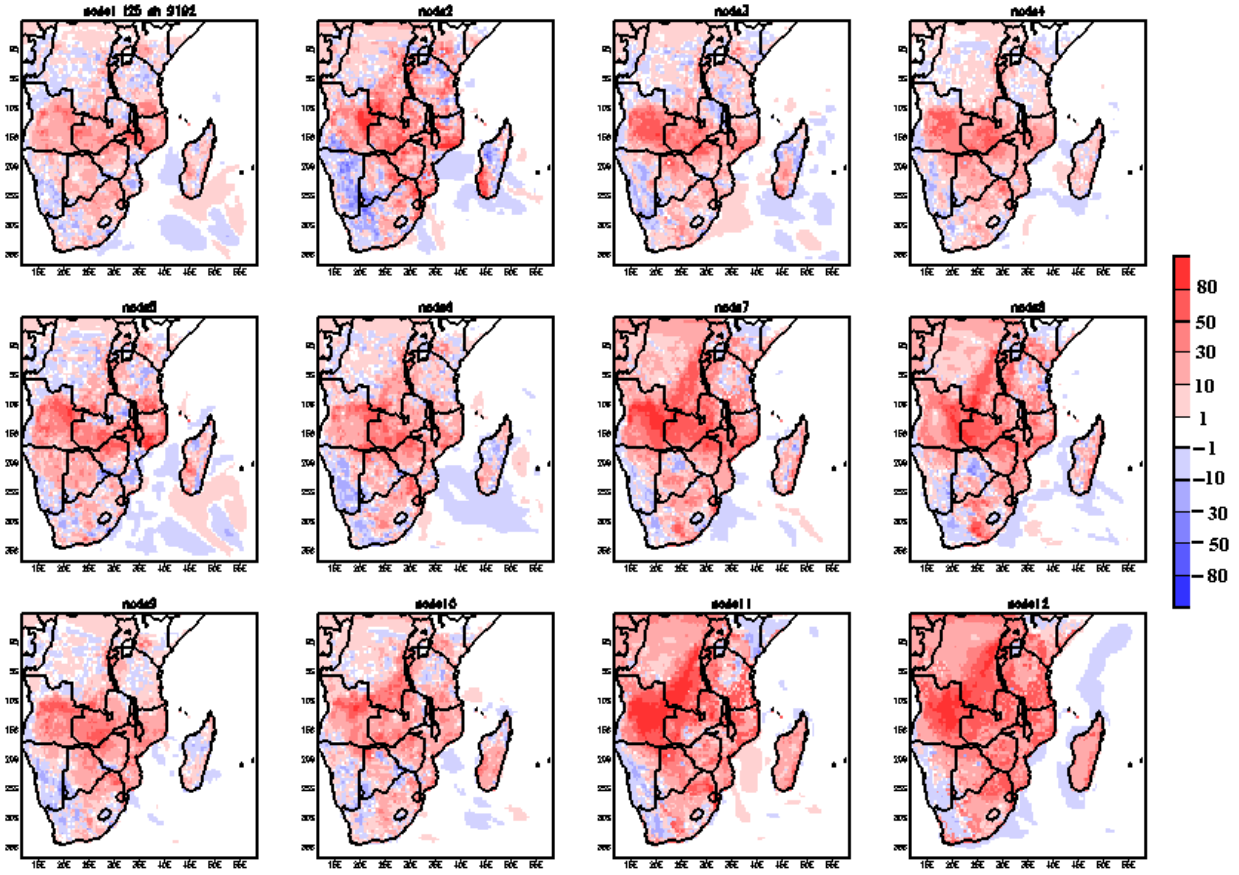

Figure B9. Sensible heat flux anomalies (W/m^2) for the 4x3 nodes from the daily RegCM3 simulation of interactive at 25% field capacity of September 1991 to March 1992. Red shading indicates positive sensible heat flux anomalies and blue shading indicates negative sensible heat flux anomalies.

`

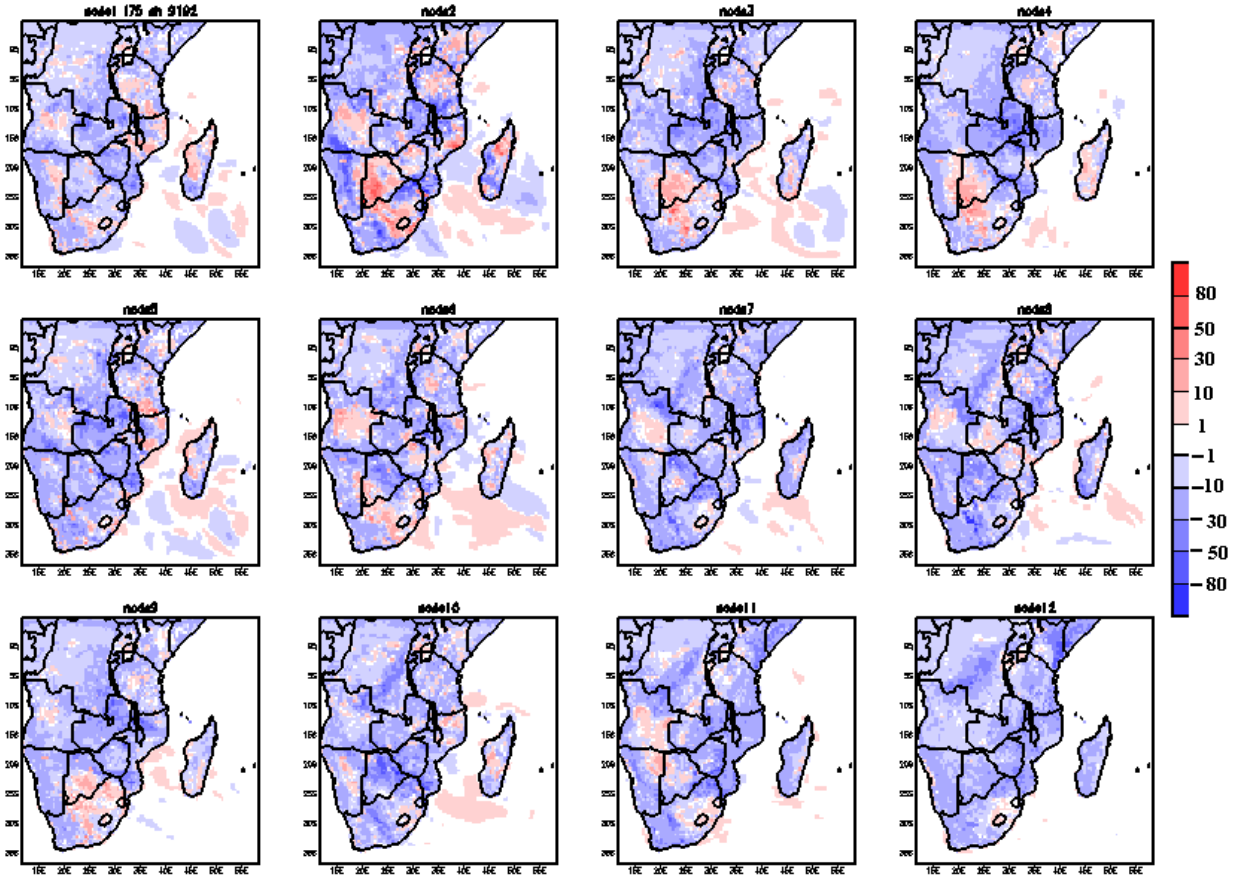

Figure B10. Sensible heat flux anomalies (W/m^2) for the 4x3 nodes from the daily RegCM3 simulation of interactive at 75% field capacity of September 1991 to March 1992. Red shading indicates positive sensible heat flux anomalies and blue shading indicates negative sensible heat flux anomalies.

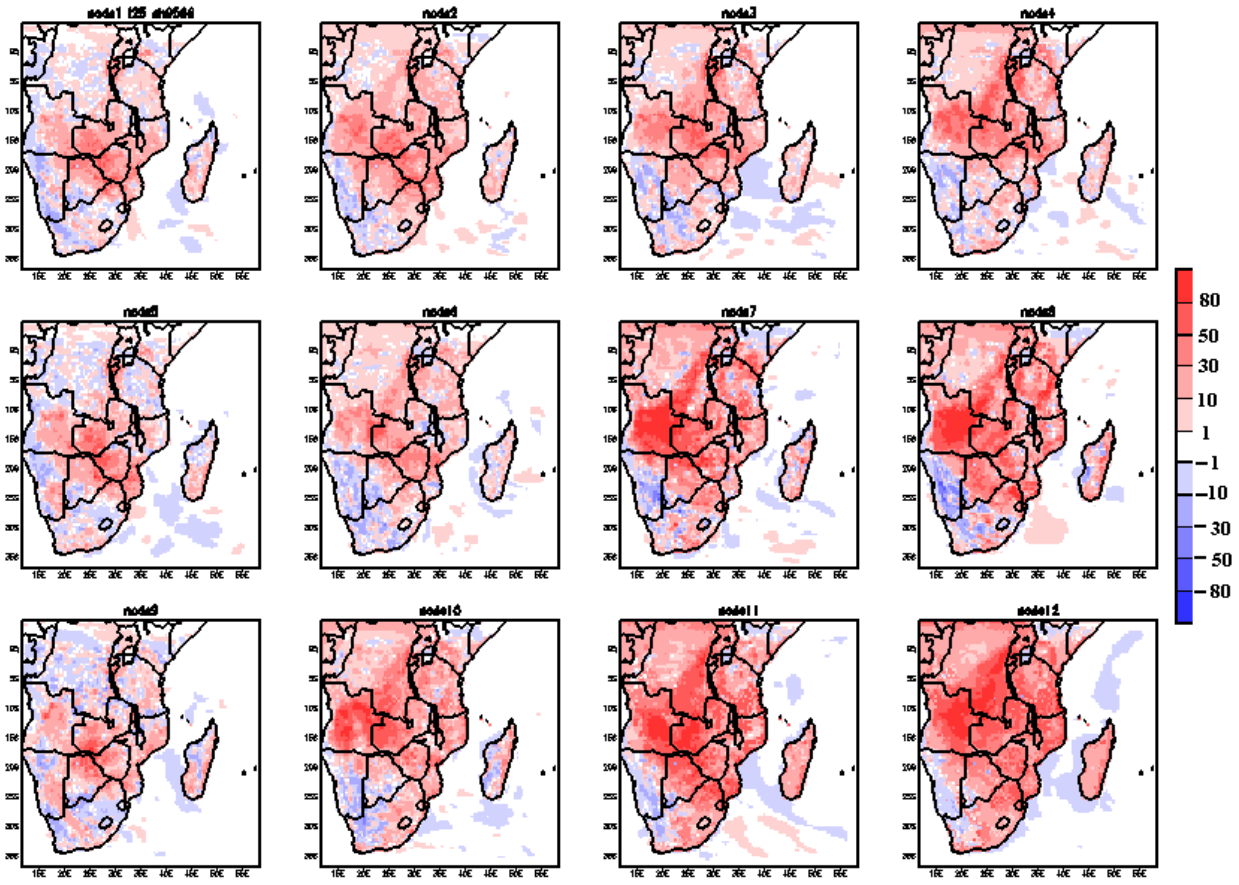

Figure B11. Sensible heat flux anomalies (W/m^2) for the 4x3 nodes from the daily RegCM3 simulation of interactive at 25% field capacity of September 1995 to March 1996. Red shading indicates positive sensible heat flux anomalies and blue shading indicates negative sensible heat flux anomalies.

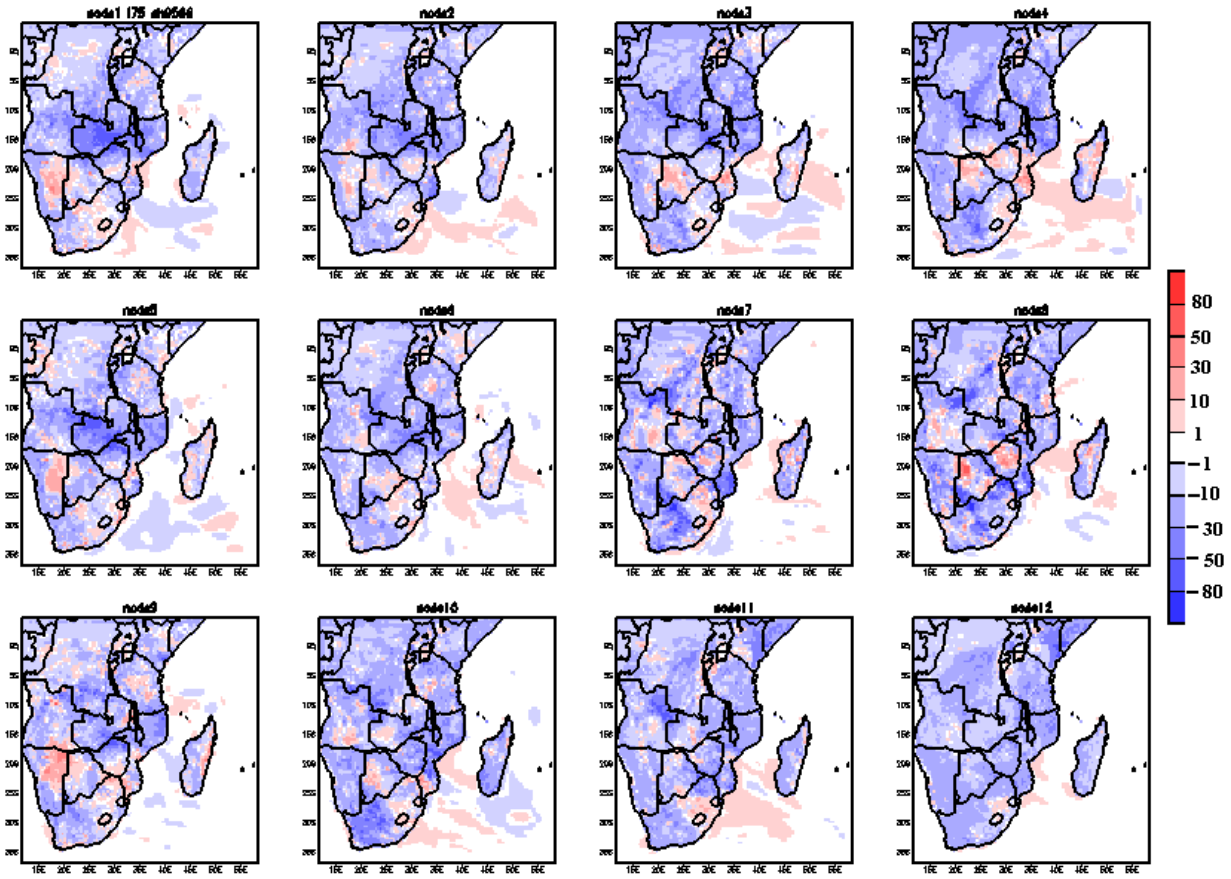

Figure B12. Sensible heat flux anomalies (W/m^2) for the 4x3 nodes from the daily RegCM3 simulation of interactive at 75% field capacity of September 1995 to March 1996. Red shading indicates positive sensible heat flux anomalies and blue shading indicates negative sensible heat flux anomalies.

Appendix B-4: Latent Heat Flux

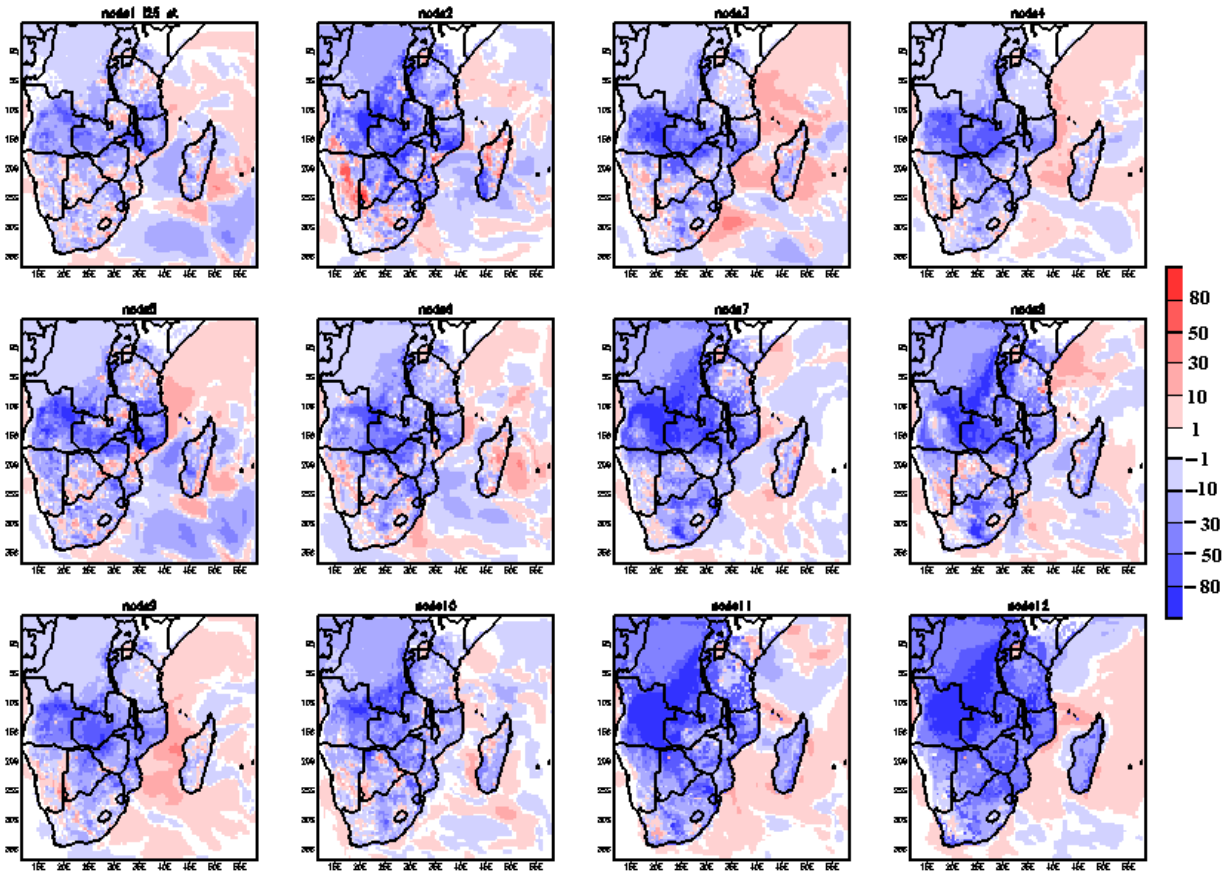

Figure B13. Latent heat flux anomalies (W/m^2) for the 4x3 nodes from the daily RegCM3 simulation of interactive at 25% field capacity of September 1991 to March 1992. Red shading indicates positive latent heat flux anomalies and blue shading indicates negative latent heat flux anomalies.

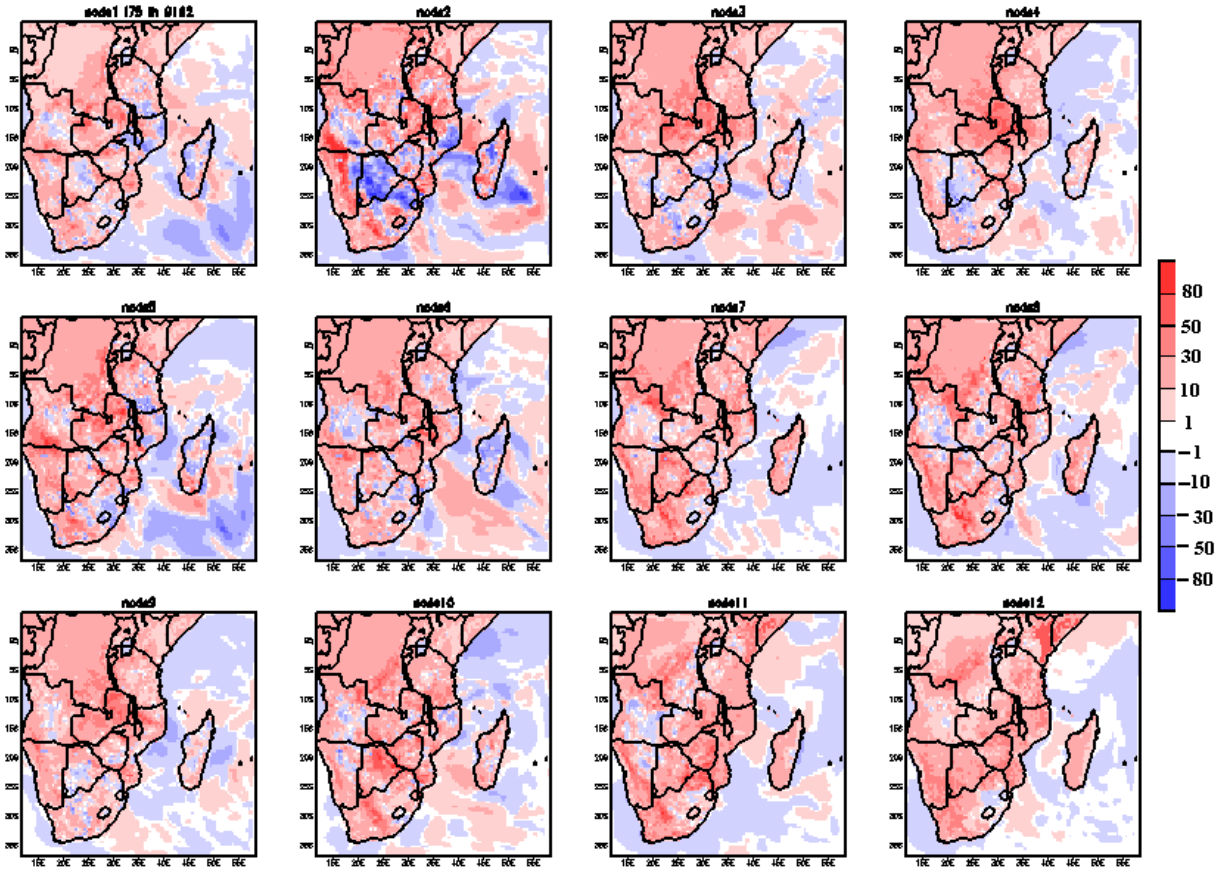

Figure B14. Latent heat flux anomalies (W/m^2) for the 4x3 nodes from the daily RegCM3 simulation of interactive at 75% field capacity of September 1991 to March 1992. Red shading indicates positive latent heat flux anomalies and blue shading indicates negative latent heat flux anomalies.

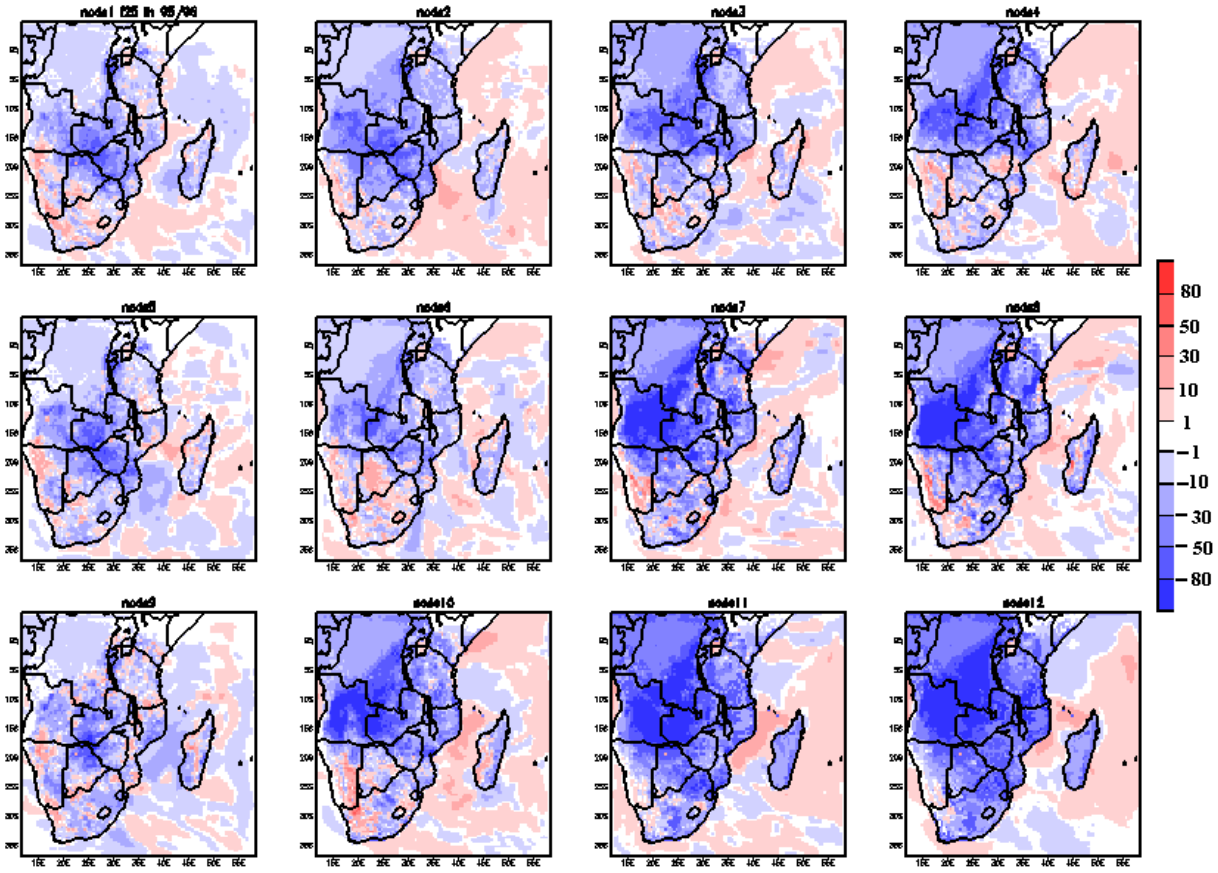

Figure B15. Latent heat flux anomalies (W/m^2) for the 4x3 nodes from the daily RegCM3 simulation of interactive at 25% field capacity of September 1995 to March 1996. Red shading indicates positive latent heat flux anomalies and blue shading indicates negative latent heat flux anomalies.

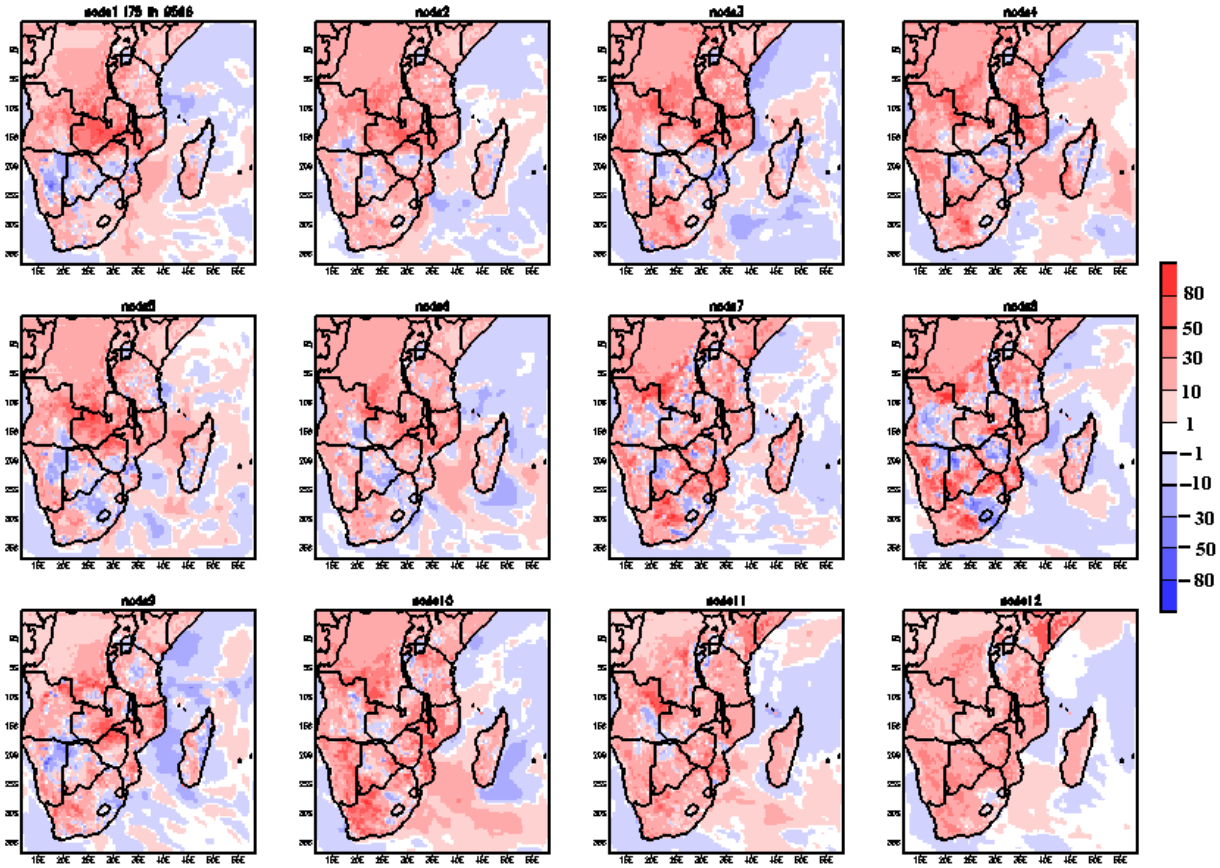

Figure B16. Latent heat flux anomalies (W/m^2) for the 4x3 nodes from the daily RegCM3 simulation of wet soil moisture perturbation – control of September 1995 to March 1996. Red shading indicates positive latent heat flux anomalies and blue shading indicates negative latent heat flux anomalies.